HYPERBRANCHED POLY(ETHYLENEIMINE) DERIVATIVES AS MODIFIERS IN EPOXY NETWORKS

Cristina Acebo Gorostiza

Cristina Acebo Gorostiza

Hyperbranched poly(ethyleneimine) derivatives as modifiers in epoxy networks

Doctoral Thesis

Supervised by Prof. Àngels Serra i Albet

and Prof. Xavier Ramis i Juan

Department of Analytical Chemistry and Organic Chemistry

UNIVERSITAT ROVIRA I VIRGILI

Tarragona, Spain

2016

UNIVERSITAT ROVIRA I VIRGILI
HYPERBRANCHED POLY(ETHYLENEIMINE) DERIVATIVES AS MODIFIERS IN EPOXY NETWORKS
Cristina Acebo Gorostiza

Departament Química Analítica i Química Orgànica
Campus Sescelades, Edifici N4
Carrer Marcel·lí Domingo s/n
43007 Tarragona

Professor Àngels Serra i Albet of the Department of Analytical and Organic Chemistry at the Universitat Rovira i Virgili and Professor Xavier Ramis i Juan of the Department of Heat Engines at ETSEIB, Universitat Politècnica de Catalunya,

Certify:

that the Doctoral Thesis, entitled "Hyperbranched poly(ethyleneimine) derivatives as modifiers in epoxy networks " presented by Cristina Acebo Gorostiza to obtain the title of Doctor, has been carried out under our direction and meets the requirements to qualify for the European Mention.

Tarragona, April 28th, 2016

Prof. Àngels Serra i Albet

Prof. Xavier Ramis i Juan

UNIVERSITAT ROVIRA I VIRGILI
HYPERBRANCHED POLY(ETHYLENEIMINE) DERIVATIVES AS MODIFIERS IN EPOXY NETWORKS
Cristina Acebo Gorostiza

Agradecimientos

La verdad que escribir la tesis es una tarea difícil y un proceso largo, pero escribir los agradecimientos, para mí, no va a ser nada fácil. Nunca encuentro el momento de escribirlos, siempre dudo de cómo empezarlos y sobretodo siempre pienso que cómo seré capaz de expresar en palabras lo que he vivido durante estos años. Y todo esto es más difícil cuando ves que el día que los escribes está más cerca el final de esta etapa de tu vida que yo no cambiaría y nunca querría acabar (aunque en el último año lo haya repetido mil veces) … Han sido muchas personas con las que he compartido y he trabajado durante estos años y haré un gran esfuerzo por no dejarme a ninguna ya que todos de una manera u otra tienen un trocito en mi corazón.

Estas primeras líneas son sin duda para mis dos directores de tesis, Àngels y Xavier. Es complicado explicar en palabras todo lo que compartes y aprendes de ellos durante cuatro años, pero hay que hacer el esfuerzo. Hace ya 5 años Àngels me ofreció un rinconcito en su laboratorio para empezar a trabajar en este mundo. A partir de entonces empezó mi unión con ella. Apenas en 6 meses, fue capaz de transmitirme sus ganas de trabajar y enseñar y además, se convirtió en una nueva compañera de mi vida, ella estaba siempre dispuesta a todo. Gracias a ella no me pensé dos veces en que mi siguiente paso era quedarme hacer la tesis. Ahora ya tengo que decirte Àngels, que has pasado a ser algo más, como yo siempre digo: mi segunda mamá. En esta etapa, una nueva persona formó parte de ella y como ahora yo ahora te llamo Xavier: el papá de la tesis. Gracias Xavier por todo. Siempre dispuesto a ayudar en todo y transmitir calma y paciencia en los momentos en que todo lo ves negros. Siempre sonriendo y viendo las cosas de una manera positiva. Agradecer a los dos su confianza depositada en mí para llevar a cabo esta tesis, de verdad que gracias. Nunca habéis dudado de mí y siempre me habéis apoyado, jamás me he visto incapaz de conseguir algo y siempre he intentado de una manera o de otra llegar hasta el final. Yo espero no haberos defraudado, siempre he intentado hacerlo todo de la mejor manera posible y ayudar en todo lo que he podido. Espero que mis nervios no se os hayan contagiado… ☺

Dar las gracias a Xavier (el petit), gran compañero con el que he compartido grandes charlas en las que siempre intentaba transmitir con ilusión todos sus conocimientos. Siempre estaba disponible a ayudarte y a aportar su granito. También a Toni, gracias por esa alegría que siempre transmites con tus buenos días y por tu ayuda durante estos años.

El laboratorio 330 ha sido 'mi casa' durante este tiempo, y por él han pasado muchas personas sin las cuales está tesis no habría sido igual. Durante mi primer año en el laboratorio sentía que pasaba más horas haciendo el café que no trabajando, y de quién era culpa: David, Isidro y Quique (*googledor*) Siempre había que tener tiempo para el café y sino ya estabas espabilando para intentarlo…David, no me olvido que tu gran cualidad era estar picándome todo el día, te lo pasabas pipa, como te gustaba... Pero ahora lo recuerdo y pienso que bien nos lo pasábamos. Gracias David. Mireia, gracias por enseñarme la base de las 'estrellas', sin ti hubieses sido todo más difícil. No me olvido tampoco de las grandes conversaciones de la vida, y cuanto nos reíamos! Para grandes conversaciones de la vida, del mundo y del amor las que tenía con Marjorie. Siempre había un momento para desconectar del trabajo y hablar de lo que fuese. Pero te lo agradezco muchísimo ya que como tu sabes, aprendí a ver muchas cosas de otra manera y a valorar un poquito más! Esta palabra que existe en el diccionario pero que pocos usamos. Ah! Y Mireia y Marjorie, no olvido aquella noche de tótem! Siempre había chocolate en

laboratorio, siempre te encontrabas un dulce de Litúania en tu mesa…Asta! Era imposible resistirse. Gracias Asta! Siempre hacías el día un poco más dulce. Cristina Mas hizo que durante un tiempo el laboratorio cambiase de temas. Vinieron las conversaciones de niños y mamás, pero que divertidas… Y es que en el laboratorio había de todo y se aprendía de todo: clases de filosofía con Adrian y cultura india con Surya. Gracias a los dos por compartir tanto y por esas comidas en casa…. (Surya Chris aún se chupa los dedos).

Ahora toca el turno a los que todavía andan por 'mi casa'. Xavi, que faré sense tú? Sense el meu fillet? La verdad que las horas que hemos pasado juntos no son fáciles de contar. ¿Y los ratos que nos hemos reído? Tampoco. Y ¿lo que se han reído con nosotros dos? Tampoco. Piensa que ahora el laboratorio ya se queda sin telenovela en la que cada día había un culebrón ¿Quién tendrá tantas historias y conversaciones divertidas que explicar y contar? Gracias por ser mi compañero 'derecho' de la mesa; por borrarme el nombre tantas veces para preguntarme de todo (jeje)…pero cuanto echaré de menos que nadie me pregunte donde está todo o como se hace esto, echaré de menos un compañero como TU. Y no me olvido de recordarte que al final la salsa y la bachata te han marcado y ahora eres tú quien la escuchas! Alberto, lo siento, te ha tocado un laboratorio muy marchoso. Ahora ya no tendrás que mover el cuerpo mientras pules tus muestras. Pero un día te acordarás del Enrique Iglesias y compañía, ya lo verás. A pesar de eso, mil gracias por compartir estos dos últimos años conmigo tanto dentro como fuera del trabajo. Tu también has formado parte del culebrón y te uniste a nosotros desde el primer momento, y es algo que ha hecho que el laboratorio también sea diferente. Ah por cierto, nunca bajes de tu mundo yupi (tu lo sabes) que ahí se vive muy bien! Pero este laboratorio necesitaba más mujeres, y aquí llega Dailyn. Aquella persona que tiene el mismo lenguaje que yo, que nos miramos y sabemos lo que decimos, aquella persona con la que he podido hablar de todo y aquella que siempre te da calma y tranquilidad cuando te estás estirando de los pelos. Ha sido capaz de comprender todas mis crisis existenciales. Además era mi esteticista personal! Te doy mucho ánimo para lo que te queda. Como siempre te digo, siempre que te vea con pelo será buena señal! Agradezco muchísimo haberte conocido, hay muchas cosas que no aprendes si no convives con una persona como tu. Y también gracias por haber sido la espectadora de la telenovela 330, porque si alguien no la ve, no tiene éxito! Y no me olvido de agradecer a aquella persona que suele cargarnos nuestro cajón secreto de dulces de Alcalá. No pierdas la paciencia durante el tiempo que te queda y suerte. Gracias por ser un compañero más en el laboratorio y por contribuir muchas veces al culebrón Cristina & Xavi. El polaco, Krys, que dulces tan buenos nos traes siempre de Polonia. Pero no solo eso, agradecer tus ganas de ayudar siempre en todo lo que necesitas. Es el hombre del laboratorio. Isaac, tu acabas de llegar apenas hace tres meses, pero también has pasado a ser uno más como todos ellos. Ya has podido comprobar que aquí te puedes reír a todas horas y te pido que sigas manteniendo esto y que no se pierda!. El químico infiltrado! David, agradecerte tu disponibilidad y ayuda siempre que lo he necesitado y por hacerme compañía muchas mañanas. No todos madrugan…. Blai, tú también ya eres uno más, y como ves es un laboratorio molón donde no falta las ganas de reír, y si te quedas, también te toca mantenerlo. A todos, no cambiéis nunca y espero que jamás perdamos el contacto.

Agradecer a aquellas personas que han sido pasajeras: Annamaria, Oleksandra, Vincenzo, Rita, Claudio, Mimmo, Gianmarco… and Yvonne! I hope that you remember always your stage in Spain. For us it was a pleasure to have you in the lab and that you learn some sentences in our language. It was a really funny time. Sorry to make you laugh so hard.

Ahora toca el turno de los vecinos! Siempre recordaré aquellos saludos de Maryluz y la fama que me gane como polibarbie en el grupo. A ello se sumaron las turcas. Alev y Zeynep agradecer vuestras visitas al laboratorio y por tenerme siempre en cuenta. Y como no, Lorena, por entendernos una a la otra. Por ser parte de mis momentos de desconexión durante las comidas y reservar algunos de tus días por estar conmigo. Espero que sigamos teniendo un día marcado para vernos en el Chaplin! Y al resto de Suspoleros, Camilo, Rodolfo, Cristina, Marc, Carmen… Gracias, porque vuestro laboratorio siempre está abierto a todo el mundo. Los que aún os queda acabar el camino, os deseo lo mejor. Las misma palabras tengo para 'azúcares'. Agradecer a Emma, Míriam, Joan, David, Adrià, Irene, Macarena, Jordi… por su simpatía. Aunque actualmente nuestro punto de encuentro sea muchas veces la cola del office sé que estáis aquí al ladito.

A Francesc y Silvia del Departamento de Ingeniería Mecánica de la URV por su ayuda y colaboración durante todo mi trabajo y por estar siempre dispuestos a encontrar soluciones a los problemas. Los técnicos de recursos científicos de la URV: Ramón, Mercè, Núria, Mariana, Rita y Lukas, gracias por vuestra paciencia y disponibilidad.

I would like to thank Dr. Albena Lederer and Dr. Dietmar Appelhans from the Leibniz-Institut für Polymerforschung (Dresden) for giving me the possibility to be part of IPF for several months and learn about polymer synthesis and characterization. Big thanks to Susanne Boye for her help and support and for being so kind with me. Also, I would like to thank the colleagues I met there (Josef, Andrea, Laura, Mikhail, Christina, Eileen, Petra, Roland, Johannes…) especially my 'office mates' Eva and Liane. Of course, I cannot forget Alejandro, Roberto, Michela, Jan, Guido, Negin, Oksana…for their kindly attention and for being part of my life since my stay in Dresden.

Mi amigos de toda la vida! Ana, Gemma, Araceli, Paola, Sergi, Joan, Mena, Miguel…Sé que a veces he andado desparecida, la vida va cambiando pero no tengo duda, espero, de que siempre estéis ahí. La amistad es la base de muchas cosas, ¿de que serviría estar en este mundo solo para trabajar si no compartes tus cosas con los demás?. Os doy las gracias por ser esa otra parte de mi vida, parte de los momentos de alegrías y penas, de fiesta, de diversión, de comidas, cenas, cumpleaños… Que sepáis que os necesito a mi lado, porque sin amigos no hay vida. Especialmente agradecer a Laura que ni en la carrera nos separamos y aquí seguimos. Gracias por todos los años a mi lado! En la carrera fuiste mi guía, el bracito derecho pero ahora eres el ejemplo de amistad. Gracias por estar cuando lo he necesitado y por animarme en este último año, el año que viene cambiamos los papeles ;).

Sin amigos somos poco, pero sin la familia somos apenas nada. A pesar de tenerla un poco lejos, sé que siempre están a mi lado. Solo una visita de fin de semana sirve para coger fuerzas para todo un mes. Me recibís con los brazos abiertos y es una alegría. Es ilusión ver como los pequeños corren a darte un besito, como un reunión en familia siempre está llena de risas y de recuerdos…En especial, un fuerte beso a la yayi que tantos veranos hemos estado juntas. Eso jamás se puede olvidar. Y aunque ni lo lea, ni me vea también es para el yayo..Sé que el también estaría orgulloso.

Realmente no sería nada hoy sin mis padres. Ellos han sido mi mano izquierda y mi mano derecha, jamás me han dejado caer. Son esas personas que nunca se van de tu lado y que los tienes para todo con la ventaja de que para mí también son mis hermanos. Gracias por haberme acompañado siempre, y por haberme apoyado en todo! Apenas llevamos poquito recorrido de vida juntos, nos queda mucho por hacer. Espero poder compartir todo

con vosotros como hasta ahora, no perder nuestras comidas, viajes... Jamás me separaré de vosotros.

Y si parecía que había acabado…NO. No puedo acabar sin agradecer a mi compañero de vida, mi compañero que también es participé de muchos de los agradecimientos anteriores. Gracias Christofer por TODO. Creo que es imposible explicar todos los motivos por los que te doy las gracias, pero si que hay uno que es el más importante, y es, gracias por tu paciencia. Quiero agradecerte tu apoyo incondicional en todos estos años, sin ti no habría sido capaz de levantarme en muchos momentos o de haber visto la vida como la veo. Soy una afortunada por tenerte a mi lado. Sé que para nosotros el final de esta etapa es el comienzo de otras. Gracias por acompañarme de la mano durante este camino.

Cristina

UNIVERSITAT ROVIRA I VIRGILI
HYPERBRANCHED POLY(ETHYLENEIMINE) DERIVATIVES AS MODIFIERS IN EPOXY NETWORKS
Cristina Acebo Gorostiza

UNIVERSITAT ROVIRA I VIRGILI
HYPERBRANCHED POLY(ETHYLENEIMINE) DERIVATIVES AS MODIFIERS IN EPOXY NETWORKS
Cristina Acebo Gorostiza

“El futuro tiene muchos nombres. Para los débiles es lo inalcanzable. Para los temerosos, lo desconocido. Para los valientes es la oportunidad”

Víctor Hugo

UNIVERSITAT ROVIRA I VIRGILI
HYPERBRANCHED POLY(ETHYLENEIMINE) DERIVATIVES AS MODIFIERS IN EPOXY NETWORKS
Cristina Acebo Gorostiza

Table of contents

UNIVERSITAT ROVIRA I VIRGILI
HYPERBRANCHED POLY(ETHYLENEIMINE) DERIVATIVES AS MODIFIERS IN EPOXY NETWORKS
Cristina Acebo Gorostiza

UNIVERSITAT ROVIRA I VIRGILI
HYPERBRANCHED POLY(ETHYLENEIMINE) DERIVATIVES AS MODIFIERS IN EPOXY NETWORKS
Cristina Acebo Gorostiza

1.General introduction and scope

UNIVERSITAT ROVIRA I VIRGILI
HYPERBRANCHED POLY(ETHYLENEIMINE) DERIVATIVES AS MODIFIERS IN EPOXY NETWORKS
Cristina Acebo Gorostiza

1.1 General introduction

Epoxy resins are commonly used as thermosetting materials due to their excellent mechanical properties, high adhesion to many substrates and good heat and chemical resistances. This type of thermosets is intensively used in a wide range of fields, where they act as fiber-reinforced materials, general-purpose adhesives, high-performance coatings and encapsulating materials. These materials are formed by the chemical reaction of multifunctional epoxy monomers forming a polymer network produced through an irreversible way.[1]

1.1.1 General concepts of epoxy thermosets

The term epoxy or epoxide refers to compounds characterized by the presence of an oxirane or epoxy ring, a three-member ring containing an oxygen atom that is bonded with two carbon atoms as shown in **Scheme 1.1**.

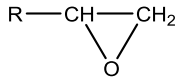

Scheme 1.1. The epoxy or oxirane ring structure

From the structural point of view of chemistry, epoxy resins are monomers or oligomers containing two or more epoxy groups in its structure. P. Castan[2] developed the first system based on the well-known diglycidyl ether of bisphenol A (DGEBA). The commercialization of this resin dates back to 1940.[3] It is obtained by the reaction of the bisphenol A with epichlorohydrin in the presence of a strong base such as NaOH. Depending on the ratio between reactants the resulting molecular weight can be tuned in order to have different resins being possible to obtain liquid, waxy or solid DGEBA resin.[4] The reaction, still used nowadays, is depicted in **Scheme 1.2**.

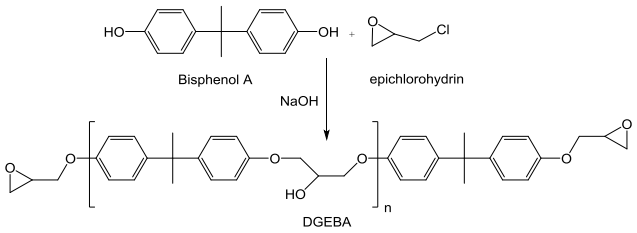

Scheme 1.2. Synthesis of DGEBA resins

There are other types of resins with different structure that leads to materials with different characteristics. Some of the most typical resins are collected in the **Scheme 1.3**. The non-epoxy part of the molecule can have an aliphatic, cycloaliphatic or aromatic structure and the functionality, related to the number of epoxide groups can also be varied.

---

[1] C. A. May, *Chemistry and Technology*, 2nd edition. Marcel Dekker, New York, **1988**.
[2] H. Lee, K. Neville, *Handbook of Epoxy Resins*, McGraw-Hill, New York, **1967**.
[3] P. Castan, *Swiss Pat.* 211,116, **1940**.
[4] B. Ellis, *Chemistry and Technology of Epoxy Resins*, Blackie Academic & Professional, London, **1993**.

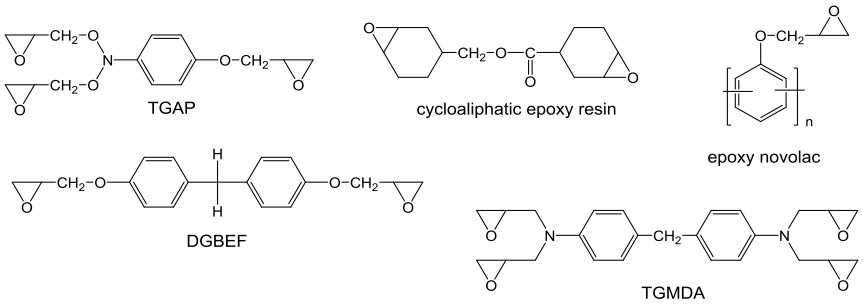

Scheme 1.3 Structure of several commercial epoxy resins

Epoxy resins are capable of reacting with different active compounds known as curing agents (with or without catalyst) or with themselves (via an initiator) to form solid, crosslinked materials. This transformation is generally referred as curing.

From a fundamental point of view, thermosetting epoxy polymers may be defined as polymer networks obtained by a chemical reaction of monomers which contain two or more epoxy groups per molecule (a functionality equal to or higher than 2).[5] The functionality of an epoxy monomer is defined by the number of arms (bonding sites) which participates in the formation of the polymer network. The functionality of the epoxy monomers depends on the curing system used and will be discuss below, but a necessary condition for the formation of a network is that at least one of the monomers involved in the reaction has a functionality higher than two, since the global functionality of the system to reach a network structure is a minimum of 4.

1.1.2 Curing agents

Crosslinked epoxy polymers are obtained by reaction of the epoxy monomers with curing agents (co-monomers or initiators). Epoxy polymers can be produced by step or chain growth polymerizations or, eventually, by a combination of both mechanisms.[5]

Step growth polymerization (polycondensation) proceeds via a step-by-step succession of elementary reactions between reactive sites. Each independent step causes the disappearance of two co-reacting sites and creates a new covalent bond between a pair of functional groups. In this case curing agents like amines, alcohols, anhydrides, isocyanates or acids have been used in stoichiometric ratio.[6]

Chain growth polymerization (ring opening) is characterized by the presence of initiation, propagation, chain transfer and termination steps. In the case of epoxies, the initiation step produces an ion (either an anion or a cation) that is called the active center of the polymerization. The ion may be generated by thermal treatment or by an adequate source of irradiation. Once active centers are generated they produce primary chains by the consecutive addition of monomers through the propagation step of the reaction.

Polycondensation curing mechanisms require an accurate knowledge of the stoichiometry of the system. Among them, the most used curing agents for epoxy resins are primary and secondary amines. In this system, DGEBA is bifunctional and a

[5] J. P. Pascault, R. J. J. Williams, *Epoxy Polymers*, Wiley VCH, Weinheim, **2010**, Chapter 1.
[6] J. P. Pascault, H. Sautereau, J. Verdu, R. J. J. Williams, *Thermosetting Polymers*, Marcel Dekker, New York, **2002**, Chapter 2.

requirement for the amines is that they must be multifunctional (more than two reacting groups). Considering that primary amines account for a functionality of two and secondary for a functionality of one, usually primary diamines are used. The reaction of epoxy with amines is depicted in the following scheme.[6]

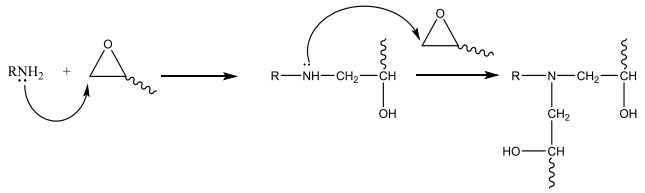

Scheme 1.4 Mechanism of reaction between epoxides and primary and secondary amines

Primary and secondary aliphatic amines react rapidly with epoxy groups at low temperature to form three-dimensional crosslinked structures. However, they can also be cured at higher temperatures to provide a more densely crosslinked structure with better mechanical properties, elevated-temperature performance and chemical resistance. Other amines, such as aromatic or cycloaliphatic, are less reactive and generally require higher curing temperatures.

After amines, acid anhydrides are the second most used group of curing agents. Among the most common anhydrides, phthalic anhydride (PA), tetrahydrophthalic anhydride (THPA), methyl tetrahydrophthalic anhydride (MTHPA) and nadic methyl anhydride (NMA) can be mentioned (**Scheme 1.5**).

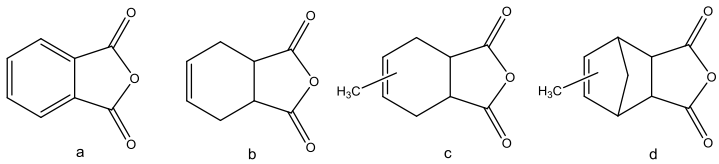

Scheme 1.5 Chemical structures of acid anhydrides used as curing agents: a) phthalic anhydride, b) tetrahydrophthalic anhydride, c) methyl tetrahydrophthalic anhydride, e) methyl nadic anhydride

The reaction of anhydrides with epoxy groups has been extensively studied and follow a complex mechanism, with several competitive reactions capable of taking place.[7,8] The limitation of the use of anhydrides as curing agents is the low reactivity and, therefore, the curing has to be carried out at high temperatures to obtain optimal properties.[9] The presence of catalyst such as tertiary amines, metallic salts and imidazoles can accelerate the curing and overcome this drawback.[10]

The main reaction that takes place on curing epoxide/anhydride mixtures without amine is illustrated in **Scheme 1.6**. The first reaction is the opening of the anhydride ring by reaction of a hydroxyl group to form the monoester (**1**) and subsequently the nascent carboxylic group reacts with the epoxy to provide an ester linkage (**2**). The reaction proceeds by the presence of existing hydroxyl groups (**3**).

[7] W. Fish, W. Hofman, J. Koskikallio, *Journal of Applied Chemistry*, **1956**, *6*, 429-441.
[8] L. A. O'Neil, C. P. Cole, *Journal of Applied Chemistry*, **1956**, *6*, 356-364.
[9] S. Montserrat, C. Flaqué, M. Calafell, G. Andreu, J. Málek, *Thermochimica Acta*,**1995**, *269*, 213-229.
[10] E. M. Petrie, *Epoxy Adhesive Formulations*, McGraw-Hill, New York, **2006**.

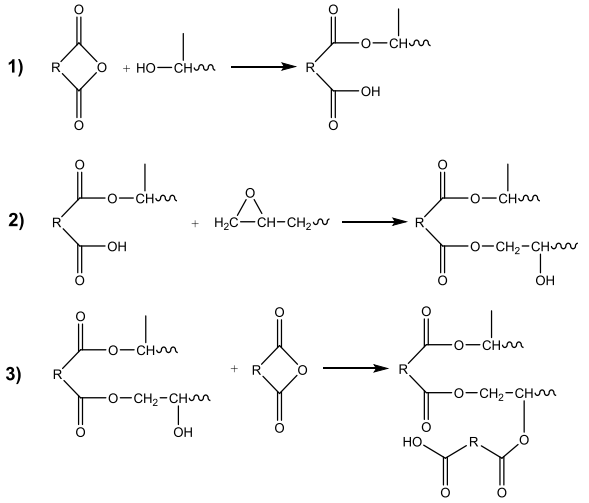

Scheme 1.6 Mechanism of uncatalyzed anhydride-epoxy reaction

In the presence of tertiary amine a different mechanism occurs (**Scheme 1.7**). It is proposed that the tertiary amine reacts with the epoxy monomer and forms a zwitterion that contains a quaternary nitrogen atom and an alkoxide (**1**). The alkoxide rapidly reacts further with an anhydride group leading to a carboxylate anion (**2**). Propagation occurs through the reaction of the generated carboxylate with an epoxy group and the formation of a new alkoxide anion (**3**). There is still no definite validation regarding the termination step and whether the initiator remains chemically attached during the whole course of the reaction. Some authors describe an irreversible bonding of the initiator[11] but there is disagreement on this point.[12,13]

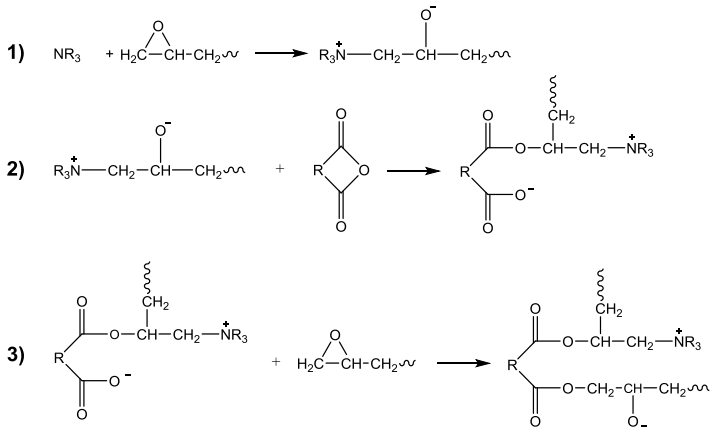

Scheme 1.7 Mechanism of anhydride epoxy reaction catalyzed by tertiary amine

The other big group of curing agents used is the one of initiators. Commonly used initiators include Lewis bases such as tertiary amines or imidazoles for anionic chain

[11] J. Leukel, W. Burchard, R. P. Krüguer, H. Munch, G. Schulz, *Macromolecular Rapid Communications*, **1996**, *17*, 359-366.
[12] M. Fedtke, F. Domaratius, *Polymer Bulletin*, **1986**, *15*, 13-19.
[13] X. Fernández-Francos, A. Rybak, R. Sekula, X. Ramis, A. Serra, *Polymer International*, **2012**, *61*, 1710-1725.

polymerization, and Lewis acids such as boron trifluoride complexes or other metal salts. These initiators are used in catalytic amounts and promote the homopolymerization of epoxides via ring opening polymerization (ROP).[14] This ring-opening mechanism is similar in terms of kinetics to polyaddition since presents an initiation step, a propagation and finally a termination, but mechanistically is more complex and leads to the introduction of heteroatoms in the network structure.

In these initiated curing systems the functionality of the epoxide group is two and therefore the global functionality of a diepoxy resin is four. Thus, from a diepoxide, crosslinked structures can be obtained by the use of the adequate initiator and conditions.

The anionic polymerization can be promoted by several initiators with high nucleophilic character or strong basic characteristics, but in the field of epoxy thermosets the most extended anionic initiators are tertiary amines,[1] such as 1-methyl imidazole (1-MI)[15] or 4-(N,N-dimethylamino)pyridine (DMAP) [16] (**Scheme 1.8**).

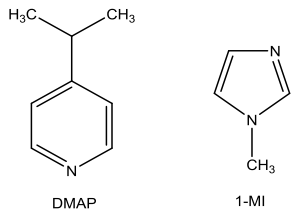

Scheme 1.8 Chemical structure of anionic initiators

The curing mechanism initiated by tertiary amines is depicted in **Scheme 1.9**. As can be seen, the opening of the epoxide by the nucleophilic attack of the amine forming an alkoxide is the first step. Initiation and propagation proceeds by nucleophilic substitution (S_N2) and as a consequence the nucleophilic attack occurs in the less substituted carbon.

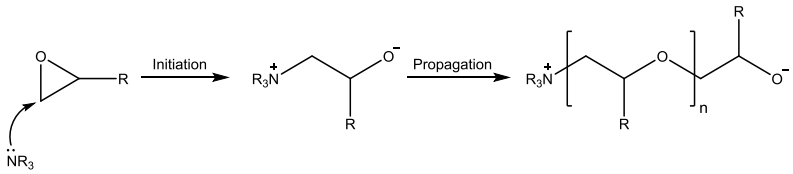

Scheme 1.9 Mechanism of polymerization of epoxides initiated by tertiary amines

Ooi et al. [17] observed by differential scanning calorimetric studies (DSC) two exothermic peaks during the curing process of N-alkyl substituted imidazole-DGEBA formulations. These results indicated that the curing mechanism represented in Scheme 1.9 was more complex. The cause of the additional peak was associated with imidazole regeneration by β-elimination or *N*-dealkylation process, which then reinitiates the polymerization, as shown in **Scheme 1.10**.

[14] D. J. Brunelle, *Ring-Opening Polymerization: Mechanism, Catalysts, Structure and Utility*, Hanser Publishers, Munich, **1993**.
[15] F. Ricciardi, W. A. Romanchick and M. M. Joullié, *Journal of Polymer Science: Polymer Chemistry Edition*, **1983**, *21*, 1475-1490.
[16] M. Galià, A. Serra, A. Mantecón, V. Cádiz, *Journal of Applied Polymer Science*, **1995**, *56*, 193-200.
[17] S. K. Ooi, W. D. Cook, G. P. Simon, C.H. Such, *Polymer*, **2000**, *41*, 3639-3649.

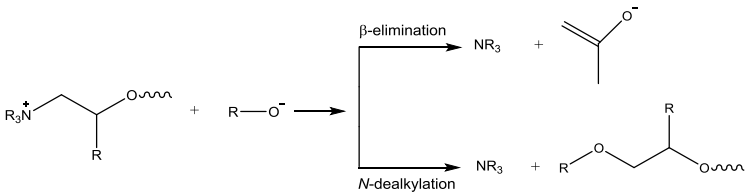

Scheme 1.10 Possible pathways of imidazole regeneration

Moreover, in previous studies it could be demonstrated that the presence of species which can coordinate with epoxides (such as hydroxyl groups) promotes the initiation step speeding up the reaction due to the interaction between the hydroxyl group and the oxygen in the oxirane ring which helps to increase the positive charge in the oxirane ring methylene carbons (**Scheme 1.11**). The imidazole regeneration can be also favored by the presence of hydroxyl groups.[18,19]

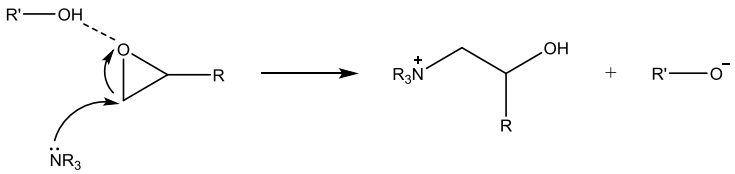

Scheme 1.11 Initiation step in the presence of hydroxyl groups

If the initiation step is catalyzed by Brönsted or Lewis acids, the propagation takes place via a cationic mechanism. $TiCl_4$, $AlCl_3$, $ZnCl_2$, BCl_3, $SiCl_4$, $FeCl_3$, $MgCl_2$, $SbCl_5$ are Lewis acids used as catalysts, but the most extended one is the BF3/amine complex.[20] In recent years also lanthanide and rare earth metal triflates have demonstrated to be good cationic initiators.[21-24]

Scheme 1.12 shows the mechanism of propagation for cationic polymerization of epoxides. In this case, there are two propagation mechanisms that coexist: activated chain end (ACE) and activated monomer (AM).[25] Both mechanisms start by the coordination of the initiator with the epoxide to promote the ring opening. ACE mechanism consists in the reaction between an activated epoxide and a non activated one. On that way, the activated epoxide is always linked to the growing chain. On the contrary, AM mechanism requires a hydroxyl group to first open an activated epoxide. Then, there is an intermolecular interchange of protons with an epoxide that becomes now activated. Thereby, the monomer is always the activated epoxide.

[18] B. A. Rozenberg, *Advances in Polymer Science*, **1986**, *75*, 113-165.
[19] X. Fernández-Francos, W. D. Cook, A. Serra, X. Ramis, G.G. Liang, J. M. Salla, *Polymer*, **2010**, *51*, 26-34.
[20] M. Ghaemy, M. H. Khandani, *European Polymer Journal*, **1998**, *34*, 477-486.
[21] P. Castell, M. Galià, A. Serra, J. M. Salla, X. Ramis, *Polymer*, **2000**, *41*, 8465-8474.
[22] C. Mas, A. Serra, A. Mantecón, J. M. Salla, X. Ramis, *Macromolecular Chemistry and Physics*, **2001**, *202*, 2554-2564.
[23] S. J. García, X. Ramis, A. Serra, J. Suay, *Thermochimica Acta*, **2006**, *441*, 45-52.
[24] S. J. García, X. Ramis, A. Serra, J. Suay, *Journal of Thermal Analysis and Calorimetry*, **2006**, *83*, 429-438.
[25] P. Kubisa, S. Penczek, *Progress in Polymer Science*, **1999**, *24*, 1409-1437.

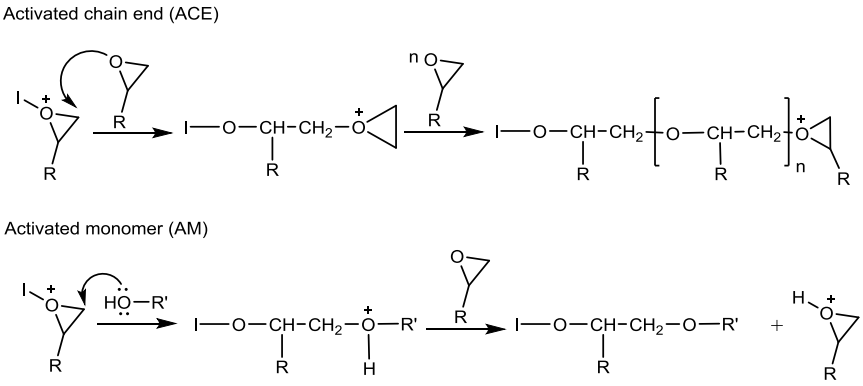

Scheme 1.12 Mechanism of propagation of the cationic polymerization of epoxides

All these systems described constitute a two-component system in which monomer and curing agents are stored separately and they are mixed in the correct quantity just prior to use. However, one-component systems in which the mixture of epoxy resin and curing agent is commercially supplied, also called one-pot resins, have considerable advantages over the other since they are easier to use. One-pot epoxy resins require a latent curing agent which does not react at room temperature, but react with epoxy resins under external stimulation, heat or irradiation.[26] Thermal latent curing agents can act mainly by two different mechanisms: the first one is based on their low compatibility in epoxy resin because of their crystalline character or by encapsulation of the active species.[27] The second mechanism is based on the use of a precursor compound, inactive at room temperature, but which under triggering by heat it transforms into an active curing agent.[28] Photoirradiation can also lead to the formation of active species, which originate homopolymerization by cationic or anionic processes.[29] Although photoirradiation is a more convenient way of triggering from the point of view of the energy savings, it presents some disadvantages, such as the curing of thick samples or with a complex geometry.[30] The initiation by heat is easier from the experimental point of view and can be applied to thicker samples or to hidden parts of surfaces.

The selection of the curing agent is the key point in the application, workability of the curing mixture, characteristics of the final thermosets and other factors.

1.1.3 Characteristics of epoxy thermosets

The degree of crosslinking and the nature of the bonds in the cured epoxies give them many desirable characteristics that have placed these thermosets as the standard option for a variety of applications such as adhesives, coatings, composites for structural applications, and so on.

One of the most important characteristics of these materials are the absence of volatile matter on curing and the capacity to adhere to most substrates due to the presence of polar

[26] T. Endo, F. Sanda, *Macromolecular Symposia*, **1996**, *107*, 237-242.
[27] A. M. Tomuta, X. Ramis, F. Ferrando, A. Serra, *Progress in Organic Coatings*, **2011**, *74*, 59-66.
[28] C. Z. Hua, S. J. Wan, L. Wang, X. D. Liu, T. Endo, *Journal of Polymer Science, Part A: Polymer Chemistry*, **2014**, *52*, 375–382.
[29] J. V. Crivello, M. Sangermano, *Journal of Polymer Science, Part A: Polymer Chemistry*, **2001**, *39*, 343-356.
[30] D. He, H. Susanto, M. Ulbricht, *Progress in Polymer Science*, **2009**, *34*, 62-98.

groups like hydroxyl or ether.[10] In addition, epoxy resins are resistant to the thermal degradation and are stable in front of the attack by corrosive chemicals. This properties are related to the covalent bonds present in the network which define their stability. The presence of groups that can be removed by chemical reactions using weak alkalis, strong acids and organic solvents reduce the chemical resistance.[31,32] Moreover, by the addition of cleavable linkages in the structures allow thermosetting materials can be removed under thermal controlled conditions.[33,35]

Epoxy thermosets are amorphous and highly crosslinked materials. The crosslinking density is a key parameter in determining the mechanical properties of an epoxy resin after cure. The higher crosslinked density allows these thermosetting materials having high glass transition temperatures and useful properties like high values of hardness, tensile strength, shear strength or Young modulus.

However, in terms of structural applications they have some disadvantages that limit their range of applications. Epoxy resins are in general brittle due to their high crosslinked character which confers low impact strength and poor resistance to crack propagation.[2] The fracture resistance decreased with increasing the crosslinking density.[35] Moreover, the tight structure implies a shrinkage that undergoes during the curing process that finally leads to the apparition of stresses and defects in the material. The crosslinked nature enhances the thermal resistance so they cannot be removed from a substrate without damaging it. In coatings technology the resistance to scratch is another issue interesting to be improved. Thus, new strategies to overcome these drawbacks are needed, but these strategies should not compromise other properties.

Toughness

Toughness of a specimen refers to the total energy required to cause failure, i.e., the total area under the stress-strain curve or the energy absorbed in an impact test. Toughening of the epoxy resins by addition of toughening agents or modifiers means to improve the amount energy absorption capacity. As a result, tremendous effort has been focused on improving the toughness of such materials during past decades and many reviews in this area are available.[36-38]

There are many approaches for improving toughness in epoxy resins which include: a) chemical modification of the network structure to make it more flexible, b) increasing the molecular weight of the epoxy resin to improve the molecular weight between crosslinks, c) lowering the crosslink density of the matrix by adjusting the ratio epoxy resin/crosslinking agent, d) adding reactive diluents, e) adding toughness modifiers in the formulation or f) incorporating of inorganic fillers/reinforcements into the neat resin.[36]

The most promising strategy for increasing the toughness of epoxy thermosets is the incorporation of plasticizers, like thermoplastic or rubbers, which increase the flexibility of

[31] D. Foix, M. Erber, B. Voit, X. Ramis, A. Mantecón, A. Serra, *Polymer Degradation and Stability*, **2010**, *95*, 445-452.
[32] A. Tomuta, X. Ramis, X. Fernández-Francos, F. Ferrando, A. Serra, *Progress in Organic Coatings*, **2013**, *76*, 1616-1624
[33] J. S. Chen, C. K. Ober, M. D. Poliks, *Polymer*, **2002**, *43*, 131-139.
[34] J. S. Chen, C. K. Ober, M. D. Poliks, Y, Zhang, U. Wiesner, C. Cohen, *Polymer*, **2004**, *45*, 1939-1950.
[35] G. Levitas, S. De Petris, A. Marchetti, A.Lazzeri, *Journal of Materials Science*, **1991**, *26*, 2348-2352.
[36] R. Bagheri, B. T. Marouf, R. A. Pearson, *Polymer Reviews*, **2009**, *49*, 201 - 225.
[37] C. B. Arends, *Polymer Toughening*, Marcel Dekker, New York, **1996**.
[38] K. P. Unnikrishnan, E. T. Thachil, *Designed Monomers and Polymers*, **2006**, *9*, 129-152.

the final network by the incorporation of a second dispersed phase.[39,40] However, the addition of these modifiers usually compromise the modulus and thermomechanical characteristics of the thermosets, leading to a reduction of Young modulus and T_g, and worsening the processability of the formulation by increasing its viscosity.[36]

Another method of prevent the crack from freely develop after impact is the addition of a modifier that induces the formation of particles that absorb the impact energy and deflect the crack. The formation of micro/nanostructures in multi-component thermosets can further optimize the interactions between the thermosetting matrix and the modifiers and thus the mechanical properties of materials can be significantly improved. This is known as "toughening by micro/nanostructures" and can be achieved, among other procedures, following the chemical induced phase separation methodology (CIPS).[41,42] It starts from an initial homogenous mixture composed of the resin, curing agent and modifiers. On curing, a blend of epoxy matrix filled with rubber or thermoplastic microspheres is formed, with a final size of these particles controlled by the viscosity of the reacting mixture during curing.[43]

Alternatively, new strategies as the incorporation of hyperbranched polymers (HBPs)[44,45] or multiarm star polymers (SPs)[42] have been applied with good results in improving toughness without affecting other properties of the resin.[46] The improvement in toughness in the case of HBPs is attributed either to the flexibilizing effect induced by the homogeneous incorporation of the HBP[47] or to local inhomogeneities created in the crosslinked network by the formation of phase separated nanoparticles with good interfacial adhesion between phases.[48] The particles hinder the propagation of a certain crack in the material as seen in **Figure 1.1**. Since the interaction between phases plays a key role in this toughness reinforcement mechanism, the structure of the HBP must be carefully selected in order to obtain the desired properties.

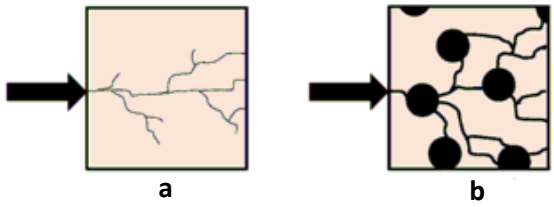

Figure 1.1 Crack propagation in materials: a) without particles and b) with dispersed particles

[39] L. T Manzione, J. K. Gillham, C. A. McPherson, *Journal of Applied Polymer Science*, **1981**, *26*, 889-905.
[40] A. C. Garg, Y. W. Mai, *Composites Science and Technology*, **1988**, *31*, 179-223.
[41] L. Ruiz-Pérez, G. J. Royston, J. P. A. Fairclough, A. J. Ryan, *Polymer*, **2008**, *49*, 4475-4488.
[42] Y. Meng, X.-H. Zhang, B.-Y. Du, B.-X. Zhou, X. Zhou, G.-R. Qi, *Polymer*, **2011**, *52*, 391-399.
[43] R. Mezzenga, C. J. G. Plummer, L. Boogh, J. A. E. Manson, *Polymer,* **2001**, *42*, 305-317.
[44] D. Ratna, R. Varley, G. P. Simon, *Journal of Applied Polymer Science*, **2003**, *89*, 2339-2345.
[45] L. Boogh, B. Pettersson, J-A. E. Månson, *Polymer*, **1999**, *40*, 2249-2261.
[46] J-F. Fu, L-Y. Shi, S. Yuan, Q-D. Zhong, D-S. Zhang, Y. Chen, J. Wu, *Polymer for Advanced Technologies*, **2008**, *19*, 1597-1607.
[47] D. Zahng, Y. Chen, D. Jia, *Polymer Composites*, **2009**, *30*, 918-925.
[48] V. Mital, *Optimization of Polymer Nanocomposite Properties*, Wiley VCH, Weinheim, **2010**, Chapter 2.

Shrinkage

When any type of monomers undergoes polymerization and crosslinking, shrinkage occurs throughout the cure process. Shrinkage is the reduction in volume brought about by increase in density. The curing process of epoxy resins entails shrinkage which is a critical point in the field of coatings since can lead to the appearance of internal stresses and consequently to defects in the materials, such as microvoids, microcracks or warping.[49] For this reason the reduction of stresses is an important goal since the protection capability is reduced when thermosets are used as coatings.

One should distinguish between thermal and chemical shrinkage. Thermal shrinkage occurs in the thermal curing because after curing the thermosets obtained at high temperature should be cooled down until room temperature and therefore the contraction is hard to be avoided. On the other hand, chemical shrinkage occurs because the formation of new covalent bonding in the reactions taking place during the curing process. In general, as monomer polymerizes, its density changes as a direct result of the bond changes being affected during polymer formation. Usually, the new bonds formed are shorter in the polymer than the distances between monomers.[50] This shrinkage is caused by the chemical reactions that take place during curing and it is described that the shrinkage during ring opening polymerization (ROP) is lower than chain growth and step growth polymerizations.[50] This is due to the fact that per each Van der Waals distance that becomes a covalent bond there is one covalent bond going to a nearly Van der Waals distance (**Scheme 1.13**). For this reason the use of ROP is a good strategy to produce the minimal shrinking epoxy thermosets.

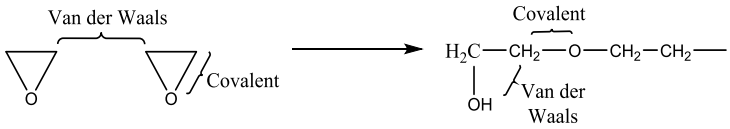

Scheme 1.13 Changes of distances during ring opening polymerization

Many approaches have been attended in order to solve the shrinkage issue related with the chemical reactions during the curing process like the addition of inorganic inert charges (silica, quartz or mica) or polymeric charges (polyurethane foams, PVC or polystyrene). Unfortunately, the main problem of this strategy is that the T_g of the resulting thermosets falls dramatically down, reduces toughness, increases the viscosity and worsens the material properties limiting their range of applications.[2]

New strategies as the addition of HBPs as modifiers in epoxy thermosets can reduce the shrinkage during curing by reducing the internal stresses.[51] The incorporation of HBPs in the network decreases the coefficients of thermal expansion (CTEs) due to the higher degree of crosslinking coming from the high number of reactive groups in the HBP and does not reduced the T_g of the final materials.[52] Moreover, it has been described that the increase in the amount of HBP added to the formulation reduces not only the global shrinkage but even more, the shrinkage after gelation, which is the true responsible of the

[49] H. Davies, *Proceedings of the IEE - Part B: Electronic and Communication Engineering*, **1962**, *109*, 259-265.
[50] R. K. Sadhir, M. R. Luck. *Expanding Monomers. Synthesis, Characterization and Applications*. CRC Press, Boca Raton, **1992**.
[51] X. Fernández-Francos, J. M. Salla, A. Cadenato, J. M. Morancho, A. Serra, A. Mantecón, *Journal Applied of Polymer Science*, **2009**, *111*, 2822-2929.
[52] M. Morell, X. Ramis, F. Ferrando, Y. Yu, A. Serra, *Polymer*, **2009**, *50*, 5374-5383.

apparition of stresses.[51] It is worth to note that after the gelation the material losses its mobility and therefore the shrinkage produced after gelation produces tensile, compressive and shear forces within the resin.

Reworkability

The concept of reworkability in thermosets is related to the ability of a material to break-down under controlled conditions in order to be removed from a given substrate (**Figure 1.2**), but it does not mean that the polymeric material can be reused or recycled.[34]

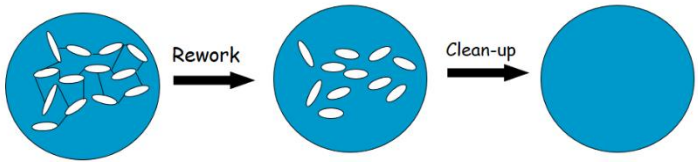

Figure 1.2 Scheme of the process of the elimination of a reworkable coating

The decomposition of the degradable linkages upon heating is expected to lead to a decrease in crosslinking density and modulus of the adhesive or coating, allowing its removing and replacement. The optimal temperature range for safe re-work operation is desired to be within 200–250 ºC.[33,53]

In order to obtain thermally reworkable epoxy thermosets, one of the first approaches was the introduction of di-sulphure linkages in the amine curing agent which allows the fragmentation of the thermoset with the temperature.[54] Other authors proposed the introduction of thermally labile groups in the structure of the resin.[55,56] The introduction of ester groups improve the reworkability since they can be broken by a *β*-elimination process (**Scheme 1.14**) at temperatures about 235ºC.[33]

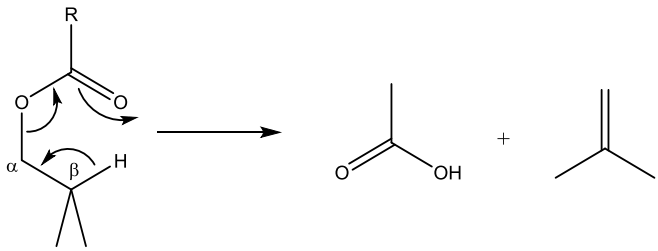

Scheme 1.14 Mechanism of pyrolytic *β*-elimination of esters

Alternatively, it also exists the possibility to introduce groups that can be eliminated by chemical reactions. This is the so called “chemical reworkability”. There are many strategies based on this principle. For instance, the introduction of olefinic unsaturation in the structure of the resins allows the cleavage of the network by oxidation of the double bonds with permanganate. If the groups introduced are carbamates, the cleavage is carried out by strong acid treatment.[57] Other examples are the use of epoxy resins with ketal

[53] E. Khosravi, O. M. Musa, *European Polymer Journal*, **2011**, *47*, 465-473.
[54] G. C. Tesoro, V. R. Sastri, *Journal of Applied Polymer Science*, **1990**, *39*, 1439-1457.
[55] S. Yang, J. S. Chen, H. Körner, T. Breiner, C. K. Ober, M. D. Poliks, *Chemistry of Materials*, **1998**, *10*, 1475-1482.
[56] L. Wang, H. Li, C. P. Wong, *Journal of Polymer Science, Part A: Polymer Chemistry*, **1999**, *37*, 2991-3001.
[57] J. R. Griffith, *Epoxy Resin Chemistry*, ACS, Washington DC, **1979**.

groups in their structure which can be hydrolyzed after acid treatment[58] or the copolymerization of epoxy resins with spirocyclic γ-bislactone obtaining thermosets that can be completely solubilized in 1M ethanolic KOH solutions.[59]

Scratch resistance

In many coatings systems, the uppermost layer is a thin coating which not only protects the underlying layers or substrate from chemical and UV degradation, but also provides protection from mechanical damage that can result in surface blemishes/scratches.[60] Excellent scratch resistance coatings are characterized by large plastic deformation, small cracks and high elastic recovery.[61]

There are two main ways to improve the scratch resistance of organic coatings: one is to optimize the polymer lacquer components, and the other is to reinforce the coating by embedding fillers into them.[62] The addition of nanosized silica and alumina particles having diameters of 10–50 nm represents an attractive alternative to conventional fillers. Because of their nanometer size and their large active surface, it can be expected that polymeric nanocomposites exhibit markedly improved properties as compared to pure polymers or conventional composites. Thus, different inorganic and organic nanopowders, such as SiO_2, Al_2O_3 or ZrO_2 have been employed yielding considerable mechanical reinforcement.[63]

Hybrid organic-inorganic nanocomposites have drawn considerable attention, in recent years, because they combine both the advantages of an organic polymer (flexibility, lightweight, good impact resistance and good processability) and inorganic materials (high mechanical strength, good chemical resistance, thermal stability and optical properties).[64] The formation of inorganic domains generated *in situ* for enhanced surface scratch resistance, seems to be a very promising approach towards new, multifunctional technical coatings.[65] The generation of nanostructures in the polymer matrix by sol-gel processes leads to a fine dispersion of the inorganic phase into the epoxy matrix which could be advantageous in front of the addition of performed inorganic nanoparticles, improving scratch characteristics.

Nowadays, the combined use of HBPs and sol-gel reactions in the preparation of nanocomposites seems to be advantageous as they can allow better interaction of the organic phase with the inorganic particles.[66,67] The multifunctional HBP structure allows to prepare silica hybrid coatings with strong increase in surface hardness and scratch resistance.

---

[58] S. L. Buchwalter, L. L. Kosbar, *Journal of Polymer Science, Part A: Polymer Chemistry*, **1996**, *34*, 249-260.
[59] X. Fernández-Francos, J. M. Salla, A. Mantecón, A. Serra, X. Ramis, *Polymer Degradation and Stability*, **2008**, *93*, 760-769.
[60] C. Seubert, K. Nietering, M. Nichols, R. Wykoff, S. Bollin, *Coatings*, **2012**, *2*, 221-234.
[61] V. Mittal, *Polymer Nanocomposite Coatings*, CRC Press, Boca Raton, **2014.**
[62] M. Sangermano, M. Messori, *Macromolecular Materials and Engineering*, **2010**, *295*, 603-612.
[63] F. Bauer, H. Ernst, U. Decker, M. Findeisen, H-J. Gläsel, H. Langguth, E. Hartmann, R. Mehnert, C. Peuker, *Macromolecular Chemistry and Physics*, **2000**, *201*, 2654-2659.
[64] J. E. Mark, C. Lee, P. A. Bianconi, *Hybrid Organic–Inorganic Composites*, vol. 585, ACS, Washington, **1995**.
[65] M. Toselli, M. Marini, P. Fabbri, M. Messori, F. Pilati, *Journal of Sol-Gel Science Technology*, **2007**, *43*, 73-83.
[66] M. Sangermano, M. Messori, M. Martin Galleco, G. Rizza, B. Voit, *Polymer*, **2009**, *50*, 5647-5652.
[67] M. Sangermano, H. El Sayed, B. Voit, *Polymer*, **2011**, *52*, 2103-2109.

1.4.1 Dendritic polymers

In the 1980s, a kind of highly branched three-dimensional macromolecules, also named dendritic polymers, was born, and gradually became one of the most interesting areas of polymer science and engineering.[68] Dendritic architecture is recognized as the main fourth class of polymer architecture after traditional types of linear, cross-linked, and chain-branched polymers that have been widely studied and industrially used.[69]

Dendritic molecules are composed of repeating units emanating from a central core. When the structure of the molecule is perfectly symmetric around the core, and adopts a spherical three-dimensional morphology, a dendrimer is formed. In contrast, the presence of some imperfections result in a hyperbranched polymers structures (HBPs). A schematic representation of dendrimers and HBPs is represented in **Figure 1.3**.

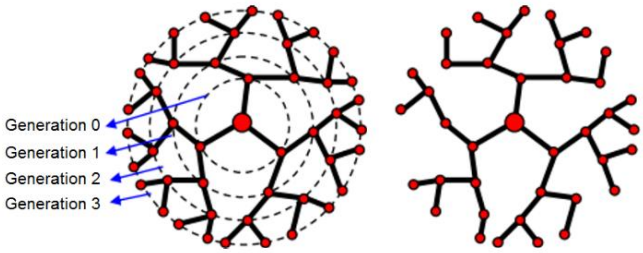

Figure 1.3 Schematic representation of a dendrimer and a hyperbranched polymer

In a perfectly branched dendrimer only one type of repeating unit can be distinguished, apart from the terminal units. However, HBPs present three different types of repeating units, named D, L and T, as illustrated in **Scheme 1.15**.

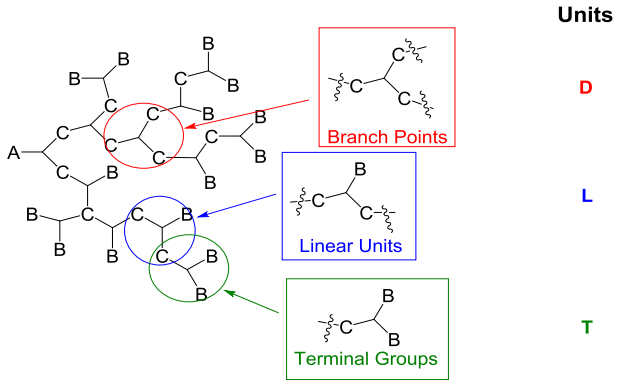

Scheme 1.15 Different units present in a HBP obtained from the polymerization of an AB_2 monomer

The degree of branching (DB) is a structural parameter used to characterize the topology of dendritic polymers and is one of the most important because it has a close

[68] J. M. J. Fréchet, D. A. Tomalia, *Dendrimers and other Dendritic Poymers*, John Wiley & Sons, Edithvale, **2001**.
[69] D. Yan, C. Gao, H. Frey, eds., *Hyperbranched Polymers. Synthesis, Properties and Applications*, 1st ed., Wiley Interscience, Hoboken, **2011**.

relationship with polymer properties such as free volume, chain entanglement, mean-square radius of gyration, glass transition temperature (T_g), degree of crystallization (DC), capability of encapsulation, mechanical strength, melting/solution viscosity, biocompatibility, and self-assembly behaviors.[70,71] Fréchet and coworkers[72] defined the DB as the ratio of the molar fraction of branched and terminal units relative to that of the total possible branching sites

$$DB = \frac{D+T}{D+T+L} \quad (1)$$

where D is the number of fully branched units and L is the number of partially reacted units. The value of the degree of branching varies from 0 for linear polymers to 1 for dendrimers or fully branched hyperbranched polymers.

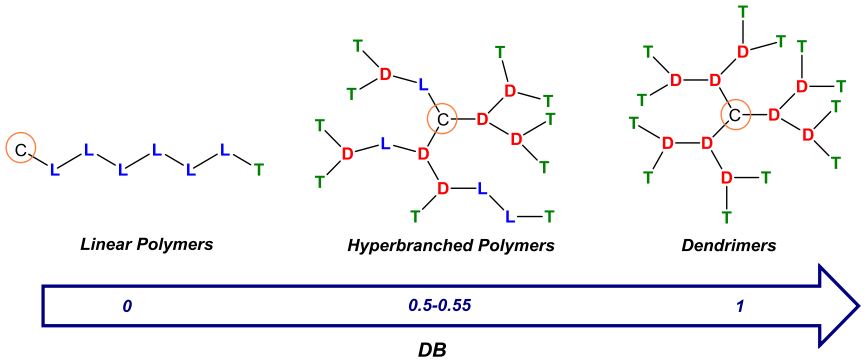

Figure 1.4 Values of the DB of linear polymers, HBPs and dendrimers

Dendritic polymers are characterized by special features that make them promising candidates for a lot of applications. One of the most interesting physical properties is their lower viscosity in comparison with their linear analogues which is a consequence of the architecture of the molecules.[73] The relationship between the molecular weight and the viscosity for various polymer topologies is represented in **Figure 1.5**. Dendrimers in solution reach a maximum of intrinsic viscosity as a function of molecular weight as their shape changes from an extended to a more compact globular structure, especially at high molecular weights.[74,75]

[70] W. Gong, Y. Mai, Y. Zhou, N. Qi, B. Wang, D. Yan, *Macromolecules*, **2005**, *38*, 9644-9649.
[71] A. Khalyavina, F. Schallausky, H. Komber, M. Al Samman, W. Radke, A. Lederer, *Macromolecules,* **2010**, *43*, 3268-3276.
[72] C. J. Hawker, R. Lee, J. M. J. Fréchet, *Journal of the American Chemical Society*, **1991**, *113*, 4583-4588.
[73] C. R. Yates, W. Hayes, *European Polymer Journal*, **2004**, *40*, 1257-1281.
[74] A. V. Lyulin, D. B. Adolf, G. R. Davies, *Macromolecules*, **2001**, *34*, 3783-3789.
[75] B. Voit, A. Lederer, *Chemical Reviews*, **2009**, *109*, 5924-5973.

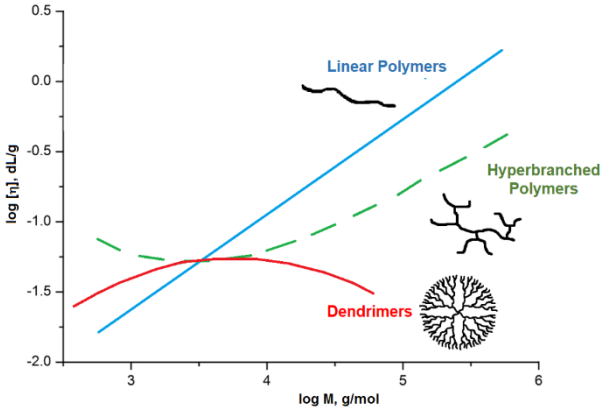

Figure 1.5 Relationship between intrinsic viscosity (η) and molecular weight (M)

Well defined structures require a step-wise synthesis and dendrimers are usually prepared by an iterative synthesis, with purification of intermediate stages or generations while hyperbranched molecules can be synthesized in one step. This characteristic and their good properties such as low viscosity, good solubility and good chemical reactivity makes HBPs suitable products for larger application scale in typical technological fields like coatings and adhesives.[76]

Hyperbranched polymers

HBPs are highly branched three-dimensional macromolecules with a large number of end groups (Figure 1.4).[77] They have special properties which are the key to their industrial applications. As it said before, one of them is low viscosity in comparison with their linear analogues.

Besides, HBPs have high chemical reactivity and enhanced solubility when compared to their linear analogues. They also exhibit enhanced compatibility with other polymers as has been demonstrated by blending studies.[73] Hyperbranched materials also have outstanding mechanical properties such as modulus, tensile strength and compressive moduli which reflect the compact highly branched structures.[73] Owing to those special properties, HBPs have been used as rheology modifiers or blend components,[44,78] toughenners for thermosets[43,45] and cross-linking or adhesive agents.[79] Also, HBPs have been used as the base for various coating resins,[80] including powder coatings,[81] flame retardant coatings[82] and barrier coatings for flexible packaging.[83]

Star polymers

Dendritic polymers with a single branch point and all arms exhibiting low degrees of compositional heterogeneity with respect to composition, molecular weight and molecular weight distribution are named stars (SPs).[84] Basically, star polymers consist of linear

[76] B. Voit, *Journal of Polymer Science, Part A: Polymer Chemistry*, **2005**, *43*, 2679-2699
[77] Y. Zheng, S. Li, Z. Weng, C. Gao, *Chemical Society Reviews*, **2015**, *44*, 4091-4130
[78] Y. H. Kim, O. W. Webster, *Macromolecules*, **1992**, *25*, 5561-5572
[79] J. H. Oh, J. Jang, S.-H. Lee, *Polymer*, **2001**, *42*, 8339-8347
[80] C. Gao, D. Yan, *Progress in Polymer Science*, **2004**, *29*, 183-275.
[81] M. Johansson, E. Malmström, A. Joansson, A. Hult, *Journal of Coatings Technology*, **2000**, *72*, 49- 54.
[82] S-W. Zhu, W-F. Shi, *Polymer Degradation and Stability*, **2002**, *75*, 543-547.
[83] J. Lange, E. Stenroos, M. Johansson, E. Malmström, *Polymer*, **2001**, *42*, 7403-7410.
[84] M. K. Mishra, S. Kobayashi, *Star and Hyperbranched Polymers*, Marcel Dekker, Inc., New York, **1999**.

polymeric chains radiating from one single branched point, called “core” or central nodule, and which can itself be polymeric. If the arms are identical, the star polymer is said to be regular. If adjacent arms are composed of different repeating subunits, the star polymer is said to be miktoarm. The copolymeric nature of the arms leads to the so named copolymeric stars (**Figure 1.6**). For the preparation of multiarm star polymers, a multifunctional core is needed. The lower cost of HBPs, the presence of reactive final groups and their easy synthesis from commercially available monomers makes them adequate cores for their synthesis.

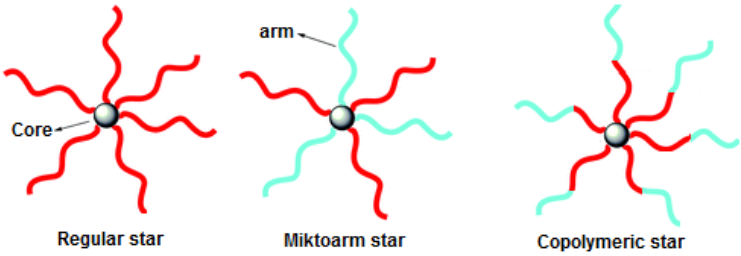

Figure 1.6 Schematic representation of star polymer structures

Star polymers resemble more closely the hard sphere model, especially when the numbers of arms in the star polymer is high. The hard sphere character of star polymer is directly correlated to the entanglement. If the number of arms is high the entanglement decreases and it is lower than in linear polymers, causing lower intrinsic viscosity of these materials as compared to linear polymers of same molecular weight, which is one of the main features of SPs.[75,85,86]

Due to their compact structures and high segment density, SPs have gained increasing interest. Nowadays, the incorporation of biocompatible segments on the star copolymers structures are of particular interest for biomedical applications.[87] Moreover, star polymers have potential applications as components of different types of complexes, hydrogels, networks, ultrathin coatings, thermoset modifiers, etc.[88-90]

1.1.5 Modified epoxy thermosets by using hyperbranched polymers and other highly branched topologies

Over the past years, hyperbranched polymers (HBPs) have received much attention as modifiers of epoxy systems to improve the mechanical properties, reduce the shrinkage on curing[51] and increase the reworkability,[31] if the structures are conveniently selected.[91,92]

[85] H. A. M. Aert, M. H. P. Genderen, E. W. Meijer, *Polymer Bulletin*, **1996**, *37*, 273-280.
[86] B. M. Erwin, M. Cloitre, M. Gauthier, D. Vlassopoulos, *Soft Matter*, **2010**, *6*, 2825-2833.
[87] W. Wu, W. Wang, J. Li, *Progress in Polymer Science*, **2015**, *46*, 55-85.
[88] J. Miao, G. Xu, L. Zhu, L. Tian, K. E. Uhrich, C. A. Avila-Orta, B. S. Hsiao, M. Utz, *Macromolecules*, **2005**, *38*, 7074-7082.
[89] K. E. Steege, J. Wang, K. E. Uhrich, E. W. Castner, *Macromolecules*, **2007**, *40*, 3739-3748
[90] M. Morell, D. Foix, A. Lederer, X. Ramis, B. Voit , A. Serra, *Journal of Polymer Science Part A: Polymer Chemistry*, **2011**, *49*, 4639-4649.
[91] L. Boogh, B. Pettersson, J-A. E. Månson, *Polymer*, **1999**, *40*, 2249-2261.
[92] R. Mezzenga, L Boogh, J-A. E. Månson, *Composites Science and Technology*, **2001**, *61*, 787-795.

One of the first HBPs used as modifier for epoxy resins was an aliphatic hyperbranched polyester based on 2,2-bis(hydroxymethyl)propionic acid (BHMPA).[93] This polymer was produced and commercialized by Perstorp as Boltorn HX (where X can be 20, 30 or 40 related with the degree of polymerization). There are several published papers on the use of Boltorn as modifier in different epoxy thermosetting systems. Ratna *et al*.[94] used Boltorn H30 as modifier in epoxy/amine thermosets. The final materials showed globular HBP particles dispersed in the epoxy matrix and the result was a significant improvement of the impact strength, approximately twice the value of the neat material, when a high concentration of HBP was used. However, Yang *et al.*[95] obtained homogeneous materials in epoxy/anhydride systems and the improvement in the impact strength was around 25% over the pure epoxy/anhydride matrix by the addition of the HBP as modifier. This could be explained by the formation of particles in the first case and a homogeneous material in the second due to the different chemistry implied in the curing process.

Different modifications of Boltorn-like polymers have been described on the field of thermosets. Varley and Tian[96] reported the use of an epoxidized Boltorn as a modifier of epoxy/anhydride systems. The addition of the HBP had a minimal effect upon the viscosity of the mixture. Furthermore, the modified materials showed excellent improvements in toughness. A 100% increase in fracture toughness was achieved by the presence of a 20%wt of HBP in the epoxy network.

Our group reported the use of HBPs as modifiers in epoxy resins and also good results were obtained, reducing some of the drawbacks commented before. The effect of the DB of the HBP in the improvement of epoxy materials cured by cationic initiator was studied.[97] In these systems, the viscosity of the formulation was lower on increasing the DB of the modifier, which confirms the advantages in the rheological behavior of HBP modified formulations. On increasing the DB the T_g was increased and the storage moduli in the rubbery state followed the same trend. The addition of the HBP to the formulation led to a reduction of the global shrinkage on the curing process, which increased with the proportion of modifier and DB. Because of the aromatic poly(ester) nature of these HBPs the thermal stability increased, but the chemical reworkability in basic solution was improved. The high thermal stability is due to the fact that aromatic ester groups cannot be broken by β-elimination processes because the absence of hydrogen in *β*-position.[31] This study put in evidence the validity of the dendritic characteristics in the improvement of epoxy thermosets.

Boltorn polyesters have also been used to control the shrinkage in the cationic polymerization of DGEBA using hydroxyl terminated hyperbranched polymers.[51] The reduction in the contraction during curing was observed because intermolecular and intramolecular H-bond interactions decreased and the free volume increased when HBP reacts and get incorporated into the network.

The large number of reactive sites present in the HBPs structure allows the possibility to change their solubility in the epoxy matrix by the attachment of polar or non-polar units

[93] A. Hult, M. Johansson, E. Malmström, *Advances in Polymer Science*, **1999**, *143*, 1-34.
[94] D. Ratna, G. P. Simon, *Polymer*, **2001**, *42*, 8833-8839.
[95] J. P. Yang, Z. K. Chen, G. Yang, S. Y. Fu, L. Ye, *Polymer*, **2008**, *49*, 3168-3175.
[96] R. J. Varley, W. Tian, *Polymer International*, **2004**, *53*, 69-77.
[97] D. Foix, A. Khalyavina, M. Morell, B. Voit, A. Lederer, X. Ramis, A. Serra, *Macromolecular Materials and Engineering*, **2012**, *297*, 85-94.

to end groups.[98] As a result, optimal shell chemistry design of the HBP could be achieved, which permits to obtain homogeneous or nano and micro structured thermosetting materials.[92] Moreover, tailoring their chemistry, can be possible to reach situable mechanical properties for inducing the most efficient toughening mechanism.[99] Flores *et. al*.[100,101] reported the use of partially modified Boltorn type polyesters and hyperbranched poly(glycidol) with 10-undecenoyl moieties as modifiers in DGEBA thermosets. The materials obtained resulted in a significant increase in impact strength, since the use of partially modified HBP led to phase-separated materials with particle sizes on the nanometric or the micrometric scale with good interaction between particles and matrix because of partial covalent bonding. Both structural facts led to a cavitation mechanism of toughness enhancement. This enhancement was possible without affecting the thermal stability, thermomechanical characteristics or processability of the formulations.

Other HBPs as poly(ester-amide) and poly(amino-ester) have been used as modifiers for epoxy resins leading to improvements in shrinkage, degradability or mechanical properties.[52,102-104] The effect of the molecular weight of different hyperbranched poly(ester-amide)s in front of the shrinkage was investigated and a progressive decrease of the global shrinkage was observed on increasing the proportion of HBP and in the higher molecular weight. [102]

Additionally to HBPs, multiarm star polymers (SPs) can also be considered as a new class of modifiers for epoxy resins. Meng *et al*.[42] obtained nanostructured diglycidylether of bisphenol A thermosets using core-crosslinked stars based on poly(styrene) core with poly(ethyleneoxide) or poly(styrene)-*b*-poly(ethyleneoxide) arms. T_gs of the epoxy thermosets containing the modifiers were clearly improved.The mechanical properties (Young modulus, impact strenght and microhardness) showed a maximum value when 10%wt of madifier was added to the formulation.

In our research team, multiarm star with poly(ε-caprolactone) (PCL) arms and different cores were used as epoxy thermoset modifiers.[90,104,105.] The addition of these polymers led to homogeneous materials with a more tough fracture while reducing the shrinkage on curing without compromising the thermomechanical properties. Multiarm star polymers with poly(styrene) and poly(methyl methacrylate) arms were also used as modifiers in epoxy systems obtaining phase separated materials or nanograined morphologies.[106,107] The impact strength was improved in the material with the highest content of modifier. Chemically reworkable epoxy coatings by addition of these star topologies were also prepared.[32] An important characteristic of these modifiers is the low viscosity of the

[98] R. Mezzenga, L Boogh, J-A. E. Månson, *Journal of Polymer Science Part B: Polymer Physics*, **2000**, *38*, 1883-1892.
[99] R. Mezzenga, L Boogh, B. Pettersson, J-A. E. Månson, *Macromolecular Symposia*, **2000**, *149*, 17-22.
[100] M. Flores, X. Fernández-Francos, F. Ferrando, X. Ramis, A. Serra, *Polymer*, **2012**, *53*, 5232-5241.
[101] M. Flores, M. Morell, X. Fernández-Francos, F. Ferrando, X. Ramis, A. Serra, *European Polymer Journal*, **2013**, *49*, 1610-1620.
[102] M. Morell, M. Erber, X. Ramis, F. Ferrando, B. Voit, A. Serra, *European Polymer Journal*, **2010**, *46*,1498-1509.
[103] M. Morell, X. Fernández-Francos, X. Ramis, A. Serra, *Macromolecular Chemistry and Physics*, **2010,** *211*, 1879-1889.
[104] M. Morell, A. Lederer, X. Ramis, B. Voit, A. Serra, *Journal of Polymer Science, Part A: Polymer Chemistry***, 2011**, *49*, 2395-2406.
[105] A. Tomuta, X. Fernández-Francos, F. Ferrando, A. Serra, X. Ramis, *Polymer-Plastics Technology and Engineering*, **2014**, *53*, 1-10.
[106] M. Morell, X. Fernández-Francos, J. Gombau, F. Ferrando, A. Lederer, X. Ramis, B. Voit, A. Serra, *Progress in Organic Coatings*, **2012**, *73*, 62-69.
[107] M. Morell, X. Ramis, F. Ferrando, A. Serra, *Macromolecular Chemistry and Physics*, **2012**, *213*, 335-343.

formulation. It could be demonstrated that on increasing the number of arms and shortening them the viscosity was lower.[108]

Miktoarm star polymers were also synthesized with a hyperbranched polyester core and poly(ethylene glycol) arms or poly(ethylene glycol)/poly(ε-caprolactone) arms.[109] The resulting materials, due to the amphiphilic character of the multiarm star, showed phase-separated morphologies with nanosized particles and a significant improvement on the impact strength. The best improvement was obtained by using the miktoarm containing poly(ethylene glycol)/poly(ε-caprolactone) arms. Due to the hydrophilic/hydrophobic character this modifier demonstrated a high self-assembly tendency, responsible of the improvement.

Taking into account that the substitution of linear thermoplastic polymers by dendritic structures as modifiers leads to an enhancement of the properties of thermosetting materials, in the present thesis we have applied this strategy to prepare epoxy coatings with improved characteristics.

1.1.6 Hyperbranched polymers and multiarm star polymers from poly(ethyleneimine)

The common terminal groups of HBPs are hydroxyl moieties. Through them, numerous functional components can be introduced into the HBP structure. However, amine terminated HBPs are also interesting and has been scarcely explored. Hyperbranched poly(ethyleneimine) (PEI) presents a high content of amino groups and is very attractive for many industrial applications.[110] One of the most important features of PEI macromolecules is their availability at industrial scale and low cost.

Nowadays, there are many companies selling HBPs which are used in many industrial applications. Among them, BASF commercializes a family of HPBs with the name of Lupasol® that consists in hyperbranched poly(ethylenimine) (PEI).[111] It should be said that firstly poly(ethyleneimine) was commercialized under the name Polymin.[112] PEI, also called polyaziridine, is a polymer with a repeating unit composed of an amino group and an ethylene spacer (**Scheme 1.16**).

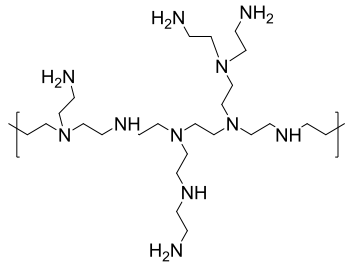

Scheme 1.16 Idealized chemical structure of poly(ethyleneimine)

[108] M. Morell, X. Ramis, F. Ferrando, A. Serra, *Polymer*, **2011**, *52*, 4694-4702
[109] C. Lagunas, X. Fernández-Francos, F.Ferrando, M. Flores, A. Serra, J. M. Morancho, J. M. Salla, X. Ramis, *Reactive and Funtional Polymers*, **2014**, *83*, 132-143.
[110] M. Krämer, J-F. Stumbé, G. Grimm, B. Kaufmann, U. Krüger, M. Weber, R. Haag, *ChemBioChem*, **2004**, *5*, 1081-1087.
[111] Available at: http://worldaccount.basf.com/wa/NAFTA~en_US/Catalog/ChemicalsNAFTA/pi/BASF/Brand/lupasol/brand_top/ accesed on 18 April 2016.
[112] D. A. Tomalia, G. R. Killat, *Encyclopedia of Polymer Science*, John Wiley & Son, New York, **1985.**

The industrial production of ethylenimine and PEI begin in Germany about 1938, when I.G. Farbenindustrie (founded as a merger of BASF, Bayer, Agfa, Hoechst, Chemische Fabrik Griesheim-Elektron and Chemische Fabrik) built and operated a plant in Ludwigshafen. In 1951, the company was split into its original constituent companies. The four largest (BASF, Bayer, Agfa and Hoechst) quickly bought the smaller ones.

Lupasol product range is extensive. Waterfree products and aqueous solutions are commercial available and applied to a huge variety of materials providing advantages and new properties. PEI was first described as an agent for producing wet-strenght papers, being usable in neutral or alkaline systems, a significant departure from the acid-requiring urea-formaldehyde resins which were extensively used. However, the use as additive in this field has been diminished, with the exception of certain special papers, by the arrival of new wet-strenght agents that can perform this function more advantageously.[113] In addition poly(ethylenimine) has been used for the preparation of cationically active papers from chromatography and electrophoresis.[114]

In the textile industry, PEI improves the dye fixation,[115] hydrophilicity[116] and flameproofing of cotton,[117] among others. Moreover, the unique properties of PEI makes its useful in many applications (plastics, metals…)[118] and can be used as flocculating agents, disinfectant, etc.[119] In coating technology, the addition of PEI makes coatings and adhesives stick better to porous and non-porous surfaces.[120] In the biomedical field, PEI has attracted an increasing interest because of its potential application in gene delivery.[121]

By modification of PEI, the application range can be further expanded. Amidation with acids, alkoxylation, alkylation and carboxylation have been done leading to PEI-modified structures used as CO_2 cells,[122,123] detectors with specific recognition elements,[124,125] drug delivery[126] or nanocarriers,[127] among others.

Recently, Appelhans *et.al.* have introduced mono- and oligosaccharide units on the PEI surface by reductive amidation or N-carboxyanhydride polymerization.[128,129] This defined

[113] Available at: http://www.innventia.com/Documents/Rapporter/STFI-Packforsk%20report%2032.pdf accessed on 18 April 2016
[114] A. Morrison, K. Murray, *Biochemical Journal*, **1974**, *141*, 321-330.
[115] Jr. Ware, D. S. Soane, D.B. Millward, M.R. Linford, US Patent 6.679.924 (to Nano Tex LLC.), 20 January **2004**.
[116] L. S. Bayer, D. Fragouli, A. Attanasio, B. Sorce, G. Bertoni, R. Bresci, R. Di Corato, T. Pellegrino, M. Kalyva, S. Sabella, P. P. Pompa, R. Cingolani, A. Athanassiou, *Applied Materials & Interfaces*, **2011**, *3*, 4024-4031.
[117] M. Andrew, M. S. Frederic, US Patent 2.472.335, 7 June **1949**.
[118] H.-G. Elias, R. Mülhaupt, *Ullmann's Polymer and Plastics: Products and Processes*, Wiley VCH, Weinheim, **2016.**
[119] A. M. Carmona-Ribeiro, L.D. Melo, *International Journal of of Moleuclar Science*, **2013**, *14*, 9906-9946.
[120] K. Bacher, K. Schmidt, G. Gardin, US Patent 20.080.199.706, 21 August **2008**.
[121] B. Abdallah, A. Hassan, C. Benoist, D. Goula, J-P. Behr, B. A. Demeneix, *Human Gene Therapy*, **1996**, *7*, 1947-1954.
[122] J. Ma, Q. Liu, D. Chen, Y. Zhou, S. Wen, *Journal of Material Science*, **2014**, *49*, 7585-7596.
[123] X. Wang, C. Song, A. M. Gaffney, R. Song, *Catalysis Today*, **2014**, 238, 95-102.
[124] Y. Shi, Z. Chen, X. Cheng, Y. Pan, H. Zhang, Z. Zhang, C-W. Li, C. Yi, *Biosensors and Bioelectronics*, **2014**, *61*, 397-403.
[125] F. Zheng, S. Guo, F. Zeng, J. Li, S. Wu, *Analytical Chemistry*, **2014**, *86*, 9873-9879.
[126] G. Lin, W. Zhu, L. Yang, J. Wu, B. Lin , Z. Cheng, C. Xia, Q. Gong, B. Song, Y. Xu, H. Ai, *Biomaterials*, **2014**, *35*, 9495-9507.
[127] Y. Chen, H. Gu, Z. Zhang, F. Li, T. Liu, W. Xia, *Biomaterials*, **2014**, *35*, 10058-10069.
[128] D. Appelhans, H. Komber, M. A. Quadir, S. Richter, S. Schwarz, J. van der Vlist, A. Aigner, M. Müller, K. Loos, J. Seidel, K-F. Arndt, R. Haag, B. Voit, *Biomacromolecules*, **2009**, *10*, 1114-1124.
[129] C. Strieglera, M. Frankea, M. Müller, S. Boye, U. Oertel, A. Janke, L. Schellkopf, B. Voit, D. Appelhans, *Polymer*, **2015**, *80*, 188–204.

novel oligosaccharide architectures on dendritic polymer surfaces have been studied as nano-sized carrier systems for gene delivery[130,131] or metal nanoparticles.[132,133]

Poly(ethyleneimine) shows high potential for the preparation of core-shell type star polymers and it has been used as macroinitiator since amines groups can react easily with many of reactive groups. Bauman *et al.*[134] grafted linear polyamide-12 into PEI by two different pathways, through transamidation of linear PA12 in the presence of PEI core or by ring opening polymerization of laurolactam.

Starting from PEI as the core, SPs have been synthesized polymerizing ε-caprolactone.[135] These polymers were used as unimolecular micellar nanocapsules for accommodating guest molecules.[121,136] Following the same methodolody, SPs containing a PEI core and poly(lactide) arms were prepared and used as nanocarriers.[137]

In our research team, PEI has been used as a curing agent of epoxy-amine system. The HBP can be incorporated into the network structure of the thermosets to improve the shape-memory behavior and an enhancement of the thermal-mechanical properties was also achieved.[138,139]

The reactivity of amino groups in the PEI structure towards acids, isocyanates, acrylates and epoxides has allowed us to prepare a series of new structures that can be used in the preparation of epoxy thermosets. The incorporation of different reactive end groups in PEI has opened the possibility to obtain thermosetting materials by different methodologies. Hybrid organic-inorganic epoxy materials could be prepared by sol-gel approach from trialkoxysilylated PEI and by using “click chemistry” different thiol reactions could be performed in addition to the epoxy curing to obtain final copolymeric materials. The possibility to growth polyester arms from PEI cores by ring opening polymerization has also been applied to prepare a family of multiarm stars that have been further used in the epoxy thermosets modification. The modification of PEI structures with terminal groups able to initiate epoxy polymerization, such as triazoles, has allowed us to study the use of these polymers as multifunctional initiators for epoxy curing.

---

[130] J. Rumschöttel, S. Kosmella, C. Prietzel, D. Appelhans, J. Koetz, *Colloids and Surfaces B: Biointerfaces*, **2016**, *138*, 78–85.
[131] S. Bekhradnia, I. Naz, R. Lund, C. Effenberg, D. Appelhans, S. A. Sande, B. Nyström, *Journal of Colloid and Interface Science*, **2015**, 458, 178–186.
[132] N. Hauptmann, M Pion, M-Á. Muñoz-Fernández, H. Komber, C. Werner, B. Voit, D. Appelhans, *Macromolecular Bioscience*, **2013**, *13*, 531-538.
[133] N. Hauptmann, M. Pion, R. Wehner, M-Á. Muñoz-Fernández, M. Schmitz, B. Voit, D. Appelhans, *Biomacromolecules,* **2014**, *15*, 957-967.
[134] F. E. Bauman, H. Haeger, O. Novikova, G. Oenbrink, R. Richter, M. Finke, *Journal of Applied Polymer Science*, **2004**, *96*, 2413-2422.
[135] X. Cao, Z. Li, X. Song, X. Cui, P. Cao, H. Liu, F. Chen, Y. Chen, *European Polymer Journal*, **2008**, *44*, 1060-1070.
[136] H. Liu, Z. Shen, S-E. Stiriba, Y. Chen, W. Zhang, L. Wei, *Journal of Polymer Science, Part A: Polymer Chemistry*, **2006,** 44, 4165–4173.
[137] M. Adeli, R. Haag, *Journal of Polymer Science, Part A: Polymer Chemistry*, **2006**, *44*, 5740–5749.
[138] D. Santiago, X. Fernández-Francos, X. Ramis, J. M. Salla, M. Sangermano, *Thermochimica Acta*, **2011**, *526*, 9-21.
[139] D. Santiago, X. Fernández-Francos, F. Ferrando, S. de la Flor, *Journal of Polymer Science, Part B: Polymer Physics,* **2015**, *53,* 924-933.

1.2 Scope and objectives

The global objective of this Doctoral Thesis is to improve the properties of epoxy thermosets and to develop new curing processes by the addition of different dendritic structures previously synthesized from hyperbranched poly(ethyleneimine).

The specific objectives can be summarized as follows:

- To synthesize 10-undecenoyl terminated poly(ethyleneimine) with different degrees of modification and study their effect as modifiers in the curing process of an epoxy resin using anhydrides as curing agents and in the properties of the final materials.
- To synthesize multiarm stars from poly(ethyleneimine)s as the core and poly(ε-caprolactone) and poly(lactide) arms and the improvement in the characteristics of the epoxy thermosets achieved by adding these dendritic structures using tertiary amines or anhydrides as curing agents.
- To prepare new hybrid organic-inorganic epoxy coatings by sol-gel methodology, using ethoxysilylated poly(ethyleneimine) as inorganic precursor to determine the improvement in scratch resistance of anionically cured epoxy resins.
- To explore the use of an allyl- and a propargyl-terminated poly(ethyleneimine) to develop a new two-stage photoinitiated/thermal dual curing system based on thiol-ene or thiol-yne/thiol-epoxy click reactions.
- To develop a new multifunctional triazole initiator for anionic curing of diglycidylic resins prepared from allyl-terminated poly(ethyleneimine).

UNIVERSITAT ROVIRA I VIRGILI
HYPERBRANCHED POLY(ETHYLENEIMINE) DERIVATIVES AS MODIFIERS IN EPOXY NETWORKS
Cristina Acebo Gorostiza

UNIVERSITAT ROVIRA I VIRGILI
HYPERBRANCHED POLY(ETHYLENEIMINE) DERIVATIVES AS MODIFIERS IN EPOXY NETWORKS
Cristina Acebo Gorostiza

2. Analysis techniques

UNIVERSITAT ROVIRA I VIRGILI
HYPERBRANCHED POLY(ETHYLENEIMINE) DERIVATIVES AS MODIFIERS IN EPOXY NETWORKS
Cristina Acebo Gorostiza

2.1 Nuclear magnetic resonance (NMR)

Nuclear Magnetic Resonance (NMR) spectroscopy is an analytical chemistry technique used for determining the content and purity of a sample as well as its molecular structure. The principle behind NMR is that many nuclei have spin and all nuclei are electrically charged. If an external magnetic field is applied, an energy transfer is possible between the base energy to a higher energy level. The energy transfer takes place at a wavelength that corresponds to radio frequencies and when the spin returns to its base level, energy is emitted at the same frequency. The signal that matches this transfer is measured and processed in order to yield an NMR spectrum.

For ^{1}H NMR and ^{13}C-NMR mesurments, A Varian Mercury VX400 spectrometer and a Varian NMR System 400 spectrometer were used in order to elucidate and confirm the chemical structures of the synthesized polymers (**Figure 2.1**). Mainly two deuterated solvents were used, *i.e.* $CDCl_3$ and DMSO-d_6. In 1H-NMR measurements at 400 MHz of magnetic field, 1 s of delay time (D1) and 14 accumulations as experimental conditions in order to obtain quantitative measurements were used. For ^{13}C-NMR measurements at 100.6 MHz magnetic field, a D1 of 0.5 s, 0.2 s acquisition time as experimental conditions were used.

Figure 2.1. Picture of the NMR devices used for the structural identification of the polymers synthesized

Solid NMR

Solid-state NMR (SSNMR) spectroscopy is a kind of nuclear magnetic resonance (NMR) spectroscopy, characterized by the presence of anisotropic (directionally dependent) interactions. Solid-state NMR spectroscopy serves as an analysis tool in organic and inorganic chemistry. Objects of SSNMR studies in materials science are inorganic/organic aggregates in crystalline and amorphous states, composite materials, heterogeneous systems including liquid or gas components, suspensions, and molecular aggregates with dimensions on the nanoscale, where different nuclei can be used as NMR probes.[1]

^{29}Si NMR mesurements were recorded on a Bruker Advance III 400 MHz at a frequency of 79.4950 MHz on a ceramic probe CP/ MAS of 4 mm. NMR spectra were obtained from

[1] L. J. Mathias, *Solid State NMR of Polymers*, Springer Science+Business Media, Toronto, **1988**.

40,000 scans using the following parameters: rotor spin rate 10,000 Hz, recycling time 5 s, contact time 2.0 ms and acquisition time 18.4 ms.

2.2 Size exclusion chromatography (SEC)

SEC, which is also well known under the name *gel permeation chromatography* (GPC), represents one of the most important methods of polymer analysis that is widely used for polymer characterization and understanding and predicting polymer performance. Gel permeation chromatography is conducted almost exclusively in chromatography columns. Samples are dissolved in an appropriate solvent and the separation of multi-component mixtures take place in the column. The constant supply of fresh eluent to the column is accomplished by the use of a pump. Since most analytes are not visible to the naked eye a detector is needed. Often multiple detectors are used to gain additional information about the polymer sample. The availability of a detector makes the fractionation convenient and accurate.[2] SEC analyses were carried out with two different equipments:

An Agilent 1200 series system (**Figure 2.2**) with PLgel 3 µm MIXED-E, PLgel 5 µm MIXED-D and PLgel 20 µm MIXED-A columns in series, and equipped with an Agilent 1100 series refractive-index detector. Calibration curves were based in polystyrene standards having low polydispersities. THF was used as the eluent at a flow rate of 1.0 mL/min, the sample concentrations were 5-10 mg/mL, and injection volumes of 100µL were used. With this technique it is possible to determine the molecular weight ($\overline{M}_n$, $\overline{M}_w$) of the synthesized HBPs as well as the molecular weight dispersity ($Đ_M$), by comparing the retention time of a diluted solution of the sample with the solution of standards, which are polymers with different molecular weight and narrow distributions.

Figure 2.2 GPC chromatograph used for the molecular weight determination

In the Leibniz-Institut für Polymerforschung (IPF) in Dresden, an Agilent 1200 pump system (US) equipped with a multi-angle light scattering (MALS) detector (Tristar MiniDawn, Wyatt Technology, DE) and refractive index (RI) detector (Knauer, DE) using LiCl(3g/L)-DMAc as an eluent in a PolarGel-M-column (Polymer Laboratories, UK) was used. An important advantage of the use of MALS detector is that the molecular weight of the sample is calculated directly from the intensity measured and the sample concentration and it eliminates the necessity to calibrate the equippment.

[2] S. Podzimek, *Light Scattering, Size Exculsion Chromatography and Asymmetric Flow Field Flow Fractionation*, John Wiley & Sons, Hoboken, **2011**.

2.3 Differential scanning calorimetry (DSC)

Differential scanning calorimetry (DSC) is the most popular thermal analysis technique. It is a technique in which the heat flow rate difference into a substance and a reference is measured as a function of temperature or time, while the sample is subjected to a controlled temperature program. Among the applications of DSC must be mentioned the easy and fast determination of the glass transition temperature the heat capacity jump at the glass transition, melting and crystallization temperatures, heat of fusion, heat of reactions, very fast purity determination, fast heat capacity measurements, characterization of thermosets, and measurements of liquid crystal transitions.[3]

For our propose a Mettler DSC821e equipped with a robotic arm TSO801RO was used to perform DSC analysis from room temperature to high temperatures. To perform tests under room temperature a Mettler DSC822e cooled with liquid nitrogen was used. Both calorimeters were calibrated using an indium standard (heat flow calibration) and an indium-lead-zinc standard (temperature calibration). Samples of 5 to 10 mg of weight were placed in covered aluminum pans to perform analysis. **Figure 2.3** shows the.calorimeters used.

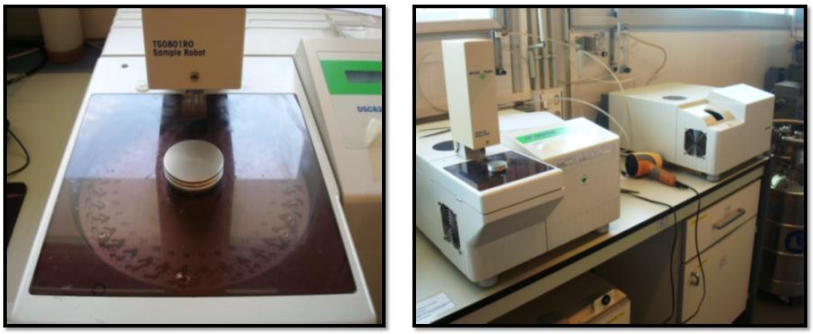

Figure 2.3 Pictures of the calorimeters and the robot used to study thermal curing systems

Curing kinetics

Cure kinetics is the mathematical relationship between time, temperature, curing rate and conversion. The kinetic study using DSC asumes that the heat released during the reaction is proportional to the conversion degree.[3] Additionally, the curing rate (*dx/dt*) is directly related to this released heat (*dH/dt*). When the reaction is completed, the integral related to the signal obtained yields the total released heat ΔH_{tot}. Reaction rate and conversion degree can be calculated with the following expression:

$$\frac{dx}{dt} = \frac{dH/dt}{\Delta H_{tot}} = \frac{dh/dt}{\Delta h_{tot}} \quad (2.1)$$

$$x = \frac{\Delta H_t}{\Delta H_{tot}} = \frac{\Delta h_t}{\Delta h_{tot}} \quad (2.2)$$

where *dh/dt* and Δh_{tot} are the heat releasing rate and the total heat released normalized in respect to the sample size, ΔH_t is the heat released up to a time *t*, and Δh_t is the heat

[3] A. Turi, *Thermal Characterization of Polymeric Materials,* 2nd edition, Academic Press, San Diego, **1997.**

released normalized in respect to the sample size. Finally *x* is the degree of curing, and can also be expressed as *α*.

The kinetics of a system can be studied in either isothermal or dynamic conditions. The dynamic experiments were preferred since they present some advantages when compared with isothermal experiments, being the most important fact using isothermal conditions the losing of information at the beginning of the curing process and, in another hand, the curing is not always completed.[3]

The reaction rate is usually expressed as $dx/dt = k\,f(x)$ being *k* the kinetic constant and *f(x)* a function depending on the conversion. The kinetic constant, *k*, usually follows the Arrhenius expression:

$$k = Ae^{\frac{-E}{RT}} \tag{2.3}$$

where *A* is the pre-exponential factor, *E* the activation energy, *R* the gas constant and *T* the absolute temperature.

In general, a kinetic process is well characterized if one knows *E*, *A* and *f(x)*, the so called kinetic triplet. Although strictly speaking this methodology should only be valid for "single-step" processes it can also be applied in systems where more than one chemical (or physical) process coexists. There are two main approaches in the kinetic analysis, isoconversional methods and model-fitting methods. In the present thesis only isoconversional kinetic analysis has been used.

The isoconversional methodology assumes that the reaction function *f(x)* is independent of the heating rate *β*.[4] On that way, the kinetics of a process only depends on the degree of conversion at a certain time. It also requires the performance of series of experiments to determine the apparent activation energy. Those experiments can be, for example, dynamic DSC curing at different heating rates.

Glass transition temperature (T_g)

The glass transition temperature is usually reported as the temperature at the half-height of the heat capacity increase (*½ΔCp* see **Figure. 2.4**). T_g can also be taken as the inflexion point, which is slightly different and corresponds to the peak on the derivative of the heat flow or heat capacity against temperature.

In order to determine the T_g of the cured materials as well as the T_g of the synthesized hyperbranched polymers DSC experiments were performed in dynamic conditions at 10 ºC/min.

[4] S. Vyazovkin, C. A. Wight, *Thermochimica Acta*, **1999**, *340-341*, 53-68.

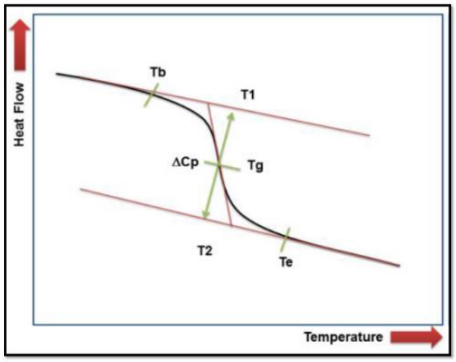

Figure 2.4 Determination of glass transition temperature in a heating experiment from an idealized DSC curve (endotherm down). *Tb*: beginning of deviation of DSC curve from linearity; *T1*: extrapolated onset temperature of T_g; T_g: glass transition temperature; *T2*: extrapolated end temperature of glass transition; *Te*: end temperature of T_g where *Cp's* dependence becomes linear again

2.4 Photo-calorimetry (photo-DSC)

The DSC-Photocalorimetry allows enthalpy changes in a material to be measured during and after exposure to light of certain wavelengths for different periods of time at different temperatures.

Photo-calorimetric experiments were performed in a Mettler DSC821e modified to irradiate the samples with a UV Hamamatsu LC5 with a double beam Hg-Xe lamp that irradiates both the sample and the reference pans simultaneously (**Figure 2.5**). The furnace of the calorimeter is covered with a silver top with two quartz windows to collimate the light beam.

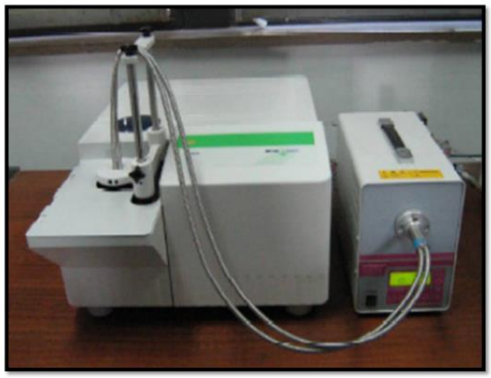

Figure 2.5 Photo-calorimeter used to perform photo-DSC experiments

The curing conversion can be determined directly from the photo-DSC curve using equation 2.2, or from the remaining heat released in a dynamic postcuring experiment as follows:

$$x = 1 - \frac{\Delta h_{post}}{\Delta h_{theor}} \tag{2.4}$$

where Δh_{post} is the heat released in the postcuring scan and Δh_{theor} is a reference value of the heat released in a complete curing.

2.5 Fourier-transformed infrared spectroscopy (FT-IR)

In infrared spectroscopy, IR radiation is passed through the sample, some is absorbed by the sample and some passes through, obtaining the absorption and transmission spectrum. IR spectroscopy has been the workhorse technique for materials analysis; an IR spectrum represents a fingerprint of a sample. The term Fourier transform is related from the fact that a mathematical process (Fourier transform) is required to convert the raw data into the FT-IR spectrum.[5] The principle which allows following the curing reaction using FT-IR measurements is the Lambert-Beer law, which is as follows:

$$A = \varepsilon \cdot C \cdot L \tag{2.5}$$

where *A* is the absorbance of a specie at a certain frequency, *ε* is the absortivity coefficient, *C* is the concentration and *L* is the optical pathway.

Since the absorbance is proportional to the concentration of different functional groups, identifying a band of a reactive group, it would be possible to follow the reaction. As an example, if a band of a functional group which reacts during the curing process is identified, and therefore disappears, it is possible to follow the curing process.

Due to the fact that absorbance is proportional to the optical pathway, *L*, it is necessary to normalize the target band in respect to a reference band that remains unaltered during the curing process. On that way the conversion *x*, determined by FT-IR measurements can be written as follows:

$$x = 1 - \frac{A\prime_t}{A\prime_0} \tag{2.6}$$

where $A\prime_t$ is the normalized absorbance at a certain time and $A\prime_0$ is the initial.

Two different FT-IR devices were used. FTIR spectrometer Bruker Vertex 70 with an attenuated total reflection accessory with thermal control and a diamond crystal (Golden Gate Heated Single Reflection Diamond ATR, Specac-Teknokroma; and FTIR-680PLUS spectrophotometer from JASCO with a resolution of 4 cm^{-1} in the absorbance mode, equipped with an attenuated total reflection accessory (ATR) with thermal control and a diamond crystal (Golden Gate heated single-reflection diamond ATR from Specac-Teknokroma) was used. Both devices are shown in **Figure 2.6**.

Figure 2.6 FT-IR devices used

[5] P. R. Griffiths, J. A. de Haseth, *Fourier Transform Infrared Spectrometry*, John Wiley & Sons, Hoboken, **2006.**

2.6 Dynamic mechanical thermal analysis (DMTA)

Dynamic mechanical thermal analysis involves imposing a small cyclic strain on a sample and measuring stress response, or equivalently, imposing a cyclic stress on a sample and measuring the resultant strain response. DMTA is used both to study molecules relaxation processes in polymers and to determine inherent mechanical or flow properties as a function of time and temperature.[6] In others words, DMTA studies the viscoelastic nature of a material by applying an oscillatory stress with a fixed frequency to the sample and monitoring its response at different temperatures. Likewise, the complex modulus (E^*) and the loss factor (tan δ) can be calculated. The modulus contains real and imaginary contributions ($E^*=E'+i\cdot E''$). The real part, E', is the elastic response measure of the material, whereas imaginary part, E'', is the viscous response. The maximum obtained on tan δ curve is, in most cases accepted as, the T of a material although it changes with the frequency used in the experiment.

Young Modulus also can be calculated by DMTA. Using three point bending assembly the Young modulus in a non-destructive flexural test at room temperature can be obtained. The modulus of elasticity is calculated using the slope of the load deflection curve in accordance with Eq. (2.7).

$$E_f = \frac{L^3 m}{4bd^3} \tag{2.7}$$

where, E_f is flexural modulus of elasticity (MPa); L is support span (mm); b is width of test beam (mm); d is depth of tested beam (mm); and m is the gradient (i.e., slope) of the initial straight-line portion of the load deflection curve (N/mm).

For this thesis a TA Instruments DMA Q800 (**Figure 2.7**) was used to carry out most of the analyses, either in three point bending mode or in single cantilever bending on prismatic rectangular samples previously cured isothermally in a mold.

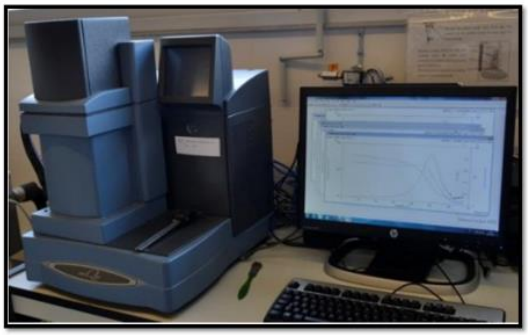

Figure 2.7 DMTA equipment used to study the viscoelastic properties

2.7 Thermal mechanical analysis (TMA)

Thermomechanical analysis (TMA) measures changes in sample length or volume as a function of temperature or time under load at atmospheric pressure. The most important TMA measurements include determination of the coefficient of linear thermal expansion

[6] R. P. Chartoff, J. D. Menczel, S. H. Dillman, *Thermal Analysis of Polymers*, John Wiley & Sons**,** Hoboken**, 2008**, chapter 5.

(CTE) and the glass transition temperature, T_g. However, several other measurements can be made by applying special modes and various attachments. These include stress relaxation, creep tensile properties of films and fibers, flexural properties and volume dilatometry.[7]

For our studies, a Mettler TMA/SDTA840 (**Figure 2.8**), were used to evaluate the thermal expansion coefficient (CTE) of cured samples.

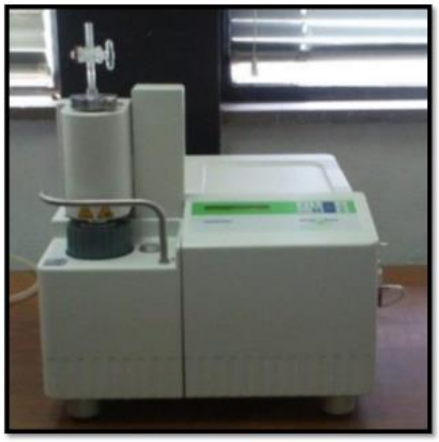

Figure 2.8 TMA apparatus used to perform thermomechanical analysis

For the determination of CTEs, prismatic rectangular samples (ca. 5 x 5 x 2.5 mm) were sandwiched between two silica discs and heated at 10ºC/min from 30 up to 150ºC for a first scan, followed by a second scan at 5ºC/min up to 180ºC. Constant force of 0.02 N was applied on the samples. The coefficients of thermal expansion α_g and α_r, below and above the T_g, respectively (**Figure 2.9**), were obtained from the second scan at 5ºC/min and calculated as follows:

$$\alpha = \frac{1}{L_0} \cdot \frac{dL}{dT} \tag{2.8}$$

where L and L_0 are the thickness at any temperature and at room temperature, respectively. The T_g was determined from the first derivative of the expansion curves L/L_0 as the half-way point in the increase of expansion coefficient step upon relaxation of the network.

[7] H. E. Bair, A. E. Akinay, J. D. Menczel, R. B. Prime, M. Jaffe, *Thermal Analysis of Polymers,* John Wiley & Sons, Hoboken, **2008**, chapter 4

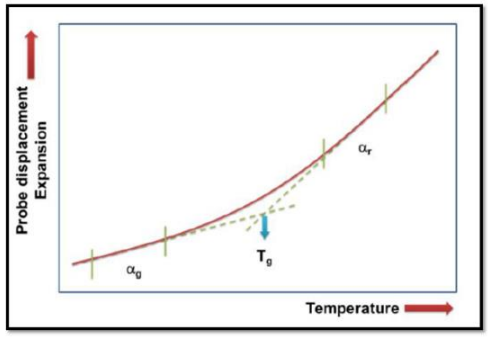

Figure 2.9 A typical TMA experiment of a cured epoxy thermoset (probe displacement is proportional to expansion) for determination of T_g; symbols α_g and α_r represent glassy and rubbery CTEs, respectively.[8]

2.8 Thermogravimetry (TGA)

Thermogravimetric analysis (TGA) is a technique where the mass of a polymer is measured as a function of temperature or time while the sample is subjected to a controlled temperature program in a controlled atmosphere.[9] The heart of the TGA is the thermobalance, which is capable of measuring the sample mass as a function of temperature and time while a purge gas flowing through the balance creates an atmosphere that can be inert, oxidizing or reducing. The moisture content of the purge gas can vary from dry to saturated.[10]

A thermobalance Mettler TGA/SDTA 851e (**Figure 2.10**) was used to analyze the thermal degradation of cured samples and of the synthesized hyperbranched polymers. The degradation was carried out in dynamic conditions, at 10 ºC/min under nitrogen or air, from 30 to 800 ºC. The most important parameters extracted from the analysis of such curves are the initial degradation temperature, the temperature of the maximum degradation rate and the char yield.

Figure 2.10 Thermobalance used for the thermal stability evaluation

[8] E. A. Turi, Y. P. Khanna, T. J. Taylor, *A guide to Materials Characterization and Chemical Analysis*, J. B. Sibilia, VCH, New York, **1988**, chapter 9.
[9] C. M. Earnest, *Compositional Analysis by Thermogravimetry*, ASTM, Philadelphia, **1988**.
[10] R. B. Prime, H. E. Bair, S. Vyazovkin, P. K. Gallagher, A. Riga, *Thermal Analysis of Polymers*, John Wiley & Sons, Hoboken, **2008**, chapter 3

2.9 Rheology

Rheology is the science of deformation and flow of materials. Actually, all materials do flow, given sufficient time. In very short processing times, the polymer may behave as a solid, while in long processing times the material may behave as a fluid. This dual nature (fluid-solid) is referred to as viscoelastic behavior.[11]

Viscosity is one of the most important flow properties to be measured by rheometry, and is the resistance to flow. Strictly speaking, it is the resistance to shearing and it can be defined as the ratio of the imposed shear stress and the shear rate. In this way, rheological measurements are based on monitoring the tension generated in the sample as a response to the application of an oscillatory shear force.[11]

The viscoelasticity of a given polymer reflects in the difference in the applied and measured angle δ. Likewise, the complex viscosity (η^*) is determined in multi-frequency experiments at a certain temperature and amplitude. This amplitude must be comprised within the range of linear viscoelasticity.

Physical transitions during the formation of polymeric networks

During the curing process of a thermoset there are two main physical transitions that can take place: gelation and vitrification. Gelation involves an abrupt change from a liquid-like to a solid like-behaviour. This transition occurs when the molar mass of the system becomes infinite, in other words, there is an only giant molecule.[12] At this moment, the material loses its ability to flow and is no longer processable above the gel point. From the applicability point of view, it is very important to know the gelation since defines the upper limit of the work life of the mixture. Vitrification is characterized by the conversion at which the polymer begins to show the typical properties of a glass and its glass transition temperature (T_g) is the same than the temperature of curing.[12]

The gel time is determined in isothermal experiments where the oscillation amplitude changes to adjust to the changes in the material. The point at which tan δ is independent of the frequency is defined as the gel point (**Figure 2.11**).[12] By stopping the experiment at that point and performing a DSC scan to determine the remaining heat it is possible to determine the conversion at gelation.

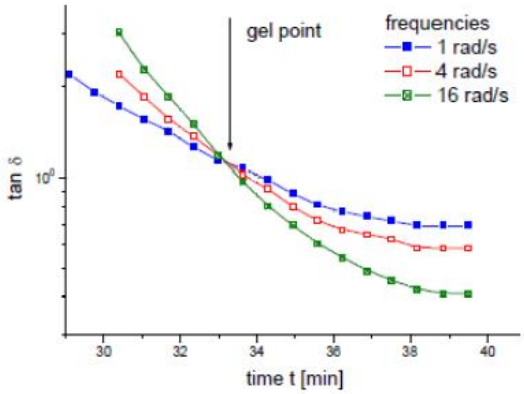

Figure 2.11 Example of gel time determination in a multifrequency experiment

[11] A.Y. Malkin, A.I. Isayev, *Rheology: Concepts, Methods & Applications*, ChemTec, Toronto, **2006.**
[12] J.P. Pascault, H. Sautereau, J. Verdu, R.J.J. Williams, *Rheological and Dielectric Monitoring of Network formation* in *Thermosetting Polymers*, Marcel Dekker, New York, **2002**.

Rheological measurements were carried out in the parallel plates (geometry of 25 mm) mode with an ARG2 rheometer (TA Instruments, **Figure 2.12**), equipped with a Peltier system for controlling the temperature. Curable formulations are placed between two aluminum plates with a distance between plates (gap) of approximately 1000 μm. By rheology it was possible to study the gel time, the conversion at the gel point, as well as determining the viscosity of uncured formulations.

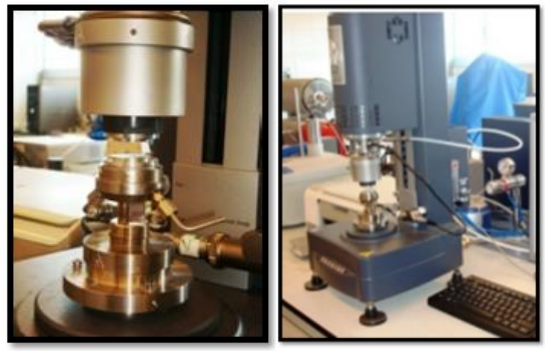

Figure 2.12 Rheometer ARG2 used, with a magnification of the geometry used

2.10 Scanning electron microscopy (SEM)

The scanning electron microscope (SEM) enables the investigation of specimens with a resolution down to the nanometer scale. Here an electron beam is generated by an electron cathode and the electromagnetic lenses of the column and finally swept across the surface of a sample. The main signals which are generated by the interaction of the primary electrons (PE) of the electron beam and the specimen´s bulk are secondary electrons (SE) and backscattered electrons (BSE) and furthermore X rays. The SE come from a small layer on the surface and yields the best resolution, which can be realized with a scanning electron microscope. The electrons interact with the atoms that make up the sample producing signals that contain information about the sample's surface topography, composition, and other properties such as electrical conductivity.[13]

A Jeol JSM 6400 with 3.5 nm resolution as a SEM was used (**Figure 2.13**). For standard analysis, samples were coated with gold.

Figure 2.13 SEM equipment used for obtaining surface images

[13] J. Goldstein, D. E. Newbury, D. C. Joy, C. E. Lyman, P. Echlin, E. Lifshin, L. Sawyer, J. R. Michael, *Scanning Electron Microscopy and X-ray Microanalysis*, Springer, New York, **2007**.

2.11 Transmission electron microscopy (TEM)

The transmission electron microscope (TEM) operates on the same basic principles as the light microscope but uses electrons instead of light. TEMs use electrons as "light source" and their much lower wavelengths make it possible to get a resolution a thousand times better than with a light microscope. The source at the top of the microscope emits the electrons that travel through vacuum in the column of the microscope. Instead of glass lenses, the TEM uses electromagnetic lenses to focus the electrons into a very thin beam. The electron beam then travels through the specimen. At the bottom of the microscope the unscattered electrons hit a fluorescent screen, which gives rise to a "shadow image" of the specimen with their different parts displayed in varied darkness according to their density.[14]

A Jeol 1011 microscope (**Figure 2.14**) was used to perform TEM images. Samples were prepared either cutting thin films with an ultramicrotome at room temperature (cured thermosets) or by deposition of diluted solutions of the samples onto support grids (hyperbranched polymers).

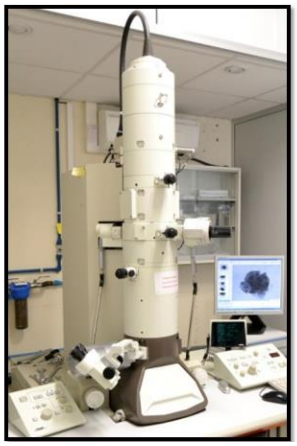

Figure 2.14 TEM equipment used to observe the morphology of the thermosets prepared

2.12 Impact test (Izod test)

Impact tests are designed to measure the resistance to failure of a material to a suddenly applied force such as collision, falling object or instantaneous blow. The test measures the impact energy, or the energy absorbed prior to fracture. The Izod test has become the standard testing procedure for comparing the impact resistances of plastics. The Izod test is most commonly used to evaluate the relative toughness or impact resistance of materials. The Izod test involves striking a test piece mounted at the end of a pendulum. The striker swings downwards impacting the test piece at the bottom of its swing.[15]

A Zwick 5110 impact tester to perform impact test at room temperature was used (**Figure 2.15**). Impact test were carried out according to ASTM D4508-10 (2010) where

[14] R. F. Egerton, *Physical Principles of Electron Microscopy*, Springer, Edmonton, **2011**.
[15] R. Brown, *Handbook of Polymer Testing - Short-Term Mechanical Tests*, Rapra Technology, United Kingdom, **2002**.

prismatic rectangular specimens were used. Adjustable pendulum at different kinetic energy was used. Afterwards, in order to correlate the energy value obtained with the impact surface morphology, the broken samples were observed by means of SEM.

Figure 2.15 Impact testing machine used for the determination of the impact strength

The impact strength (IS) is calculated using the following equation:

$$IS = \frac{E}{A} \tag{2.9}$$

where, *A* is the sample area (width (a) x thickness(b)), *E* are the energy of the pendulum after impact, respectively. *E* can be calculated as follow:

$$E = \frac{\%_{lost} \times E_p}{100} \tag{2.10}$$

being E_p the energy of pendulum before impact, %lost the difference between the measure (X) and the zero value related to the pendulum P_0 as the following equation shows:

$$\%_{lost} = X - P_0 \tag{2.11}$$

Finally, bringing everything together the impact strenght can be calculated as follow:

$$IS = \frac{(X - P_0) \times E_P}{100 \times a \times b} \left[\frac{J}{mm^2}\right] \tag{2.12}$$

2.13 Microhardness (Knoop)

A microhardness test is a mechanical hardness test used particularly for very brittle materials where only a small indentation may be made for testing purposes. Here, a pyramidal diamond point is pressed into the polished surface of the test material with a known force for a specified time. Thereby, the length of the long diagonal produced by the indentation of a rhomboidal tip can be related with the hardness of the material. Moreover, the length is directly related to the hardness of the material, so the shorter the diagonal the hardest the material.[15]

Following the ASTM D1474-98(2002) standard procedure and using a Wilson Wolpert (MicroKnoop 401MAV) the microhardness measurements were carried out (**Figure 2.16**). For each material at least 10 measurements were made with a confidence level of 95%. The Knoop microhardness (*HKN*) was calculated following:

$$HKN = \frac{L}{A_p} = \frac{L}{I^2 \times C_p} \tag{2.13}$$

where, L is the load applied to the indenter (0.025 Kg), Ap is the projected area of indentation in mm2, l is the measured length of the long diagonal of indentation in mm, C_p is the indenter constant (7.028 x 10-2) relating l^2 to A_p.

Figure 2.16 Microhardness tester used

UNIVERSITAT ROVIRA I VIRGILI
HYPERBRANCHED POLY(ETHYLENEIMINE) DERIVATIVES AS MODIFIERS IN EPOXY NETWORKS
Cristina Acebo Gorostiza

UNIVERSITAT ROVIRA I VIRGILI
HYPERBRANCHED POLY(ETHYLENEIMINE) DERIVATIVES AS MODIFIERS IN EPOXY NETWORKS
Cristina Acebo Gorostiza

3. Modification of hyperbranched poly(ethyleneimine) with long alkyl chains and its use as modifier in epoxy thermosets

UNIVERSITAT ROVIRA I VIRGILI
HYPERBRANCHED POLY(ETHYLENEIMINE) DERIVATIVES AS MODIFIERS IN EPOXY NETWORKS
Cristina Acebo Gorostiza

3.1 Introduction

The toughness of the epoxy thermosets is an important characteristic in many applications and many efforts have been done until now in order to improve it. The addition of conventional toughening modifiers such as rubbers and high performance thermoplastics is the main strategy followed by several authors.[1,2] However, these additives compromise the modulus and the thermomechanical characteristics of the thermosets (see Section 1.5), which restrict their range of application. In order to overcome these limitations, HBPs have been proposed as reactive modifiers leading to a significant improvement of this property without negatively affecting the thermomechanical characteristics.[3]

In our group, the modification of different epoxy systems using commercially available HBPs has been reported.[4-7] An increase in impact strength was achieved without sacrificing thermal and thermomechanical properties. The enhancement of the toughness could be explained by the flexible structures from the HBPs which increase the capability of the epoxy matrix to undergo plastic deformation. The high density of hydroxylic groups that can react with some curing agents allows the covalent linkage of the HBP to the epoxy matrix resulting in homogenous materials.

Poly(ethyleneimine) could be considered as an alternative to hyperbranched polyesters for the modification of DGEBA since the presence of a high content of amines can increase the compatibility between the HBP and the epoxy matrix. Santiago *et al.* reported the use of hyperbranched poly(ethyleneimines) as curing agent and studied in detail the curing kinetics in comparison with a linear aliphatic triamine.[8] As well, as epoxy modifier, the effect of the molecular weight of the PEI on the thermal, dynamomechanical and mechanical properties of 1-methyl imidazole/epoxy based materials was examined.[9] Recently, taking into account the results obtained using the PEI as a crosslinking agent, the shape-memory behavior has been studied.[10] High values of shape-recovery rate were achieved depending on the crosslinking density. However, amines are very reactive at room temperature with epoxy resins which lead to a short pot-life. Therefore, the reduction of the amino reactive groups in the structure is sometimes needed. The easy modification of the amino reactive groups allows to obtain PEI modified polymers with many different groups in order to make them suitable for different applications.

It is known that the impact resistance is determined by the morphology formed during the curing process. The addition of a modifier that can undergo phase separation during curing is an alternative approach for toughening thermoset polymers.[11] An important method to produce phase separated thermosets is the chemical induced phase separation

---

[1] K. Mimura, H. Ito, H. Fujioka, *Polymer*, **2000**, *41*, 4451-4459.
[2] N. Chikhi, S. Fellahi, M. Bakar, *European Polymer Journal*, **2002**, *38*, 251-264.
[3] F. Däbritz, B. Voit, M. Naguib, M. Sangermano, *Polymer*, **2011**, *52*, 5723-5731.
[4] D. Foix, Y. Yu, A. Serra, X. Ramis, J.M. Salla, *European Polymer Journal*, **2009**, *45*, 1454-1466.
[5] D. Foix, X. Fernández-Francos, J.M. Salla, A. Serra, J.M. Morancho, X. Ramis, *Polymer International*, **2011**, *60*, 389-397.
[6] M. Morell, X. Ramis, F. Ferrando, Y. Yu, A. Serra, *Polymer*, **2009**, *50*, 5374-5383.
[7] M. Morell, M. Erber, X. Ramis, F. Ferrando, B. Voit, A. Serra, *European Polymer Journal*, **2010**, *46*, 1498-1509.
[8] D. Santiago, X. Fernández-Francos, X. Ramis, J. M. Salla, M. Sangermano, *Thermochimica Acta*, **2011**, *526*, 9-21.
[9] X. Fernández-Francos, D. Santiago, F. Ferrando, X. Ramis, J. M. Salla, A. Serra, M. Sangermano, *Journal of Polymer Science, Part B: Polymer Physics*, **2012**, *50*, 1489-1503.
[10] D. Santiago, X. Fernández-Francos, F. Ferrando, S. de la Flor, *Journal of Polymer Science, Part B: Polymer Physics,* **2015***, 53,* 924-933*.*
[11] S. K. Siddhamalli, T. Kyu, *Journal of Applied Polymer Science*, **2000**, *77*, 1257-1268.

methodology (CIPS). CIPS generally proceeds from an initially homogeneous solution via liquid-liquid phase separation to yield a regular phase separated morphology in the course of reaction. It is due to the increase of the molecular weight of the polymer with the curing reaction resulting in a decrease in the entropy of the system. To date, there are several reviews in the preparation of micro/nanostructured thermosetting polymers by means of the CIPS methodology.[12,13]

HBPs offers the potential for tailoring their compatibility with epoxy resins through the conversion of their end-groups. The introduction of non-polar moieties reduces the polarity of HBPs with a consequent decrease in their miscibility with epoxies leading to phase separated materials by the CIPS methodology. In our research group, the modification of HBPs using long aliphatic chains has been reported.[14] Flores *et al*. prepared a series of partially modified Boltorn H30 by acylation process with 10-undecenoyl chloride.[15] Their addition to epoxy/anhydride formulations led to a great increase in the impact strength (more than 400%) in comparison with the neat material. Following the same approach, different modifications of hyperbranched poly(glycidol) were done and the epoxy thermosets prepared showing a significant increase in impact strength greater than 200% with respect to the unmodified material.[16] In both cases, the enhancement in impact strength was achieved by the formation of microphase separated particles by CIPS with a good interaction with the epoxy matrix due to the covalent linkage of the remaining OH groups of the HBPs with the curing agent.

Taking into account these results, an amidation of the amino groups from the PEI structure with 10-undecenoic acid was done. By the partial amidation of the amino groups, it is possible to tune the compatibility of the initial mixture and the formation of particles by CIPS maintaining some degree of compatibility between these particles and the matrix by partial covalent linkages of remaining amines with the epoxy network.

3.1.1 General synthetic methods of HBPs

The term hyperbranched polymer was first coined by Kim and Webster[17,18] in 1988 when the authors synthesized soluble hyperbranched polyphenylene. However, previously to this date highly branched polymers were prepared.[19] Since then, hyperbranched polymers have attracted increasing attention and many reviews on the synthetic aspects have been reported.[20,21]

Up to now, the synthetic techniques used to prepare hyperbranched polymers could be divided into two major categories.[22] The first category contains techniques of the single-monomer methodology (SMM), in which hyperbranched macromolecules are synthesized by polymerization of an AB_n or a latent AB_n monomer. According to the reaction

[12] T. Inoue, *Progress in Polymer Science*, **1995**, *20*, 119-153.
[13] L. Ruiz-Pérez, G. J. Royston, J. P. A. Fairclough, A. J. Ryan, *Polymer*, **2008**, *49*, 4475-4488.
[14] X. Fernández-Francos, D. Foix, A. Serra, J.M. Salla, X. Ramis, *Reactive and Functional Polymers*, **2010**, *70*, 798-806.
[15] M. Flores, X. Fernández-Francos, F. Ferrando, X. Ramis, A. Serra, *Polymer*, **2012**, *53*, 5232-5241.
[16] M. Flores, M. Morell, X. Fernández-Francos, F. Ferrando, X. Ramis, A. Serra, *European Polymer Journal*, **2013**, *49*, 1610-1620.
[17] Y. H. Kim, O. W. Webster, *Journal of the American Chemical Society*, **1990**, *112*, 4592-4593.
[18] Y. H. Kim, O. W. Webster, *Macromolecules*, **1992**, *25*, 5561-5572.
[19] H. R. Kricheldorf, Q. Z. Zang, G. Schwarz, *Polymer,* **1982**, *23*, 1821-1829.
[20] C. R. Yates and W. Hayes, *European Polymer Journal*, **2004**, *40*, 1257-1281.
[21] B. Voit, A. Lederer, *Chemical Reviews*, **2009**, *109*, 5924-5973.
[22] C. Gao, D. Yan, *Progress in Polymer Science*, **2004**, *29*, 183-275.

mechanism, the SMM category includes at least four specific approaches: 1) polycondensation of AB_n monomers,[18] 2) self-condensing ring opening polymerization (SCROP),[23] 3) self-condensing vinyl polymerization (SCVP)[24] and 4) proton transfer polymerization (PTP)[25] (**Scheme 3.1**).

1. Polycondensation of AB_n monomers

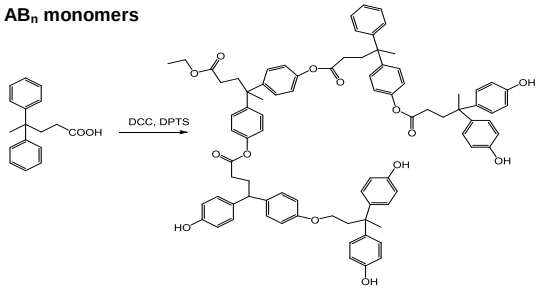

2. Self-condensing ring opening polymerization (SCROP)

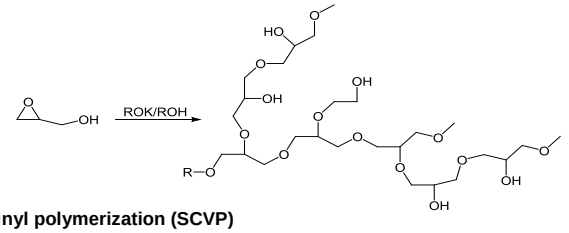

3. Self-condensing vinyl polymerization (SCVP)

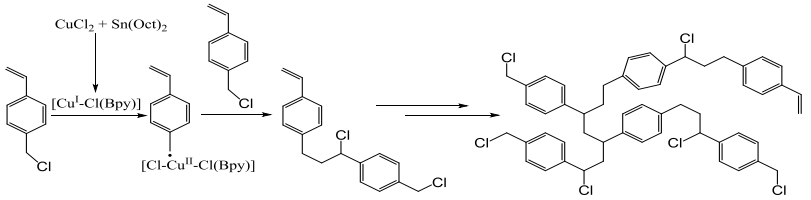

4. Proton transfer polymerization (PTP)

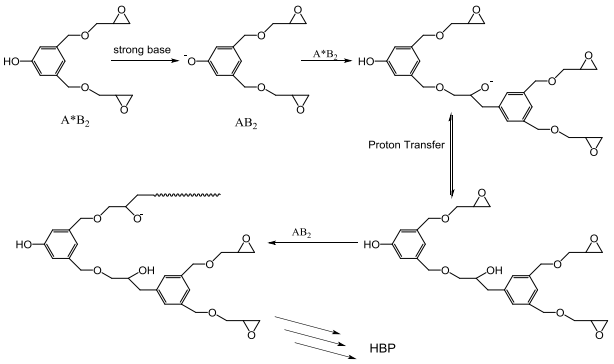

Scheme 3.1 Synthetic approaches for the preparation of HBPs through the SMM methodology

[23] A. Sunder, R. Hanselmann, H. Frey, R. Mulhaupt, *Macromolecules,* **1999**, *32*, 4240-4246.
[24] J. M. Fréchet, M. Henmi, I. Gitsov, S. Aoshima, M. R. Leduc, R. B. Grubbs, *Science*, **1995**, 269, 1080-1083.
[25] H. T. Chang, J. M. J. Fréchet, *Journal of the American Chemical Society*, **1999**, *121*, 2313-2314.

The other category contains methods of the double-monomer methodology (DMM) in which direct polymerization of two types of monomers or a monomer pair generates hyperbranched polymers (**Scheme 3.2**).[26]

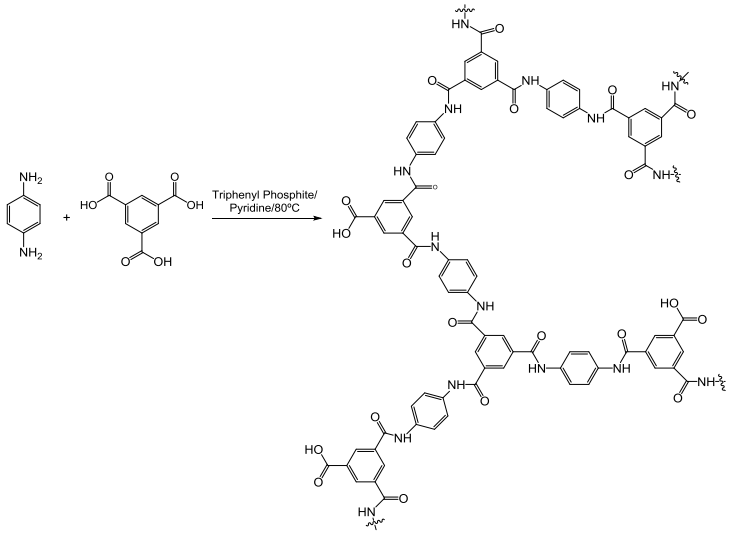

Scheme 3.2 Synthetic approach for the preparation of HBPs through the DMM methodology

Hyperbranched poly(ethyleneimine) is produced in a large scale by SCROP. In this methodology a heterocyclic monomer is used and a cationic or anionic mechanism is applied. Lupasol products are obtained through cationic polymerization of the ethylenimine monomer (aziridine) by a wide variety of acidic reagents and quaternizing agents.[27] The polymerization is terminated by reaction with water. Under these conditions, branched chain structures are formed as is shown in **Scheme 3.3**. The degree of branching is dependent upon the reaction conditions such as catalyst and ethylenimine concentration. PEI dendrimers were also prepared.[28]

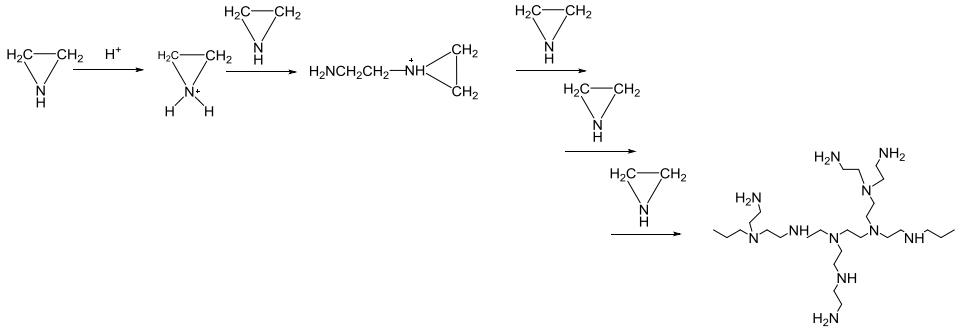

Scheme 3.3 Synthesis of poly(ethyleneimine) from aziridine monomer

[26] M. Jikei, S-H. Chon, M-A. Kakimoto, S. Kawauchi, T. Imase, J. Watenebe, *Macromolecules*, **1999**, *32*, 2061-2064.
[27] 0. C. Dermer and G. E. Ham, *Ethylenimine and Other Aziridines; Chemistry and Applications*, Academic Press, New York, **1969**, Chapter 4.
[28] O. Yemul, T. Imae, *Colloid and Polymer Science*, **2008**, *286*, 747-752.

3.1.2 Modification of hyperbranched poly(ethylenimine) with long alkyl chains

The preparation and characterization of PEI derivatives by amidation process have been followed by several authors. [29-32] For example, amidation with fatty acids leads to pigment dispersants for non-polar solvents[33] due to the decrease polar character by the reduction of amines content. PEIs modified with alkanoic acids with different alkyl chain were used as macromolecular antioxidants.[34] The reactive amines presents in the PEI structure can be modified by amidation procedure, since amines can react with acyl chlorides and acids. To form amide bonds by using acyl chlorides, an additional base is usually required to trap the formed HCl and to avoid the conversion of the amine into its unreactive HCl salt and normally N,N-dimethylaminopyridine is added.[35] Taking this into account, the modification of PEI by this procedure is limited by the presence of a high quantity of amines which can be protonated difficulting the purification process. As an alternative, N,N-carbonyldiimidazole (CDI) and dicyclohexyl carbodiimide (DCC) are frequently used for amide bond formation since they do not need an additional base.[35] CDI is the most commonly used reagent for the synthesis of amides from carboxylic acids and amines through the acyl imidazole intermediate (**Scheme 3.4**) due to the mild conditions under which it can be used, its low cost and the formation of innocuous by-products (CO_2 and imidazoles).

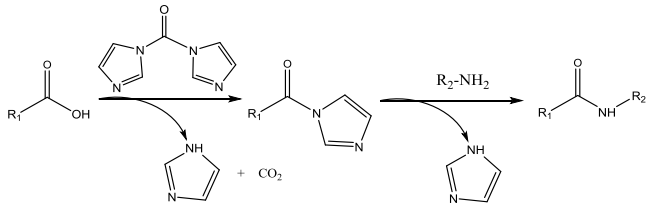

Scheme 3.4 Synthetic procedure of CDI mediated amide formation

The synthetic process is carried out in one pot and two steps: firstly, the activation of 10-undecenoic acid by reaction with CDI and then the nucleophilic substitution of imidazole group in the CDI derivative by amines of the PEI structure. On changing the proportion of CDI and 10-undecenoic acid to NH reactive groups, different modification percentages could be obtained.

This chapter will deal about the use of the modified PEI with different degrees of modification to improve the impact strength of epoxy/anhydride systems and the importance of the degree of modification of the PEI structure in the morphology of the final materials. The work herein presented has been published in the following article:

- New anhydride/epoxy thermosets based on diglycidyl ther of bisphenol A and 10-undecenoyl modified poly(ethyleneimine) with improved impact resistance. *Progress in Organic Coatings* **2015***, 85,* 52-59

[29] T. W. Johnson, I. M. Klotz, *Macromolecules*, **1974**, *7*, 149-153.
[30] L. Antonietti, C. Aymonier, U. Schlotterbeck, V. M. Garamus, T. Maksimova, W. Richtering, S. Mecking, *Macromolecules*, **2005**, *14*, 5914-5920.
[31] H. Liu, Y. Chen, D. Zhu, Z. Shen, S-E. Stiriba, *Reactive & Functional Polymers*, **2007**, *67*, 383-395.
[32] H. Qin, H. Liu, Y. Chen, *Chinese Journal of Polymer Science*, **2014**, *32*, 1338-1347.
[33] D. Thetford, J.D. Schofield ,US Patent 5.700.395, 23 December **1997**.
[34] G. Kasza, K. Mosnácková, A. Nádor, Z. Osváth, T. Stumphauser, G. Szarka, K. Czaniková, J. Rychlý, Š. Chmela, J. Mosnáčeк, *European Polymer Journal*, **2015**, *68*, 609-617.
[35] C. A. G. N. Montalbetti, V. Falque, *Tetrahedron*, **2015**, *61*, 10827-10852.

UNIVERSITAT ROVIRA I VIRGILI
HYPERBRANCHED POLY(ETHYLENEIMINE) DERIVATIVES AS MODIFIERS IN EPOXY NETWORKS
Cristina Acebo Gorostiza

3.2 New anhydride/epoxy thermosets based on diglycidyl ther of bisphenol A and 10-undecenoyl modified poly(ethyleneimine) with improved impact resistance

Cristina Acebo, Xavier Fernández-Francos, Silvia de la Flor, Xavier Ramis, Àngels Serra

Progress in Organic Coatings **2015***, 85,* 52-59

UNIVERSITAT ROVIRA I VIRGILI
HYPERBRANCHED POLY(ETHYLENEIMINE) DERIVATIVES AS MODIFIERS IN EPOXY NETWORKS
Cristina Acebo Gorostiza

Progress in Organic Coatings **2015**, *85*, 52-59

New anhydride/epoxy thermosets based on diglycidyl ether of bisphenol A and 10-undecenoyl modified poly(ethyleneimine) with improved impact resistance

Abstract

New dendritic modifiers have been synthesized by amidation of hyperbranched poly(ethylenimine) (PEIs) with 10-undecenoic acid to obtain hyperbranched polymers (HBPs) with different degree of modification. These HBPs have been used as toughness modifiers in a proportion of 10 and 20% in reference to the epoxy resin in diglycidyl ether of Bisphenol A (DGEBA) / methyltetrahydrophthalic anhydride (MTHPA) formulations. The curing process has been studied by dynamic scanning calorimetry and by rheometry, which allow the kinetic constants and the gel and vitrification times to be evaluated. The materials obtained have been thermally characterized and their mechanical properties have been evaluated. An increase in impact resistance has been achieved and the T_g of all thermosets prepared was higher than 100ºC in spite of the flexible structure of the PEI modifiers.

Keywords: thermosetting resins, hyperbranched, toughness, anhydride, rheology

Introduction

Epoxy resins are ideal materials in the field of coatings, adhesives, molding compounds and polymer composites due to their excellent thermomechanical properties and chemical and environmental stability. They also present good processability before curing.[1] Their broad range of applications can be explained by the fact that they are probably one of the most versatile thermosets not only because the type of resin and the chemistry of the curing can be varied, but also a huge number of organic and inorganic modifiers and fillers can be added to improve their properties.[2] Although rigidity and strength are desired properties in engineering applications, toughness is one of the restrictions in the use of epoxy resins.

During the past decades considerable efforts have been made to improve the toughness of these materials. Toughness implies energy absorption and it is achieved through various deformation mechanisms before failure occurs. One of the most effective methods of preventing the crack from freely developing after impact is the addition of a second phase that induces the formation of particles that absorb the impact energy and deflect the crack. A combination of cavitation around the rubber particles with shear yielding in the matrix produces a cooperative effect in the energy dissipation.[3] It has been reported that the formation of micro- or nanostructures in epoxy thermosets improves the overall properties without reducing crosslinking degree of the epoxy matrix and glass transition temperatures.[4] Chemically induced phase separation (CIPS) is one of the methodologies in which the morphology develops during curing. It starts from an initial homogenous mixture composed of the resin, curing agent and modifiers.[5,6] On curing, a blend of epoxy matrix filled with rubber or thermoplastic microspheres is formed, with a final size of these particles controlled by the viscosity of the reacting mixture during curing.

The first attempts to improve toughness were based on the addition of liquid rubbers or thermoplastics. However, these additives usually compromise the modulus and thermomechanical characteristics of the thermosets and the processability of the formulation.[7] Some years ago the use of hyperbranched polymers (HBPs) was proposed to overcome the limitations of traditional modifiers[8] and since then a significant number of research groups have adopted this strategy.[9-12] The dendritic structure of HBPs makes

these modifiers very promising in terms of processability because of the low entanglement that leads to low viscosities in comparison to rubbers or linear polymers.[13] By partial or total modification of their reactive terminal groups, it is possible to tune their interaction or covalent linkage with the epoxy matrix. This can lead to phase separated or homogenous morphologies.

In previous papers we demonstrated that the addition of HBPs to a curing system improves mechanical properties.[14-16] In these cases, the chemical incorporation of hydroxyl ended HBPs to the epoxy matrix led to materials with homogenous appearances without any phase separation.

We reported the use of partially modified Boltorn type polyesters with 10-undecenoyl moieties in DGEBA thermosets cured with anhydrides, resulting in a significant increase in impact strength, up to 400% with respect to the neat formulation, without sacrificing thermal and mechanical properties.[17] Efficient toughening was obtained because of the CIPS process leading to well dispersed hyperbranched particles covalently attached to the thermosetting matrix by the unmodified hydroxyl groups of the HBP. Following the same approach, we synthesized end-capped multiarm star polymers as modifiers in the curing of DGEBA with anhydride and a significant increase in impact strength was also achieved, attributed to the nanophase separation observed. [18]

In the present work, we propose the use of a series of partially modified poly(ethyleneimine) (PEI) with 10-undecenoyl chains as modifier of DGEBA thermosets cured with anhydride in the presence of a tertiary amine as a catalyst. Our interest is to investigate the influence of the degree of modification of the PEI structure with 10-unedecenoyl groups and the proportion of this modifier in the formulation on the curing evolution and on the mechanical and thermal characteristics of the materials obtained, emphasizing toughness improvement.

Experimental section

Materials

Poly(ethyleneimine) (PEI) (Lupasol®FG, 800 g/mol, BASF) was used after drying under vacuum. From the molecular weight of the polymer and of the repeating unit an average degree of polymerization of 18.6 was calculated. According to the data sheet, the relationship (NH_2/NH/N) was (1/0.82/0.53) and thus by calculations the equivalent number of primary, secondary and tertiary amines resulted to be 0.010, 0.00837, and 0.0053 eq/g. 10-Undecenoic acid was purchased from Fluka and 1,1-carbonyldiimidazole (CDI) was purchased from Sigma-Aldrich. Chloroform ($CHCl_3$) was dried under $CaCl_2$ and distilled before used. Diglycidylether of bisphenol A (DGEBA, Araldite GY 240, Huntsman, 182 g/eq) and methyl tetrahydrophthalic anhydride (MTHPA, Aradur HY 918, Huntsman) (166 g/mol) were used as received. Benzyl dimethylamine (BDMA, DY 062, Huntsman) was used as catalyst.

Amidation of hyperbranched polyethylenimines

The amidation of PEIs was performed according to a reported procedure.[19,20] The modified PEIs were achieved by reaction of the PEI with different ratio of 10-undecenoic acid and the degree of modification was calculated by means of ^{1}H-NMR spectroscopy. The synthesis of amidated PEIs were exemplified for the polymer PEI_{91}: 8.49 g (52 mmol) of CDI were slowly added to a solution of 9.66 g (52 mmol) of 10-undecenoic acid in 40 mL of chloroform. The solution was stirred at room temperature for 1h, and then 3 g (3.75

mmol) of PEI in 10 mL of chloroform were added. The mixture was stirred at room temperature for 4h, and then at 50ºC overnight. After cooling down, the mixture was washed several times with NaCl aqueous solution. The organic phase was dried by anhydrous $MgSO_4$ and after filtration and removal of the volatiles, the residue was kept at 40ºC in vacuum oven overnight and a honey-like polymer was obtained. ^{1}H NMR (400 MHz, $CDCl_3$), δ (ppm): 1.20-1.36 (-C**H**$_2$-, **4-8**), 1.59 (-C**H**$_2$-CH$_2$-CO-, **3**), 2.04 (-C**H**$_2$-CH=CH$_2$, **9**), 2.15 (-C**H**$_2$-CO-NH, **2**), 4.77 (-N**H**-, **1**), 4.95 (C**H**$_2$=CH-, **11**), 5.80 (CH$_2$=C**H**-, **10**) and 3.46-2.55 (PEI core) (**Figure 1**).

Average molecular weights and thermal data of all the modified HBPs obtained are collected in Table 1.

Table 1. Characteristics of the modified HBPs synthesized

Notation	*DA* [a] *(%)*	M_n [b] (g/mol)	T_g [c] (ºC)	$T_{5\%}$ [d] (ºC)
PEI_{91}	91	2925	-56	204
PEI_{78}	78	2626	-49	196

[a] Degree of amidation calculated by ^{1}H-NMR.
[b] Determined by ^{1}H-NMR spectroscopy.
[c] Determined by DSC.
[d] Temperature of 5% of weight loss determined by TGA under N_2 atmosphere.

Preparation of mixtures

Neat formulations were prepared by mixing the DGEBA with the stoichiometric amount of MTHPA. Then, the selected proportion of BDMA was added and the mixture was homogenized by mechanical stirring. The formulations containing 10-20% wt of PEIs (by weight of DGEBA) were prepared by first adding the required amount of PEIs to the epoxy resin and gently heating until they were dissolved and subsequently mixing with MTHPA and BDMA by mechanical stirring. For all the formulations, the quantity of MTHPA was calculated taking into account that 1 mol of anhydride reacts with 1 mol of epoxide group and the amount of BDMA was always 1 phr (1 part per hundred) with respect to the anhydride. The samples were kept at -20ºC before use to prevent polymerization. **Table 2** collects the composition of the formulations studied.

Table 2. Composition of DGEBA/MTHPA/BDMA formulations with different percentages of modifiers

Formulation	Modifiers wt (g)	DGEBA wt (g)	MTHPA wt (g)	BDMA wt (g)
Neat	-	1	0.912	0.00912
10% PEI_{91}	0.1	1	0.912	0.00912
20% PEI_{91}	0.2	1	0.912	0.00912
10% PEI_{78}	0.1	1	0.912	0.00912
20% PEI_{78}	0.2	1	0.912	0.00912

Characterization

^{1}H NMR measurements were carried out at 400 MHz in a Varian Gemini 400 spectrometer. $CDCl_3$ was used as the solvent. For internal calibration, the middle solvent signal corresponding to $CDCl_3$ was taken as δ (^{1}H) = 7.26 ppm.

Calorimetric analyses were carried out on Mettler DSC 822e and Mettler DSC 821e calorimeter with a TSO01RO robotic arm. The kinetic studies were performed at heating

rates of 2, 5, 7.5, 10ºC/min to determine the kinetic parameters and the reaction heat. The glass transition temperatures (T_g) of the HBPs were determined from a dynamic scan from -100ºC to 200ºC at 10ºC/min. The glass transition temperatures of the completely cured materials (T_g^{∞}) were determined by means of a heating scan at 10ºC/min, after isothermal curing process performed during 3h at 100ºC and 1h at 150ºC.

The curing kinetics of non-isothermal DSC experiments was analyzed by means of isoconversional and model-fitting procedures applied to non-isothermal DSC data.[21]

The isoconversional activation energy at different degrees of conversion *x* was determined from multiple heating rate experiments using the Kissinger-Akahira-Sunose method:

$$ln\left(\frac{\beta}{T^2}\right) = ln\left(\frac{A \cdot R}{g(x) \cdot E}\right) - \frac{E}{R \cdot T} \quad (1)$$

where *β* is the heating rate, *A* is the pre-exponential factor, *E* is the activation energy and *g(x)* is an integral function corresponding to the kinetic model. The time needed to reach a given conversion in an isothermal experiment can be determined from the results of the isoconversional analysis of non-isothermal experiments using the following expression:

$$lnt = ln\left(\frac{g(x)}{A}\right) + \frac{E}{R \cdot T} \quad (2)$$

The kinetic model was determined using a 2nd order autocatalytic kinetic model with $g(x) = (1/(n-1)) \cdot ((1-x)/x)^{1-n}$ and rearranging the above expressions as:

$$ln\left(\frac{g(x) \cdot \beta}{T^2}\right) = ln\left(\frac{A \cdot R}{E}\right) - \frac{E}{R \cdot T} \quad (3)$$

Thermogravimetric analyses were carried out in a nitrogen atmosphere with a Mettler TGA/SDTA 851e thermobalance. Samples with an approximate mass of 8 mg were degraded between 40 and 800 ºC at a heating rate of 10 ºC/min in N_2 (100 cm^3/min measured in normal conditions).

Rheological measurements were carried out in the parallel plates (diameter of 25 mm) mode with an ARG2 rheometer (TA Instruments, UK, equipped with an electrically heated plates system, EHP). The curing of the mixtures was monitored in an isothermal experiment at 100 ºC by means of a multiwave frequency sweep (1, 3 and 5 Hz). The frequency independent crossover of *tan*δ was used to determine the gel time [22]. The vitrification time was taken as the maximum of *tan*δ at 5 Hz. The conversion at gelation (x_{gel}) was determined by stopping the rheology experiment at gelation and performing a subsequent dynamic DSC scan of the gelled sample to measure the remnant heat of curing. The degree of curing achieved in gelation was determined using the following equation:

$$x_{gel} = 1 - \frac{\Delta H_{t,gel}}{\Delta H_{dyn}} \quad (4)$$

where $\Delta H_{t,gel}$ is the heat of the sample obtained by rheological experiment at gelation and ΔH_{dyn} is the total reaction heat.

Dynamic mechanical thermal analyses were carried out with a TA Instruments DMA Q800. The samples were cured isothermally in a mold (5 mm width and 3 mm thick) at

100 ºC for 3 h and then post-cured for 1 h at 150 ºC. Single cantilever bending at 1 Hz and deformation of 0.05% was performed at 3ºC/min, from 30ºC to 230ºC on prismatic rectangular samples (10x10x1 mm^3).

Impact tests were performed at room temperature by means of a Zwick 5110 impact tester according to ASTM D 4508-05 (2008) standard using rectangular samples (25 x 12 x 2.5 mm^3) cured by the same thermal process scheduled for DMTA samples. The pendulum employed had a kinetic energy of 0.5 J. For each material 9 determinations were made. The impact strength (IS) was calculated from the energy absorbed by the sample upon fracture as:

$$IS = \frac{E - E_0}{S} \quad (5)$$

where E and E_0 are the energy loss of the pendulum with and without sample respectively, and S is the cross-section of the samples.

The fracture area of impacted samples was metalized with gold and observed with a scanning electron microscope (SEM) Jeol JSM 6400 with a resolution of 3.5 nm.

Results and discussion

Synthesis and characterization of 10-undecenoyl modified PEI

Poly(ethyleneimine) possesses high number of reactive amines as end groups that can be modified to different extents. In the present study, total and partial modifications with 10-undecenoyl chains of this polymer were attempted. From the degree of polymerization of PEI, the proportion of NH_2/NH/N and the equivalent number of primary and secondary amines by molecule we calculated the number of reactive groups capable of being modified (NH_2 and NH), which resulted to be 14 per PEI molecule. From this number and desired degree of modification the quantity of 10-undecenoic acid and CDI used in the chemical modification was calculated. In the notation of the modified polymers, the subscript indicates the percentage of modification attained. The idealized structure and the synthetic procedure are represented in **Scheme 1**.

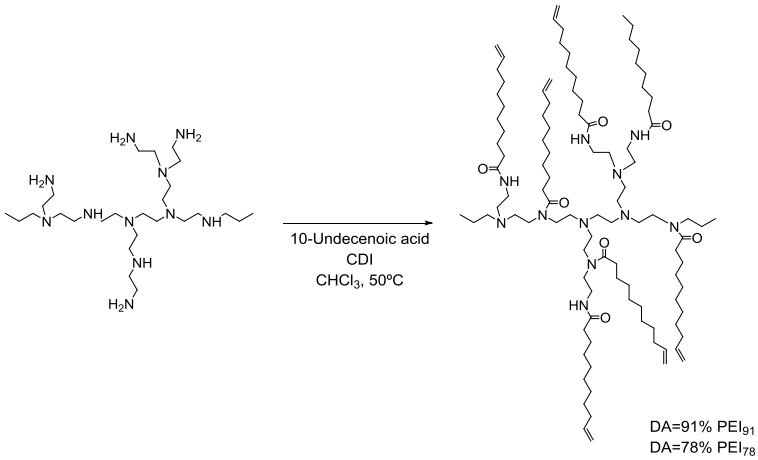

Scheme 1. Synthetic route to the modified PEIs

In previous studies[17,23] the modification of hydroxyl ended HBPs with 10-undecenoyl groups was performed by reaction with 10-undecenoyl chloride in the presence of 4-(N,N-dimethylamino) pyridine (DMAP) as hydrochloric acid acceptor. However, when we used PEI as HBP the elimination of DMAP by acidic extraction was impossible because the basic character of the modified polymer. Therefore, as the alternative synthetic procedure we selected the one proposed by Antonietti *et al*.[19] for the modification of PEI with palmitic acid which consists in two steps: the first one is the activation of 10-undecenoic acid by reaction with CDI in chloroform. The second step is the nucleophilic substitution of imidazole group in the CDI derivative by amines of the PEI structure. By selecting the proper amount of CDI derivative in reference to the active amine groups in the PEI core, different degrees of modification were reached, 91% and 78%. No complete modification could be reached similarly to that described in PEI modification with long-chain aliphatic acids.[19,20]

The degree of modification was calculated by ^{1}H-NMR, following a previously reported method.[19] **Figure 1** shows the spectrum for the partially modified polymer with the signal assignments. From the intensities of signal 2, corresponding to methylene protons directly attached to amide group divided by two (*A*) and the area in the region between 3.6 and 2.4 ppm which corresponds to the core of PEI (*P*), we determined the value of *x.* This value corresponds to the ratio of alkyl chains introduced per amine moiety in the starting PEI, which includes tertiary, secondary and primary amines. From *x* and the values of the primary amine end groups (*T*), secondary amine linear units (*L*), and tertiary amine branched units (*D*) it is possible to calculate the degree of amidation (*DA*) by using the following equations:

$$x = A/\left[\frac{P}{(5-x)}\right] \quad (6)$$

$$DA = x(L+T+D)/(L+T) \quad (7)$$

The values of *DA* were slightly lower than expected. In the case of adding the stoichiometric amount of CDI derivative to PEI, an only 91% of the total reactive amines could be modified, whereas the difference between the expected and the reached degree of modification is lower for lower degrees of modification. Probably the aliphatic shell formed in the modification of PEI hinders the possibility of nucleophilic attack of amine groups to the carbonyl group of the CDI derivative.

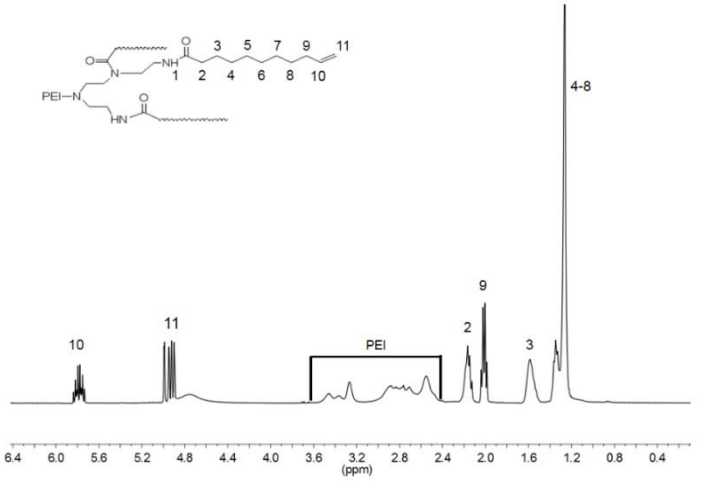

Figure 1. ^{1}H NMR spectrum in $CDCl_3$ of the PEI_{78}

From the thermogravimetric data shown in Table 1 it was observed that the higher the degree of modification the higher the temperature of initial degradation. However, there is a decrease in their T_g as the degree of modification increases. This is a feature that was observed in modified hyperbranched poly(glycidol) with 10-undecenoyl chains[23] caused by both the decrease in the intensity of inter- and intra-molecular H-bonding interactions and the increased in free volume associated with the presence of the 10-undecenoyl chains.[24,25]

Effect of the 10-undecenoyl modified PEI on the curing kinetics

Figure 2 represents the curing thermograms and conversion evolution of the DGEBA neat formulation and the formulations containing 10% and 20% of the PEI_{78} cured with MTHPA in the presence of BDMA. **Table 3** summarizes the most relevant data obtained from the curing of the formulations.

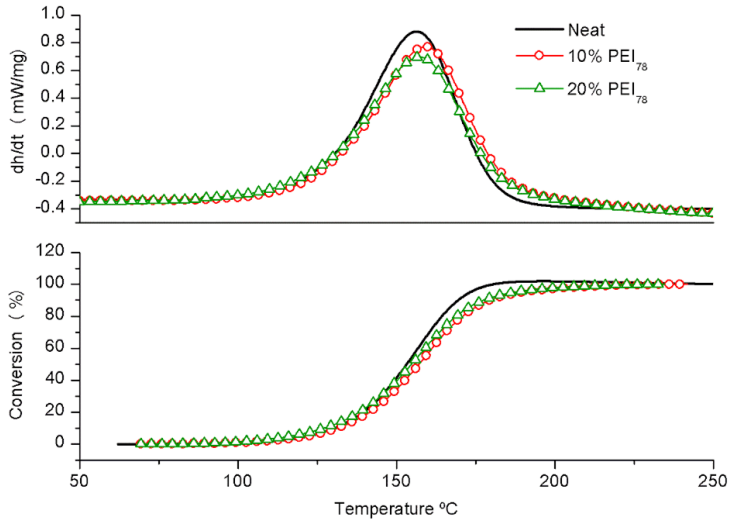

Figure 2. DSC scanning curves (top) and degree of conversion (bottom) against temperature of the curing of the neat and the modified formulations with 10% and 20% of the PEI_{79} at a heating rate of 10ºC/min.

Table 3. Calorimetric data of the curing of the different formulations studied

Formulation	T_{peak}[a] (°C)	E_a[b] (kJ/mol)	$k_{150ºC} \cdot 10^3$[c] (s^{-1})	$k_{100ºC} \cdot 10^3$[c] (s^{-1})	Δh[d] (J/g)	Δh[e] (kJ/ee)	T_g[f] (°C)
Neat	158	78.8	0.759	0.038	290	101	123
10% PEI_{91}	158	75.7	0.659	0.036	291	106	110
20% PEI_{91}	157	69.7	0.653	0.046	304	107	101
10% PEI_{78}	159	72.3	0.582	0.037	304	111	117
20% PEI_{78}	158	65.5	0.655	0.054	282	109	103

[a] Temperature of the maximum of the exothermic DSC curve
[b] Activation energy at 0.5 of conversion evaluated by isoconversional non-isothermal integral procedure.
[c] Rate constants at 150ºC and 100ºC calculated using the 2nd order autocatalytic kinetic model with n=1.6, determined using eq (3) and the Arrhenius expression for the kinetic constant $k=A \cdot exp(-E/R \cdot T)$.
[d] Reaction heat per gram determined by DSC.
[e] Reaction heat per epoxy equivalent determined by DSC.
[f] Glass transition temperature of thermosetting samples prepared for DMTA analysis

If we observe the shape of the crosslinking exotherm, it seems that there is no much influence on adding the PEI_{78} to the reactive mixture. The curing exotherms for formulations with PEI_{91}, although not shown in the figure, had similar appearance, without differences in the temperature of the maximum of the peak.

The calculated activation energy decreases proportionally to the amount of PEI in the formulation, being the lower the one calculated for the curing of the formulation containing 20% of PEI_{78}. Following the procedure described in a previous paper,[18] we determined the constant rates of the curing processes at 150 ºC and observed that the addition of PEI modifier retarded the curing. At 100 ºC, the kinetic constants indicate that the curing process is only slightly retarded in the presence of 10 % of the PEI modifiers and even significantly accelerated when 20% of the modifiers are used. This change in trend is caused by the lowering of the overall activation energy when the PEI modifiers are used.

Curing processes of epoxy-anhydride formulations are complex and involve a number of competitive reactions[26] that may have different temperature dependence. The remaining unreacted amine groups in the PEI modifiers may react with either epoxy or anhydride groups, leading to hydroxyl or carboxyl chain ends that can participate actively in the curing process and even have a catalytic effect.[27,28]

We can see in Table 3 that the average reaction heat released per epoxy equivalent is around 100-110 kJ for all formulations and within the reported literature values for analogue epoxy-anhydride systems.[29-31] The addition of the PEI modifiers to the formulation slightly decreases the value of the T_g but temperatures higher than 100ºC were determined for all the materials.

Rheological studies of the curing of the formulations

Gelation and vitrification processes are important phenomenological issues taking place during curing and processing of epoxy formulations. Gelation corresponds to the formation of a giant macromolecular structure that percolates the reaction medium. Then, the gel fraction extends and increases crosslinking as the curing advances leading to an insoluble, fully three-dimensional network at the end of the curing process. Macroscopically, a change from a liquid to a solid mass can be observed (the sample viscosity tends to infinite). The material ceases to flow and starts to build-up mechanical properties.[22] As a consequence, internal stresses can appear after gelation owing to curing shrinkage. The knowledge of the conversion and gelation time is also of the main importance from the processing point of view. Vitrification may occur if the T_g of the system equals and becomes higher than the reaction temperature, decreasing the mobility of the reactive species because of the reduction of the free volume. Thus, the curing dramatically slows down and the reaction stops, preventing the curing from reaching completion and producing materials with lower crosslinking density than expected. Therefore, vitrification should be surpassed in order to get complete cure by increasing the curing temperature above the T_g of the fully cured material. Rheometric monitoring of curing processes is a methodology used to determine accurately the gel point and vitrification because it is highly sensitive to the dramatic changes in the viscoelastic properties that occur.[31-33]

The values of gelation and vitrification times and conversion at the gel point are collected in **Table 4**.

Table 4. Data obtained from rheometric monitoring of the curing of the formulations at 100 ºC.

Formulation	t_{gel} [a] (min)	x_{gel} [b]	t_{vit} [c] (min)
Neat	33	31	103
10% PEI_{91}	32	40	90
20% PEI_{91}	34	44	67
10% PEI_{78}	31	43	100
20% PEI_{78}	35	49	71

[a] Gel time determined from the frequency independent crossover of tan δ.
[b] Determined as the conversion reached by rheometry and DSC tests at 10ºC/min.
[c] Vitrification time determined as the tan δ peak time at the frequency of 5 Hz.

As can be seen, there is a small effect of the addition of modifier on the gelation time. However, the conversion at gelation increases notably, and this should have a positive effect in terms of internal stresses because of the reduced curing shrinkage after gelation, assuming that curing shrinkage is proportional to conversion.[34] The conversion at gelation is higher than in the curing of DGEBA/MTHPA mixtures modified with poly(ε-caprolactone) multiarm stars[18] possibly due to the participation of unreacted amine groups of the modified PEI in the curing process. Thus, the higher the proportion of PEI in the formulation or the lower the modification degree, the higher the conversion at the gelation is. Because of the faster curing kinetics at 100 ºC when PEI modifiers are added, gelation times are comparable in spite of the higher degree of conversion at the gel point.

On comparing the vitrification times of the formulations studied it can be seen that on increasing the proportion of modifier this value is reduced. Possibly the network build-up process during curing of the modified formulations is affected by the presence of the modified PEI, leading to a faster increase in the T_g of the curing formulation, but the trend is consistent with the overall positive effect of PEI modifiers on the curing kinetics at 100 ºC, especially when a proportion of 20% is used.

Thermal and thermomechanical properties of the thermosets obtained

The thermosets prepared were studied by DMTA. **Figure 3** represents the mechanical spectra of the thermosets and the main parameters determined are collected in **Table 5.**

Table 5. Thermomechanical and thermogravimetric data of the thermosets prepared

Formulation	DMTA		TGA	
	$T_{tan\delta}$ [a] (ºC)	E'_r [b] (MPa)	$T_{5\%}$ [c] (ºC)	T_{max} [d] (ºC)
Neat	146	17	345	406
10% PEI_{91}	129	17	345	406
20% PEI_{91}	119	14	328	401
10% PEI_{78}	134	16	352	409
20% PEI_{78}	123	14	326	393

[a] Temperature of maximum of tan δ.
[b] Storage modulus in the rubbery state determined at tan δ peak + 50ºC
[c] Temperature of the onset decomposition on TGA data at 10ºC/min calculated for a 5% weight loss.
[d] Temperature of the maximum decomposition rate based on the TGA data at 10ºC/min

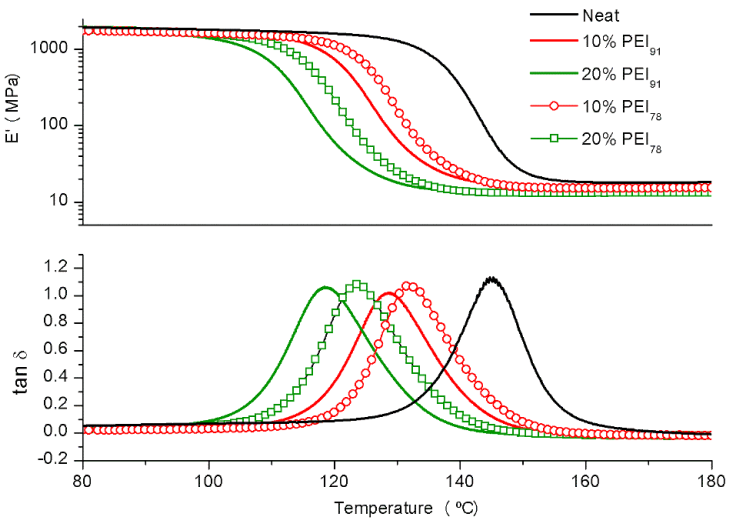

Figure 3. Storage modulus and tan δ against temperature at 1Hz for neat DGEBA and the thermosets containing different amounts of PEIs.

As we can see in the figure, the tan δ curves are unimodal as correspond to homogeneous material although relaxations corresponding to the PEI modifier added could appear under ambient temperature. On increasing the proportion of PEI modifier, the transitions are shifted toward lower temperature which indicates partial or total compatibility of the modifier with the epoxy network. On the other hand, on decreasing the degree of 10-undecenoyl modification in the PEI structure the decrease is reduced. This can be due to the plasticizing effect of the flexible 10-undecenoyl moieties of the PEI structure, which is predominant for PEI_{91} formulations. However, this effect is not as evident in the modulus in the rubbery state, parameter which is more affected by the molecular weight between crosslinks, which does not change significantly.

From the values of the table we can observe that the addition of the 10-undecenoyl modified PEI to the formulations reduces the temperature of the maximum of the α-relaxation, as seen with DSC. The reduction in this temperature is more notable than in thermosets with 10-undecenoyl modified hyperbranched polyesters previously reported.[17] The highly flexible structure of the PEI core and the higher compatibility between the matrix and the modifier can explain the differences in the behavior.

The modified materials have a slightly lower modulus in the rubbery state than the neat thermoset, which indicates a less crosslinked network, due to the presence of the modifier. As discussed in the preceding sections, the remaining amine groups of the PEI modifier may react with epoxy and anhydride groups leading to species that can participate in the epoxy-anhydride curing mechanism and can catalyze the process. In previous works it was observed that the crosslinking density in epoxy-anhydride thermosets decreased upon addition of reactive hyperbranched.[27] This could be rationalized by the participation of the reactive hydroxyl groups of the hyperbranched modifier in the complex reaction mechanism during curing of epoxy-anhydride thermosets, in spite of the presence of internal branching points in the hyperbranched structure. It is hypothesized that the effect should be similar in the present case, especially taking into account the small number of available unmodified amine groups. The trend in crosslinking density and decrease in T_g, reflecting a loosening

of the network structure, is also consistent with the increasing conversion at gelation upon addition of the modifiers.

The thermal stability of these materials was rated by thermogravimetry. The shape of the thermogravimetric curves was unimodal indicating a single degradative process or overlapping processes with comparable thermal dependence. From the values of the table we can state that a proportion of 10% of PEIs does not compromise the stability of the material, since the temperature of the initial degradation ($T_{5\%}$) is maintained. However, this temperature is reduced on adding a 20% of the modifier in the formulation. The presence of 20% of PEI_{79} in the material produces a reduction in the temperature of the maximum rate of degradation.

Mechanical characterization and morphology

Toughness is one the weakest properties of epoxy resins and for that reason a lot of efforts have been made to improve it. The addition of flexible structures in a thermoset helps to dissipate the energy of impact, increasing toughness. Thus, the structure of the modifiers studied in the present work, seems to be good candidates to dissipate impact energies, taking also into account that they can be mixed easily to prepare the DGEBA/MTHPA formulation and that T_gs are not much influenced by the addition of this modifier. As it can be seen in **Figure 4**, the addition of modified PEI improves the impact resistance of the resulting thermosets in comparison with the neat material.

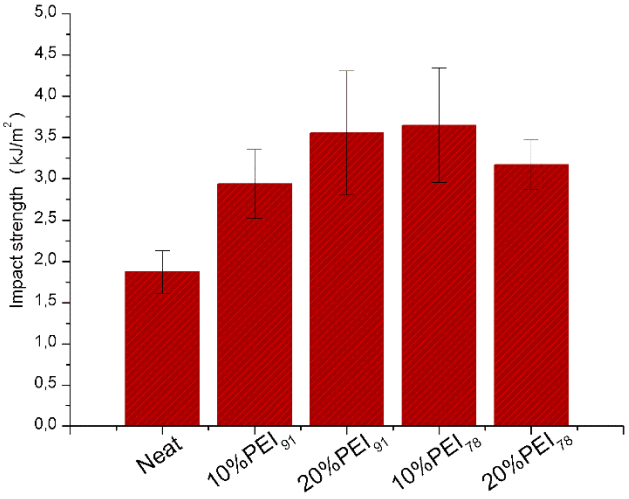

Figure 4. Impact strength values for thermosets prepared

In the case of using PEI_{91} as modifier, on increasing its proportion impact resistance is improved. This fact can be explained in terms of the morphology of samples observed by SEM. The fracture surfaces after impact tests were investigated by this technique and all micrographs are shown in **Figure 5**. In the micrographs of the formulations with PEI_{91} it can be observed the presence of a nanograined morphology more evident on increasing the proportion of modifier. When 10% of PEI_{78} was used as modifier, the increase in impact strength was higher than with any proportion of PEI_{91}, but further addition decreased the impact strength. The inspection of the impacted surfaces of these samples by SEM does

not show any clear phase separation or nanograined morphology and both surfaces are quite smooth at this magnification.

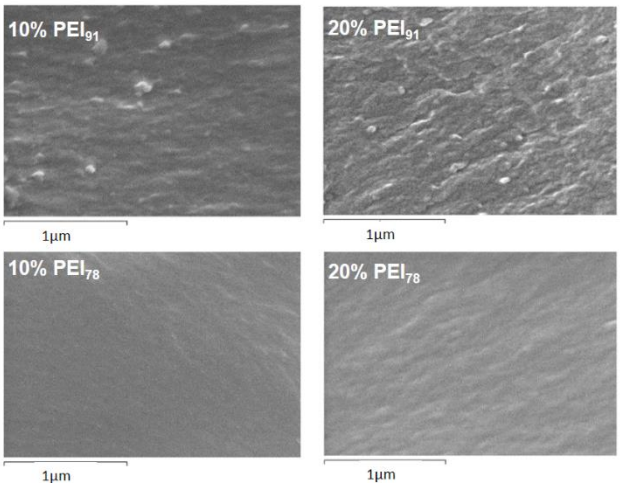

Figure 5. SEM micrographs of the surface of fracture of the modified thermosets

From the surface inspection of all the samples, no clear phase separation was put in evidence, in contrast with our previous report on epoxy/anhydride thermosets modified with 10-undecenoyl terminated hyperbranched polyesters.[17] In that work, an increase in the impact resistance higher than 400% was achieved and it was explained by a cavitation mechanism, based in the phase separation and in the covalent linkage of the remaining hydroxyl terminal groups of the HBP to the epoxy matrix. As it has been commented, cavitation around rubber particles in combination with shear yielding in the matrix produces a cooperative effect in the energy dissipation. In the present study, improvements below 200% were reached and fracture mechanisms of *in situ* reinforcing or plasticization of the matrix can be considered as responsible. The higher reactivity of unreacted amine groups towards anhydrides and epoxy than hydroxyl groups and the lower molecular weight of the PEI structures in comparison to the modified polyesters can explain the final compatibility of PEIs with the epoxy matrix. Thus, PEI_{78}, with a higher proportion of unreacted amines leads to the smoother surfaces observable in Figure 5. Although the modification of poly(ethyleneimine) with higher molecular weight (Lupasol WF®, 25000 g/mol) with 10-undecenoyl moieties was performed, there was a lack of compatibility with the DGEBA/MTHPA mixture that hindered the preparation of homogeneous samples to make mechanical and thermomechanical tests.

Conclusions

Amine groups of poly(ethyleneimine) could be amidated by using a synthetic procedure consisting in the previous activation of 10-undecenoic acid with carbonyldiimidazole and further reaction of this derivative with PEI. However, the complete modification of all amine groups could be not achieved reaching a 91% of maximum modification degree. The degree of modification was determined by ^{1}H-NMR spectroscopy.

The curing kinetics was accelerated by the presence of the PEI modifiers at moderate curing temperatures. However, rheological measurements showed that gelation time was hardly affected because of the increasing degree of conversion at gelation. The addition of

the PEI modifiers to the DGEBA/MTHPA formulation slightly decreased the value of *Tg* but they were higher than 100ºC for all the thermosets.

Thermosets containing modified PEI showed improved impact resistance in reference to the neat material. Nanograined morphology was observed by SEM for materials containing PEI_{91}, whereas materials with PEI_{78}, because of the chemical bonding of remaining amine groups to the epoxy matrix, showed a smoother surface of impact.

References

[1] May C.A. (Ed.): Epoxy Resins. Chemistry and Technology, Marcel Dekker, New York, Chapter 1 (1988)
[2] Petrie E.M.: Epoxy Adhesives Formulations, McGraw-Hill, New York (2006)
[3] Brooker R.D., Kinloch AJ., Taylor AC: The morphology and fracture properties of thermoplastic-toughened epoxy polymers. The Journal of Adhesion, 86, 726-741 (2010)
[4] Meng F., Xu Z., Zheng S.: Microphase separation in thermosetting blends of epoxy resin and poly(ε-caprolactone)-*block*-polystyrene block copolymers. Macromolecules, 41, 1411-1420 (2008)
[5] Ruiz-Perez L., Royston G.J., Fairclough J.P.A., Ryan A.J.: Toughening by nanostructure. Polymer, 49, 4475-4488 (2008)
[6] Mezzenga R., Plummer C.J.G., Boogh L., Manson J.A.E.: Morphology build-up in dendritic hyperbranched polymer modified epoxy resins: modelling and characterization. Polymer, 42, 305-317 (2001)
[7] Pascault J.P., Williams R.J.J.: Epoxy Polymers, Wiley VCH, Weinheim, Chapter 1 (2010)
[8] Boogh L., Pettersson B., Mänson J-A.E.: Dendritic hyperbranched polymers as toughеners for epoxy resins. Polymer, 40, 2249-2261 (1999)
[9] Ratna D., Simon GP.: Thermomechanical properties and morphology blends of a hydroxyl-functionalized hyperbranched polymer and epoxy resin. Polymer, 42, 8833-8839 (2001)
[10] Ratna D., Varley R., Simon GP.: Toughening of trifunctional epoxy using and epoxy-functionalized hyperbranched polymer. Journal of Applied Polymer Science, 89, 2339-2345 (2003)
[11] Sangermano M., Malucelli G., Bongiovanni R., Priola A., Harden A.: Investigation on the effect of the presence of hyperbranched polymers on termal and mechanical properties of an epoxy UV-cured system. Polymer International, 54, 917-921 (2005)
[12] Zhang D., Jia D.: Toughness and strength improvement of diglycidyl ether of bisphenol A by low viscosity liquid hyperbranched epoxy resin. Journal of Applied Polymer Science, 101, 2504-2511 (2006)
[13] Voit B., Lederer A.: Hyperbranched and highly branched polymers architectures-synthetic strategies and major characterization aspects. Chemical Reviews; 109, 5924-5973 (2009)
[14] Morell M., Erber M., Ramis X., Ferrando F., Voit B., Serra A.: New epoxy thermosets modified with hyperbranched poly(ester-amide) of different molecular weight. European Polymer Journal, 46, 1498-1509 (2010)
[15] Morell M., Ramis X., Ferrando F., Yu Y., Serra A.: New improved thermosets obtained from DGEBA and a hyperbranched poly(ester-amide). Polymer, 50, 5374-5383 (2009)
[16] Foix D., Rodriguez M.T., Ferrando F., Ramis X., Serra A.: Combined use of sepiolite and a hyperbranched polyester in the modification or epoxy/anhydride coatings: A study of the curing process and the final properties. Progress in Organic Coatings, 75, 364-372 (2012)
[17] Flores M., Fernández-Francos X., Ferrando F., Ramis X., Serra A.: Efficient impact resistance improvement of epoxy/anhydride thermosets by adding hyperbranched polyesters partially modified with undecenoyl chains. Polymer, 53, 5232-5241 (2012)
[18] Acebo C., Picardi A., Fernández-Francos X., De la Flor S., Ramis X., Serra A.: Effect of hydroxyl ended and end-capped multiarm star polymers on the curing process and mechanical characteristics of epoxy/anhydride thermosets. Progress in Organic Coatings, 77, 1288-1298 (2014)
[19] Antonietti L., Aymonier C., Schlotterbeck U., Garamus V.M., Maksimova T., Richtering W., Mecking S.: Core-Shell-Structured Highly Branched Poly(ethylenimine amide)s: Synthesis and Structure. Macromolecules, 38, 5914-5920 (2005)

[20] Liu H., Chen Y., Zhu D., Shen Z., Stiriba S.E.: Hyperbranched polyethylenimines as versatile precursors for the preparation of different type of unimolecular micelles. Reactive & Functional Polymers, 67, 383-395 (2007)
[21] Ramis X., Salla JM., Mas C., Mantecón A., Serra A.: Kinetic study by FTIR, TMA, and DSC of the curing of a mixture of DGEBA resin and γ-butyrolactone catalyzed by ytterbium triflate. Journal of Applied Polymer Science, 92, 381-393 (2004)
[22] Pascault J.P., Sauterau H., Verdu J., Williams R.J.J.: Thermosetting Polymers, Marcel Dekker, New York, Chapter 6 (2002)
[23] Flores M., Morell M., Fernández-Francos X., Ferrando F., Ramis X., Serra A.: Enhancement of the impact strength of cationically cured cycloaliphatic diepoxide by adding hyperbranched poly(glycidol) partially modified with 10-undecenoyl chains. European Polymer Journal, 49, 1610-1620 (2013)
[24] Sunder A., Bauer T., Mülhaupt R., Frey H.: Synthesis and thermal behaviour of esterified aliphatic hyperbranched polyether polyols. Macromolecules, 33, 1330-1337 (2000)
[25] Luciani A., Plummer C.J.G., Nguyen T., Garamszegi L., Manson J-AE.: Rheological and physical properties of aliphatic hyperbranched polyesters. Journal of Polymer Science, Part B: Polymer Physics, 42, 1218-1225 (2004)
[26] Rocks J., Rintoul L., Vohwinkel F., George G.: The kinetics and mechanism of cure of an amino-glycidyl epoxy resin by a co-anhydride as studied by FT-Raman spectroscopy. Polymer, 45, 6799-6811 (2004)
[27] Fernández-Francos X., Rybak A., Sekula R., Ramis X., Serra A. Modification of epoxy-anydride thermosets using a hyperbranched poly(ester-amide): Kinetic study. Polymer International, 61, 1710-1725 (2012)
[28] Fernandez-Francos X., Ramis X., Serra A.: From curing kinetics to network structure: A novel approach to the modeling of the network buildup of epoxy–anhydride thermosets. Journal of Polymer Science, Part A: Polymer Chemistry, 52, 61-75 (2014)
[29] Flores M., Fernández-Francos X., Ramis X., Serra A.: Novel epoxy-anhydride thermosets modified with a hyperbranched polyester as toughness enhancer. Thermochimica Acta, 544, 17-26 (2012)
[30] Ivin K.J., Brandrup J., E.H. Immergut (Eds.); Polymer Handbook, Wiley, New York, (1975)
[31] Fernández-Francos X., Cook W.D., Salla J.M., Serra A., Ramis X.: Crosslinking of mixtures of diglycidylether of bisphenol-A with 1,6-dioxaspiro[4.4] nonan-2,7-dione initiated by tertiary amines: III. Effect of hydroxyl groups on network formation. Polymer International, 58, 1401-1410 (2009)
[32] Raghavan S.R., Chen L.A., McDowell C., Khan S.A., Hwang R., White S.: Rheological study of crosslinking and gelation in chlorobutyl elastomer system. Polymer, 37, 5869-5875 (1996)
[33] Eloundou J.P., Gerard J.F., Harran D., Pascault J.P. Temperature Dependence of the Behavior of a Reactive Epoxy−Amine System by Means of Dynamic Rheology. 2. High-T_g Epoxy−Amine System. Macromolecules, 29, 6917-6927 (1996)
[34] Fernández-Francos X., Kazarian S.G., Ramis X., Serra A.: Simultaneous monitoring of curing shrinkage and degree of cure of thermosets by attenuated total reflection fourier transform infrared (ATR FT-IR) spectroscopy. Applied Spectroscopy, 67, 1427-1436 (2013)

UNIVERSITAT ROVIRA I VIRGILI
HYPERBRANCHED POLY(ETHYLENEIMINE) DERIVATIVES AS MODIFIERS IN EPOXY NETWORKS
Cristina Acebo Gorostiza

UNIVERSITAT ROVIRA I VIRGILI
HYPERBRANCHED POLY(ETHYLENEIMINE) DERIVATIVES AS MODIFIERS IN EPOXY NETWORKS
Cristina Acebo Gorostiza

4.Synthesis of multiarm star polymers by ring opening polymerization and their use as modifiers in epoxy thermosets

4

UNIVERSITAT ROVIRA I VIRGILI
HYPERBRANCHED POLY(ETHYLENEIMINE) DERIVATIVES AS MODIFIERS IN EPOXY NETWORKS
Cristina Acebo Gorostiza

4.1 Introduction

Star polymers (SPs) are characterized as the simplest case of branched species where all chains of a given macromolecule are connected to a core. The preparation methods and properties of star-branched polymers were examined in detail several years ago.[1]

Commonly, star polymers have been widely used as well-defined nanoparticles for applications in nanomedicine, catalysis, drug and gene delivery, among others.[2,3] Different functional cores can be used to synthesize multiarm star polymers[4,5] and the arms can be obtained using different synthetic methods.[6,7] The possibility to modify the structure by the conjugation of different segments to their end functional groups is an advantage to find out the good host-guest properties. Moreover, star-like topologies have attracted considerable interest as a toughness modifiers of thermally cured epoxy thermosets because of their unusual physical and rheological properties.[8] The properties of the final materials are related to the SPs structure, the amount of end groups and the molecular weight and length of the arms.

In our group it has been tested the use of SPs as modifiers in epoxy resins. Different mutiarm star polymers were synthesized using poly(glycidol)[9] and poly(styrene)[10] as a macroinitiator and poly(ε-caprolactone) arms. As a conclusion, star like structures are suitable epoxy resin modifiers due to their potential as toughening agents together with the capacity to improve other characteristics, without negatively affecting the curing and processability as well as the final thermomechanical properties of the materials.

4.1.1 Synthesis of star-shaped polymers

Generally, star polymers can be prepared by “core-first” and “arm-first” methodologies. In the first method, the polymerization of the monomer to growth the arms is conducted from either a well-defined initiator with a known number of initiating groups or a less defined multifunctional macromolecule or HBP (**Figure 4.1, 1**).[11]

In the arm first synthesis two different approaches are possible: one is where a linear polymer, previously synthesized, with a reactive chain end is directly attached to a multifunctional core (**Figure 4.1, 2A**). The other, is the direct copolymerization of a macromonomer with a di or multifunctional monomer in the presence of an initiator (**Figure 4.1, 2B**).[1]

---

[1] M. K. Mishra, S. Kobayashi, *Star and Hyperbranched Polymers*, Marcel Dekker, Inc., New York, **1999**.
[2] J. Liu, H. Duong, M. R. Whittaker, T. P. Davis, C. Boyer, *Macromolecular Rapid Communications*, **2012**, *33*, 760-766.
[3] V. Rodionov , H. Gao , S. Scroggins , D. A. Unruh , A.-J. Avestro , J. M. J. Fréchet , *Journal of the American Chemical Society*, **2010**, *132*, 2570-2572.
[4] W. Xia, G. Jiang, W. Chen, *Journal of Applied Polymer Science*, **2008**, *109*, 2089-2094.
[5] X. Zhang, J. Cheng, Q. Wang, Z. Zhong, R. Zhuo, *Macromolecules*, **2010**, *43*, 6671-6677.
[6] D. J. A. Cameron , M. P. Shaver , *Chemical Society Reviews*, **2011**, *40*, 1761-1776.
[7] A. Duréault , D. Taton , M. Destarac , F. Leising , Y. Gnanou , *Macromolecules*, **2004**, *37*, 5513-5519.
[8] Y. Meng, X.-H. Zhang, B-Y. Du, B-X. Zhou, X. Zhou, G-R Qi, *Polymer*, **2011**, *52*, 391-399.
[9] M. Morell, A. Lederer, X. Ramis, B. Voit, A. Serra, *Journal of Polymer Science, Part A: Polymer Chemistry*, **2011**, *49*, 2395-2406.
[10] M. Morell, D. Foix, A. Lederer, X. Ramis, B. Voit, A. Serra, *Journal of Polymer Science, Part A: Polymer Chemistry*, **2011**, *49*, 4639-4649.
[11] S. Maier, A. Sunder, H. Frey, R. Mülhaupt, *Macromolecular Rapid Communications*, **2000**, *21*, 226-230.

1. Core first

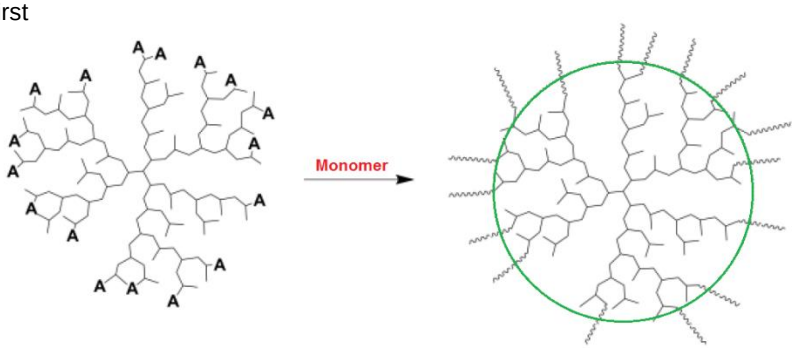

2. Arm first

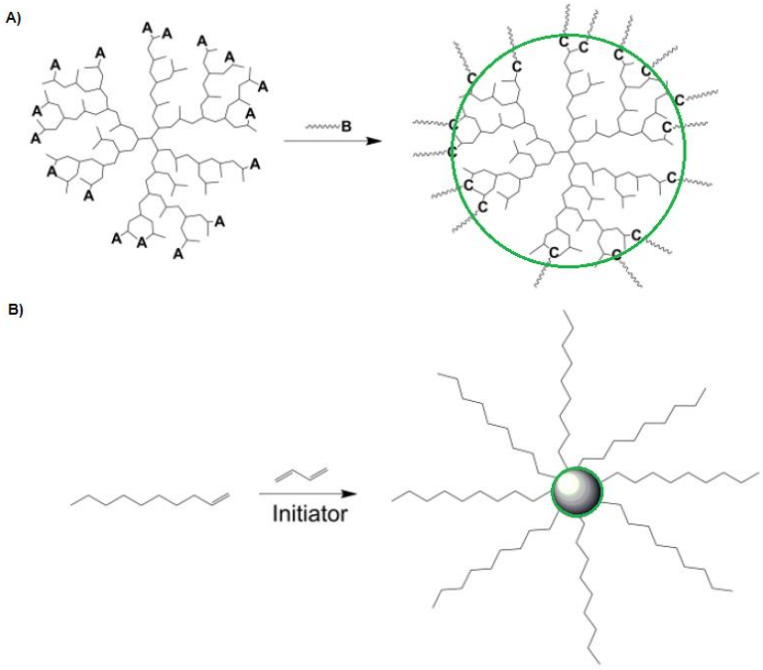

Figure 4.1 Synthesis of multiarm star polymers by different methods

In the core first methodology the arm length can be tailored by the ratio of active sites to the amount of added monomer obtaining well-defined star polymers with a known number of arms. High yields are achieved with only simple purification methods in comparison with the arm first in which the purification processes are much more complex since the impurities consist in polymer that has not been attached to the star structure. Moreover, the number of arms in “arm-first” methodology is not always well-controlled. Despite of the approach used, obtaining star polymer with a high number of arms is a tough task since a macroinitiator is needed (i.e. HBP) and the molecular weight of the arms can

be only determined by indirect methods. In most of the core-first syntheses, HBPs like polyesters, polyethers or poly(ethyleneimine) have been used as macroinitiator.[12-14]

4.1.2 Synthesis of multiarm star polymers by ring opening polymerization using poly(ethyleneimine) as a core

To date, well-defined stars have been prepared through the ring opening polymerization (ROP) of lactide (LA) and ε-caprolactone (CL) using polyhydroxyl compounds as co-initiators.[13,15] ROP processes, which take place by a living polymerization, provides a sufficient polymerization control, giving polymers of the expected molar masses and leads to the desired end-groups.[16] The mechanism allows to prepare defined arms in the SPs structures. It has been shown that LA and CL can be polymerized in a controlled manner using Sn-based catalysts in combination with initiating hydroxyl or amine groups. However, references devoted SPs prepared through the poly(ethyleneimine) initiated ROP of LA and CL were scarce.[17,18]

The polymerization mechanism of CL and LA co-initiated with amines, involves several steps to obtain the desired products.[19] The reaction of PEI with CL is preceded by the carboxylate-imine groups exchange at the tin atom in $Sn(Oct)_2$, accompanied by the octanoic acid (OctH) release (**Scheme 4.1**).

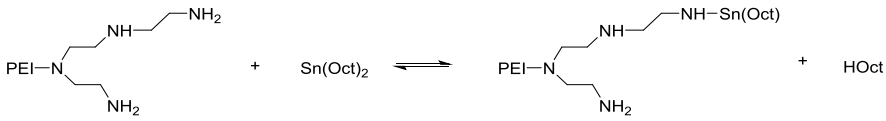

Scheme 4.1 Activation of the macroinititor (PEI) using $Sn(Oct)_2$

The polymerization follows by CL monomer insertion forming a new tin(II)-alkoxide specie (**Scheme 4.2.a**) initiating the propagation step (**Scheme 4.2.b**).

[12] M. Trollsås, C.J. Hawker, J.F. Remenar, J.L. Hedrick, H. Johanson, H. Ihre, A. Hult, *Journal of Polymer Science, Part A: Polymer Chemistry,* **1998**, *36*, 2793-2798.
[13] A. Burgath, A. Sunder, I. Neuner, R. Mülhaupt, H. Frey, *Macromolecular Chemistry and Physics*, **2000**, *201*, 792-797.
[14] P. F. Cao, R. Xiang, X. Y. Liu, C.X. Zhang, F. Cheng, Y. J. Chen, *Journal of Polymer Science, Part A: Polymer Chemistry*, **2009**, *47*, 5184-5193.
[15] M. Schömer, H. Frey, *Macromolecular Chemistry and Physics*, **2011**, *212*, 2478-2486.
[16] T. Biela, A. Kowalski, J. Libiszowski, A. Duda, S. Penczek, *Macromolecular Symposia*, **2006**, *240*, 47-55.
[17] M. Adeli, R. Haag, *Journal of Polymer Science, Part A: Polymer Chemistry*, **2006**, *44*, 5740-5749.
[18] X. Cao, Z. Li, X. Song, X. Cui, P. Cao, H. Liu, F. Cheng, Y. Chen, *European Polymer Journal*, **2008**, *44*, 1060-1070.
[19] A. Kowalski, J. Libiszowski, T. Biela, M. Cypryk, A. Duda, S. Penczek, *Macromolecules*, **2005**, *38*, 8170-8176.

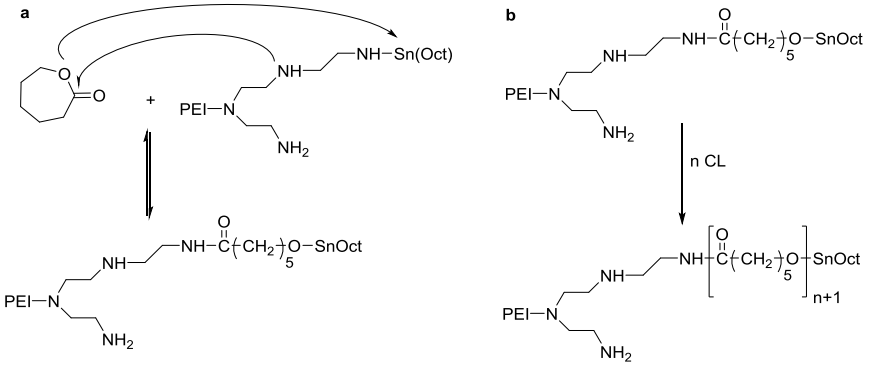

Scheme 4.2 Initiation (a) and propagation (b) of the polymerization reaction

Finally, the exchange reaction with octanoic acid results in the final product and the $Sn(Oct)_2$ is recovered again (**Scheme 4.3**).

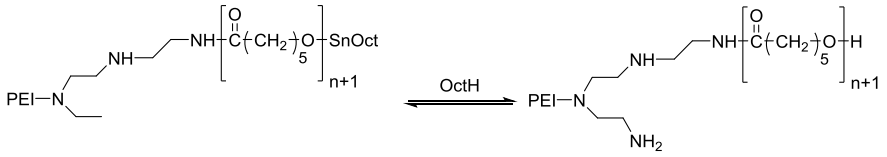

Scheme 4.3 Termination step

By this mechanism, different degrees of polymerization in the arms can be achieved taking into account the ratio of CL and LA to reactive amine groups. The different structures of the repetitive units in the arms can tailor the characteristics of SPs modifiers.

PCL is a hydrophobic, semi-crystalline polyester with a high chain flexibility, which is miscible in most epoxy systems.[20] The use of PCL to modify epoxy resins appears as a good choice due to the presence of OH groups as chain end that could be covalently linked to the epoxy network if the proper curing agent is used. Its flexible structure is capable to promote crazing and shear yielding leading to a toughened material.[21] Moreover, the presence of aliphatic esters, which can undergo thermal degradation by a pyrolytic elimination process, allows the reworkability of the modified coating.

In the same way, the incorporation of PLA in the SPs can enhance the final mechanical properties of the thermosetting materials and it is expected a higher thermal reworkability by the lower thermal stability of the secondary ester groups of PLA in comparison to ester of primary alkyl groups of PCL.[22]

It is known, that the formation of micro- or nanostructures improves the overall properties of thermosetting materials.[23] One strategy to reduce the compatibility of the SPs and to form well dispersed SPs microparticles in the final materials could be the modification of the hydroxyl groups to obtain end-capped multiarm star polymers. In this

[20] N. Hameed, Q. Guo, T. Hanley, Y. W. Mai, *Journal of Polymer Science, Part B: Polymer Physics*, **2010**, *48*, 790-800.
[21] H. Lützen, P. Bitomsky, K. Rezwan, A. Hartwig, *European Polymer Journal*, **2013**, *49*, 167–176.
[22] J. S .Chen, C. K. Ober, M. D. Poliks, *Polymer*, **2002**, *43*, 131–139.
[23] F. Meng, Z. Xu, S. Zheng, *Macromolecules*, **2008**, *41*, 1411-1420.

study, the modification of hydroxyl groups by acetylation process has been carried out to obtained the unreactive multiarm stars desired.

Given that SPs are good candidates as modifiers for epoxy materials, in this chapter we will discuss about the ring polymerization of CL and LA monomers initiated by hyperbranched poly(ethyleneimine) leading to multiarm star polymers by the first core approach and their use as modifiers in different DGEBA formulations. The influence of the arm length and molecular weight of the core in the toughness improvement will be studied. Furthermore, the influence of end-capped multiarm stars on the mechanical properties will be evaluated. The work herein presented has been published in the following articles that compose this chapter:

- Multiarm Star with Poly(ethyleneimine) core and Poly(ε-caprolactone) arms as Modifiers of Diglycidylether of Bisphenol A Thermosets cured by 1-methylimidazole. *Reactive & Functional Polymers* **2013**, *73,* 431-441
- New epoxy thermosets modified with multiarm star poly(lactide) with poly(ethylenimine) as core of different molecular weight. *European Polymer Journal* **2013**, *49,* 2316-2326
- Effect of hydroxyl ended and end-capped multiarm star polymers on the curing process and mechanical characteristics of epoxy/anhydride thermosets. *Progress in Organic Coatings* **2014**, *77,* 1288-1298
- Epoxy/anhydride thermosets modified with end-capped star polymers with poly(ethyleneimine) cores of different molecular weight and poly(ε-caprolactone) arms. *eXPRESS Polymer Letters* **2015**, *9*, 809-823

UNIVERSITAT ROVIRA I VIRGILI
HYPERBRANCHED POLY(ETHYLENEIMINE) DERIVATIVES AS MODIFIERS IN EPOXY NETWORKS
Cristina Acebo Gorostiza

4.2 Multiarm star with poly(ethyleneimine) core and poly(*ε*-caprolactone) arms as modifiers of diglycidylether of bisphenol A thermosets cured by 1-methylimidazole

Cristina Acebo, Xavier Fernández-Francos, Francesc Ferrando, Àngels Serra, Josep M. Salla, Xavier Ramis

Reactive & Functional Polymers **2013***, 73,* 431-441

UNIVERSITAT ROVIRA I VIRGILI
HYPERBRANCHED POLY(ETHYLENEIMINE) DERIVATIVES AS MODIFIERS IN EPOXY NETWORKS
Cristina Acebo Gorostiza

Reactive & Functional Polymers **2013**, *73*, 431-441

Multiarm star with poly(ethyleneimine) core and poly(ε-caprolactone) arms as modifiers of diglycidylether of bisphenol A thermosets cured by 1-methylimidazole

Abstract

Well-defined multiarm star copolymers, with hyperbranched poly(ethyleneimine) (PEI) as the core and poly(*ε*-caprolactone) (PCL) arms with different degree of polymerization were synthesized by cationic ring-opening polymerization of *ε*-caprolactone from a hyperbranched poly(ethyleneimine) core and used to modify diglycidylether of bisphenol A formulations cured with 1-methylimidazole as anionic initiator. The curing process was studied by dynamic scanning calorimetry (DSC) and FTIR. By rheometry the complex viscosity of the multiarm stars synthesized and the influence of their addition to the reactive mixture was analyzed in detail. The resulting materials were characterized by thermal and mechanical tests. The addition of the multiarm star to the formulation led to homogeneous materials with a slightly toughened fracture in comparison to neat DGEBA thermosets without compromising thermal characteristics.

Keywords: Star polymers, hyperbranched, epoxy resin, anionic polymerization, thermosets.

Introduction

Epoxy resins are widely used as coatings, electrical and electronic materials because of their high adhesion and other attractive properties such as thermal stability and electrical insulation.[1-3] The objectives of our research on epoxy based materials are to face some of the limitations of this kind of materials for instance, the enhancement of toughness or the reduction of the internal stresses, maintaining their thermomechanical characteristics and easy processability.

In previous works it was proved the convenience of star-like topologies to enhance some characteristics of epoxy thermosets.[4-11] Star-like polymeric structures were also used in the improvement of other matrices, such as poly(vinyl ester urethane)s with a great success.[12]

In general, the modification with dendritic structures like hyperbranched or star polymers leads to a significant improvement of mechanical properties of the thermosets without affecting thermomechanical characteristics.[13-16] Moreover, low shrinking thermosets have been prepared by the use of these structures[17,18] and chemically or thermally reworkable thermosets can be reached when the dendritic structure presents labile groups such as esters.[13,19] However, the most interesting item is that dendritic polymers offer a low formulation viscosity since the highly branched structure prevent chain entanglement, thus reducing the viscosity in comparison to linear polymeric modifier analogs.[20]

In previous studies of our research team, we have synthesized multiarm stars with poly(glycidol) core and poly(ε-caprolactone) arms, which have been studied as modifiers in the curing of DGEBA using cationic and anionic initiators as curing agents.[5,8] In both studies the processability of the reactive mixtures was not worsened in reference to the neat formulation and even the viscosity was reduced when the multiarm star had arms with a degree of polymerization of 10. T_gs of the final materials were not much reduced and

were even higher than those of the thermosets modified with linear poly(ε-caprolactone). In cationic cured materials the thermal stability was practically maintained whereas the use of anionic curing initiators allowed us to reach reworkable thermosets, because of the temperature of initial degradation was reduced more than 100ºC. Toughness characteristics were improved in both materials.

Following the "core-first" approach, which involves the living polymerization of a monomer from a multifunctional core,[21-24] in the present study we have synthesized new multiarm stars with poly(ε-caprolactone) (PCL) arms of different lengths using as the multifunctional core a poly(ethyleneimine) (PEI) from a commercial source, with trade name Lupasol®. This is a promising strategy to reach star modifiers at low price by an easy procedure, which allows facing advantageous technological applications in the field of epoxy coatings.

In a recent study, Lupasol® has been explored as a multifunctional crosslinker of epoxy resins, but its reactivity is too high and the short gelation time prevents technological applicability.[25,26] Thus, the modification of the amine terminal and linear active groups, capable of directly reacting with epoxides, with poly(ε-caprolactone) arms, changes dramatically its reactivity and applicability. This polymer, which is a hydrophobic semi-crystalline polyester with a high chain flexibility, is miscible in most epoxy resins.[27,28] Its flexible structure is capable of promoting crazing and shear yielding and to absorb the energy locally. Therefore it can improve the toughness characteristics on incorporating it to the epoxy matrix.[29]

The presence of tertiary amine groups in the core of the multiarm star prevents the use of cationic initiators such as rare earth metal triflates. Thus, 1-methylimidazole has been selected in the present work as anionic initiator. Tertiary amines help to covalently link the multiarm stars ended with OH groups to the epoxy matrix, as has been demonstrated previously by us.[5,30] This is due to the fact that the initiation by the tertiary amine generates an alkoxide anion, responsible for the propagation by reaction with epoxides by a typical anionic ring-opening mechanism. Thus, a proton exchange can take place between this anion and the hydroxyl groups present in the reactive system, which allows the chemical incorporation of hydroxyl-terminated polymers into the network structure.

The goal of the present work is the improvement of DGEBA epoxy thermosets cured by 1MI by adding poly(ethyleneimine)-poly(ε-caprolactone) multiarm stars with different arm length in proportions of 5 and 10% w/w and the evaluation of the curing process.

Experimental section

Materials

Polyethyleneimine (PEI) Lupasol®FG (800 g/mol) was purchased from BASF and used without further purification. From the molecular weight of the polymer and of the repeating unit an average degree of polymerization of 18.6 was calculated. According to the data sheet, the relationship (NH_2/NH/N) was (1/0.82/0.53) and thus by calculations the equivalent number of primary, secondary and tertiary amines is 0.010, $8.37 \cdot 10^{-3}$, and $5.3 \cdot 10^{-3}$ eq/g. *ε*-Caprolactone (ε-CL, 97 %) was distilled under vacuum. Tin (II) 2-ethylhexanoate ($Sn(oct)_2$, 98 %) and 1-methylimidazole (1MI, 99 %) were used without further purification. All these chemicals were purchased from Sigma-Aldrich. Solvents were purchased from Scharlab. Diglycidylether of bisphenol A (DGEBA) Araldite GY 240 was provided by Huntsman (EEW = 182 g/eq).

Reactive & Functional Polymers **2013**, *73*, 431-441

Synthesis of poly(ethyleneimine)-b-poly(ε-caprolactone) multiarm stars (PEI-PCLX)

In the acronym PEI-PCLX, X accounts for the degree of polymerization of the ε-caprolactone arms in the star and can take the values 10, 30 and 50.

The synthesis is exemplified for PEI-PCL10. PEI (0.5 g, 0.625 mmol) and 10.28 g of *ε*-CL (90.06 mmol) were placed at room temperature in a two-necked flask equipped with a magnetic stirrer and a gas inlet to fill the flask with argon. Then, 0.12 g of $Sn(oct)_2$ (0.3 mmol) was added to the solution mixture and the flask was immersed in an oil bath thermostatized at 130 ºC during 48 hours. After that, the crude product was dissolved in chloroform and the polymer was isolated by precipitation in methanol and then filtered and dried at 45 ºC under vacuum for two days.

^{1}H NMR (400 MHz, $CDCl_3$, δ in ppm): 4.08 (-C**H$_2$**-OCO-, **5**), 3.66 (-C**H$_2$**-OH, **5'**), 2.32 (-NHCO-C**H$_2$**-, -C**H$_2$**-COO, **1** and **1'**), 1.70-1.40 (-C**H$_2$**-, **2-4** and **2'-4'**) and 3.5-1.5 (PEI core) (see Figure 1).

Average molecular weights and thermal data of all the multiarm stars obtained are given in **Table 1.**

Table 1. Data of the multiarm stars PEI-PCLX synthesized in this study

Entry	*CL/NH*[a] *(mol/eq)*	*Yield* (%)	$\overline{M}_{n,\exp 1}$ [b] *(g/mol)*	$\overline{M}_{n,\exp 2}$ [c] *(g/mol)*	$\frac{\overline{M}_w}{\overline{M}_n}$ [c]	$\overline{DP}_{arm}$ [b]	T_g [d] (ºC)	T_m [d] (ºC)	Δh_m [d] (J/g)	X [e] (%)	$T_{5\%}$ [f] (ºC)
PEI-PCL10	10	70	18371	6108	1.33	12	-79	62	72	53	312
PEI-PCL30	30	72	40735	6909	1.42	26	-74	63	86	63	312
PEI-PCL50	50	89	83865	11902	1.75	53	-	66	89	66	331

[a] Feed ratio between caprolactone monomer and active NH groups
[b] Determined by ^{1}H-NMR spectroscopy
[c] Determined by SEC
[d] Determined by DSC
[e] Degree of crystallinity determined by DSC
[f] Temperature of 5% of weight loss determined by TGA

Preparation of epoxy thermosets

The mixtures were prepared by adding the required amount of PEI-PCLX to the epoxy resin and gently heating until it was dissolved and the solution became clear. Then, 5 phr of 1MI (part of initiator per hundred parts of mixture) were added and the resulting solution was stirred and cooled down to -10 ºC to prevent polymerization. Mixtures containing 5-10 wt% (by weight) of PEI-PCLX were prepared. The compositions of the formulations studied are detailed in **Table 2.**

Table 2. Composition and curing enthalpies of DGEBA/1-MI mixtures with different percentages of PEI-PCLX and T_g of the thermosets prepared

Formulation (wt.%)	Eq_{epoxy}: $Eq_{1\text{-}MI}$	Eq_{epoxy}: Eq_{OH}	Δh (J/g)	Δh (kJ/ee)	T_g[a] (ºC)
0	9.10	0	515	96	145
PEI-PCL10					
5	9.99	85.82	491	98	123
10	9.11	43.81	487	102	111
PEI-PCL30					
5	9.10	246.22	504	103	122
10	9.23	119.04	462	97	110
PEI-PCL50					
5	9.33	636.04	492	98	129
10	9.11	316.19	490	101	117

[a] Glass transition temperature of the thermosets obtained after the dynamic curing in the DSC

Characterization

^{1}H NMR measurements were carried out at 400 MHz and in a Varian Gemini 400 spectrometer. $CDCl_3$ was used as the solvent. For internal calibration, the middle solvent signal corresponding to $CDCl_3$ was taken as δ (^{1}H) = 7.26 ppm.

Molecular weight and molecular weight distribution was determined by means of an Agilent 1200 series SEC-system with a combination of PL-GEL 3, PL-GEL 5 and PL-GEL 20 µm mixed A columns in series, equipped with an Agilent 1100 series Refractive Index detector. Calibration curves were based in polystyrene standards having low molecular weight dispersity using a flow rate of 1 mL/min and THF as eluent, the sample concentrations were between 5 and 10 mg/mL and injection volumes of 100 µL were used.

Calorimetric analyses were carried out on a Mettler DSC-822e thermal analyzer. Samples of approximately 10 mg were placed in aluminum pans under nitrogen atmosphere. The calorimeter was calibrated using an indium standard (heat flow calibration) and an indium-lead-zinc standard (temperature calibration).

Multiarm star polymers (PEI-PCLX) were heated from 25 to 120 ºC with a heating rate of 20 ºC/min, cooled down to -120 ºC with a cooling rate of -10 ºC/min and then heated again to 120 ºC with a heating rate of 20ºC/min. Melting temperature (T_m), the heat of fusion (Δh_m) and the glass transition temperature (T_g) were obtained from the second heating curves. The degree of crystallinity (χ) was calculated as the quotient between the experimental heat of fusion and the theoretical heat of fusion of a perfect crystal of infinite size, obtained from additive group contributions[31] for poly(ε-caprolactone). Thermal data are collected in Table 1.

Non-isothermal curing of DGEBA/PEI-PCLX/1MI mixtures was performed from 30 to 300 ºC at heating rate of 10 ºC/min to determine the reaction heat associated with the complete conversion of all reactive groups.

The glass transition temperatures ($T_{g\infty}$s) of the completed cured materials were determined, by means of a second heating scan at 10 ºC/min after dynamic curing at 20 ºC/min, as the temperature of the half-way point of the jump in the heat capacity when the material changed from glassy to the rubbery state under N_2 atmosphere and the error is estimated to be approximately ± 1 °C.

Thermogravimetric analyses were carried out in a Mettler TG50 thermobalance. Samples with an approximate mass of 8 mg were degraded between 40 and 800 ºC at a heating rate of 5 ºC/min in N_2 (100 cm^3/min measured in normal conditions).

A Bruker Vertex FTIR spectrometer equipment (resolution of 4 cm^{-1}) with an attenuated-total-reflectance accessory with a diamond crystal (Golden Gate heated single-reflection diamond ATR, Specac-Teknokroma) was used to study the curing by FTIR spectroscopy. The evolution of the epoxy band at 915 cm^{-1} was monitored during curing at 80, 100 and 120 ºC, taking the band at 1605 cm^{-1} attributed to the phenyl ring as a reference. The conversion was determined by the Lambert-Beer law from the normalized change of absorbance at 915 cm^{-1}:

$$\alpha_{epoxy} = 1 - \frac{A\prime_{epoxy,t}}{A\prime_{epoxy,0}} \quad (1)$$

where $A'_{epoxy,t}$ and $A'_{epoxy,0}$ are respectively the normalized absorbance of the reactive group before curing and after a reaction time *t*.

Dynamic mechanical thermal analyses were carried out with a TA Instruments DMA Q800. The samples were cured isothermally in a mould at 100 ºC for 1 h and then post-cured for 1 h at 200 ºC. Single cantilever bending at 1 Hz and deformation of 0.05% was performed at 3 ºC/min, from 35 ºC to 230 ºC on prismatic rectangular samples (10 x 10 x 1 mm^3).

Thermomechanical analyses were carried out on a Mettler TMA40 thermomechanical analyzer. The samples were supported by two silica discs and heated at 5ºC/min from 30 up to 150ºC by application of a force of 0.02N. The thermal expansion coefficients (CTEs) below and above the T_g were calculated as follows:

$$CTE = \frac{1}{L_0} \cdot \frac{dL}{dT} = \frac{1}{L_0} \cdot \frac{dL/dt}{dT/dt} \quad (2)$$

where, *L* is the thickness of the sample, L_0 the initial length, *t* the time, *T* the temperature and *dT/dt* the heating rate.

Rheological measurements were carried out in the parallel plates (geometry of 25 mm) mode with an ARG2 rheometer (TA Instruments, UK, equipped with an electrically heated plates system, EHP).

Complex viscosity (η^*) of the mixtures and the multiarm star polymers were recorded as function of angular frequency (0.1-100 rad/s) under a constant deformation of 3 % at 40, 60, 80 y 100ºC for the mixtures and at 80, 100, 120 y 140ºC for the multiarm star polymers.

Impact tests were performed at room temperature by means of a Zwick 5110 impact tester according to ASTM D 4508-05 (2008) standard using rectangular samples (25 x 12 x 2.5 mm^3) cured by the same thermal process schedule than for DMTA samples. The

pendulum employed had a kinetic energy of 0.5 J. For each material 9 determinations were made. The impact strength (IS) was calculated from the energy absorbed by the sample upon fracture as:

$$IS = \frac{E - E_0}{S} \quad (3)$$

where *E* and E_0 are the energy loss of the pendulum with and without sample respectively, and *S* is the cross-section of the samples.

The fracture area of impacted samples was metalized with gold and observed with a scanning electron microscope (SEM) Jeol JSM 6400 with a resolution of 3.5 nm.

Results and discussion

Synthesis and characterization of multiarm stars

The synthesis of multiarm star polymers can be carried out by means of two major strategies: (1) the core first approach, which consists in a living polymerization from a multifunctional molecule as initiator, and (2) the "arm-first" approach, which consists in linking reactive polymer chains to a functionalized core or polymerize vinyl terminated polymer chains with a small amount of bifunctional vinyl compounds capable of crosslinking.[32-34] In the present study we used the core first approach taking a commercial polyethyleneimine (Lupasol®) as the multifunctional core and forming the arms from ε-caprolactone by a living cationic polymerization employing $Sn(oct)_2$ as the catalyst.[35] Tailoring the ratio of active sites to the amount of monomer is possible to control the arm length. The synthetic pathway is depicted in **Scheme 1**.

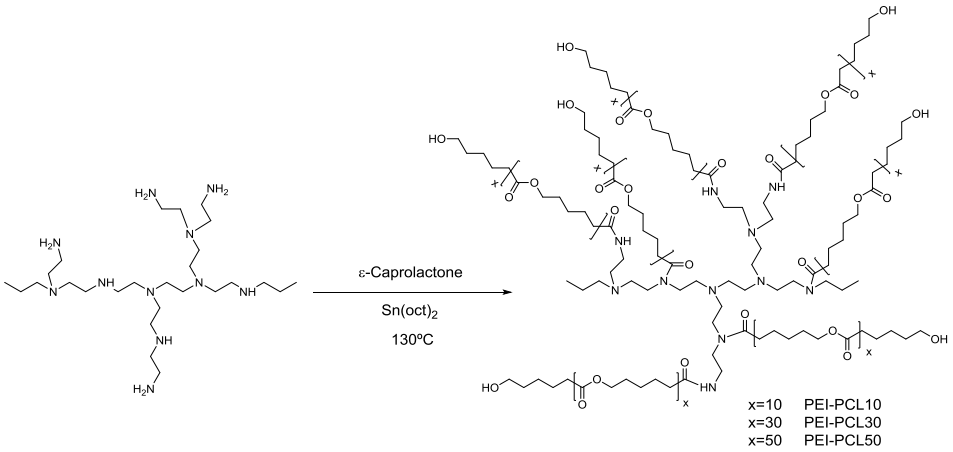

Scheme 1. Synthetic route to the mutiarm star copolymers PEI-PCLX

From the degree of polymerization of PEI, the proportion of NH_2/NH/N and the equivalent number of amines by gram of PEI we calculated the number of active groups capable to act as initial growing of PCL chain (only NH_2 and NH), which resulted to be 0.0184 eq/g. From this number and the desired degrees of polymerization of PCL the quantity of ε-caprolactone to be polymerized was calculated. The reaction was performed in bulk at 130 ºC for 48 h under argon atmosphere. After precipitation in methanol and drying in vacuum, the polymers were obtained as a yellowish powder.

To evaluate the real degree of polymerization achieved in the PCL arms and confirm the chemical structure of the multiarm star, ^{1}H-NMR spectra were registered. **Figure 1** shows the ^{1}H-NMR spectrum in $CDCl_3$ of PEI-PCL10 multiarm star as an example with the corresponding assignments.

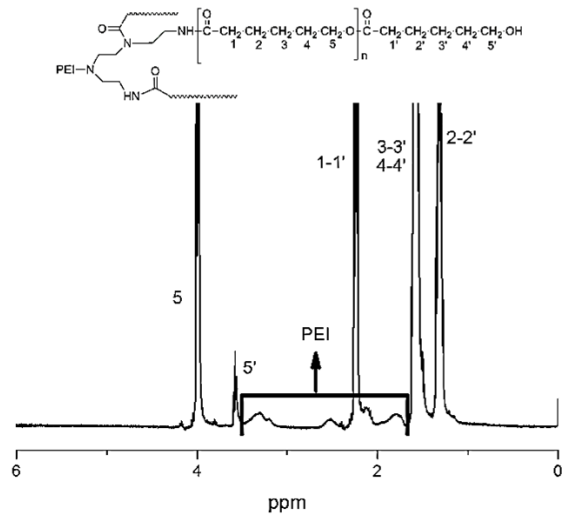

Figure 1. ^{1}H NMR spectrum in $CDCl_3$ of PEI-PCL10 multiarm star copolymer

In addition to the broad signals attributed to the PEI core three groups of signals clearly appear. The central methylene protons of the ε-caprolactone unit appear between 1.4 and 1.7 ppm. The protons directly attached to carbonyl group (1 and 1') appear overlapped at 2.3 ppm. Thus, the only signals that can be used to evaluate the degree of polymerization are the methylene protons 5 and 5', attached to the oxygen of ester in the repeating unit or to hydroxyl terminal group, which appear separately. Thus, the degree of polymerization of PCL arms ($\overline{DP}_{arm}$) was calculated from the integration of these signals by dividing peak **5** by peak **5'** and adding a terminal unit, as follows:

$$\overline{DP} = \frac{I_5}{I_{5'}} + 1 \qquad (4)$$

The use of the signals of carbons **5** and **5'** for DP evaluation of the arms is possible due to the absence of PCL homopolymer, which was confirmed by SEC experiments, which show a curve with unimodal distribution and the absence of signals at lower molecular weight, meaning no detectable PCL homopolymer formed during the ring-opening polymerization process. The characterization data listed in Table 1 show that the experimental values $\overline{DP}_{arm}$ were slightly higher than expected. This fact can be rationalized because of the incomplete initiation of all the amine sites. Primary amines are more nucleophylic than the secondary ones, and therefore some linear units of the core could remain unreacted.

By using linear standards, the molecular weights of star polymers are usually underestimated by SEC. However, the values obtained by this technique are also collected in Table 1 together with the molecular weight dispersity, and compared with the ones calculated from the molecular weight of the core and the degree of polymerization of the

arms, determined by NMR. As can be seen, the average number molecular weight determined by NMR spectroscopy, considered to be more real, is much higher than this parameter determined by SEC. As collected in Table 1, the molar-mass dispersity is quite narrow which indicates that polymers were synthesized in a controlled manner. Furthermore, the increase of the molecular weight with increasing the ratio ε-CL/OH is evident according to SEC and NMR results.

From thermal data it was observed that the melting temperature (T_m), heat of fusion (Δh_m), crystallinity (χ) and glass transition temperature increased with increasing the molecular weight of the star polymer and the length of the arm (Table 1). This had been expected due to the effect of molecular weight on the thermal transitions of semi-crystalline polymers. The glass transition temperature is slightly lower than -62ºC, which is the value associated to the neat poly(ε-caprolactone) and neat PEI (measured by us) and are difficult to be determined when the crystallinity increases. The obtained PEI-PCLX showed thermal stability up to 310 ºC.

The complex viscosity (η^*), as a function of angular frequency, at different temperatures for the multiarm star polymers prepared was studied. Within the experimental range of frequencies all polymers showed a constant value for η^* with an Arrhenius temperature dependence. **Figure 2** shows the complex viscosity against temperature for all multiarm stars synthesized. It can be observed that the viscosity exponentially increases on increasing the arm length (or the molecular weight), reaching an exceptionally large value for PEI-PCL50. Tonhauser *et al.,*[36] studying a family of hyperbranched polyglycerol with different molecular weight, observed that the viscosity remained practically constant up molecular weights close 10000 g·mol^{-1}, but considerably increased when the molecular weight exceeded a critical molar mass of 20000 g-mol^{-1}. These authors rationalized this behavior in terms of leveling phenomenon.[37] While the molecular weight is low, there exists a constant density of the star structures (similar to hard spheres) and the viscosity hardly increases. Above of a critical molecular weight, the viscosity exponentially increases, as a consequence of the increasing significance of entanglements between star-like structures with the densely packed core region. The viscosity behavior observed for PEI-PCLX polymers can be understood likewise in terms of entanglement transition when the arm length increases.

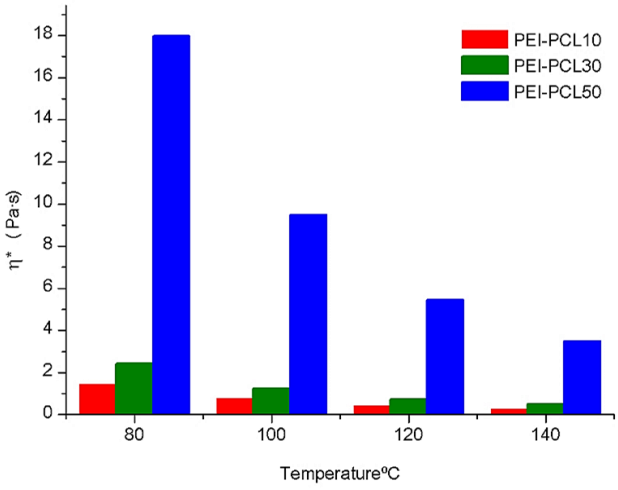

Figure 2. Complex viscosity against temperature for all multiarm stars synthesized

Curing of DGEBA with different proportions of PEI-PCLX

In a previous work it was confirmed that 5 phr of 1-methylimidazole (1MI) (0.61 mmol of initiator per gram of mixture) were necessary to assure the complete cure of DGEBA.[18] Therefore, this amount of anionic initiator was selected to prepare the formulations studied, which are collected in Table 2.

Figure 3 shows the DSC exotherms and the plots of degrees of conversion against temperature recorded at 10 ºC/min of neat DGEBA and PEI-PCL10 formulations. It can be observed, that there is not much influence on the curing exotherm when PEI-PCL10 is added. PEI-PCL30 and PEI-PCL50 formulations showed similar DSC traces than PEI-PCL10. Although these results suggests that the arm length and the proportion of modifier do not exert a significant effect on the kinetic of curing, a more detailed inspection of DSC thermogram allow to see a slight acceleration at the beginning of the curing and a deceleration as the curing progresses. This effect is slightly more pronounced with increasing PEI-PCLX content. The existence of a higher content of hydroxyl groups in PEI-PCLX formulations than in neat formulation, could increase the curing rate in the initiation step of the curing because of more activating species were formed.[30] The retarding effect observed can be attributed to the effect of the increased viscosity of the mixture and to the decrease of concentration of reactive species during curing.

Table 2 collects the main features of the curing process. The similarity between enthalpies per epoxy equivalent (value close to 100 kJ/ee) and the reported for other similar epoxy systems indicates that epoxides have reacted almost completely.[38] By FTIR-ATR spectroscopy we could prove the complete curing of the formulations, since all the epoxy groups were reacted as shown by the disappearance of the absorption at 915 cm^{-1}.

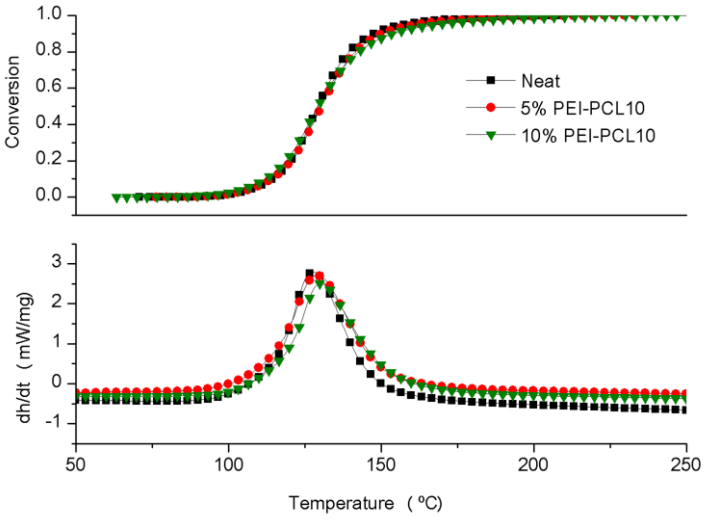

Figure 3. Calorimetric non-isothermal curves and degree of conversion against temperature of DGEBA/PEI-PCL10 formulation at 10ºC min^{-1}

In order to deeply investigate the curing, it was monitored under isothermal conditions by FTIR. **Figure 4** plots the FTIR spectra collected during isothermal curing of DGEBA with 5 phr of 1MI at 120ºC. The general features of the epoxy homopolymerization can be observed: the decrease of the epoxy band (915 cm^{-1}) and the increase of the ether band (1100 cm^{-1}) formed during ring opening polymerization of epoxy groups. It is also noticed

the growth of two bands at 1660 cm^{-1} and 1730 cm^{-1} and the grown of the hydroxyl band at 3500 cm^{-1} (inset of Figure 4). These three bands had been previously related with the mechanisms of regeneration of the 1MI during epoxy curing.[30] The bands at 1660 cm^{-1} and 1730 cm^{-1}, corresponding to the vinyl group of the enol ether and the carbonyl group of the ketone respectively, were formed during regeneration via N-dealkylation. The hydroxyl band increases due to the transformation of the alkoxide to an alcohol during regeneration via β-elimination. The relevant features of epoxy curing shown in Figure 4 are similar for all the PEI-PCLX formulations studied. In general, the results obtained were equivalent to those obtained by non-isothermal curing, and showed only a slight influence of the length of the arms and of the amount of modifier on the curing. **Figure 5** shows the conversions of epoxide groups during isothermal curing at 120ºC of DGEBA with 10% of different multiarm stars. We can see how some formulations accelerate and others decelerate the curing evolution in reference to the neat formulation, but always in little extension and without a regular trend

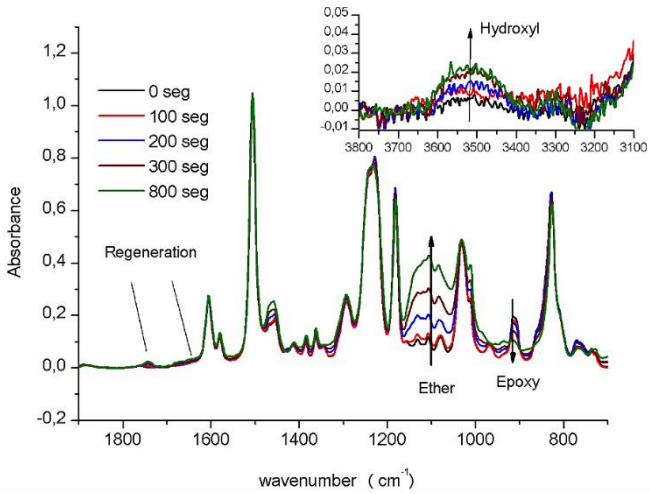

Figure 4. FTIR spectra recorded during curing of DGEBA neat formulation at 120ºC. The inset details the hydroxyl group absorption band

.

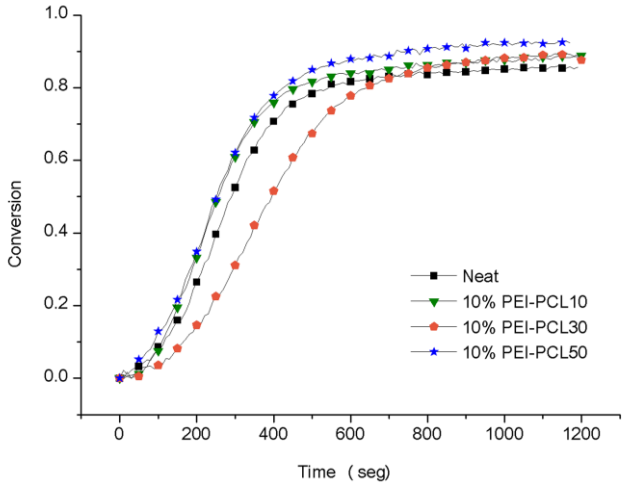

Figure 5. Conversion of epoxide groups during isothermal curing at 120ºC of DGEBA with 10% of different multiarm stars

It can be concluded that the curing kinetics of DGEBA/PEI-PCLX formulations is complex and therefore not easy to predict the effect of PEI-PCLX in the curing. Different factors such as: viscosity of the formulation, regeneration of the initiator, hydroxyl group content and amount of active species can accelerate or decelerate the process. The rate of curing is a compromise between all these factors.

On increasing the proportion of PEI-PCLX multiarm star in the formulation the T_g of the material decreases, but this decrease is not further affected by the length of the arms when PEI-PCL10 and PEI-PCL30 are compared (see Table 2). The modifiers reduce the density of croslinking of the thermoset due two different facts: 1) the chain transfer reaction between terminal hydroxyl groups and the activated epoxy groups, which stops chain growth, and 2) the plasticizing effect of flexible PEI-PCLX multiarm star. PEI-PCL50 shows higher T_g than the equivalent formulations with shorter arm length (PEI-PCL10 and PEI-PCL30). Probably, the higher entanglement of PEI-PCL50, that makes difficult the hydroxyl-induced chain-transfer reactions and the lower hydroxyl content can justify this behavior.

Rheological properties, thermal expansion coefficient and internal stress of the formulations

In order to establish the processability of the formulations, the complex viscosity of the mixtures before curing was determined by rheological experiments on varying the angular frequency. **Figure 6** shows the results at 40ºC for formulations containing 10% of modifier and for neat DGEBA catalyzed by 1MI. All formulations show a Newtonian behavior, similar to the pure stars, and the viscosity increases with the length of the arms of the star modifier. As expected, PEI-PCL50 formulations show a much higher viscosity as a result of the higher viscosity and entanglement of PEI-PCL50. The flow activation energy was determined using the Arrhenius equation and it was 53, 60 and 70 $kJ \cdot mol^{-1}$ for formulations containing a 10% of PEI-PCL10, PEI-PCL30 and PEI-PCL50, respectively. These data agree with the increase of viscosity observed (Figure 6), and could be related with the increase of the entanglement on increasing the length of the arms.

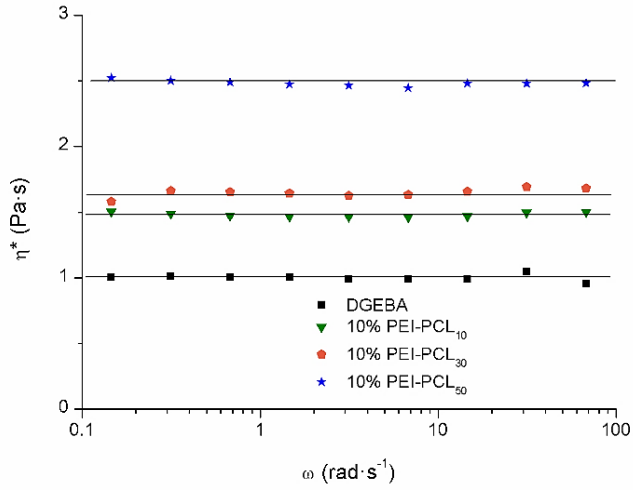

Figure 6. Complex viscosity against angular frequency at 40ºC for neat DGEBA and DGEBA containing 10% of modifier

In all cases the viscosity values, even in the PEI-PCL50 formulation, are relatively low and do not compromise the processability of the mixtures. In contrast, other authors described significant increases in viscosity when using hyperbranched hydroxyl-terminated polyesters as epoxy modifiers, because of the hydroxyl groups gave rise to hydrogen bonding.[39]

One of the most common causes of internal stresses in coatings is produced by the mismatch in the thermal expansion coefficients (CTEs) between the coating and the substrate. **Table 3** collects the CTE values in the glassy and rubbery states determined by TMA expansion experiments. In general, it can be observed that on increasing the proportion of multiarm star and the length of the arms the CTEs increase due to the introduction of flexible structures within the network structure.

Table 3. Thermal expansion coefficient and internal stresses of the DGEBA and DGEBA/PEI-PCL thermosets studied.

Formulation (wt.%)	$CTE_{glass} \cdot 10^6$ (K^{-1})	$CTE_{rubber} \cdot 10^6$ (K^{-1})	σ_{glass} (MPa)	σ_{rubber} (MPa)	σ_{total} (MPa)
0	68	175	20.46	0.13	20.59
PEI-PCL10					
5	64	174	15.00	0.64	15.64
10	72	173	14.88	0.81	15.69
PEI-PCL30					
5	71	178	17.46	0.68	18.14
10	76	179	14.70	0.87	15.57
PEI-PCL50					
5	77	185	20.89	0.64	21.53
10	74	181	18.07	0.75	18.82

In order to determine the influence of CTE increase, the generation of internal stresses during cooling of DGEBA and DGEBA/PEI-PCLX thermosets on steel rigid substrate was investigated, according to Lange *et al.* metodology.[40] Table 3 shows the calculated stresses generated during cooling above (σ_{rubber}) and below (σ_{glass}) glass transition temperature and the total stress (σ_{tot}). The following features can be observed in Table 3. The stress generated above T_g during cooling is not significant despite the high CTE, due to the low elastic modulus in the rubbery state. On the contrary, below T_g the residual stress is much higher and by far the most relevant contribution to the total stress, because of the high elastic modulus value in the glassy state and the higher temperature range during cooling below T_g. Thus, the addition of PEI-PLCX multiarm star to DGEBA reduces significantly the stress generated in the glassy state and consequently the total stress. Although the increase of CTEs on adding the multiarm star tends to increase stresses, the lower T_g values of modified formulations compensate this effect leading to a reduction of internal stresses. Formulations with 5% of PEI-PCL10 and 10% of PEI-PCL30 have lower stresses below T_g according to their lower T_g value. It can be concluded that T_g is one of the key parameters that control the residual stress build-up and therefore the stress originated can be decreased by adding modifiers that decrease the T_g of the thermoset, without much increasing the CTEs in both states.

Dynamomechanical properties of the thermosets obtained

The materials obtained were characterized by DMTA. **Figure 7** shows the mechanical relaxation spectra at 1 Hz for neat DGEBA and DGEBA/PEI-PCL10 formulations. As we can see, the curves are unimodal and as the proportion of PEI-PCL10 increases, the modulus-temperature and the tan δ-temperature curves are shifted towards lower temperature. Formulations containing PEI-PCL30 and PEI-PCL50 show a similar mechanical relaxation pattern. **Table 4** collects the dynamomechanical data for all the formulations studied. The decrease of the modulus after relaxation on adding the modifier can be appreciated. The behavior observed by DMTA is consistent with the lower T_g values revealed by DSC, and agree with the decrease of croslinking density and with the flexibilizing effect of PEI-PCL. Table 4 also shows that the width of the tan δ curves barely change on increasing the proportion of modifier, indicating that the homogeneity of the network is not significantly affected.

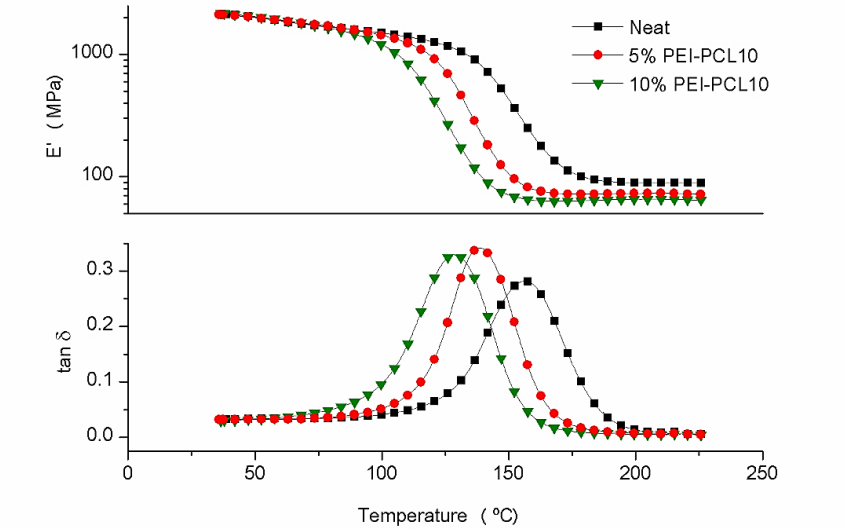

Figure 7.Tan δ against temperature at 1Hz and storage modulus against temperature at 1Hz for neat DGEBA and DGEBA containing different amounts of PEI-PCL10

The absence of mechanical relaxation, at temperatures below ambient, associated to PEI-PCLX, suggests that the materials do not present phase separation. The β-relaxation peak of DGEBA (at -60ºC, figure not shown) does not increase on adding PEI-PCL. It is generally accepted that the increase in the area of the β-relaxation correlates with the increase in impact resistance.[41] Consequently, it is not expected that PEI-PCL can enhance the toughness to a significant extent.

Table 4. Results of the DMTA (1 Hz) and TGA analysis for the thermosets obtained from DGEBA and DGEBA/PEI-PCL formulations

Formulation (wt.%)	DMTA				TGA	
	$T_{tan\delta}$ [a] (ºC)	E'_u [b] (MPa)	E'_r [c] (MPa)	FWHM [d] (ºC)	$T_{5\%}$ [e] (ºC)	T_{max} [f] (ºC)
0	157	2125	90	36	408	454
PEI-PCL10						
5	139	2093	72	30	408	454
10	129	2042	64	34	400	454
PEI-PCL30						
5	141	2087	78	30	400	454
10	139	2035	68	34	400	454
PEI-PCL50						
5	147	2170	95	32	392	454
10	130	2087	68	32	385	454

[a] Temperature of maximum of tan δ
[b] Storage modulus in the glassy state determined at 40ºC
[c] Storage modulus in the rubbery state determined at tan δ peak + 50ºC
[d] FWHM stands for full width at half maximum
[e] Temperature of the onset decomposition on TGA data at 10ºC·min^{-1} calculated for a 5% weight loss
[f] Temperature of the maximum decomposition rate based on the TGA data at 10ºC·min^{-1}

Thermal stability of the thermosets obtained

Table 4 shows the results of the thermogravimetric analysis in nitrogen atmosphere. The addition of PEI-PCL barely modifies the thermal stability, since the temperature of the maximum degradation rate remains constant and only the onset temperature slightly decreases. This result is completely different from the previously obtained using multiarm stars with poly(glycidol) core and poly(ε-caprolactone) arms of the same length as DGEBA modifier, in which the thermal stability of the materials decreases dramatically.[6] Probably, the higher stability of amide bonds between the core and the arms in PEI-PCL in comparison to the ester bonds between the poly(glycidol) core and the poly(ε-caprolactone) arms can justify these results, since the length and the chemical nature of arms are the same for both multiarm stars. Other dendritic polymers containing aliphatic ester groups used as epoxy modifiers show a low thermal stability, due to the β-elimination reaction that take place through the labile ester groups.[42] In reworkable materials this characteristic can be useful, but not for other applications where high thermal stalility is required. In the light of the present results, it can be envisioned the use of DGEBA/PEI-PCL thermosets for structural applications.

Mechanical characterization and morphology

The toughness behavior of neat DGEBA and DGEBA/PEI-PCLX modified thermosets has been investigated by impact test, and the morphology has been analyzed by SEM on the fracture surface of the samples. The results of the impact tests are collected in **Figure 8** for all the materials prepared. We can see that only two formulations, 10% PEI-PCL30 and 5% PEI-PCL50, have higher impact strength than neat DGEBA. Moreover, there is not a clear relationship between the length of the arms or the amount of modifier and the values of impact strength.

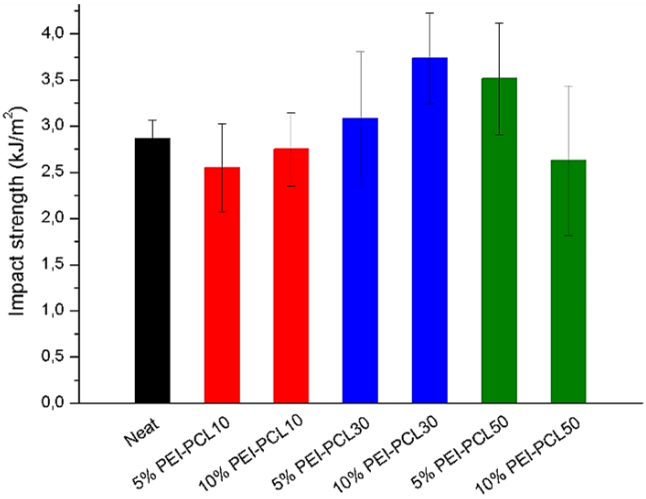

Figure 8. Dependence of impact strength of DGEBA thermosets containing different weight percentages of PEI-PCL10, PEI-PCL30 and PEI-PCL50

Figure 9 shows the SEM micrographs for the fracture surface for all the thermosets prepared. As it can be seen, the fracture surfaces of all materials consist of only one phase, are relatively fragile and present a homogenous appearance, due to the good compatibility between PCL and the DGEBA matrix. Although, the differences are not very important, the fracture surface of the material containing a 10% of PEI-PCL30 shows more yielding than the others, with thicker cracks, in agreement with the higher impact strength value measured for this formulation.

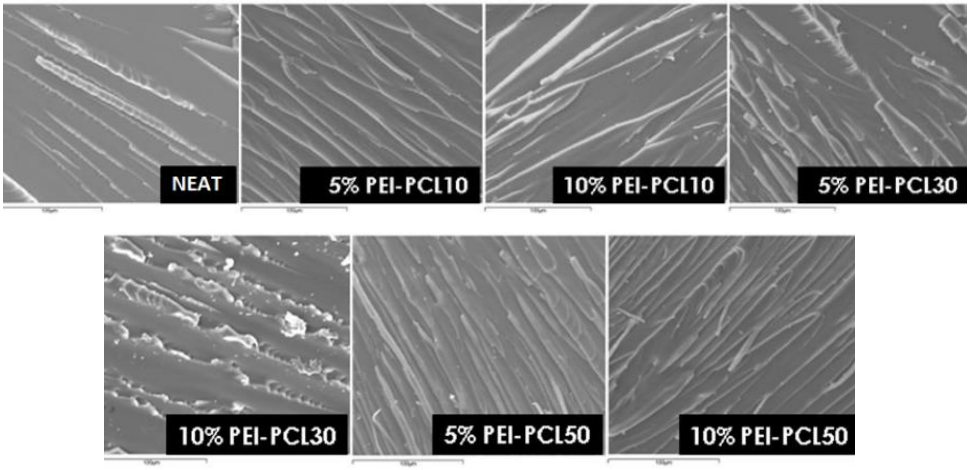

Figure 9. SEM micrographs at 500 magnifications for the fracture surface for all the thermosets prepared

Conclusions

Following a “core-first” strategy, multiarm star polymers based on hyperbranched poly(ethyleneimine) core and poly(ε-caprolactone) arms with different lengths were obtained by a cationic ring-opening polymerization of ε-caprolactone from a commercially

available hyperbranched poly(ethyleneimine) core and used as modifier in the curing of DGEBA with 1-methyl imidazole as an anionic initiator.

The addition of these novel star polymers synthesized barely modified the curing kinetics, which are controlled by different factors such as: the viscosity, the regeneration of initiator, the hydroxyl group content and the amount of active species.

New thermosetting materials with slightly improved toughness and low stress generation during cooling were obtained without compromising the thermal stability and without much affecting the glass transition temperature. The new thermosets obtained are homogeneous without any phase separation. The best improvement in impact resistance was obtained with the addition of a 10% of PEI-PCL30 or 5% of PEI-PCL50.

The modified materials showed some differences in reference to the neat DGEBA but they were quite similar regardless of the length of the arms of the star modifier, due to their special topology.

From the point of view of the processability, the addition of the synthesized multiarm stars to DGEBA formulations did not increase much the viscosity of mixtures, even when stars with long arms that allow entanglement were used.

Thus, one can conclude that PEI-PCLX star-like structures are suitable modifiers for epoxy resins enhancing toughness, reducing internal stresses without affecting negatively other properties and processability.

References

[1] C.A. May, (ed.), Epoxy Resins. Chemistry and technology, Marcel Dekker, New York, 1988, Chapter 1.
[2] E.M, Petrie, Epoxy Adhesive Formulations, McGraw-Hill, New York, 2006.
[3] J.P. Pascault, R.J.J. Williams, Epoxy Polymers, Wiley VCH, Weinheim, 2010, Chapter 1.
[4] Y. Meng, X.-H. Zhang, B.-Y. Du, B.-X. Zhou, X. Zhou, G.-R.Qi, Polymer 52 (2011) 391-399.
[5] M. Morell, A. Lederer, X. Ramis, B. Voit, A. Serra, J. Polym. Sci. Part A: Polym. Chem. 49 (2011) 2395-2406.
[6] M. Morell, D. Foix, A. Lederer, X. Ramis, B. Voit, A. Serra, J. Polym. Sci. Part A: Polym. Chem. 49 (2011) 4639-4649.
[7] D. Foix, E. Jiménez-Piqué, X. Ramis, A. Serra, Polymer 52 (2011) 5009-5017.
[8] M. Morell, X. Ramis, F. Ferrando, A. Serra, Polymer 52 (2011) 4694-4702.
[9] M. Morell, X. Fernández-Francos, J. Gombau, F. Ferrando, A. Lederer, X. Ramis, B. Voit, A. Serra, Prog. Org. Coat. 73 (2012) 62-69.
[10] M. Morell, X. Ramis, F. Ferrando, A. Serra, Macromol. Chem. Phys. 213 (2012) 335-343.
[11] F. Däbritz, B. Voit, M. Naguib, M. Sangermano, Polymer 52 (2011) 5723-5731.
[12] J. Karger-Kocsis, J. Fröhlich, O. Gryshchuk, H. Kautz, H. Frey, R. Mülhaupt, Polymer 45 (2004) 1185-1195
[13] M. Morell, M. Erber, X. Ramis, F. Ferrando, B. Voit, A. Serra, Eur. Polym. J. 46 (2010) 1498-1509.
[14] J.P. Yang, Z.K. Chen, G. Yang, S.Y. Fu, L. Ye, Polymer 49(2008) 3168-3175.
[15] M. Morell, X. Ramis, F. Ferrando, Y. Yu, A. Serra, Polymer 50 (2009) 5374-5383
[16] J. Zhang, Q. Guo, B. Fox, J. Polym. Sci. Part B: Polym. Phys. 48 (2010) 417-424.
[17] J.E. Klee, C. Schneider, D. Hölter, A. Burgath, H. Frey, R. Mülhaupt, Polym. Adv. Technol.12 (2001) 346-354.
[18] X. Fernández-Francos, J.M. Salla, A. Mantecón, A. Serra, X. Ramis, J. Appl. Polym. Sci. 109 (2008) 2304-2315.
[19] D. Foix, M. Erber, B. Voit, A. Lederer, X. Ramis, A. Mantecón, A. Serra, Polym. Degrad. Stab. 95 (2010) 445-452.
[20] E. Zagar, M. Zigon, Prog. Polym. Sci. 36 (2011) 53-88.
[21] S. Maier, A. Sunder, H. Frey, R. Mülhaupt, Macromol. Rapid. Commun. 21 (2000) 226-230.

[22] C. Liu, Y. Zhang, J. Huang, Macromolecules 41 (2008) 325-331.
[23] H. Gao, K. Matyjaszewski, Macromolecules 41 (2008) 1118-1125.
[24] M. Mendrek, B. Trzebicka, W. Walach, A. Dworak, Eur. Polym. J. 46 (2010) 2341-2351.
[25] D. Santiago, X. Fernández-Francos, X. Ramis, J.M. Salla, M. Sangermano, Thermochim. Acta 526 (2011) 9-21.
[26] X. Fernández-Francos, D. Santiago, F. Ferrando, X. Ramis, J.M. Salla, A. Serra, M. Sangermano, J. Polym. Sci. Part B: Polym. Phys. 50 (2012) 1489-1503.
[27] W. Fan, L. Wang, S. Zheng, Macromolecules 42 (2009) 327-336.
[28] N. Hameed, Q. Guo, T. Hanley, Y.W. Mai, J. Polym. Sci. Part B: Polym. Phys. 48 (2010) 790-800.
[29] L.H. Sperling, Introduction to Physical Polymer Science, Wiley Interscience, Hoboken, 2006, p 573.
[30] X. Fernández-Francos, W.D. Cook, A. Serra, X. Ramis, G.G. Liang, J.M. Salla, Polymer 51 (2010) 26-34.
[31] D.W. van Krevelen, Properties of Polymers, 3rd ed., Elsevier, Amsterdam, 1994.
[32] S. Kanaoka, M. Sawamoto, T. Higashimua, Macromolecules 24 (1991) 2309-2313.
[33] J. Xia, X. Zhang, K. Matyjaszewski, Macromolecules 32 (1999) 4482-4484.
[34] B. Voit, A. Lederer, Chem. Rev. 109 (2009) 5924-5973.
[35] T. Biela, A. Kowalski, J. Libiszowski, A. Duda, S. Penczek Macromol. Symp. 240 (2006) 47-55.
[36] C. Tonhauser, D. Wilms, Y. Korth, H. Frey, C. Friedrich, Macromol. Rap. Commun. 31 (2010) 2127-2132.
[37] M.J.A. Hule, M. Johansson, E. Malmström, Adv. Polym. Sci. 143 (1999) 1-34.
[38] K.J. Ivin, in: J. Brandrup, E.H. Immergut (Eds.), Polymer Handbook, Wiley, New York, 1975.
[39] G. Cicala, A. Recca, C. Restuccia, Polym. Eng. Sci. 45 (2006) 225-237.
[40] J. Lange, S. Toll, J.-A.E.Manson, A. Hult, Polymer 36 (1995) 3135-3141.
[41] J. Kager-Kocsis, V.N. Kuleznev, Polymer 23 (1982) 699-705.
[42] X. Fernández-Francos, J.M. Salla, A. Cadenato, J.M. Morancho, A. Serra, A. Mantecón, X. Ramis, J. Appl. Polym. Sci., 111 (2009) 2822-2829.

4.3 New epoxy thermosets modified with multiarm star poly(lactide) with poly(ethylenimine) as core of different molecular weight

Cristina Acebo, Xavier Fernández-Francos, Francesc Ferrando, Àngels Serra, Xavier Ramis

European Polymer Journal **2013***, 49,* 2316-2326

UNIVERSITAT ROVIRA I VIRGILI
HYPERBRANCHED POLY(ETHYLENEIMINE) DERIVATIVES AS MODIFIERS IN EPOXY NETWORKS
Cristina Acebo Gorostiza

European Polymer Journal **2013**, *49*, 2316-2326

New epoxy thermosets modified with multiarm star poly(lactide) with poly(ethyleneimine) as core of different molecular weight

Abstract

Multiarm stars containing a hyperbranched poly(ethyleneimine) core of different molecular weight and poly(lactide) arms were synthesized by cationic ring-opening polymerization of lactide from a hyperbranched poly(ethyleneimine) core. After characterization by rheometry, calorimetry, thermogravimetry and nuclear magnetic resonance, these polymers were used as chemically modifiers in the anionic curing of diglycidylether of bisphenol A epoxy resin. The curing process was studied by dynamic scanning calorimetry, demonstrating the influence of the mobility of the reactive species and the hydroxyl content on the curing kinetics. The resulting materials were characterized by thermal and mechanical tests. The addition of the multiarm stars led to homogeneous materials with a slight improvement on the impact strength in comparison with the neat material, without compromising the glass transition temperature. The reworkable nature of the materials was demonstrated by monitoring the changes in their glass transition under thermal rework conditions.

Keywords: Star polymers, poly(ethyleneimine), poly(lactide), epoxy resin, anionic polymerization.

Introduction

Epoxy resins have been widely used in technological applications such as adhesives, matrices in advanced composites, surface coatings and electronic device assemblies because of their good combination of high strength and stiffness, excellent corrosion protection and good electrical properties.[1-3] However, the high crosslinking density and chain stiffness of the cured network leads to low impact resistance, which places a limitation on their potential range of applications. In addition, when epoxy resins are used as coatings, the curing shrinkage promotes the appearance of internal stresses, which can lead to the generation of microvoids and microcracks, the loss of adhesion and deformation due to warping. Stresses can also appear during their processing and service life due to the mismatch between the thermal expansion coefficients of the polymer coating and the metallic substrate, the former being significantly higher. These drawbacks reduce the protection capability and durability of the coating materials and allow corrosion of the substrate to take place as a result of the penetration of moisture. On the other hand, it is difficult to recycle or repair coated devices at the end of their service life because the thermosetting coating cannot be easily removed by solvents or thermal treatment; only pyrolysis can be used, which involves a significant waste of energy in addition to some other problems.

The aim of this manuscript is the preparation and characterisation of novel thermosets, based on epoxy resins and dendritic polymers, with enhanced toughness, reworkability and with low internal stresses while maintaining their thermomechanical characteristics and processability.

Recently, star-like topologies have attracted considerable interest because of their unusual physical and rheological properties, which allow the enhancement of some characteristics of epoxy thermosets.[4-12] The properties of the final materials and the

processability can be tailored as a function of the core and arms structures, the type and amount of functional end groups, the molecular weight and length and number of the polymeric arms.

In previous studies, multiarm stars with poly(ε-caprolactone) arms with hyperbranched poly(glycidol) or poly(ethyleneimine) as a core have been synthesized and studied as modifiers in the curing of diglycidylether of bisphenol A epoxy resin, using cationic and anionic initiators as curing agents.[8,9,12] In general, the processability of the reactive mixtures was barely worsened in comparison with the neat formulation and even the viscosity was reduced when poly(glycidol)-*b*-poly(ε-caprolactone) multiarm stars had arms with a degree of polymerization of 10. The T_gs of the cured materials were hardly reduced. The thermal stability of all materials was not affected with the exception of poly(glycidol)-*b*-poly(ε-caprolactone)/epoxy formulations, which had a significantly lower initial degradation temperature than the unmodified formulation. Impact strength was improved in all cases to a greater or lesser extent.

Recently Lupasol®, which is the trade name of a hyperbranched poly(ethyleneimine) produced by BASF, has been used as a multifunctional crosslinker for epoxy resins. The densely branched architecture of high molecular weight Lupasol® created significant mobility restrictions, which had a strong effect on the glass transition temperature and on the degree of croslinking of the cured materials.[13]

Taking into account these previous works, in the present study we have synthesized, following the “core-first” approach,[14-18] multiarm stars with poly(lactide) (PLA) arms and hyperbranched poly(ethyleneimine)s (PEI) of different molecular weight core. These multiarm star polymers have been used to modify diglycidylether of bisphenol A using 1-methylimidazole as an anionic initiator. The crosslinking process has been monitored by differential scanning calorimetry and the obtained materials have been characterized by thermal and mechanical tests and electron microscopy.

Given that PLA arms contain rigid esters of secondary alkyl groups in their structural units, it is expected to produce materials with a higher reworkability and higher glass transition temperature than those obtained with similar stars with PCL arms, which are more flexible and have primary ester linkages that are less thermally degradable. We have limited the degree of polymeritzation of the arms to about 10 in order to ensure that the weight of the arms is not much larger than that of the core. Thus it is expected that both the arms and the core structure will tailor the final material properties. 1-methylimidazole has been selected in the present work as anionic initiator with the purpose of allowing the incorporation of hydroxyl-terminated polymers into the network structure, through the chain-transfer reactions between hydroxyl terminal groups of star and epoxide groups.[8,12]

Although amphiphilic poly(ethyleneimine)-*b*-poly(lactide) multiarm stars have been used as nanocarriers,[17,18] to the best of our knowledge, this is the first time that this kind of polymers has been used as epoxy modifier.

Experimental

Materials

Poly(ethyleneimine) (PEI) Lupasol®FG (PEI800, 800 g/mol) and Lupasol®PR 8515 (PEI2000, 2000 g/mol) were kindly donated by BASF and used without further purification.

From the molecular weight of the polymer and of the repeating unit an average degree of polymerization of 18.6 for Lupasol®FG and 46.5 for Lupasol®PR 8515 were calculated. According to the data sheet, the relationship (NH_2/NH/N) was (1/0.82/0.53) for Lupasol®FG and (1/0.92/0.70) for Lupasol®PR 8515 thus by calculations the equivalent number of primary, secondary and tertiary amines is 0.010, 0.00837, and 0.0053 eq/g for Lupaso®FG and 0.0089, 0.0082, and 0.0062 eq/g for Lupasol®PR 8515. Lactide (LA), tin (II) 2-ethylhexanoate ($Sn(oct)_2$, 98 %) and 1-methylimidazole (1MI, 99 %) were purchased from Sigma-Aldrich and used without further purification. Solvents were purchased from Scharlab and were purified by standard procedures. Diglycidylether of bisphenol A (DGEBA, Araldite GY 240) was kindly provided by Huntsman (EEW = 182 g/eq).

Synthesis of poly(ethyleneimine)-poly(lactide) multiarm stars (PEIX-PLA)

In the acronym PEIX-PLA, X accounts for the molecular weight of the poly(ethyleneimine) core in the star and can take the values of 800 g/mol and 2000 g/mol. The degree of polymerization of poly(lactide) arms in the star is similar.

The synthesis is exemplified for PEI800-PLA. 0.73 g of PEI800 (0.91 mmol) and 9.47 g of LA (65.7 mmol) were placed at room temperature in a two-necked flask equipped with a magnetic stirrer and a gas inlet to fill the flask with argon. Then, $Sn(oct)_2$ was added to the solution mixture with a feed molar ratio of [LA]/[$Sn(oct)_2$], 155:1 (0.17 g, 0.42 mmol) and the flask was immersed in a thermostated oil bath at 130 ºC during 24 hours [19]. After cooling down, the mixture was dissolved in a mixture of chloroform and methanol (2:1 v/v), and stirred at room temperature for 4 h. Subsequently, the mixture was precipitated in diethyl ether, filtered and then dried at 40ºC under vacuum for one day. ^{1}H NMR (400 MHz, $CDCl_3$, in ppm): 5.16 (-OCOC<u>H</u>(CH_3), -NHCOC<u>H</u>(CH_3), **a** and **a'**), 4.35 (-OCOC<u>H</u>(CH_3)OH, **b**), 3.5-2.5 (broad signals, PEI core), 1.57 (-NHCOCH(C<u>H</u>$_3$), -OCOCH(C<u>H</u>$_3$), **c'** and **c**) and 1.46 (-COCH(C<u>H</u>$_3$)OH, **d**) (see **Figure 1**). Average molecular weights and thermal data of all the multiarm stars obtained are given in **Table 1.**

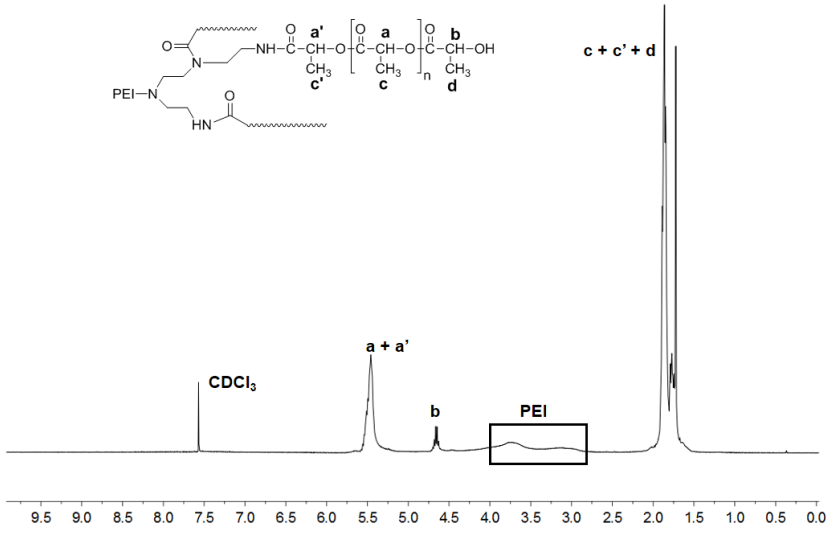

Figure 1. ^{1}H-NMR spectrum in $CDCl_3$ of PEI800-PLA multiarm star copolymer.

Table 1. Data of the mutiarm stars PEIX-PLA synthesized in this study.

Polymers	LA/NH[a]	Yield (%)	$\overline{DP}_{arm}$ [b]	$\overline{M}_{n,\exp 1}$ [c]	$\overline{M}_{n,\exp 2}$ [d]	$\frac{\overline{M}_w}{\overline{M}_n}$ [e]	T_g [f] (ºC)	$T_{5\%}$ [g] (ºC)
PEI800-PLA	5	57	8	8872	1334	1.87	39	212
PEI2000-PLA	5	52	8	22178	2108	1.44	42	208

[a] Feed ratio lactide monomer/NH active groups
[b] Average number of repeating lactic units in the arms determined by ^{1}H-NMR spectroscopy
[c] Average molecular weight in number calculated by ^{1}H-NMR spectroscopy
[d] Average molecular weight in number determined by SEC
[e] Molar-mass dispersity determined by SEC
[f] Glass transition temperature determined by DSC
[g] Temperature of the 5% weight loss determined by TGA

Preparation of reactive mixtures

The mixtures were prepared by adding the required amount of PEIX-PLA to the epoxy resin and gently heating until it was dissolved and the solution became clear. Then, 5 phr of 1MI (part of initiator per hundred parts of DGEBA)[12] were added and the resulting solution was stirred and cooled down to -20 ºC to prevent polymerization. Mixtures containing 5 and 10 phr of PEIX-PLA in reference to DGEBA were prepared. The compositions of the studied formulations are detailed in **Table 2.**

Table 2.Composition and calorimetric data of DGEBA/1-MI mixtures with different percentages of PEIX-PLA

Formulation (wt.%)	Eq_{OH}: Eq_{epoxy} [a]	E_a [b] (kJ/mol)	ln A [c] (s^{-1})	$k_{150ºC}\cdot 10^3$ [d] (s^{-1})	Δh [e] (J/g)	Δh [e] (kJ/ee)	$T_{g\infty}$ [f] (ºC)
0	0	59.8	16.77	13.1	515	96	156
PEI800-PLA							
5	0.0143	63.3	17.21	7.65	495	99	143
10	0.0286	67.6	18.67	9.58	488	102	124
PEI2000-PLA							
5	0.0144	64.1	17.63	9.24	499	100	138
10	0.0287	66.0	18.16	9.11	486	102	123

[a] Equivalent ratio (OH in PEIX-PLA/epoxide groups)
[b] Values of activation energy at 0.5 of conversion were evaluated by isoconversional non-isothermal integral procedure
[c] Values of pre-exponential factor at 0.5 of conversion for A_2 kinetic model with $g(\alpha)=[-\ln(1-\alpha)^{1/2}]$
[d] Values of rate constant at 0.5 of conversion and 150ºC calculated using the Arrhenius equation
[e] Reaction heats determined by DSC
[f] Glass transition temperature of the thermosets obtained of an isothermal cured samples (1 hour at 100ºC + 1 hour at 140ºC)

Characterization

^{1}H NMR measurements were carried out at 400 MHz and in a Varian Gemini 400 spectrometer. $CDCl_3$ was used as the solvent. For internal calibration, the middle solvent signal corresponding to $CDCl_3$ was taken as δ (^{1}H) = 7.26 ppm.

Molecular weight and molecular weight distribution was determined by means of an Agilent 1200 series SEC-system with a combination of PL-GEL 3, PL-GEL 5 and PL-GEL 20 µm mixed A columns in series, equipped with an Agilent 1100 series refractive index

detector. Calibration curves were based in polystyrene standards having low molecular weight dispersity using a flow rate of 1 mL/min and THF as eluent. The sample concentrations were between 5 and 10 mg/mL and injection volumes of 100 µL were used.

Calorimetric analyses were carried out on a Mettler DSC-822e thermal analyzer. Samples of approximately 10 mg were placed in aluminum pans under nitrogen atmosphere. The calorimeter was calibrated using an indium standard (heat flow calibration) and an indium-lead-zinc standard (temperature calibration).

Multiarm star polymers were analyzed from -50 to 150 ºC at a heating rate of 10 ºC/min in order to determine their glass transition temperature (T_g). Thermal data are collected in Table 1.

Non-isothermal curing of DGEBA/PEIX-PLA/1MI mixtures was performed from 30 to 300 ºC at heating rates of 2, 5, 10 and 20 ºC/min in order to determine the reaction heat associated with the complete conversion of all reactive groups and study the curing kinetics.

The kinetic triplet [pre-exponential factor, activation energy, and the kinetic model] of the curing was determined using integral isoconversional non-isothermal kinetic analysis, Kissinger-Akahira-Sunose equation, combined with the Coats-Redfern procedure. Details of the kinetic methodology are given in previous studies.[19]

The glass transition temperatures ($T_{g\infty}$s) of the fully cured materials, after an isothermal curing schedule of 1h at 100ºC and 1 h at 140ºC, were determined from a non-isothermal scan at 10 ºC/min as the temperature of the half-way point of the jump in the heat capacity when the material changed from glassy to the rubbery state under N_2 atmosphere. The error is estimated to be approximately ± 1 °C. No residual curing exotherm was detected.

Thermogravimetric analyses were carried out in a Mettler TG50 thermobalance. Samples with an approximate mass of 8 mg were heated from 30 to 800 ºC at 10 ºC/min in N_2 (100 cm^3/min measured in normal conditions).

Dynamic mechanical thermal analyses were carried out with a TA Instruments DMA Q800. The samples were cured isothermally in a mould at 100 ºC for 1 h and then post-cured for 1 h at 140 ºC. Single cantilever bending at 1 Hz and deformation of 0.05% was performed at 3 ºC/min, from 35 ºC to 230 ºC on prismatic rectangular samples (10 x 10 x 1 mm^3).

Thermomechanical analyses were carried out on a Mettler TMA40 thermomechanical analyzer. The samples were supported by two silica discs and heated at 5ºC/min from 40 up to 180ºC, applying of a force of 0.02N. The thermal expansion coefficients (CTEs) below and above the T_g were calculated as follows:

$$CTE = \frac{1}{L_0} \cdot \frac{dL}{dT} = \frac{1}{L_0} \cdot \frac{dL/dt}{dT/dt} \quad (1)$$

where, L is the thickness of the sample, L_0 the initial length, t the time, T the temperature and dT/dt the heating rate.

Rheological measurements were carried using an ARG2 rheometer (TA Instruments, UK) equipped with an electrically heated plates system, EHP and disposable parallel plates (25 mm diameter).

Complex viscosity (η^*) of the mixtures at 40 and 60ºC and of the multiarm star polymers at 60, 80 and 100ºC was recorded as function of angular frequency under a constant deformation. At each temperature strain-sweep and frequency sweep experiments were performed to determine the linear viscoelastic region. For the mixtures, it was determined varying the angular frequency (0.05-10 Hz) with a constant deformation of 15% and for the multiarm star polymers it was determined varying the angular frequency (0.02-20 Hz) and using a constant deformation of 2% (PEI2000-PLA) and 10% (PEI800-PLA).

Impact tests were performed at room temperature by means of a Zwick 5110 impact tester according to ASTM D4508-10 standard using rectangular samples (25 x 12 x 2.5 mm^3) cured using the same temperature schedule for as the DMTA samples. The pendulum employed had a kinetic energy of 0.5 J. For each material 8 determinations were made. The impact strength (IS) was calculated from the energy absorbed by the sample upon fracture as:

$$IS = \frac{E - E_0}{S} \quad (2)$$

where E and E_0 are the energy loss of the pendulum with and without sample respectively, and S is the cross-section of the samples.

The fracture area of impacted samples was metalized with gold and observed with a scanning electron microscope (SEM) Jeol JSM 6400 with a resolution of 3.5 nm.

Results and discussion

Synthesis and characterization of multiarm stars

The synthesis of the multiarm star polymers was carried out by the core first approach, which consists in a living polymerization of lactide from a poly(ethyleneimine) multifunctional core. We used commercial poly(ethyleneimine) (Lupasol®) of different molecular weight and different equivalents of reactive groups as the multifunctional core to form the arms from lactide by a living cationic polymerization employing $Sn(oct)_2$ as the catalyst.[18] The synthetic pathway is depicted in **Scheme 1**.

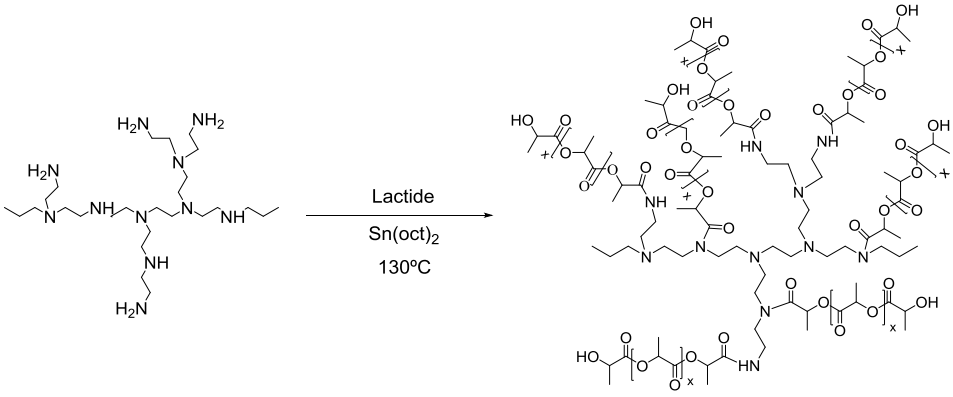

Scheme 1. Synthetic route to the multiarm star copolymers PEIX-PLA

From the degree of polymerization of PEI, the proportion of NH_2/NH/N and the equivalent number of amines by gram of PEI we calculated the average number of active

groups per molecule, only NH_2 and NH, capable of acting as initial growing sites for PLA chains, which resulted to be 14 for PEI800 and 35 for PEI2000. From this number and the desired degrees of polymerization of PLA the quantity of lactide to be polymerized was calculated.

Zhang *et al.*[18] reported a reinvestigation of the synthesis of PEI-PLA multiarm stars, which was previously reported by Adelli *et al.*[17] They concluded that the efficiency of initiation of NH_2 groups is about 100%, whereas the initiation efficiency of NH is about 89%. However, they used PEI cores of 10000 g/mol, which can lead to higher steric hindrances in the initiation step than in our case. These authors optimized the proportion of LA/$Sn(oct)_2$ to 155/1, which was used in our experiments, and the temperature of polymerization to 130ºC, which gave the best control of the polymerization degree. However, they described that higher degrees of LA polymerization than expected were obtained, and some linear PLA was also formed.

The reaction was performed in bulk at 130 ºC for 24 h under argon atmosphere and produced a solid which was solubilized in a mixture of $CHCl_3$/MeOH, then precipitated in diethyl ether and dried in vacuum. The polymers were obtained as brownish powders. It should be noted that the yield was not high due to the fact that the polymerization of lactide was not complete. Thus, in the diethyl ether solution the presence of unpolymerized lactide was always observed. Previous studies[18,20] reported similar results and pure lactide was separated or remained unreacted as impurities in the synthesized star. The precipitation of the solution over diethyl ether led to the complete elimination of unreacted lactide. The elimination of lactide by sublimation or by dialysis gave not as good results.

To evaluate the degree of polymerization achieved in the PLA arms and to confirm the chemical structure of the multiarm stars, ^{1}H-NMR spectra were registered. Figure 1 shows the ^{1}H-NMR spectrum in $CDCl_3$ of PEI800-PLA multiarm star with the corresponding assignments. In addition to the broad signals attributed to the PEI core three groups of signals clearly appear. The methyl protons of the lactide of the final and repetitive unit (**d** and **c**+**c'**) appear at 1.3-1.6 ppm and the methine protons of the final and repetitive unit (**b** and **a**+**a'**) at 4.35 and 5.2 ppm. By integration of these methine signals and applying the following equation, the degree of polymerization of the arms ($\overline{DP}_{arm}$) could be calculated.[18]

$$\overline{DP}_{arm} = \frac{[I(a+a')+I(b)]}{I(b)} \quad (3)$$

This calculation can be performed because of the absence of linear lactide homopolymer, which was confirmed by SEC experiments. A unimodal distribution was obtained in the chromatograms which confirmed the well-defined multiarm star structures of the synthesized products. The expected $\overline{DP}_{arm}$ was 10, taking into account that lactide molecule introduces two lactic repetitive units, and including the unit directly attached to the PEI core and the final unit. However, Table 1 shows that the experimental values $\overline{DP}_{arm}$ were lower than expected, due to incomplete reaction of lactide.

The molecular weight of PEI800-PLA and PEI2000-PLA determined with SEC are collected in Table 1 together with the molecular weight dispersity, and compared with the molecular weight calculated from ^{1}H-NMR spectroscopic analysis. The values determined with SEC are underestimated because of the use of linear standards and the compact

structures of the multiarm stars. In contrast, the calculation by ^{1}H-NMR, which takes into account the molecular weight of the PEI core, the number of arms and their molecular weight, is significantly higher and far more realistic. The molar-mass dispersity is quite narrow which indicates that polymers were synthesized in a controlled manner.

By calorimetric measurements we determined the glass transition temperature of both polymers. The larger star presents a slightly higher value, as expected. The presence of the PLA arms increases the T_g value of the PEI core which is below 0ºC.

PLA is a thermally degradable polymer[21] because of the presence of ester groups of secondary alkyl moieties in the main chain that can break by a thermal β-elimination process at about 200-250ºC.[22] Low temperatures of 5% of weight loss were determined by TGA, as shown in Table 1**.** PEIX-PLA decompose in two well-resolved degradation steps (figure not shown), the first one with a peak temperature around 260ºC corresponding to the decomposition of PLA arms and the second one with a peak temperature around 350ºC associated to the decomposition of PEI core. The assignment of both peaks was made by comparison between TGA traces of PEIX-PLAs and neat PLA, neat PEI800 and neat PEI2000 and taking account the relative amount of PEI and PLA in the multiarm star.

The rheologic behavior of the multiarm star polymers was studied, taking into account the effects of the angular frequency and temperature (T > T_g). The dynamic frequency sweeps experiments showed that both star polymers did not have a constant value of η^* with frequency at the different temperatures. This result is different from that in the previous work using multiarm stars with poly(ethyleneimine) core and poly(*ε*-caprolactone) arms.[12] In order to understand their complex behaviour, a different strategy was used, based on the combination of frequency sweep experiments at different temperatures and the application of the time-temperature superposition principle, in order expand the frequency range at a given temperature. Only shifts along the frequency scale were performed and were fitted with the Williams-Landel-Ferry equation (WLF equation).

$$\log a_T = \frac{-C_1(T-T_{ref})}{C_2+T-T_{ref}} \quad (4)$$

where a_T is the shift factor, T_{ref} the reference temperature and C_1 and C_2 (K) are fitting parameters.[23] Master curves were obtained at 60, 80 and 100ºC.

Figure 2 shows the master curves for both multiarm star polymers (T_{ref} =60ºC). For the PEI2000-PLA, the storage modulus G' is below the loss modulus G'' throughout a large frequency range investigated, although at lower frequencies there is a moduli crossover with a constant G', around 10-20 Pa down to the lowest frequencies, which is evidence of some weak structure. Moreover, it is also observed a significant increase in complex viscosity towards the lowest frequencies. Both phenomena can be related to the yield stress, the minimum shear stress corresponding to the first evidence of flow. A minimum shear stress is needed to break this weak structure of 10-20 Pa and make the molecules flow. This kind of solid-like to liquid-like transition is also evidenced by the G'-G'' crossover at low frequencies. Helgeson *et al.* observed a similar behavior, but they didn't explain the reasons of that.[24] The underlying phenomena to this dynamic response would be (1) the topology of the multiarm stars, with a high degree of arm interpenetration between neighboring stars due to their high core functionality and (2) the strong intermolecular H-bonding interactions between the arms of one star and the core of a neighboring star or

between neighboring cores. A Newtonian behaviour, with constant η^*, is observed in the middle frequency range, while at higher frequencies the complex viscosity decreases. This shear-thinning at high frequencies is commonly observed in the rheological analysis of polymers.[25] Vukovic *et al.* investigated the rheological properties of aliphatic hyperbranched polyesters and attributed the strong viscosity decrease with increasing shear rate to the cleavage of the intermolecular hydrogen bonds.[26]

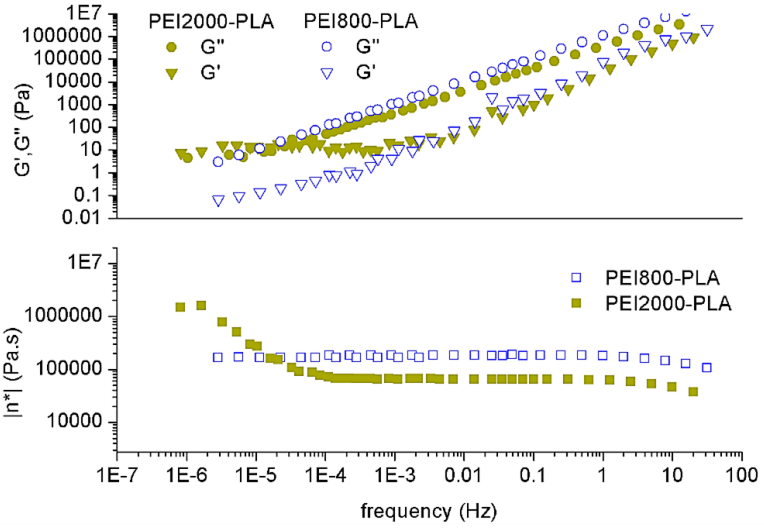

Figure 2. Master curves for the viscosimetric properties of PEI800-PLA and PEI2000-PLA multiarms star polymers at T_{ref} =60ºC

In the case of PEI800-PLA, whose core has a lower functionality, G' still lies below G'' within the whole experimental range. It can be observed a slight deviation of G' at the lowest frequencies towards a somewhat constant but small value of G', an indication of the existence of a weak structure. This behavior resembles that of PEI2000-PLA but the strength of the structure is much smaller. This can be rationalized on the basis of the lower molecular weight and functionality of the hyperbranched core, which reduces the intensity of the intermolecular interactions between neighboring stars, thus reducing the structure strength and the stress needed to make the molecules start to flow. At higher frequencies, though, the same decrease in complex viscosity is observed.

The TTS fitting produced C_1 = 8.90 and C_2 = 53.51 K for PEI800-PLA and C_1 = 9.61 and C_2 = 66.26 K for PEI2000-PLA, using in both cases a reference temperature T_{ref} =60ºC. The constants C_1 and C_2 are material dependent parameters that have been associated with fractional free volume f_0 and it was calculated as: $f_0=(B)/(2.303 \cdot C_1)$, where B is an empirical constant that related viscosity an free volume and has a value close to unity for most polymers.[27] The values for PEI800-PLA were f_0=0.049 and for PEI2000-PLA f_0=0.045. The free volume is higher in PEI800-PLA because of the lower functionality and molar mass of the core, indicating that it presents a topology more similar to that of linear polymers, in contrast with PEI2000-PLA, which has a more dense structure due to the higher molar mass and functionality of the hyperbranched core.

As stated above, a Newtonian plateau in the middle frequency range was found at the three temperatures for both polymers, as shown in Figure 2. **Table 3** collects the complex

viscosity in this Newtonian plateau for the multiarm star polymers synthesized. As expected, the viscosity decreases on increasing the temperature. It is also observed that, in spite of the lower molecular mass of PEI800-PLA, its viscosity is higher at any temperature than that of PEI2000-PLA. This can be rationalized in terms of the more linear character of PEI800-PLA because of the lower functionality of the PEI800 core in comparison with the PEI2000 core, which is also in agreement with comments above on the free volume fraction.

Table 3.Complex viscosity at different temperatures for both multiarm stars synthesized.

Temperature (ºC)	|η*| (Pa·s)		
	60	80	100
PEI800-PLA	175000 ($3\cdot10^{-6}$-0.4 Hz)[a]	620 ($1\cdot10^{-3}$-100 Hz)[a]	25 (0.02-2000 Hz)[a]
PEI2000-PLA	66020 ($3\cdot10^{-4}$-0.2 Hz)[a]	368 (0.04-100 Hz)[a]	18 (4-20000 Hz)[a]

[a] Interval of frequency that multiarm stars show a Newtonian behavior

Curing of DGEBA with different proportions of PEIX-PLA

Prior to study the curing we analyzed the processability of the formulations by rheological experiments. **Figure 3** shows the complex viscosity at 40ºC versus angular frequency for formulations containing 10% of modifiers and for neat DGEBA. All formulations show a Newtonian behavior in the experimental range of frequencies. From the viscosity values, we can see that the addition of PEIX-PLA to the reactive mixtures increases the viscosity without compromising the processability. Moreover, these viscosities are always much lower than the obtained with poly(ε-caprolactone) linear analog, because of the low entanglement of the short arms of the multiarm stars.[9] Although neat PEI800-PLA showed higher viscosity than neat PEI2000-PLA (Table 3), mixtures containing both modifiers have similar viscosity. Probably the balance between two opposite factors, the density of the structure of the modifier and the hydrogen bond content, contribute to this behavior. PEI2000-PLA has probably high dense structure than PEI800-PLA because of its higher generation number,[28] but higher amine content leading to higher hydrogen-bonding interactions. Consequently formulations with PEI2000 core can have similar viscosity than formulations containing PEI800 core.

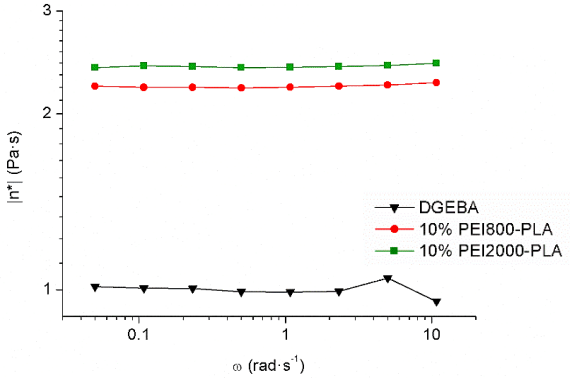

Figure 3. Complex viscosity against angular frequency at 40ºC for neat DGEBA and DGEBA containing 10% of PEI800-PLA and PEI2000-PLA

In order to characterize the curing kinetics, DGEBA/PEIX-PLA mixtures and neat DGEBA were cured with 5 phr of 1-MI at several heating rates in the DSC. All the formulations had reacted completely, since no residual heat was observed in a second DSC scan and FTIR showed that the characteristic band at 915 cm^{-1}, associated with epoxy groups, had disappeared completely after curing. The similarity between reaction heats per epoxy equivalent (Table 2) and the reported data for other similar epoxy systems agree with this conclusion.[29]

Figure 4 shows the heat flow and conversion curves of neat DGEBA and PEI2000-PLA formulations at $10^{o}C \cdot min^{-1}$. It can be observed that PEI2000-PLA produces a significant decelerative effect in all stages of the curing regardless of the amount of modifier. DGEBA/PEI800-PLA mixtures showed a similar trend (figure do not shown) with similar rate of curing than DGEBA/PEI2000-PLA formulations. In general, it is accepted that different factors such as: viscosity and mobility of the reactive species, regeneration of initiator, and hydroxyl content control the kinetics of curing. While high hydroxyl content and regeneration accelerate the process, the participation of less mobile species such as these multiarms stars may decelerate the curing significantly, being this latter factor the one controlling the curing rate of DGEBA/PEIX-PLA mixtures at low modifier content. The increase of hydroxyl content when 10% of modifier is used instead of 5% may partially offset this effect, explaining why both formulations, with 5% and 10% of modifier, react at similar rate of curing (see Table 2 and Figure 4).

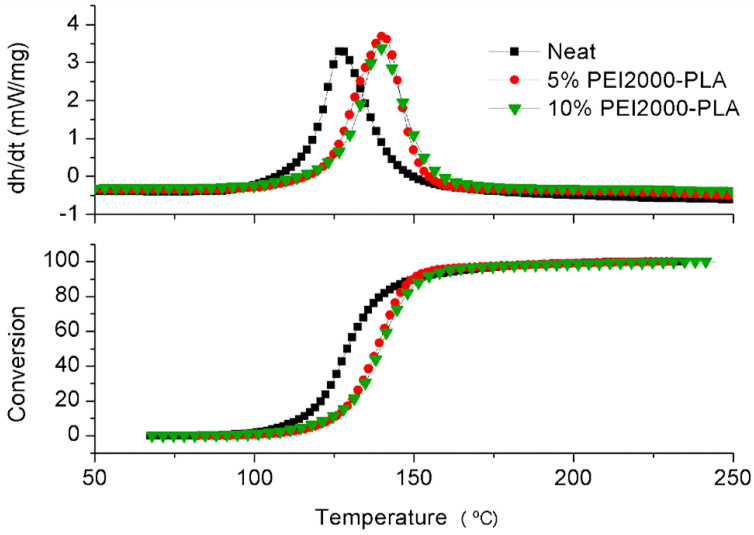

Figure 4. Calorimetric non-isothermal curves and degree of curing against temperature of DGEBA/PEI2000-PLA formulation at $10^{o}C \cdot m^{-1}$

The kinetics of the curing process was analyzed by non-isothermal integral isoconversional procedure and revealed the quasi-constancy of activation energy for all formulations in the whole range of conversion (figure not shown). The calculated values of rate constants (Table 2**)** demonstrate the retarding effect of PEIX-PLA, in agreement with the calorimetric data (Figure 4).

Thermal properties of the thermosets obtained

The T_g of the isothermally cured samples, determined by DSC, decreases progressively on increasing the modifier content (Table 2). This decrease is similar for both PEIX-PLAs, although their core, molecular weight and number of arms are quite different. The fact that both modifiers leads to materials with similar properties could be rationalized taking into account that the relationship between arms weight and core weight (≈90/10) is very similar for both multiarm stars. In a previous work we observed a decrease on the T_g when the weight ratio between arms and core increases.[12]

Figure 5 shows the mechanical relaxation spectra at 1 Hz for neat DGEBA and DGEBA/PEI2000-PLA formulations and **Table 4** summarizes the results obtained by dynamomechanical analysis.

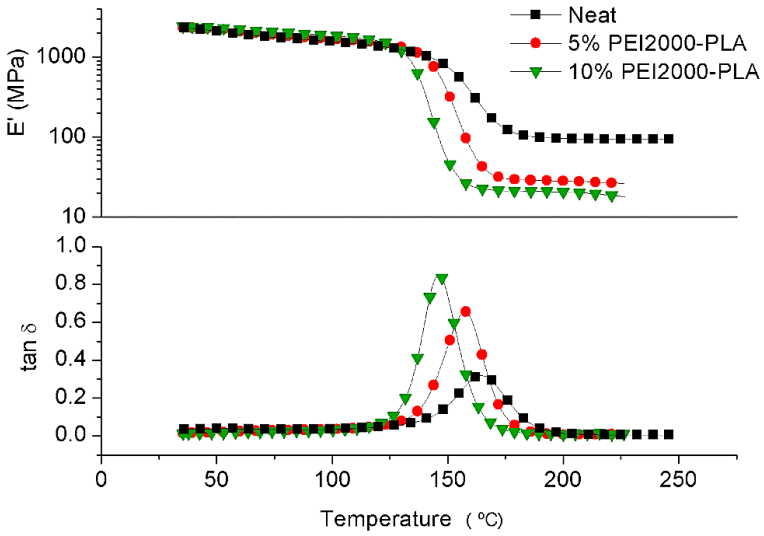

Figure 5. Tan δ and storage modulus against temperature at 1 Hz for neat DGEBA and DGEBA containing different amounts of PEI2000-PLA

As it can be observed, the DMTA curves show a single and unimodal α relaxation, which is typical of single-phase materials, as will be further demonstrated by electronic microscopy. It can also be seen that on increasing the modifier proportion in the formulation, the dynamomechanical relaxations shift to slightly lower temperatures, indicating that T_g slightly decreases, as seen above by DSC. According to the rubber elasticity theory,[30] the relaxation moduli in the rubbery state are directly proportional to the crosslinking density. Table 4 and Figure 5 show that on increasing the PEIX-PLA the rubbery modulus strongly decreases due to the formation of a less crosslinked structure. This result contrasts with the relatively high T_g values of the DGEBA/PEIX-PLA thermosets, which can be explained by the high stiffness of the lactide units. The presence of a pendant methyl group in the polymeric chain and the high proportion of ester bonds in PLA reduce the conformational freedom of the arms. Using PEI-PCL stars of similar molecular weight as modifiers,[12] materials with a higher crosslinking density were obtained but with a T_g around 20ºC below those of the present study, because of the higher flexibility of the PCL

arms. Thermomechanical results show again that both PEIX-PLAs have a similar influence on the final characteristics of the cured thermosets.

Table 4. Results of the DMTA and TGA analysis for the thermosets obtained from DGEBA and DGEBA/PEI-PLA formulations

Formulation (wt.%)	DMTA				TGA	
	$T_{tan\delta}$ [a] (ºC)	E'_u [b] (MPa)	E'_r [c] (MPa)	FWHM [d] (ºC)	$T_{5\%}$ [e] (ºC)	T_{max} [f] (ºC)
0	165	2257	94	27	396	435
PEI800-PLA						
5	156	2297	26	22	357	428
10	149	2243	22	21	311	419
PEI2000-PLA						
5	157	2324	29	19	346	427
10	146	2385	21	18	320	418

[a] Temperature of maximum of tan δ
[b] Storage modulus in the glassy state determined at 40ºC
[c] Storage modulus in the rubbery state determined at tan δ peak + 50ºC
[d] FWHM stands for full width at half maximum
[e] Temperature of the onset decomposition on TGA data at 10ºC·min^{-1} calculated for a 5% weight loss
[f] Temperature of the maximum decomposition rate based on the TGA data at 10ºC·min^{-1}

In order to determine the potential application of the obtained thermosets as coatings, the generation of internal stresses during cooling of DGEBA and DGEBA/PEIX-PLA formulations on steel as a rigid substrate was investigated using the methodology described in detail by Lange *et al*.[31] In this methodology the stress during cooling can be estimated from the mechanical and thermal properties of the polymer and substrate (modulus, thermal expansion coefficient CTE, Poisson's ratio…) and on the basis of the difference between the CTEs of the polymer and substrate.

Table 5 collects the CTE values in the glassy and rubbery state, determined by TMA expansion experiments, and the calculated stresses that are generated during cooling above (σ_{rubber}) and below T_g (σ_{glass}) and the total stress ($\sigma_{total}=\sigma_{rubber}+\sigma_{glass}$). It can be seen that all formulations exhibit no significant stress during cooling above T_g, but develop stress on cooling below T_g. Although the addition of PEIX-PLA gives an increase in CTE and glassy modulus (see Tables 4 and 5) that contributes to increase the stress, the decrease in T_g is sufficient to compensate for it and reduce the stress in the glassy state and the overall stress. It can be concluded that by controlling the T_g of thermosets it is possible to decrease the stress build-up during cooling.

Table 5. Thermal expansion coefficient and internal stresses of the DGEBA and DGEBA/PEIX-PLA thermosets studied

Formulation (wt.%)	$CTE_{glass} \cdot 10^6$ (K^{-1})	$CTE_{rubber} \cdot 10^6$ (K^{-1})	σ_{glass} (MPa)	σ_{rubber} (MPa)	σ_{total} (MPa)
0	69	171	24.11	0.12	24.23
PEI800-PLA					
5	66	175	20.85	0.14	20.99
10	70	185	18.45	0.27	18.71
PEI2000-PLA					
5	73	198	23.03	0.23	23.26
10	74	186	20.85	0.26	21.12

The thermal stability of the materials obtained was tested by thermogravimetry. **Figure 6** shows the thermogravimetric traces in nitrogen atmosphere of neat DGEBA and PEI800-PLA formulations and the results for all formulations are summarized in Table 4. On increasing the modifier content, the onset temperature and the temperature of the maximum decomposition rate clearly decrease, irrespective of the type of multiarm star used. The breakage of polyester structures in the multiarm star through a β-elimination process and the decrease in crosslinking density may account for the observed decrease in thermal stability. When PEI-PCL stars were used as DGEBA modifiers, the stability of the thermosets remained unchanged.[12] The difference between PEI-PLA and PEI-PCL formulations should be attributed to the lower thermally stability of secondary ester groups of PLA in comparison to ester of primary alkyl groups of PCL.[32]

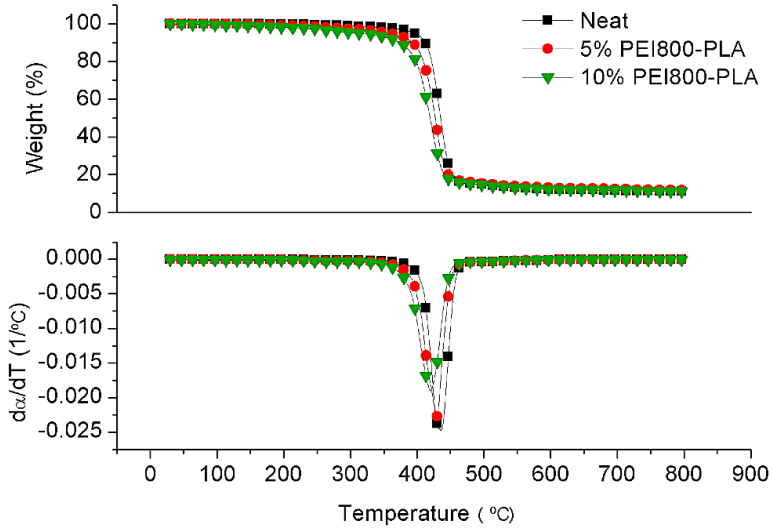

Figure 6. Thermogravimetric traces at 10 ºC·min^{-1} under nitrogen atmosphere for neat DGEBA and DGEBA containing different amounts of PEI800-PLA

The term reworkable applied to epoxy thermosets refers to the ability of the network structure to breakdown under controlled conditions in order to remove it from the substrate. Thermosets are usually considered thermally reworkable if they begin to decompose at

temperature ranging from 200 up to 300ºC but do not degrade during the curing process. Chen *et al*.[32] found that the most useful technique for directly evaluate a reworkable network breakdown is by following the evolution of the glass transition temperature during thermal treatment. In order to evaluate the thermal reworkability of the prepared materials, samples were placed at 230ºC in the DSC during different times and after degradation the T_g's were determined. **Figure 7** shows the evolution of the glass transition temperatures of the samples against isothermal degradation time. Samples containing PEIX-PLA show a continuous decrease in T_g until it stabilizes at long rework times (time > 30 minutes). As expected, neat DGEBA does not degrade at 230ºC within the experimental time interval. The differences observed between neat DGEBA and PEIX-PLA formulations should be related with the breaking of secondary ester bonds in PLA arms. Due to the reworkable nature of PEIX-PLA formulations, the effective crosslink density decreases as the ester linkages cleave, leading to a decrease in the glass transition temperature.

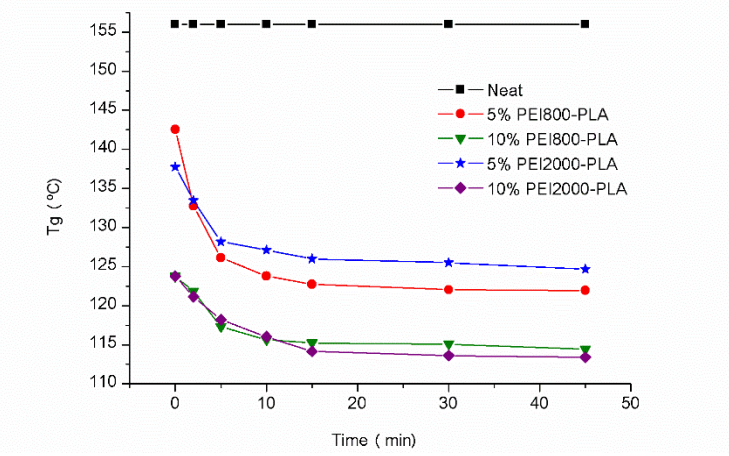

Figure 7. Glass transition temperature against degradation time for samples heat-treated isothermally at 230ºC

Mechanical characterization and morphology of the thermosets obtained

The toughness of neat DGEBA and DGEBA/PEIX-PLA formulations has been determined by impact tests and examination of the morphology of the fracture surface of impacted materials by SEM.

The effect of the addition of PEI2000-PLA and PEI800-PLA to the formulations in the impact strength is shown in **Figure 8**. It is possible to observe that the modification of DGEBA with PEIX-PLAs slightly improves this value in comparison with the neat material. The higher improvement obtained with 10% of PEI2000-PLA can be explained by the flexibilization of the network structure, with a lower T_g and crosslinking density.

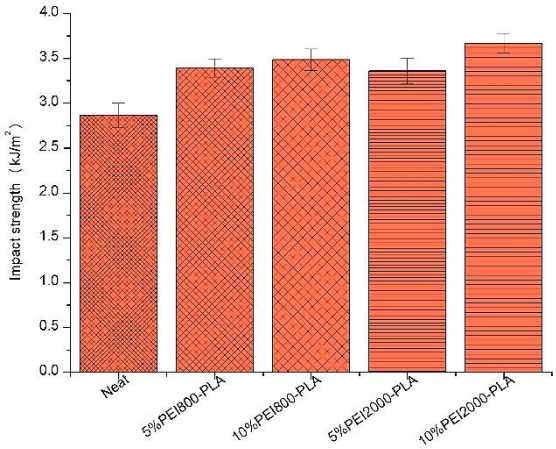

Figure 8. Impact strength values for the thermoset prepared

Figure 9 shows the most representative SEM micrographs for the fracture surface for some thermosets prepared. All the micrographs presented a homogeneous appearance without any sign of phase separation, as it was deduced by DMTA analysis. This is explained by the high compatibility between poly(lactide) arms and DGEBA, favored by the reaction of hydroxyl terminals groups of the star with activated epoxy groups through chain transfer mechanisms. The differences are relatively small, but 10%PEI2000-PLA modified material shows a more yielding fracture than the other formulations, in agreement with its higher impact strength.

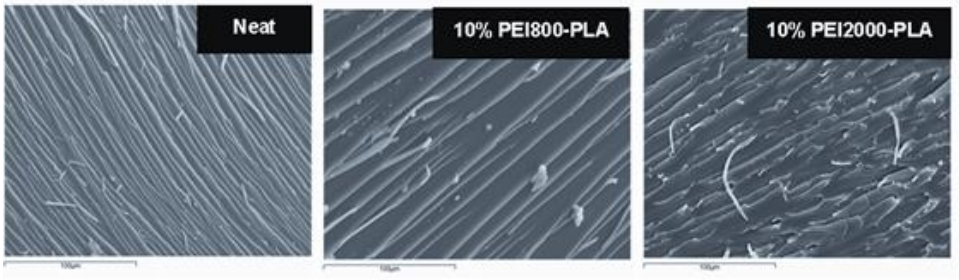

Figure 9. SEM micrographs at 500 magnifications for fractured surfaces of some impacted samples studied

Conclusions

Following a “core-first” strategy, multiarm star polymers based on hyperbranched poly(ethyleneimine) core and poly(lactide) arms were obtained by a cationic ring-opening polymerization of lactide from a hyperbranched poly(ethyleneimine) core of different molecular weight and used as modifier in the curing of DGEBA by 1-methyl imidazole as an anionic initiator.

The addition of these multiarm star polymers reduced the curing rate of DGEBA formulations with 1-methylimidazole as anionic initiator. The reaction rate is primarily controlled by the low mobility of the reactive species by the participation of the multiarm stars in the curing process and to a lower extent by the hydroxyl group content.

Novel thermosetting materials with slightly improved toughness and low stress generation during cooling were obtained without compromising processability and hardly affecting the glass transition temperature. The new thermosets obtained were homogeneous without any sign of phase separation. The highest improvement in impact resistance was obtained with the addition of a 10% of PEI2000-PLA.

Although no significant influence of the molecular weight of the core on the curing and on the final properties was found, it has been found that the weight ratio between arms and core, the length of the arms, the arm entanglement and the intermolecular interactions between arms and core are the key parameters that controlled the properties of multiarm stars and final properties of the modified epoxy thermosets.

The thermal reworkability of the modified thermosets was proved by a decrease in the glass transition temperature under thermal rework conditions. The esters of secondary alkyl groups in the poly(lactide) arms are responsible for this behaviour.

References

[1] May CA, Tanaka GY Eds. Epoxy resin chemistry and technology. New York: Marcel Dekker: 1973.
[2] Bauer RS Ed. Epoxy resin chemistry I. Advances in chemistry series. Washington: Am. Chem. Soc.: 1979 [Vol 114].
[3] Pascault JP, Williams RJJ. Epoxy Polymers. Wiley VCH: Weinheim: 2010 [Chapter 1].
[4] Meng Y, Zhang XH, Du BY, Zhou BX, Zhou X, Qi GR. Polymer 2011;52:391-399.
[5] Fröhlich J, Kautz H, Thomann R, Frey H, Mülhaupt R. Polymer 2004;45:2155-2164.
[6] Fan W, Zheng S. Polymer 2008;49-3157-3167.
[7] Turunen MPK, Laurila T, Kivilahti JK. J Appl Polym Sci 2006;101:3677-3688.
[8] Morell M, Foix D, Lederer A, Ramis X, Voit B, Serra A. J Polym Sci Part A: Polym Chem 2011;49:4639-4649.
[9] Morell M, Ramis X, Ferrando F, Serra A. Polymer 2011;52:4694-4702.
[10] Morell M, Ramis X, Ferrando F, Serra A. Macromol Chem Phys 2012;213:335-343.
[11] Däbritz F, Voit B, Naguib M, Sangermano M. Polymer 2011;52:57235723-5731.
[12] Acebo C, Fernández-Francos X, Ferrando F, Serra A, Salla JM, Ramis X. React Funct Polym 2013;73:431-441.
[13] Fernández-Francos X, Santiago D, Ferrando F, Ramis X, Salla JM, Serra A, Sangermano M, J Polym Sci Part B: Polym Phys 2012;50:1489-1503.
[14] Maier S, Sunder A, Frey H, Mülhaupt R. Macromol Rapid Commun 2000;21:226-230.
[15] Gao H, Matyjaszewski K. Macromolecules 2008;41:1118-1125.
[16] Mendrek M, Trzebicka B, Walach W, Dworak A. Eur Polym J 2010;46:2341-2351.
[17] Adeli M, Haag R. J Polym Sci Part A: Polym Chem 2006;44:5740-5749.
[18] Zhang CX, Wang B, Chen Y, Cheng F, Jiang SC. Polymer 2012;53:3900-3909.
[19] Ramis X, Salla JM, Mas C, Mantecón A, Serra A. J Appl Polym Sci 2004;92:381-393.
[20] Liu C, Zhang Y, Huang J. Macromolecules 2008;41:325-331.
[21] Kopinke FD, Remmler M, Mackenzie K, Möder M, Wachsen O. Polym Degrad Stab 1996;53:392-242
[22] Sivasamy P, Palaniandavar M, Vijayakumar CT, Ledered K. Polym Degrad Stab 1992;38:15-21.
[23] Ferry JD. Viscoelastic properties of polymers. 3 ed. Wiley: New York: 1980.
[24] Helgeson ME, Wagner NJ, Vlassopoulos D. J. Rheol 2007;51:297-316.
[25] Barnes HA, Hutton JF, Walters K. An Introduction to Rheology. Rheology Series 3. Amsterdam: Elsevier: 1989.
[26] Vukovic J, Lechner MD, Jovanovic S. Macromol Chem Phys 2007;208:2321-2330.
[27] Doolittle AK. J Appl Phys 1951;22:1471-1474.
[28] Lederer A, Hartmann T, Komber H, Macromol Rapid Commun 2012;33:1440-1444.
[29] Ivin KJ, in: Brandrup J, Immergut EH Eds. Polymer Handbook. Wiley: New York: 1975.
[30] Nielsen LE. J Macromol Sci Rev Macromol Chem 1969;C3:69-193.

[31] Lange J, Toll S, Manson JAE, Hult A. Polymer 1995;36:3135-3141.
[32] Chen JS, Ober CK, Poliks MD. Polymer 2002;43:131-139

4.4 Effect of hydroxyl ended and end-capped multiarm star polymers on the curing process and mechanical characteristics of epoxy/anhydride thermosets

Cristina Acebo, Annamaria Picardi, Xavier Fernández-Francos, Silvia de la Flor, Xavier Ramis, Àngels Serra

Progress in Organic Coatings **2014***, 77,* 1288-1298

UNIVERSITAT ROVIRA I VIRGILI
HYPERBRANCHED POLY(ETHYLENEIMINE) DERIVATIVES AS MODIFIERS IN EPOXY NETWORKS
Cristina Acebo Gorostiza

Progress in Organic Coatings **2014**, *77*, 1288-1298

Effect of hydroxyl ended and end-capped multiarm star polymers on the curing process and mechanical characteristics of epoxy/anhydride thermosets

Abstract

Multiarm star polymers have been synthesized by cationic ring-opening polymerization of *ε*-caprolactone from a hyperbranched poly(ethyleneimine) core and end-capped with acetic anhydride. These star polymers have been used as modifiers in diglycidylether of bisphenol A/methyl tetrahydrophthalic anhydride/benzyl dimethylamine formulations. The curing process is studied by dynamic scanning calorimetry and rheometry and the resulting thermosets are characterized by dynamic mechanical thermal analysis and thermogravimetry. Internal stresses generated during curing are measured and interpreted in terms of the thermal-mechanical properties of the cured materials. The influence of the modifier in the toughness improvement of the cured thermosets is determined by standardized impact tests and the microstructure of the material observed by scanning electron microscopy.

Keywords: Star polymers, hyperbranched, epoxy resin, anhydrides, thermosets, stress, toughness.

Introduction

Epoxy resins are commonly used as thermosetting materials due their good thermomechanical, adhesive and electrical properties and ease of processing. Due to their good characteristics, epoxy-based thermosets are widely used in technological applications such as surface coatings, adhesives and assemblies for electronic devices.[1-3] Although rigidity and strength are desired properties in engineering applications, toughness is one of the restrictions in the use of epoxy resins. The low toughness, coming from the high crosslinking density, in addition to the internal stresses appearing during processing, affects the durability of coatings and places strong constraints on design parameters.[4]

The first attempts to improve toughness were based on the addition of liquid rubbers or thermoplastics, but usually these additives compromise the modulus and thermomechanical characteristics of the thermosets and the processability of the formulation.[5] Toughness implies energy absorption and it is achieved through various deformation mechanisms before failure occurs. One of the most effective methods to prevent free crack propagation after impact is the addition of a modifier that leads to the formation of particles that absorb the impact energy and deflect the crack. It has been recognized that a combination of cavitation around the rubber or thermoplastic particles with shear yielding in the matrix produces a cooperative effect in the energy dissipation.[6] It has been described that the formation of micro- or nanostructures in epoxy thermosets improves the overall properties without reducing crosslinking degree of the epoxy matrix.[7] Chemically induced phase separation (CIPS) is one of the methodologies in which the morphology develops during curing from an initial homogenous mixture composed of the resin, curing agent and modifiers[8-10] to form a blend of epoxy matrix filled with rubber or thermoplastic microspheres, with a final size of these particles controlled by the viscosity of the reacting mixture during curing.

To overcome the limitations before mentioned for rubbers or linear thermoplastics used as toughenners, the use of dendritic structures was proposed by several authors.[11-14]

Recently, star-like topologies are used to enhance some characteristics of epoxy thermosets because of their unusual physical and rheological properties which allow the enhancement of some characteristics of epoxy thermosets.[15-17] Depending on the chemistry of the curing and the structure of the stars, homogeneous or nanostructured materials were obtained.

In coating applications the formation of internal stresses during curing usually leads to the appearance of defects that finally leads to the reduction of the protection capability. The mismatch between the thermal expansion coefficients of the coating and the substrate, along with the glass transition temperature (T_g) of the coating, are relevant parameters with a strong influence on the generation of internal stresses. In previous studies we reported that dendritic structures not only lead to a reduction of the shrinkage during curing which produces the apparition of internal stresses, but also to a reduction of the thermal expansion coefficients (*CTEs*).[11]

The aim of the present work is the preparation and characterization of new epoxy thermosets to overcome the above mentioned drawbacks, namely, the enhancement of toughness or the reduction of the internal stresses on curing while maintaining the thermomechanical characteristics of the thermosets and the easy processability of the formulation.

In recent publications, we reported the use of multiarm stars with poly(ethyleneimine) core and poly(ε-caprolactone) or poly(lactide) arms as modifiers in the curing of DGEBA using 1-methylimidazole (1-MI) as anionic curing agent.[18,19] The T_g's of the final materials were not greatly affected while toughness was slightly improved in spite of the different flexibility and length of the poly(ε-caprolactone) and poly(lactide) arms.

We reported a significant increase in impact strength up to 400% with respect to the neat formulation without sacrificing thermal and thermomechanical properties by the addition of partially modified Boltorn type polyesters with 10-undecenoyl moieties in DGEBA thermosets cured with anhydrides.[20] Efficient toughening was obtained because of the formation of well dispersed hyperbranched microparticles covalently attached to the thermosetting matrix by the unmodified hydroxyl groups of the HBP.

Taking all of these precedents into account, in the present work we compared the properties of epoxy thermosets cured with anhydrides in the presence of a tertiary amine as a catalyst on adding multiarm stars with polyethylene imine core and poly(ε-caprolactone) arms in different proportions and arms lengths. These stars, which have hydroxyl end-groups, have been end-capped with acetyl moieties to investigate the influence of unreactive multiarm stars on the possible phase separation during curing and on the mechanical and thermal characteristics of the prepared material, with a focus on toughness and internal stresses formation.

Experimental Part

Materials

The hydroxyl terminated star polymers (PEI-PCLX) were synthesized as previously described.[19] To perform the end-capping process by acetylation, extra pure acetic anhydride was used and purchased from Scharlau. Triethyl amine (TEA) and *N,N*-dimethylamino pyridine (DMAP) were purchased from Fluka. Chloroform ($CHCl_3$) was dried under $CaCl_2$ and distilled before used. Solvents were purchased from Scharlab. Diglycidylether of bisphenol A (DGEBA; Araldite GY 240, Huntsman) (182 g/eq) and methyl

tetrahydrophthalic anhydride (MTHPA; Aradur HY 918, Huntsman) (166 g/mol) were used as received. Benzyl dimethylamine (BDMA; DY 062, Huntsman) was used as the catalyst.

General procedure for acetylation of poly(ethyleneimine)-b-poly(ε-caprolactone) multiarm stars (PEI-PCLX and PEI-PCLX-B)

In the acronyms for both types of stars, X accounts for the degree of polymerization of the ε-caprolactone arms and can take the values 10 or 30 and B in multiarm star polymers PEI-PCLX-B, indicates that the multiarm star polymers were end-capped by acetylation.

The synthesis was performed using the same procedure that in the acryloyl functionalization of stars[21] and is exemplified for PEI-PCL10-B. PEI-PCL10 (5 g, 0.32 mmol) was dissolved in $CHCl_3$ in a two-necked round-bottomed flask equipped with a magnetic stirrer and a gas inlet to fill the flask with argon and cooled on a water/ice-bath. Triethylamine (0.097 g, 0.96 mmol) and a catalytic amount of DMAP were added to the solution. Acetic anhydride (0.4 g, 3.8 mmol) was then added dropwise and the solution stirred at room temperature overnight. After that, the reaction mixture was further diluted with $CHCl_3$ before precipitation into methanol and then filtered and dried at 40 ºC under vacuum for one day to give a white crystalline powder. ^{1}H NMR (400 MHz, $CDCl_3$, δ in ppm): 4.08 (-C**H**$_2$-OCO-, **5** and **5'**), 2.32 (-NHCO-C**H**$_2$-, -C**H**$_2$-COO, **1** and **1'**), 1.92 (-C**H**$_3$, **6**), 1.70-1.40 (-C**H**$_2$-, **2-4** and **2'-4'**) and 3.5-1.5 (PEI core) (see Figure 1).

Average molecular weights and thermal data of all the multiarm stars obtained are collected in **Table 1.**

Table 1. Data of the multiarm star polymers PEI-PCLX/PEI-PCLX-B synthesized in this study

Entry	Yield (%)	M_n [a] (g/mol)	T_g [b] (ºC)	T_m [b] (ºC)	$T_{5\%}$ [c] (ºC)
PEI-PCL30	72	40749	-74	63	312
PEI-PCL10	70	16780	-79	62	312
PEI-PCL30-B	80	41351	-58	56	307
PEI-PCL10-B	82	17382	-57	48	299

[a] Determined by 1H-NMR spectroscopy
[b] Determined by DSC
[c] Temperature of 5% of weight loss determined by TGA

Preparation of epoxy thermosets

The mixtures were prepared by adding the required amount of PEI-PCLX or PEI-PCLX-B to the epoxy resin and gently heating until it was dissolved and the solution became clear. Then, stoichiometric amount of MTHPA and 1 phr (parts per hundred of anhydride) of BDMA were added and the resulting solution was stirred and cooled down to -10 ºC to prevent polymerization. Mixtures containing 10-20 wt% (by weight of DGEBA) of PEI-PCLX or PEI-PCLX-B were prepared. The compositions of the formulations studied are detailed in **Table 2.**

Table 2. Composition of DGEBA/MTHPA/BDMA formulations with different percentages of star modifiers.

Formulation	Star modifiers		DGEBA		MTHPA		BDMA	
	wt (g)	mol OH	wt (g)	mol	wt (g)	mol	wt (g)	mol (%)
Neat	-	-	12.067	0.033	10.814	0.065	0.107	0.8
10% PEI-PCL30	1.200	0.4	12.081	0.033	10.959	0.066	0.108	0.8
20% PEI-PCL30	2.397	0.8	12.072	0.033	11.081	0.067	0.115	0.9
10% PEI-PCL10	1.211	1.1	12.070	0.033	11.030	0.066	0.113	0.8
20% PEI-PCL10	2.406	2	11.982	0.033	11.061	0.067	0. 113	0.8
10% PEI-PCL30-B	1.231	-	12.026	0.033	11.137	0.067	0.109	0.8
20% PEI-PCL30-B	2.134	-	10.652	0.029	9.845	0.059	0.095	0.8
10% PEI-PCL10-B	1.196	-	12.091	0.033	11.041	0.067	0.111	0.8
20% PEI-PCL10-B	2.144	-	10.631	0.029	9.785	0.059	0.095	0.7

Characterization

^{1}H NMR measurements were carried out at 400 MHz and in a Varian Gemini 400 spectrometer. $CDCl_3$ was used as the solvent. For internal calibration, the solvent signal corresponding to $CDCl_3$ was taken as δ (^{1}H) = 7.26 ppm.

Calorimetric analyses were carried out on a Mettler DSC-822e thermal analyzer. Samples of approximately 10 mg were placed in aluminum pans under nitrogen atmosphere. The calorimeter was calibrated using an indium standard (heat flow calibration) and an indium-lead-zinc standard (temperature calibration). In the dynamic curing process the degree of conversion by DSC (x_{DSC}) was calculated as follows:

$$x_{DSC} = \frac{\Delta h_T}{\Delta h_{tot}} \quad (1)$$

where Δh_T is the heat released up to a temperature T, obtained by integration of the calorimetric signal up to this temperature, and Δh_{tot} is the total reaction heat associated with the complete conversion of all reactive groups. The kinetic studies were performed at heating rates of 2, 5, 10 and 20ºC/min in N_2 atmosphere.

Multiarm star polymers were heated from 25 to 100 ºC with a heating rate of 20 ºC/min, cooled down to -120 ºC with a cooling rate of -10 ºC/min and then heated again to 120 ºC with a heating rate of 20ºC/min. Melting temperature (T_m) and the glass transition temperature (T_g) were obtained from the second heating curves.

The glass transition temperatures ($T_{g\infty}$)s of the isothermally cured materials were determined, by means of a heating scan at 10 ºC/min, as the temperature of the half-way point of the jump in the heat capacity when the material changed from glassy to the rubbery state under N_2 atmosphere and the error is estimated to be approximately ± 1 °C.

The curing kinetics of non-isothermal DSC curing experiments was analyzed by means of isoconversional and model-fitting procedures applied to non-isothermal DSC data.[22-24] The isoconversional activation energy at different degrees of conversion *x* was determined from multiple heating rate experiments using the Kissinger-Akahira-Sunose method:

$$ln\left(\frac{\beta}{T^2}\right) = ln\left(\frac{A \cdot R}{g(x) \cdot E}\right) - \frac{E}{R \cdot T} \quad (2)$$

where *β* is the heating rate, *A* is the pre-exponential factor, *E* is the activation energy and *g(x)* is an integral function corresponding to the kinetic model. The time needed to reach a given conversion in an isothermal experiment can be determined from the results of the isoconversional analysis of non-isothermal experiments using the following expression:

$$\ln t = ln\left(\frac{g(x)}{A}\right) + \frac{E}{R \cdot T} \quad (3)$$

The kinetic model was determined using a 2nd order autocatalytic kinetic model with $g(x) = (1/(n-1)) \cdot \left((1 - x/x)\right)^{1-n}$ and rearranging the above expressions as:

$$ln\left(\frac{g(x) \cdot \beta}{T^2}\right) = ln\left(\frac{A \cdot R}{E}\right) - \frac{E}{R \cdot T} \quad (4)$$

Thermogravimetric analyses were carried out in a Mettler TG50 thermobalance. Samples with an approximate mass of 8 mg were degraded between 40 and 800 ºC at a heating rate of 10 ºC/min in N_2 (100 cm^3/min measured in normal conditions).

Thermomechanical analyses were carried out on a Mettler TMA40 thermomechanical analyzer. The samples were supported by two silica discs and heated at 5ºC/min from 30 up to 150ºC by application of a force of 0.02N. The thermal expansion coefficients (*CTEs*) below and above the T_g were calculated as follows:

$$CTE = \frac{1}{L_0} \cdot \frac{dL}{dT} = \frac{1}{L_0} \cdot \frac{dL/dt}{dT/dt} \quad (5)$$

where, *L* is the thickness of the sample, L_0 the initial length, *t* the time, *T* the temperature and *dT/dt* the heating rate. T_g was taken as the temperature of the intersection of the extrapolated dilatation in the glassy and rubbery state.

Rheological measurements were carried out in the parallel plates (diameter of 25 mm) mode with an ARG2 rheometer (TA Instruments, UK, equipped with an electrically heated plates system, EHP). The curing of the mixtures was monitored in an isothermal experiment at 100ºC by means of a multiwave frequency sweep (1, 3 and 5 Hz). The frequency independent crossover of *tan δ* was used to determine the gel time. The vitrification time was taken as the maximum of *tan δ* at 5 Hz.

Dynamic mechanical thermal analyses were carried out with a TA Instruments DMA Q800. The samples were cured isothermally in a mold (5 mm width and 3 mm thick) at 100 ºC for 2 h and then post-cured for 2 h at 180 ºC. The samples were carefully polished to ensure constant dimensions inasmuch as little variations of dimensions lead to erroneous measurements. The samples were analyzed in three-point bending mode with a support span of 15 mm. The viscoelastic properties of the cured materials were determined by means of a temperature ramp at 3 ºC/min from 40 to 250 ºC, frequency 1 Hz, and 10

microns of oscillation amplitude. The modulus of elasticity was determined at 35 ºC by means of a force ramp at constant load rate, from 0.001 N to 10 N at 0.01 N/min. Three samples of each material were analyzed and the results were averaged. The modulus of elasticity is calculated using the slope of the load deflection curve in accordance with the following equation:

$$E = \frac{L^3 m}{4bt^3} \quad (6)$$

where, *E* is the elastic modulus of epoxy sample (MPa), *L* is the support span (mm), *b* and *t* are the width and the thickness of test sample (mm), and *m* is the gradient (i.e., slope) of the initial straight-line portion of the load-deflection curve obtained from the test.

The residual stresses of all the materials were computed using the beam bending technique. A stainless steel feeler gauge (0.1 mm thickness, 50 mm longitude and 3 mm width) was used as the substrate and it was coated on one side with the analyzed epoxy formulations. The stainless steel sheets were degreased and polished using ultrafine sandpaper (P1500) to help the adhesion of the epoxy and finally cleaned with acetone.

The uncovered stainless steel sheet was positioned onto a borosilicate glass slide covered with Teflon. Two gauges of 0.5 mm thickness were laterally positioned to ensure the final accurate desired epoxy thickness. A layer of the epoxy formulation was deposited onto the stainless steel sheet with a doctor blade and covered with another borosilicate glass slide (also with Teflon). The steel-epoxy beam was then tightened rigidly with a fastened system and cured. After the curing process, the system was held in this situation until it reached room temperature, the constraints were then released and the samples adopted the curvature shape. The total specimen's thickness was then determined to within ± 0.001 mm using a micrometer. To ensure that the thickness was constant five measures were taken along the total longitudinal direction. The mean value was adopted and the sample was rejected if the standard deviation was greater than 0.5%. Midpoint deflection *f* (maximal deflection at the center of the beam) was measured to within ± 0.02 mm with a caliper measuring system. At least, three samples of each epoxy formulation were obtained.

The mathematical expression for computing the residual stress found to match these conditions and assuming small deflections was that derived from Benabdi-Roche expression:[25]

$$\sigma_R = -\frac{8 \cdot f}{L^2} \cdot \frac{E_s \cdot t_s^2}{6t_e} \cdot \frac{1}{(1+\alpha\beta)} \cdot \left[1 + \beta(4\alpha - 1) + \beta^2 \left[\alpha^2(\beta - 1) + 4\alpha + \frac{(1-\alpha)^2}{(1+\beta)}\right]\right] \quad (7)$$

where $\beta = t_e/t_s$ and $\alpha = E_e/E_s$, *f* is the midpoint deflection, *L* is the length of the beam, E_i is the elastic modulus and t_i is the layer thickness. The subscript *s* is used for stainless steel and *e* for epoxy material.

The contribution of thermal stress (i.e. the influence of *CTE*) to the total measured stress can be computed taking into account the thermal uniform misfit strain. This misfit depends on the thermal expansions coefficients (CTE_s for the stainless steel and CTE_e for the epoxy), the elastic modulus for the epoxy (E_e), and the drop in temperature ($\Delta T = SFT - T_{amb}$).

SFT is the stress free temperature, which can be considered close to T_g if T_g is lower than T_{cure}.[26] In this study, *SFT* is assumed to be equal to the T_g obtained from TMA expansion experiments. For stainless steel sheets, the elastic modulus (E_s) is 180053 MPa and the thermal expansion coefficient $16 \cdot 10^{-6}$ ºC^{-1}.

Thermal stress also depends on the geometrical parameters of the sample and elastic modulus of substrate (E_s). Adapting the expression derived by Timoshenko,[25] thermal stress can be computed with the following expression:

$$\sigma_{th} = \frac{6 \cdot (1+\beta)^2 \cdot (SFT - T_{amb}) \cdot (CTE_e - CTE_s)}{(t_e - t_s) \cdot [3 \cdot (1+\beta)^2 + (1+\alpha\beta)(\beta^2 + (1/\alpha\beta))]} \cdot \frac{E_s \cdot t_s}{6} \cdot \left[\frac{1}{\beta(\beta+1)}(\alpha\beta^3 + 1) + 3\alpha\beta\right] \quad (8)$$

It is important to point out that all mechanical properties of the thermoset are assumed constant once cure is complete. Therefore, the analysis predictions for this assumption may provide upper bonds on process-induced stresses, since no stress relaxation is considered.

Impact tests were performed at room temperature by means of a Zwick 5110 impact tester according to ASTM D 4508-05 (2008) standard using rectangular samples (25 x 12 x 2.5 mm^3) cured by the same thermal process schedule than for DMTA samples. The pendulum employed had a kinetic energy of 0.5 J. For each material 9 determinations were made. The impact strength (IS) was calculated from the energy absorbed by the sample upon fracture as:

$$IS = \frac{E - E_0}{S} \quad (9)$$

where E and E_0 are the energy loss of the pendulum with and without sample respectively, and S is the cross-section of the samples.

The fracture area of impacted samples was metalized with gold and observed with a scanning electron microscope (SEM) Jeol JSM 6400 with a resolution of 3.5 nm.

Microhardness was measured with a Wilson Wolpert (MicroKnoop 401MAV) device following the ASTM D1474-98 (2002) standard procedure. For each material 10 determinations were made with a confidence level of 95%. The Knoop microhardness (HKN) was calculated from the following equation:

$$HKN = \frac{L}{A_p} = \frac{L}{l^2 \times C_p} \quad (10)$$

where, L is the load applied to the indenter (0.025 kg), A_p is the projected area of indentation in mm^2, l is the measured length of long diagonal of indentation in mm, C_p is the indenter constant (7.028×10^{-2}) relating l^2 to A_p.

Results and discussion

Synthesis and characterization of end-capped multiarm stars

In the present study the hydroxyl end-groups of the previously synthesized PEI-PCLX multiarm stars[18] were end-capped by acetylation with acetic anhydride. The synthetic pathway with the structures and acronyms are depicted in **Scheme 1**.

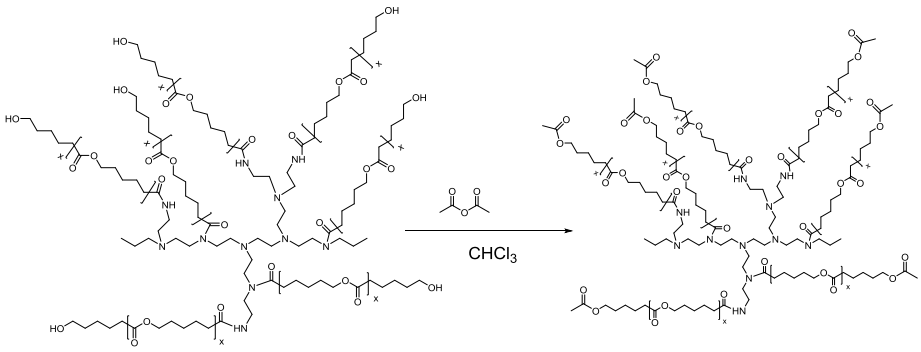

Scheme 1. Synthetic route to the end-capped multiarm star polymers PEI-PCL-X

It was assumed that the number of reactive hydroxyl groups was the same of the number of initial reactive amines (only NH and NH_2),[18] which render a 0.0184 eq OH/g. From this number the quantity of acetic anhydride needed was calculated. The reaction was performed in $CHCl_3$ at room temperature overnight under argon atmosphere. After precipitation in cold methanol and drying in vacuum, the end-capped multiarm stars were obtained as a yellowish powder.

These polymers were characterized by ^1H NMR (see Figure 1). The ratio between the signals **5** and **5'** is used for the calculation of the degree of polymerization of the arms. After acetylation, the signal **5'** disappears, which indicates that all hydroxyl groups have been reacted. A new signal clearly appears at 1.92 pm (signal **6**) attributable to the methyl of the acetyl group.

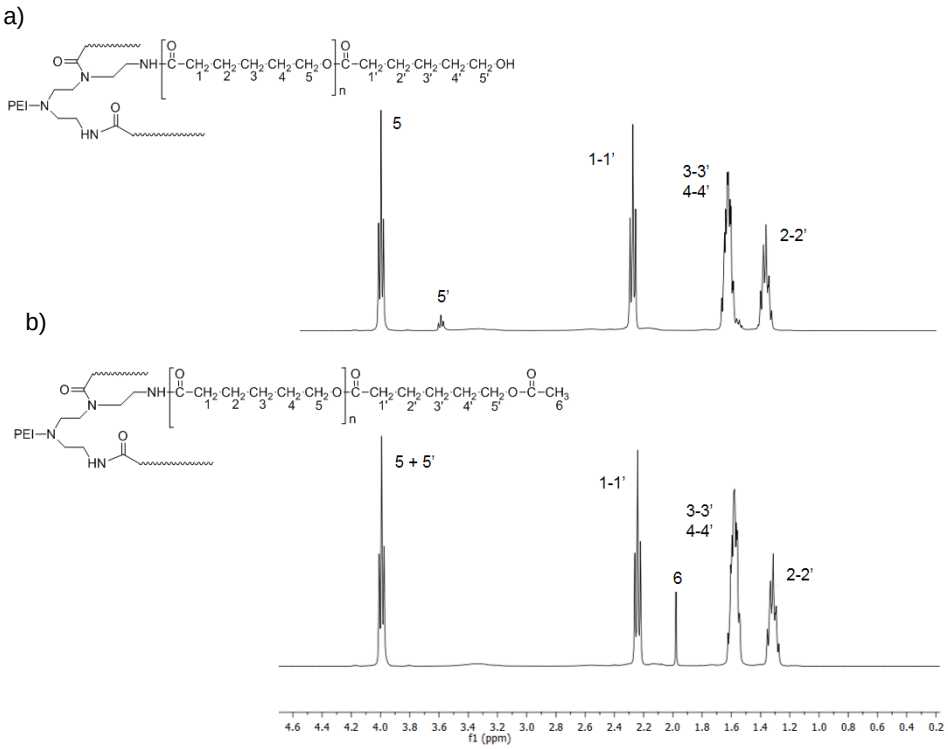

Figure 1. ^{1}H NMR spectra of (a) PEI-PCL10 and (b) PEI-PCL10-B

By calorimetric studies it was observed that the melting temperatures decreased when the star polymers were end-capped, while their T_gs were increased. The thermal stability was slightly reduced after acetylation (see Table 1).

Curing of DGEBA with different proportions of PEI-PCLX/PEI-PCLX-B

The reaction of DGEBA with anhydrides as curing agents has been widely reported.[11-13,27] The role of hydroxyl ended HBPs in epoxy formulations has been studied in the past.[11,12,20] Recently, we demonstrated by FTIR that HBPs were incorporated into the matrix by esterification of end hydroxyl groups with the anhydride giving rise to carboxyl groups that could subsequently react with epoxides.[11] The incorporation of OH groups takes place in the first stages of the reaction and their presence in the formulation produces an accelerative effect in the curing process.[20] **Scheme 2** depicts the reactions taking place during the curing process in the presence of hydroxyl ended HBPs.

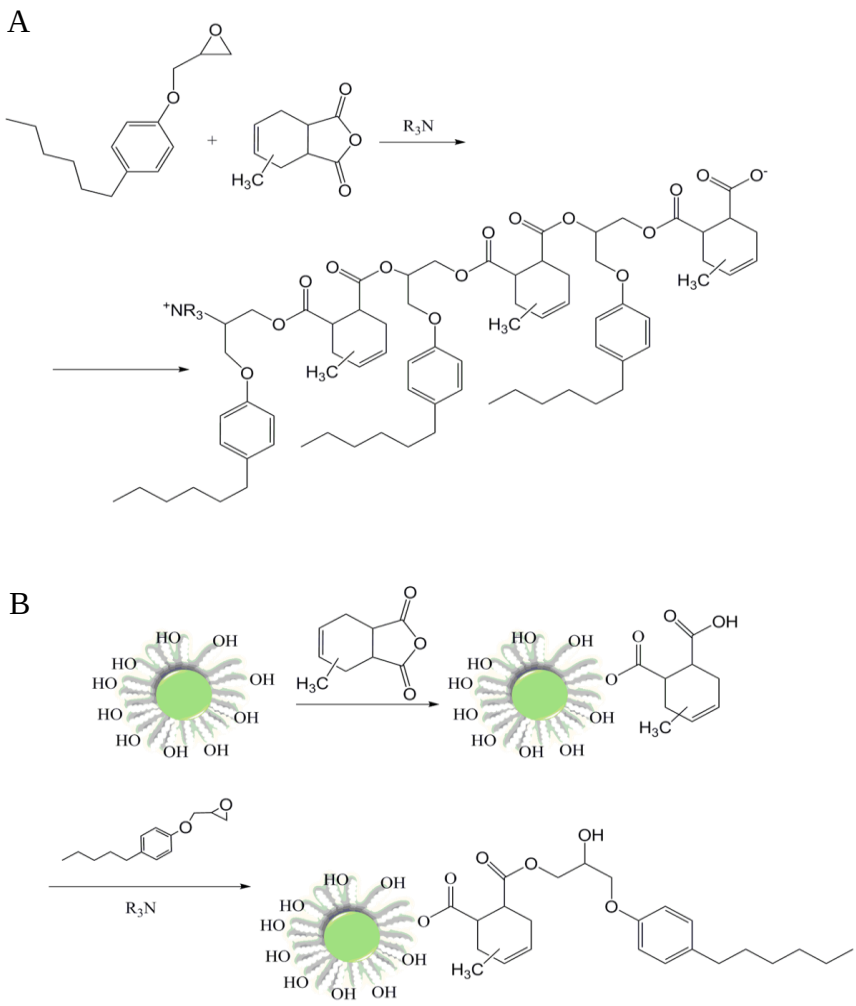

Scheme 2. Reaction processes taking place during curing of the modified formulations

In order to characterize the curing kinetics, neat and modified formulations were cured at several heating rates in the DSC. **Table 3** collects the main data of the curing process. The enthalpies per epoxy equivalent are all around 100-110 kJ/ee, a value comparable to those reported for other similar epoxy systems, indicating that epoxides have reacted almost completely.[24,28-30]

Table 3. Calorimetric data of the curing of the different formulations studied

Formulation	E_a[a] (kJ/mol)	$k_{150ºC} \cdot 10^3$[b] (min^{-1})	Δh[c] (J/g)	Δh[d] (kJ/ee)	T_g[e] (°C)
Neat	83.0	0.765	300	105	126
10% PEI-PCL30	77.4	0.625	282	104	121
20% PEI-PCL30	82.2	0.515	257	99	116
10% PEI-PCL10	74.4	0.574	294	109	114
20% PEI-PCL10	76.9	0.435	282	110	110
10% PEI-PCL30-B	78.9	0.595	281	103	123
20% PEI-PCL30-B	79.9	0.464	250	97	119
10% PEI-PCL10-B	80.8	0.560	285	107	112
20% PEI-PCL10-B	78.1	0.525	280	109	109

[a] Values of activation energy at 0.5 of conversion were evaluated by isoconversional non-isothermal integral procedure using eq. (2)
[b] Values of rate constant at 150ºC calculated using the 2nd order autocatalytic kinetic model with n=1.6, determined using eq (4) and the Arrhenius expression for the kinetic constant $k=A \cdot exp\ (-E/R \cdot T)$
[c] Reaction heat determined by DSC
[d] Reaction heat determined by DSC in kJ/ee
[e] Glass transition temperature of thermosets obtained of isothermal cured samples (2h at 100 ºC and 2 h at 180 ºC)

Figure 2 illustrates the effect of the addition of PEI-PCLX and PEI-PCLX-B on the dynamic curing at 10 ºC/min of DGEBA/anhydride formulations. It can be clearly observed that the addition of PEI-PCL30-B produces a decelerative effect which is proportional to the amount of modifier. Other modifiers have a similar effect, regardless of the chain length or the presence of hydroxyl or acetyl end groups. Although it is reported that the presence of reactive hydroxyl groups accelerates the curing process in epoxy-anhydride formulations,[29] the amount of hydroxyl end-groups in the PEI-PCLX stars is too small to have an effect on the curing kinetics. The effect of the different modifiers on the curing kinetics can therefore be explained on the basis of the lower mobility of the species in the increasingly viscous formulation and the dilution effect of the reactive groups on adding the modifier.

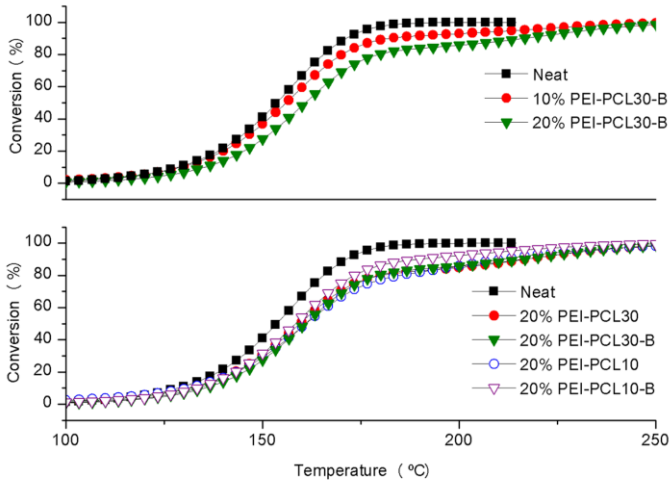

Figure 2. Degree of curing against temperature of some formulations at 10ºC/min

The kinetic parameters of the curing processes were calculated according to the procedures described in the experimental section and references therein. The results of the analysis are summarized in Table 3. It can be seen that there is no significant influence on the E_a, determined using equation (2), when the modifiers were added, indicating that all the systems follow a similar curing profile. The 2nd order autocatalytic model with n=1.6 was found to describe reasonably well the curing kinetics of all the formulations. The calculated values of rate constant demonstrate the slight retarding effect of the modifiers, in agreement with the conversion curves (Figure 2).

Table 3 shows that the T_g of the thermosets is progressively reduced upon addition of PEI-PCLX and PEI-PCLX-B multiarm stars. While the effect of the end-capping is not significant, it is clearly observed that multiarm stars with longer arms produce a smaller decrease in the T_g than those with shorter arms. This fact could be explained by the higher proportion of flexible poly(ethylene imine) core in the materials modified by the stars with shorter arms.

Rheological characterization

The special architecture of multiarm stars has the advantage to produce low viscosity polymers, even at high molecular weights, because of the low entanglement of the arms. In a previous publication,[18] we reported that PEI-PCL10 and PEI-PCL30 multiarm stars had a very low melt viscosity because of the absence of chain entanglement. If the arm length was further increased, the melt viscosity of the stars increased dramatically because of the occurrence of chain entanglement above a critical arm length. The effect of PEI-PCL10 and PEI-PCL30 on the viscosity of DGEBA formulations was likewise small. Due to the small amount of hydroxyl groups, the acetylation should not affect much the viscosity and therefore the good processability of the formulations studied in the present work should be maintained.

Gelation and vitrification are key phenomena taking place during curing and processing of epoxy formulations. Gelation is characterized by the formation of a three-dimensional network percolating the bulk of the material as a consequence of the increasing molecular weight and branching as the curing advances. Then, the gel fraction extends and becomes more densely crosslinked as the curing advances leading to an insoluble, fully crosslinked network at the end of the curing process. Gelation leads to a dramatic change in the viscoelastic properties during processing, as the material ceases to flow and starts to build-up mechanical properties. Another consequence is the apparition of internal stresses due to the curing shrinkage after this point. From the processing point of view, precise knowledge of the conversion and time at gelation is of key importance to avoid clogging of injectors or reactors. Vitrification during curing is characterized by a decrease in mobility as the glass transition temperature of the curing material approaches the curing temperature, because of the reduction in the available free volume for cooperative molecular rearrangement. As a consequence, the curing rate is dramatically slowed down and virtually halted, leading to incomplete cure. For this reason, vitrification should be surpassed in order to get complete cure by increasing the curing temperature above the T_g of the fully cured material.

Rheometric monitoring of curing processes in the oscillatory mode allows one to determine accurately the gel point and vitrification,[31-33] because it is highly sensitive to the dramatic changes in viscoelastic properties that take place. **Figure 3** plots the storage modulus *G'*, the loss modulus *G"* and the loss factor *tan* δ, recorded on curing at 100 ºC the unmodified formulation, at the oscillation frequency of 5 Hz. Although it is acknowledged

that the frequency-independent crossover of *tan δ* is more accurate, the *G'-G"* crossover around 30 min is also a good approximation because it represents a transition from a liquid-like to solid-like behaviour. Upon gelation, *G'* rises proportionally to the increase in crosslinking density as the curing advances. Vitrification can be identified from the maxima in *G"* and *tan δ* and the increase in *G'*, around 100 min.

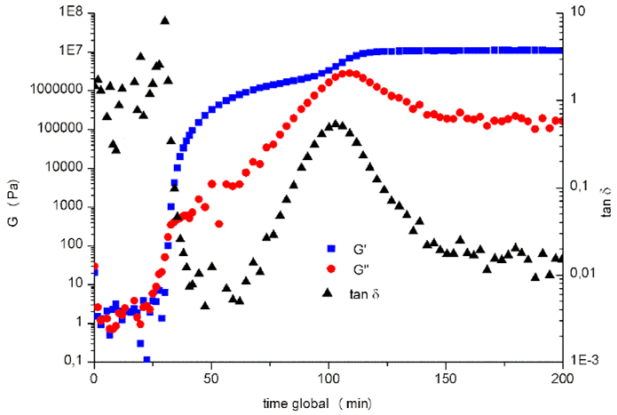

Figure 3. Rheologic monitoring of the curing of the neat formultation at 100ºC. Plotted data corresponds to a measuring frequency of 5 Hz.

Table 4 collects the gel time determined from the *tan δ* crossover and the vitrification time determined from the *tan δ* peak at 5 Hz. It is generally observed that the use of PEI-PCLX/PEI-PCLX-B leads to an increase in the gel time, in accordance of the decelerating effect of these modifiers on the curing process, as seen in the kinetic analysis of the curing process. The gel point conversion x_{gel} was calculated by isothermal simulation of the experimental DSC data, using Eq. (3), and the experimental gel time. In **Table 4** it can be seen that, taking into account the error associated with the comparison of kinetic DSC data and the rheological experiments, x_{gel} is not greatly affected by the presence of the multiarm star polymer, indicating that the curing mechanism is not greatly disturbed by the presence of the modifiers. The values of x_{gel} are within the same range of magnitude as shown in previous reports on the curing of epoxy-anhydride formulations[34-36] indicating that the curing process is practically not affected by the polymeric modifiers.

Table 4. Summary of the rheological monitoring of the curing of different formulations at 100ºC

Formulation	t_{gel}[a] (min)	x_{gel}[b]	t_{vitr}[c] (min)
Neat	33.0	0.31	102.6
10% PEI-PCL30	33.1	0.34	103.0
20% PEI-PCL30	37.2	0.30	100.0
10% PEI-PCL10	38.0	0.34	105.5
20% PEI-PCL10	37.4	0.28	112
10% PEI-PCL30-B	33.2	0.31	98.8
20% PEI-PCL30-B	n/d	n/d	n/d
10% PEI-PCL10-B	36.6	0.32	116.8
20% PEI-PCL10-B	40.2	0.34	113

[a] Gel time determined from the frequency independent crossover of tan δ
[b] Gel point conversion determined using Eq. (3) and t_{gel}
[c] Vitrification time determined as the tan d peak time at the frequency of 5 Hz

If one compares the values of vitrification times of the different formulations, it can be seen that, in spite of the decelerating effect of the polymeric modifiers, vitrification takes place around 100-120 min. Given that curing in the vitrified state is extremely slow, it is not necessary to extend the curing process far beyond the vitrification time. A conversion of *ca*. 70-80 % can be estimated using eq. (3) at the vitrification for all the formulations, indicating the need of a postcuring above the glass transition temperature in any case. Therefore, the curing schedule consisting of 2 h at 100 ºC and 2 h at 180 ºC used for the sample preparation seems adequate to obtain fully cured samples.

Thermal properties of the thermosets obtained

The materials obtained were characterized by DMTA. **Figure 4** shows the storage modulus and *tan δ* curves registered at 1 Hz for neat DGEBA and DGEBA/PEI-PCLX-B formulations. DMTA curves show a single and unimodal relaxation, typical of homogeneous materials. For PEI-PCL10-B formulations both, storage modulus and tan δ-temperature curves, are shifted towards lower temperature, indicating that T_g slightly decreases, as seen above by DSC. The *tan δ* curve becomes broader due to the heterogeneity of the network structure at molecular level. In contrast, formulations containing PEI-PCL30-B have similar characteristics to neat materials and *tan δ* has a similar shape and temperature of the maximum of the peak. The shorter arm length and higher relative amount of PEI in PEI-PCL10-B may facilitate plasticization of the network in comparison with PEI-PCL30-B, thus explaining the difference in relaxation temperatures.

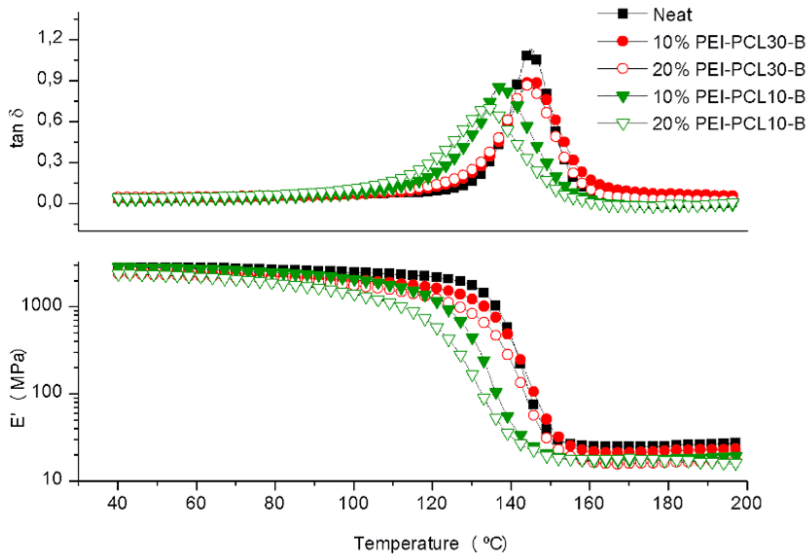

Figure 4. Storage modulus and tan δ curves against temperature for neat DGEBA and DGEBA/PEI-PCLX-B modified materials

Table 5 collects all thermomechanical data obtained. It can be observed that the presence of hydroxyl or acetyl end groups in the polymeric modifiers does not have a significant effect on the network relaxation behavior, given by the values of tan *δ*. The values of tan *δ* follow a similar trend to that of T_g determined by DSC analysis of cured samples (see **Table 3**). All the modified thermosets present a lower value of the modulus in the rubbery region than the neat material, indicating a lower density of crosslinking. The moduli obtained were much lower than the ones of similar materials but cured by 1-MI,[18]

because of the loosening of the network structure taking place when epoxides are cured with anhydrides, which act as chain extenders thus increasing the chain length between crosslinks.

Table 5. Thermomechanical and thermogravimetric data of the thermosets prepared

Formulation	DMTA		TGA	
	$T_{tan\ \delta}$ [a] (°C)	E'_r [b] (MPa)	$T_{5\%}$ [c] (ºC)	T_{max} [d] (ºC)
Neat	146	26	348	401
10% PEI-PCL30	145	22	347	400
20% PEI-PCL30	142	25	348	398
10% PEI-PCL10	136	20	351	399
20% PEI-PCL10	128	14	343	398
10% PEI-PCL30-B	146	23	351	398
20% PEI-PCL30-B	145	17	346	395
10% PEI-PCL10-B	138	18	344	400
20% PEI-PCL10-B	132	17	344	394

[a] Temperature of the maximum of *tan δ* peak.
[b] Storage modulus in the rubbery state determined at *tan δ* peak + 50 ºC
[c] Temperature of the initial degradation calculated at 5% of weight loss.
[d] Temperature of the maximum decomposition rate

Table 5 also reports the thermal stability of the cured samples determined by thermogravimetric analysis. Although not shown, the thermogravimetric curves presented an only degradation step, indicating random and homogeneous bond breaking in the network structure. As previously reported for DGEBA/PEI-PCLX cured by 1-MI, the addition of these star modifiers barely affects the thermal stability in reference to the neat material.[18] In the present study, the higher proportion of ester groups, coming from the anhydride reaction, leads to a reduction of the temperature of initial weight loss ($T_{5\%}$) and temperature of the maximum degradation rate (T_{max}) in about 50 ºC in comparison with 1-MI cured thermosets.[18]

Evaluation of the internal stresses appeared during curing

The analysis of residual stresses in thermosetting polymers usually involves the two main sources of stresses: intrinsic stresses due to rearrangement of molecular structure and thermal stresses based on a thermal expansion mismatch between the epoxy and the adjacent substrate and a uniform temperature difference between cooling down from the T_g to ambient temperature.[37] Normally, it is assumed that there is a low stress development prior to completion of the curing process caused by the volumetric shrinkage of the epoxy, after gelation, due to the cross-link polymerization reaction and the main contribution to the residual stress arises from mismatch in thermal expansion coefficients (*CTEs*) between the coating and the substrate. [38]

Table 6 collects the *CTE* values in the glassy state determined by TMA expansion experiments and the stress results for all the epoxy formulations studied. In general, it can be observed that on increasing the proportion of multiarm star the *CTE* increases due to the introduction of flexible structures within the network structure. The higher *CTEs* correspond to the materials containing PEI-PCL10-B. It should be noticed that on comparing these materials with the ones previously obtained by curing with 1-MI as anionic initiator,[18] the present materials have a slightly higher *CTE* due to the more open structure

of the anhydride cured network that allows a higher expansion on increasing the temperature.

Table 6. Thermal data of the materials and stresses generated on curing for the different formulations

Formulation	E_e[a] (MPa)	SFT[b] (ºC)	CTE_e[c] ($\cdot 10^{-6}$) (ppm/ºC)	σ_R[d] (MPa)	σ_{th}[e] (MPa)
Neat	2884	118.2	85	11.18	10.56
10% PEI-PCL30	2542	110.6	91	9.30	8.95
20% PEI-PCL30	2280	104.9	95	7.83	7.62
10% PEI-PCL10	2816	105.8	78	7.36	7.27
20% PEI-PCL10	2545	99.2	84	6.27	6.18
10% PEI-PCL30-B	2486	120.0	80	9.91	8.79
20% PEI-PCL30-B	2258	110.5	88	8.61	7.66
10% PEI-PCL10-B	2707	109.9	100	10.58	10.53
20% PEI-PCL10-B	2572	98.1	119	10.15	9.66

[a] Elastic modulus obtained by DMA three point bending test
[b] Stress free temperature which is assumed to be equal to the T_g obtained from TMA expansion experiments
[c] Thermal expansion coefficient in glassy state for epoxy thermosets
[d] Experimental residual stress obtained using Eq (7)
[e] Thermal stress obtained using Eq (8)

Comparing experimental and thermal stresses for all the samples, thermal stresses are lower than the experimental ones. This difference can be attributed to the chemical shrinkage on curing, although it may be minimal since chemical shrinkage strains occur at high temperature (early in the cure cycle) when the stress relaxation effects are significant and sufficient time is allowed for relaxation before cooling down. So the stress generated above *SFT* (stress free temperature) can be considered insignificant due to low elastic modulus in rubbery state. On the contrary, below *SFT* (*i.e.* T_g) the residual stress is much higher and by far the most relevant contribution to the total stress, because of the high elastic modulus value in the glassy state and the higher temperature range during cooling below T_g.

Analyzing residual stresses, (σ_R) all samples present lower values in reference to the neat material although in the thermoset containing a 10% of PEI-PCL10-B the difference is not significant. Reduction in residual stress is much notable in the samples containing PEI-PCL10 and 20% PEI-PCL30, with a reduction of 44% for 20% PEI-PCL10, 34% for 10% PEI-PCL10 and 30% for 20% PEI-PCL30. In the sample with a 20% PEI-PCL30-B the relative reduction in reference to the neat one is around 23%. The trend in thermal stress is the same, with similar reductions respect to the neat one. Thus, the addition of PEI-PCLX multiarm stars to DGEBA/anhydride reduces significantly the stress generated in the glassy state and consequently the total stress. Although the increase of *CTEs* on adding the multiarm star tends to increase stresses, the lower *SFT* values of modified formulations compensate this effect leading to a reduction of internal stresses. Formulations with 10% and 20% of PEI-PCL10 have lower stresses according to their lower *SFT* value with respect to the neat one and despite the similar *CTE* value between thermosets with 20% of PEI-PCL10 and neat. The material containing a 20% PEI-PCL30 also presents the lowest residual stress although its *CTE* is higher than the one determined for the neat material, but its elastic modulus is considerably lower.

Consequently, the most decisive parameters affecting the residual stress in an epoxy thermoset are: the glass transition temperature or the stress-free temperature, *SFT*; thermal expansion coefficient (CTE_e) in the glassy state and the elastic modulus (E_e). A decrease in any of these parameters contributes to reduce the residual stresses. As seen above, the incorporation of the different modifiers leads to an increase in *CTE*, but this is offset by a decrease in *SFT* or T_g, which leads to decrease in residual stress.

Mechanical characterization and morphology

Coatings applications require a high hardness in order to keep the good appearance of the surface after an extensive use and prevent protection capacity reduction. Microhardness measurements are the adequate in rating coatings and evaluating the resistance against penetration by a static force. As can be seen in **Figure 5**, all the modified materials have a lower microhardness value. This decrease is more evident for the thermosets containing a 20 wt. % of modifier, but even in these cases the reduction is not dramatic. The end-capping of the multiarm stars does not produce any regular effect. Multiarm stars with shorter arms cause a greater reduction in microhardness, which would indicate a softening of the matrix. However, the effect of multiarm stars on the mechanical properties is more complex. As a means of comparison, ***Table 6*** shows that the decrease in elastic modulus is larger when multiarm stars with longer arms are used, following the opposite trend. In contrast, Table 5 shows that the reduction in T_g is more significant when shorter arms are used, following the same trend as microhardness.

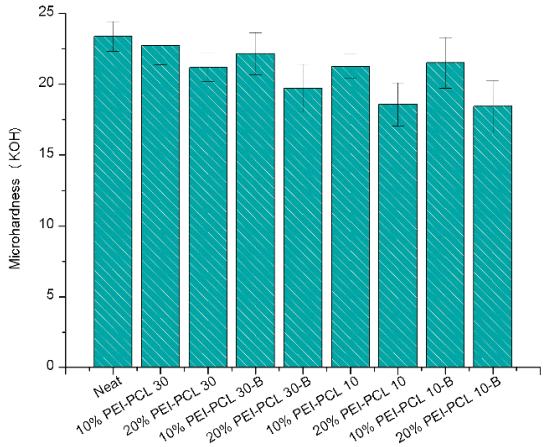

Figure 5. Microhardness values for the thermosets obtained

It is commonly reported in the literature that phase separated materials forming micro or nanoparticles in the epoxy matrix can lead to significant toughness enhancement with respect to homogenous materials.[20,39] In a recent publication, we reported that multiarm PCL stars with hyperbranched poly(ethylenimine) cores used as additives in anionically initiated epoxy formulations have a positive effect on impact strength.[18] However, the materials were homogenous and the effect was discrete.

To evaluate the toughness behavior of neat DGEBA and DGEBA/PEI-PCLX modified thermosets we performed impact test measurements with an Izod pendulum. Then, the morphology of the fracture surfaces were analyzed by SEM inspection. The results of the impact tests are collected in **Figure 6**.

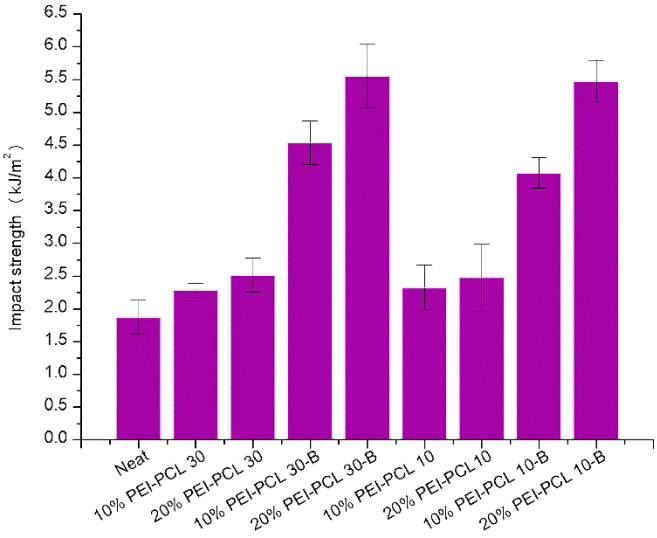

Figure 6. Impact strength values for the thermosets prepared

A great increase of 300%, in reference to the neat material, was observed when a 20% of PEI-PCL30-B was added to the formulation. The superior increase in toughness of end-capped stars modified thermosets obtained in the present study could be explained in the basis of a slight phase separation or nanostructuration of the material. The unreactive character of the end-capped stars with the anhydride could facilitate their separation or nanostructuration producing irregularities in the matrix that can divert the crack propagation. In contrast, the reactive character of unblocked stars may prevent such separation, leading to homogeneous materials with only a small increase in toughness.

In the SEM micrographs collected in **Figure 7** it can be observed the presence of some nanometric structures in the matrix for the materials containing the end-capped multiarm stars. These micrographs present a nanograined morphology similar to the one observed in a previous work in which PCL multiarm stars were used in DGEBA thermosets cured by 1-MI.[17] On the contrary, the SEM micrographs of the material containing the hydroxyl-ended stars showed a smooth surface accounting for a lower fracture resistance. In microphase separated epoxy thermosets obtained by partially end-capping hydroxyl end-groups of HBPs we observed an increase in the β-relaxation at low temperatures, which was related to the hyperbranched separated structure,[20] differently to what happens in the present study.

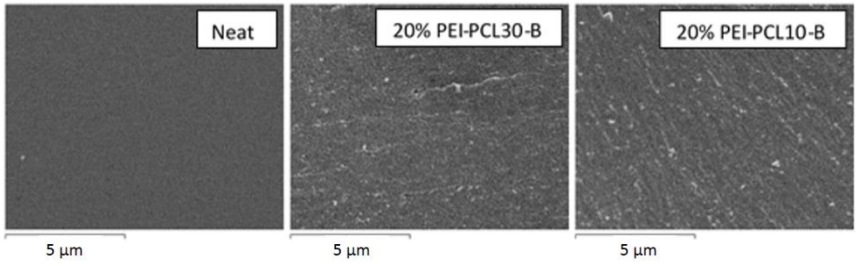

Figure 7. Micrographs of the surface of fracture of the thermosets modified with PEI-PCL30-B and PEI-PCL10-B

It should be noted that, in the case of the material with 20% of PEI-PCL30-B, this optimum toughness enhancement has been achieved to the detriment of elastic modulus which, as seen in Table 6, decreases moderately from 2.9 to 2.3 GPa, a slight decrease in microhardness but no appreciable change in T_g and a significant decrease in internal stresses. Therefore, the addition of blocked multiarm stars seems a promising way to increase the impact strength without compromising significantly other thermal and mechanical characteristics or even processability, but even improving some of them.

Conclusions

The effect of multiarm star polymers based on hyperbranched poly(ethyleneimine) core and poly(ε-caprolactone) arms with a DP of 10 or 30 and hydroxyl or acetyl end-groups, added as modifiers of DGEBA/MTHPA formulations was studied.

The addition of these star polymers slightly delayed the curing process regardless of the arm length or end-capping of the multiarm stars. Accordingly, the gel time was increased upon addition of all the multiarm stars, with no well-defined trend. In spite of this decelerative effect, the curing process was not greatly disturbed by the presence of the polymeric modifiers.

The T_g of the resulting materials was reduced upon addition of the multiarm stars. However, this effect was almost negligible for the stars with longer arm length. The thermal stability of the materials was not affected by the addition of the multiarm stars.

The effect of the multiarm stars on the mechanical properties is complex. In general, a gradual reduction in elastic modulus and microhardness was observed. However, the effect in elastic modulus was larger when multiarm stars with longer arms were used, while the effect on microhardness was more significant with shorter arm length. The addition of the multiarm stars reduced the generation of internal stresses, but the effect was complex, depending on the thermomechanical properties of the thermosets.

Impact strength was notably increased by adding the end-capped multiarm stars to the formulations, which was attributed to a nanostructuration that led to the observation of a nanograined morphology by SEM inspection. The greatest increase measured was a 300%, when a 20% of PEI-PCL30-B was in the thermoset. Hydroxyl ended multiarm stars did not produce any appreciable nanostructuration and thus, the improvement in toughness characteristics was only moderate.

To sum up, one can conclude that the end-capping of hydroxyl groups in PEI-PCLX multiarm stars is greatly beneficial in terms of toughness enhancement without any detriment of thermal and thermo mechanical characteristics.

References

[1] C.A. May, (ed.), Epoxy Resins. Chemistry and Technology, Marcel Dekker, New York, 1988 (Chapter 1).
[2] E.M. Petrie, Epoxy Adhesive Formulations, McGraw-Hill, New York, 2006.
[3] J.P. Pascault, R.J.J. Williams, Epoxy Polymers, Wiley VCH, Weinheim, 2010 (Chapter 1).
[4] R. Bagheri, BT. Marouf BT, RA. Pearson, Polym. Rev. 49 (2009) 201-225.
[5] S. Zheng. In: J.-P. Pascault, R.J.J Williams (Eds). Epoxy Polymers: New materials and Innovations. Wiley-VCH, Weinheim, 2010.
[6] R.D. Brooker, AJ. Kinloch, AC. Taylor, J. Adhes. 86 (2010) 726-741.
[7] F. Meng, Z. Xu, S. Zheng, Macromolecules 41 (2008) 1411-1420.
[8] M.E. Frigione, L. Mascia, D. Acierno, Eur. Polym. J. 31 (1995) 3649-3659.

[9] L. Ruiz-Pérez, G.J. Royston, J.P.A. Fairclough, A.J. Ryan, Polymer 49 (2008) 4475-4488.
[10] R. Mezzenga, C.J.G. Plummer, L. Boogh, J.A.E. Månson, Polymer 42 (2001) 305-317.
[11] M. Morell, M. Erber, X. Ramis, F. Ferrando, B. Voit, A. Serra, Eur. Polym. J. 46 (2010) 1498-1509.
[12] J.P. Yang, Z.K. Chen, G. Yang, S.Y. Fu, L. Ye, Polymer 49 (2008) 3168-3175.
[13] M. Morell, X. Ramis, F. Ferrando, Y. Yu, A. Serra, Polymer 50 (2009) 5374-5383.
[14] J. Zhang, Q. Guo, B. Fox, J. Polym. Sci. Part B: Polym. Phys. 48 (2010) 417-424.
[15] Y. Meng, X-H. Zhang, B-Y.Du, B-X. Zhou, X. Zhou, G-R.Qi, Polymer 52 (2011) 391-399.
[16] M. Morell, A. Lederer, X. Ramis, B. Voit, A. Serra, J. Polym. Sci. Part A: Polym. Chem. 49 (2011) 2395-2406.
[17] M. Morell, D. Foix, A. Lederer, X. Ramis, B. Voit, A. Serra, J. Polym. Sci. Part A: Polym. Chem. 49 (2011) 4639-4649.
[18] C. Acebo, X. Fernández-Francos, F. Ferrando, A. Serra, J.M. Salla, X. Ramis. React. Funct. Polym. 73 (2013) 431-441.
[19] C. Acebo, X. Fernández-Francos, F. Ferrando, A. Serra, X. Ramis, Eur. Polym. J. 49 (2013) 2316-2326.
[20] M. Flores, X. Fernández-Francos, F. Ferrando, X. Ramis, A. Serra, Polymer 53 (2012) 5232-5241.
[21] H. Claesson, E. Malmström, M. Johansson, A. Hult, Polymer 43 (2002) 3511-3518.
[22] S. González, X. Fernández-Francos, JM. Salla, A. Serra, A. Mantecón, X. Ramis. J. Appl. Polym. Sci. 104 (2007) 3407-3416.
[23] X. Ramis, J.M. Salla, C. Mas, A. Mantecón, A. Serra. J. Appl. Polym. Sci. 92 (2004) 381-393.
[24] M. Flores, X. Fernàndez-Francos, X. Ramis, A. Serra. Thermochim. Acta. 544 (2012) 17-26.
[25] M. Benabdi, A.A. Roche, J. Adhes. Sci. Technol 11 (1997) 281-289.
[26] L.F.M. Da Silva, R.D. Adams, Int. J. Adh. Adhesiv. 27 (2007) 362–379.
[27] R.J. Varley, W. Tian, Polym. Int. 53 (2004) 69-77.
[28] K.J. Ivin, in: J. Brandrup, E.H. Immergut (Eds.), Polymer Handbook, Wiley, New York, 1975.
[29] X. Fernández-Francos, A. Rybak, R. Sekula, X. Ramis, A. Serra. Polym. Int. 61 (2012) 1710-1725.
[30] J. Xu, M. Holst, M. Wenzel, I. Alig. J. Polym. Sci.Part B: Polym. Phys. 46 (2008) 2155-2165.
[31] S.R. Raghavan, L.A. Chen, C. McDowell, S.A. Khan, R. Hwang, S. White. Polymer 37 (1996) 5869-5875.
[32] J.P. Eloundou, J.F. Gerard, D. Harran, J.P. Pascault. Macromolecules. 29 (1996) 6917-6927.
[33] X. Fernández-Francos, W.D. Cook, J.M. Salla, A. Serra, X. Ramis. Polym.Int. 58 (2009) 1401-1410.
[34] H. Teil, S.A. Page, V. Michaud, J.A.E. Manson JAE. J. Appl.Polym. Sci. 93 (2004) 1774-1787.
[35] X. Fernández-Francos, X. Ramis, A. Serra. J. Polym. Sci. Part A: Polym. Chem. 52 (2014) 61-75.
[36] Z. Zhang, T. Yamashita, C.P. Wong CP. Macromol. Chem. Phys. 206 (2005) 869-877.
[37] J. Lange, S. Toll, J.-A.E.Manson, A. Hult, Polymer 36 (1995) 3135-3141.
[38] R. K. Sadhir, M. R Luck, Expanding Monomers: Synthesis, Characterization and Applications, CRC, Boca Raton, FL, 1992.
[39] J.F. Fu, L.Y. Shi, S. Yuan, Q.D. Zhong, D.S. Zhang, Y. Chen, J. Wu, J. Polym. Adv. Technol. 19 (2008) 1597-1607.

4.5 Epoxy/anhydride thermosets modified with end-capped star polymers with poly(ethyleneimine) cores of different molecular weight and poly(ε-caprolactone) arms

Cristina Acebo, Miquel Alorda, Francesc Ferrando, Xavier Fernández-Francos, Àngels Serra, Josep M. Morancho, Josep M. Salla, Xavier Ramis

eXPRESS Polymer Letters **2015***, 9,* 809-823

UNIVERSITAT ROVIRA I VIRGILI
HYPERBRANCHED POLY(ETHYLENEIMINE) DERIVATIVES AS MODIFIERS IN EPOXY NETWORKS
Cristina Acebo Gorostiza

eXPRESS Polymer Letters **2015**, *9*, 809-823

Epoxy/anhydride thermosets modified with end-capped star polymers with poly(ethyleneimine) cores of different molecular weight and poly(ε-caprolactone) arms

Abstract

Multiarm star polymers, with a hyperbranched poly(ethyleneimine) (PEI) core and poly(ε-caprolactone) (PCL) arms end-capped with acetyl groups were synthesized by ring-opening polymerization of ε-caprolactone from PEI cores of different molecular weight. These star polymers were used as toughening agents for epoxy/anhydride thermosets. The curing process was studied by calorimetry, thermomechanical analysis and infrared spectroscopy. The final properties of the resulting materials were determined by thermal and mechanical tests. The addition of the star polymers led to an improvement up to 130 % on impact strength and a reduction in the thermal stresses up to 55%. The structure and molecular weight of the modifier used affected the morphology of the resulting materials. Electron microscopy showed phase-separated morphologies with nano-sized fine particles well adhered to the epoxy/anhydride matrix when the higher molecular weight modifier was used.

Keywords: Thermosetting resins, star polymers, epoxy resin, toughness, thermal stress.

Introduction

Epoxy resins are extensively used in technological fields such as electricity and electronics. They are employed as adhesives, matrices in advanced composites, surface coatings and device assemblies because of their combination of high strength and stiffness, excellent corrosion resistance and good electrical properties.[1-3] However, their inherent rigidity and high crosslinking density makes them brittle, thus limiting their potential range of applications. In addition, when epoxy thermosets are used as coatings, thermal stresses generated from the mismatch between the thermal expansion coefficients (*CTE*) of the coating and of the metallic substrate can lead to the appearance of defects that can limit their service life, such as the generation of microvoids and microcracks, the loss of adhesion due to warping. Thermal stress generated during cooling from the curing temperature down to operating conditions, typically room temperature, tends to be more severe than that consequence of heating or during service at constant temperature, especially when the temperature is below glass transition temperature (T_g) of the thermoset.[4]

One of the most successful routes towards toughness improvement is to incorporate polymeric modifiers into the thermosetting matrix to form fine morphological structures. Some effective polymer modifiers are liquid rubber,[5] thermoplastics[6] or core-shell particles.[7] In general, these modifiers are initially miscible with the uncured thermoset precursors but partially or completely phase-separate to typically form spherical structures or bicontinuous structures. The problem of this strategy is a sharp increase of the viscosity of the blends, the drop in the modulus and glass transition temperature and sometimes the poor interfacial adhesion between phases. Recently, a significant toughening effect has been achieved without compromising other properties and processability by using dendritic polymers, especially if the structure and properties of the modifier have been tailored to

enhance the physical and chemical interaction between them and the matrix. The improvement in toughness can be achieved by chemically induced phase separation (CIPS) or by *in situ* homogeneous reinforcing and toughening mechanism, but in both cases covalent linkages or a good compatibility between the modifier and the matrix are necessary.[8-16]

The thermal stresses generated during cooling of thermosetting coatings applied over metal can be minimized by reducing the *CTE* and elastic modulus in the glassy state of the coating, as well as by decreasing its T_g, which in certain applications may not be desired. We recently reported the use of multiarm stars with poly(ethyleneimine) core and poly(ε-caprolactone) or poly(lactide) arms as modifiers in the curing of DGEBA using a tertiary amine as anionic curing agent.[17,18] Upon addition of the modifiers, the decrease on T_g and glassy modulus led to a significant reduction in internal stresses, in spite of the increase in the glassy *CTE*. In another work, it could be seen that the addition of hyperbranched poly(ester-amide)s to epoxy/anhydride systems allowed reaching a significant reduction of the *CTE* in the glassy state and consequently on the thermal stress,[19] the effect being more important when higher molecular weight modifiers were used. Recently, we used multiarm star polymers with hyperbranched poly(ethyleneimine) core and poly(ε-caprolactone) arms of different length with reactive and unreactive terminal groups as modifiers of epoxy/anhydride thermosets.[20] The overall stresses, measured on a steel substrate using the beam bending technique, were significantly reduced with modifiers containing reactive hydroxyl terminal groups and low degree of polymerization of the poly(ε-caprolactone) arms.

Taking all these precedents into account, in the present work we synthesized, following the “core-first” approach, multiarm star polymers with hyperbranched poly(ethyleneimine) cores of different molecular weight and poly(ε-caprolactone) short arms. All the end hydroxyl groups resulting from the polymerization of ε-caprolactone were end-capped with acetyl moieties, but some amine groups of the poly(ethyleneimine) remain unmodified and can potentially react with epoxy groups. These multiarm star polymers were used to modify diglycidylether of bisphenol A/methyl hexahydrophthalic anhydride formulations in the presence of benzyl dimethyl amine as catalyst.

The synthesis of an amphiphilic modifier with hydrophilic core and hydrophobic shell, aimed at reaching phase-separated morphologies. The existence of reactive amino groups in the hyperbranched core would permit the incorporation of the modifier into the network structure, enhancing the interfacial adhesion between phases, if present. Moreover, the hydrophobic poly(ε-caprolactone) arms could contribute to the good interfacial adhesion between the hydrophobic matrix and the modifier-rich phase. To summarize, the goal of the present work is to enhance the toughness and reduce the internal stress in epoxy/anhydride formulations using amphiphilic star polymers with cores of different molecular weight, end-capped arms and reactive amine groups in the core structure.

The curing process was studied by calorimetry, infrared spectroscopy and thermomechanical analysis and the curing kinetics was analyzed by model-free and model-fitting methods. The final properties of the resulting materials were characterized by means of thermogravimetry, thermomechanical analysis and electron microscopy on the fracture surface. Impact resistance was evaluated by Izod impact tests and thermal stresses were estimated on the basis of *CTE*, T_g and elastic modulus measurements.

eXPRESS Polymer Letters **2015**, *9*, 809-823

Experimental

Materials

Poly(ethyleneimine) (PEI) Lupasol®FG (M_w = 800 g/mol, data sheet) and Lupasol®WF (M_w = 25000 g/mol, data sheet) were kindly donated by BASF (Ludwigshafen, Germany) and used without further purification. From the molecular weight of the polymer and of the repeating unit, average degrees of polymerization of 18.3 for Lupasol®FG and 581.4 for Lupasol®WF were calculated. According to the data sheet, the relationship (NH_2/NH/N) was (1/0.82/0.53) for Lupasol®FG and (1/1.2/0.76) for Lupasol®WF, therefore the equivalent number of primary, secondary and tertiary amines is 10, 8.4, and 5.3 meq/g for Lupasol®FG and 8.0, 9.6, and 6.1 meq/g for Lupasol®WF.

ε-Caprolactone (ε-CL, 97 %) was distilled under vacuum before use. Tin (II) 2-ethylhexanoate ($Sn(oct)_2$, 98 %), *N*,*N*-dimethylbenzylamine (BDMA, >99%) and methyl hexahydrophthalic anhydride (MHHPA) were used without further purification. All these chemicals were purchased from Sigma-Aldrich (St. Louis, MO, USA). For the end-capping process by acetylation, extra pure acetic anhydride was used and purchased from Scharlau (Sentmenat, Spain). Triethyl amine (TEA) and *N*,*N*-dimethylamino pyridine (DMAP) were purchased from Fluka (Sentmenat, Spain). Chloroform ($CHCl_3$) was dried under $CaCl_2$ and distilled before use. Solvents were purchased from Scharlab (Sentmenat, Spain).

Diglycidylether of bisphenol A (DGEBA) with an epoxy equivalent of 187 g/eq (Epikote 828, Hexion Speciality Chemicals B.V. Louvain, Belgium) was dried for 4 hours at 40ºC under vacuum before use.

Synthesis of poly(ethyleneimine)-poly(ε-caprolactone) end-capped multiarm stars (PEIX)

In the acronyms for both types of stars (PEIX), X accounts for the data sheet molecular weight times 10^{-2} and take the values of 8 and 250 for Lupasol®FG and Lupasol®WF, respectively. The hydroxyl terminated star polymers were synthesized by ring-opening polymerization of ε-caprolactone from a hyperbranched poly(ethyleneimine) core in bulk at 130ºC. The acetylation to obtain PEIX was performed with acetic anhydride at room temperature overnight in the presence of TEA and a catalytic amount of DMAP in $CHCl_3$ solution as previously described.[17,20] **Figure 1** depicts the synthetic procedure applied in the preparation of the stars.

For both PEIX star polymers ^{1}H NMR (400 MHz, $CDCl_3$, δ in ppm): 4.08 (-C**H$_2$**-OCO-), 2.32 (-NHCO-**CH$_2$**-, -**CH$_2$**-COO), 1.92 (OCO-**CH$_3$**), 1.70-1.30 (-**CH$_2$**-,CL chain) and 3.5-1.5 (PEI core).

The structural data of the stars prepared determined by ^{1}H NMR and values in data sheet were as follows:

PEI8: polymerization degree of arms is 11.8. Fraction of unmodified primary/secondary amines of 0.15. T_g=-54ºC, T_m=58ºC, Δh_m=96 J/g, T_{max}= 390ºC (temperature of the maximum rate of weight loss calculated by TGA).

PEI250: polymerization degree of arms is 13.5. Fraction of unmodified primary/secondary amines of 0.26. T_g=-59ºC, T_m=50ºC, Δh_m=75 J/g, T_{max}= 390ºC.

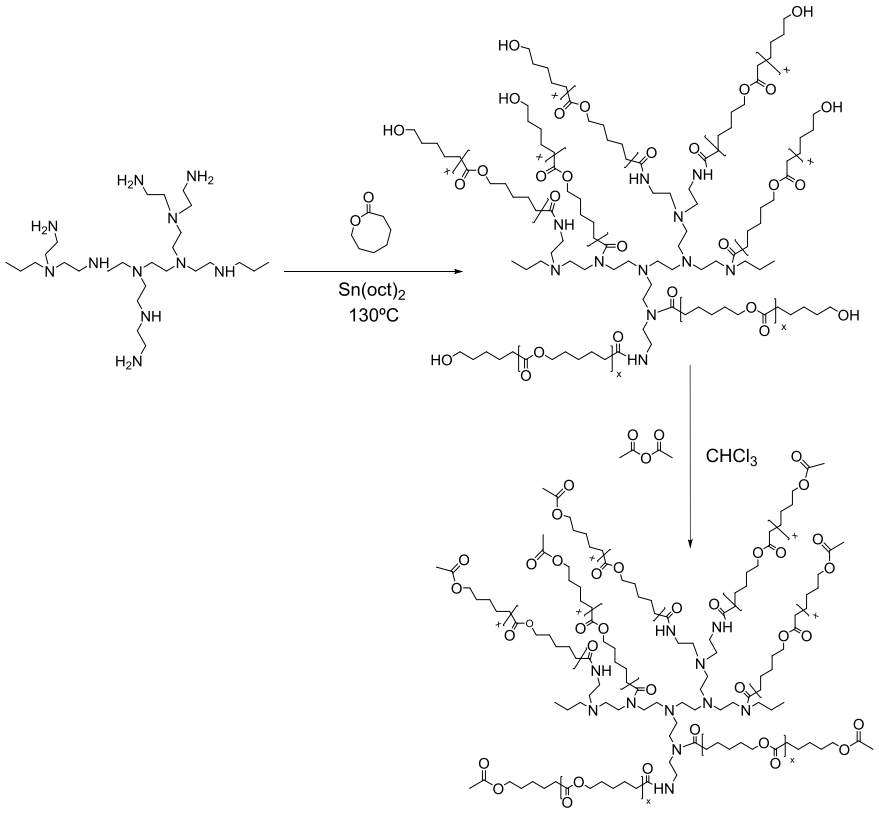

Figure 1. Synthetic procedure for the preparation of the multiarm stars PEI8 and PEI250

Preparation of curing formulations

Mixtures containing MHHPA and the selected proportion of the star polymer were heated mildly until the modifier was dissolved and the solution became clear. The mixture was then cooled down to room temperature and added to the corresponding amount of DGEBA and catalyst. Finally, samples were carefully stirred and degassed under vacuum (at 40ºC) during 15 min to prevent the appearance of bubbles during curing. The catalyst, BDMA, was used at a concentration of 1 phr (1 part of catalyst per hundred parts of DGEBA/MHHPA mixture). The modifier was added at concentrations of 5, 10 and 20% with respect to DGEBA/MHHPA/BDMA mixture. **Table 1** collects the notation and composition of the different formulations studied.

Fully cured samples for DMA, TMA, TGA, DSC, impact and SEM assays were prepared by isothermal curing in oven at 100ºC for 2 h followed by a postcuring at 180ºC for one hour.

Table 1. Notation and composition of the neat and modified formulations in weight percentage (wt. %) and in equivalents per gram of mixture. The weight percentage of the star polymer is indicated in formulation.

Formulation	DGEBA		MHHPA		BDMA		NH from SP
	[wt.%]	[eq/g]	[wt.%]	[eq/g]	[wt.%]	[eq/g]	eq/g
Neat	52.1	$2.79 \cdot 10^{-3}$	46.9	$2.79 \cdot 10^{-3}$	0.99	$7.32 \cdot 10^{-5}$	0
5% PEI8	49.6	$2.65 \cdot 10^{-3}$	44.7	$2.65 \cdot 10^{-3}$	0.94	$6.97 \cdot 10^{-5}$	$3.95 \cdot 10^{-6}$
10% PEI8	47.4	$2.53 \cdot 10^{-3}$	42.6	$2.53 \cdot 10^{-3}$	0.90	$6.66 \cdot 10^{-5}$	$7.54 \cdot 10^{-6}$
20% PEI8	43.4	$2.32 \cdot 10^{-3}$	39.1	$2.32 \cdot 10^{-3}$	0.83	$6.10 \cdot 10^{-5}$	$1.38 \cdot 10^{-5}$
5% PEI250	49.6	$2.65 \cdot 10^{-3}$	44.7	$2.65 \cdot 10^{-3}$	0.94	$6.97 \cdot 10^{-5}$	$1.00 \cdot 10^{-5}$
10% PEI250	47.4	$2.53 \cdot 10^{-3}$	42.6	$2.53 \cdot 10^{-3}$	0.90	$6.66 \cdot 10^{-5}$	$1.92 \cdot 10^{-5}$
20% PEI250	43.4	$2.32 \cdot 10^{-3}$	39.1	$2.32 \cdot 10^{-3}$	0.83	$6.10 \cdot 10^{-5}$	$3.51 \cdot 10^{-5}$

Characterization

^{1}H NMR and ^{13}C NMR measurements were carried out at 400 MHz and 100.6 MHz, respectively, in a Varian Gemini 400 spectrometer (Palo alto, USA). $CDCl_3$ was used as solvent. For internal calibration the solvent signals were used: δ (^{13}C) = 77.16 ppm and δ (^{1}H) = 7.26 ppm for $CDCl_3$.

Calorimetric analyses were carried out on a Mettler DSC-822e thermal analyser (Greifensee, Switzerland). The calorimeter was calibrated using an indium standard (heat flow calibration) and an indium-zinc standard (temperature calibration).

Samples of approximately 10 mg were placed in aluminium pans with pierced lids and cured non-isothermally from 0 to 300ºC at heating rates of 2, 5, 10 and 15 ºC/min, under nitrogen atmosphere, to determine the reaction heat associated with the complete conversion of all reactive groups and study the curing kinetics. In a non-isothermal curing process, the degree of conversion by DSC was calculated as follows:

$$\alpha = \frac{\Delta h_T}{\Delta h_{dyn}} \tag{1}$$

where Δh_T is the heat released up to a temperature T, obtained by integration of the calorimetric signal up to this temperature, and Δh_{dyn} is the total reaction heat associated with the complete conversion of all reactive groups. The reaction rate $d\alpha/dt$ was calculated as the first derivative of the conversion with respect to time.

The glass transition temperatures ($T_{g\infty}$s) of the obtained thermosets, uncured materials and star polymers were determined by means of a scan at 10 ºC/min under nitrogen atmosphere, as the temperature of the half-way point of the jump in the heat capacity when the material changed from glassy to the rubbery state under N_2 atmosphere and the error is estimated to be approximately ± 1°C.

In order to predict the theoretical glass transition temperature of the formulations, Fox equation was used:

$$\frac{1}{T_g} = \frac{w}{T_{g,SP}} + \frac{1-w}{T_{g,matrix}} \quad (2)$$

where $T_{g,SP}$ and $T_{g,matrix}$ are the glass transition temperatures of the star polymer and neat epoxy/anhydride matrix respectively and w is the weight fraction of star polymer in the formulation.

The linear integral isoconversional, model-free method of Kissinger-Akahira-Sunose (KAS) was used for the determination of the activation energy based on the non-isothermal curing curves:

$$ln\left(\frac{\beta}{T^2}\right) = ln\left(\frac{A \cdot R}{g(\alpha) \cdot E}\right) \quad (3)$$

β is the heating rate, T the temperature, E the activation energy, A the pre-exponential factor, R the gas constant, and $g(\alpha)$ the integral conversion function. For each conversion degree, the representation of $\ln(\beta/T^2)$ versus $1/T$ produces a straight line and makes it possible to determine E and $\ln[AR/g(\alpha)E]$ from the slope and the intercept without knowing the kinetic model.

Isoconversional isothermal curing times, t, were estimated taking the non-isothermal data $\ln[AR/g(\alpha)E]$ and E, determined from equation (3), and applying the rate equation integrated in isothermal conditions:

$$ln\ t = ln\left(\frac{g(\alpha)}{A}\right) + \frac{E}{RT} \quad (4)$$

Assuming that the approximation given by expression (3) is valid, we can determine the kinetic model that best describes the curing process by rearranging expression (3) as shown in equation (5):

$$ln\left(\frac{g(\alpha) \cdot \beta}{T^2}\right) = ln\left(\frac{A \cdot R}{E}\right) - \frac{E}{R \cdot T} \quad (5)$$

which is the basis for the composite integral method for the determination of the kinetic model. Given that the curing of epoxy-anhydride can be satisfactory modelled using autocatalytic-like models with an overall reaction order around 2, we have fitted using equation (5) the experimental data to autocatalytic kinetic models with $n+m=2$, where n and m are the order of reaction.

The results of the kinetics analysis were used to model the curing and to determine the optimum curing times to achieve fully cured thermosets. In addition, isothermal curing times determined by simulation of non-isothermal kinetic data (equations 3 and 4) were compared with experimental isothermal curing times obtained by means of FTIR experiments.

Details of the kinetic methodology used can be found in previous works.[21,22]

A Bruker Vertex FTIR spectrometer (Ettlinge, Germany) equipped with an attenuated-total-reflectance accessory with a diamond crystal (Golden Gate heated single-reflection diamond ATR, Specac-Teknokroma, Sant Cugat del Vallés, Spain) was used to monitor the curing process. Spectra were acquired in the mid-infrared region (spectral range of 600-4000 cm^{-1}) with a resolution of 4 cm^{-1}. 20 scans were averaged for each spectrum. The

evolution of the functional groups was monitored during isothermal curing at 100ºC, taking the band at 1508 cm^{-1}, attributed to the DGEBA aromatic rings, as a reference. The conversion was determined by the Lambert-Beer law from the normalized change of absorbance at 1732 cm^{-1} (formation ester groups) and at 1860+1785 cm^{-1} (disappearance of anhydride group) as explained in a previous work.[22]

A thermo-mechanical analyzer Mettler thermomechanical analysis SDTA840 (Greifensee, Switzerland) was used to determine the conversion at the gel point and the thermal expansion coefficients.

A silanized glass fiber disc about 5 mm in diameter was impregnated with the liquid formulation and sandwiched between two aluminium discs. The sample was heated up from 40 to 200 ºC at 2 ºC/min and subjected to an oscillatory force from 0.005 to 0.01 N with an oscillation frequency of 0.083 Hz. The gel point temperature was taken as the onset in the decrease of the oscillation amplitude measured by the probe. The conversion at the gel point was determined from the gel point temperature and a dynamic curing experiment in the DSC at 2 ºC/min.

Cured samples (1.5 x 8 x 8 mm^3) were supported by two silica discs and heated at 5ºC/min from 30 up to 150ºC by application of a force of 0.02N. Two heating were performed, the first one to erase the thermal history and the second one to determine the thermal expansion coefficients (*CTE*s), below and above the T_g , calculated as follows:

$$CTE = \frac{1}{L_0} \cdot \frac{dL}{dT} = \frac{1}{L_0} \cdot \frac{dL/dt}{dT/dt} \tag{6}$$

where, *L* is the thickness of the sample, L_0 the initial length, t the time, *T* the temperature and d*T*/d*t* the heating rate.

DMA was carried out with a TA Instruments DMA Q800 (New Castle, DE, USA). Three point bending of 10 mm at 1 Hz and 0.05 % strain was performed at 3 ºC/min from -150 to 250ºC on prismatic rectangular samples (ca. 2 x 12 x 20 mm^3).

The thermal stress caused by the variation of the temperature, σ_{th}, in a bi-layer strip (epoxy-anhydride coating/steel substrate) was determined from the radius of curvature, *R*, in the assumptions of the simple beam theory and from the free body analysis of strains in the two layer. The calculation was made taking account the dependence on the geometrical parameters and properties of the sample and substrate, according to Benabdi and Roche methodology,[23] see equation (7) and (8):

$$\frac{1}{R} = \frac{6 \cdot (1+\beta)^2 \cdot (SFT - T_{amb}) \cdot (CTE_c - CTE_s)}{(t_c + t_s) \cdot \left[3 \cdot (1+\beta)^2 + (1+\alpha\beta)\left(\beta^2 + \frac{1}{\alpha\beta}\right)\right]} \tag{7}$$

$$\sigma_{th} = \frac{1}{R} \cdot \frac{E_s \cdot t_s}{6} \left[\frac{1}{\beta(\beta+1)}(\alpha\beta^3 + 1) + 3\alpha\beta\right] \tag{8}$$

where the subscripts *c* and *s* mean coating and substrate respectively, *t* is the thickness, *E* the elastic modulus, $\alpha = E_c/E_s$, $\beta = t_c/t_s$, *SFT* is the stress free temperature taken as the transition glass transition temperature determined by TMA and T_{amb} is the ambient temperature taken as 40ºC.

In this study a stainless steel, with an elastic modulus of 180,053 MPa and thermal expansion coefficient of $16 \cdot 10^{-6}$ ºC^{-1}, was selected as the substrate and the thickness of the steel substrate and the epoxy/anhydride coating was respectively 0.1 mm and 0.4 mm. The elastic modulus of epoxy/anhydride sample was determined by DMA.

Thermogravimetric analysis was carried out with a Mettler TGA/SDTA 851e/LF/1100 thermobalance (Greifensee, Switzerland). Samples with an approximate mass of 10 mg were degraded between 30 and 800ºC at a heating rate of 10 ºC/min in a nitrogen atmosphere (50 cm^3/min measured in normal conditions).

The impact test was performed at room temperature by means of an Zwick 5110 impact tester (Ulm, Germany) according to ASTM D 4508-10 (2010) using rectangular samples (2 x 12 x 25 mm^3). The pendulum employed had a kinetic energy of 0.5 J. For each material, nine determinations were made. The impact strength (*IS*) was calculated from the energy absorbed by the sample upon fracture as:

$$IS = \frac{E - E_0}{S} \quad (9)$$

where *E* and E_0 are the energy loss of the pendulum with and without sample respectively, and S is the cross-section of the samples.

The fracture surface of the samples, previously fractured by impact at room temperature, was coated with a conductive gold layer and then examined with a Jeol JSM 6400 SEM (JEOL Ltd., Tokyo, Japan) with a resolution of 3.5 nm and different magnifications (100, 500 10,000 and 50,000).

Results and discussion

Synthesis and characterization of multiarm stars

The synthesis of the multiarm stars was performed as previously described in two different papers, one of them describing the growing of the poly(ε-caprolactone) arms from the PEI core and the other to the blocking of hydroxyl end-groups by reaction with acetic anhydride.[17,20] The length of the arms can be adjusted, in principle, from the amount of ε-CL per reactive group in the core (NH and NH_2). In this paper, PEI cores of 800 and 25000 g/mol of mass-average molecular weight were employed.

The multiarm star molecules where characterized by ^{1}H NMR spectroscopy as done in the previous works.[17,20] It could be seen that the increase in the molecular weight of the core did not change significantly the ^{1}H NMR spectrum. From the spectra of the hydroxyl-ended stars we could determine the degree of polymerization of the arms. However, in both cases the arms were longer (*DP* = 11.8 and 13.5) than expected (*DP* = 10) and the difference was higher for the larger core. Since all the ε-CL reacts, the higher polymerization degree of the arms calculated from the spectra led us to the conclusion that part of the NH- and NH_2 groups could not initiate the growth of an arm. From these values we estimated a degree of modification of 0.85 for the PEI8 core and of 0.74 for the PEI250 core. The effect of the core size is noteworthy, as the degree of modification of the PEI250 core is significantly lower. The hydrogen bond interactions and the steric hindrance could be the responsible for these differences. Although the evaluation of the modification achieved in terminal and linear units could not be accomplished, linear units seem to be less reactive because of the lower nucleophilicity of secondary amines and the more internal position of these units in the PEI structure. Moreover, intra-molecular hydrogen

bonding in PEI may difficult the penetration of ε-CL into the core structure and subsequent polymerization reaction.

The acetylation of the hydroxyl groups at the end of the arms was performed as described and the spectra obtained were similar to the ones published before.[20] The complete disappearance of $–CH_2OH$ signals showed that all hydroxyl groups were blocked. The intensity of the methyl signals (at 1.92 ppm) allowed us to determine that unreacted NH groups were still in PEI8 and PEI250 structures.

By using linear standards the molecular weight of star polymers are usually underestimated by GPC and this method does not rend accurate molecular weights. However, the GPC analysis did not produce signals at low molecular weight, meaning that no detectable poly(ε-caprolactone) homopolymer was formed during the ring-opening polymerization. In addition, the shape of the curves was unimodal in both PEI8 and PEI250, due to the living characteristics of the ε-CL polymerization.

Study of the curing and thermal properties of DGEBA/MHHPA/PEIX mixtures

The presence of hydroxyl groups and tertiary amines in epoxy-anhydride formulations, leads to a complex competitive mechanism consisting of polycondensation, initiated by hydroxyl groups, and ring opening polymerization, initiated by tertiary amine.[19,24] Moreover the existence of secondary and/or primary amines in the reaction medium may also lead to a polycondensation between these groups and epoxy resin or even anhydrides and the concomitant appearance of new tertiary amines or amides. In previous works we reported the use of hyperbranched poly(ethyleneimine)s as crosslinking agents in epoxy formulations,[25,26] reacting by an epoxy-amine condensation mechanism and getting thus incorporated into the network structure of the thermoset. The curing kinetics was slowed down by their lower mobility in comparison with smaller amines and they led to more densely crosslinked materials due to the presence of internal branching points in the hyperbranched polymer structure. However, the total number of reactive amino groups introduced in the formulation is very small taking into account the elevated molecular weight of the stars polymers, and the effect would be difficult to quantify. It should be also noticed that not all the amine groups would be able to react because of steric hindrance or topology restrictions**.**

Figure 2 shows the plots of degree of conversion and reaction rate against temperature recorded at 10ºC/min of neat formulation and formulations containing different amounts of PEI250. Calorimetric curves for neat and 5% showed a unimodal shape, which indicates that, the different curing mechanism takes place at the same time or that one of them predominates, in particular the epoxy-anhydride alternating copolymerization mechanism, due to the presence of BDMA. Formulations containing 10% and 20% of PEI250 show a secondary process at conversions above 0.8. Because epoxy-amine condensation may take place at a relatively low temperature[25,26] this process, at high temperature and slow rate, could be related with the non-catalytic epoxy/anhydride curing mechanism or epoxy homopolymerization, although this is generally observed in anhydride-deficient formulations.[27]

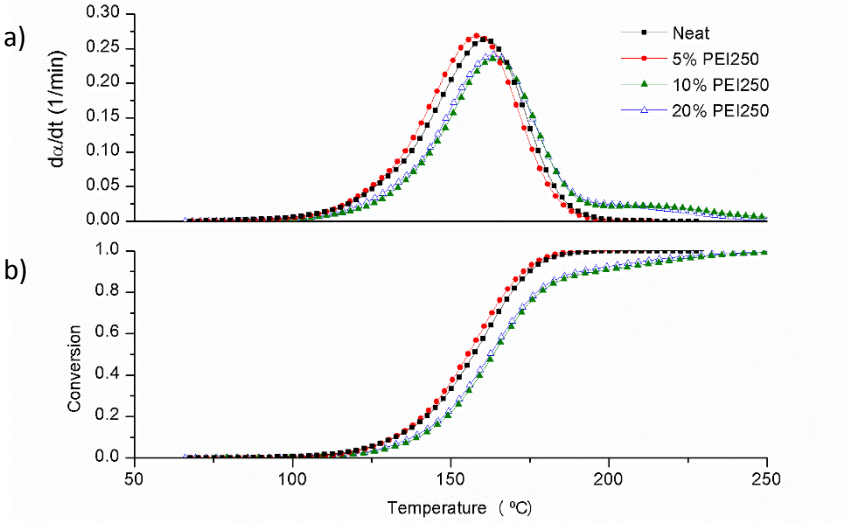

Figure 2. Reaction rate da/dt (a) and degree of conversion (b) against temperature of neat and PEI 250 formulations at 10ºC/min

In the presence of a small amount of star polymer the curing is slightly accelerated possibly due to the additional tertiary amines coming from the modifier. When a higher amount of modifier is used (10 and 20%) the reaction rate decrease and the conversion-temperature curves shift at higher temperatures (Figure 2). In these last cases the higher viscosity of the formulations, the lower mobility of the reactive species and the lower content of epoxides may contribute to decelerate the curing rate of the epoxy/anhydride/PEIX formulations. Although the differences between formulations are not large, the relative influence of the discussed parameters can lead to acceleration or deceleration of the curing.

When PEI8 was used as modifier a similar trend was observed (not shown), although both effects, acceleration at low modifier content and deceleration at high modifier content, take place to a lesser extent. This result can be rationalized on the basis of the lower tertiary amine content and viscosity of PEI8 than PEI250.

The nonisothermal curing kinetics were analyzed using the isoconversional KAS methodology (eq.3). **Figure 3** shows that *E* remains constant during the entire range of conversions for neat and 5% formulations, whereas for 10 and 20% *E* is maintained constant up to a conversion of 0.8, to decrease sharply between 0.8 and 1. This result is consistent with the existence of two curing mechanisms, activated at different temperatures, in modifier-rich formulations (Figure 2).

As described in the experimental section, model fitting was performed using suitable phenomenological model, autocatalytic model with $n + m = 2$,[22,24] which may generally describe the autocatalytic behaviour of the catalyzed epoxy-anhydride curing. Non-isothermal data at different heating rates were simultaneously fitted by linear regression (eq.5), in the conversion range 0.1-0.8, where activation energy is nearly constant for all formulations.

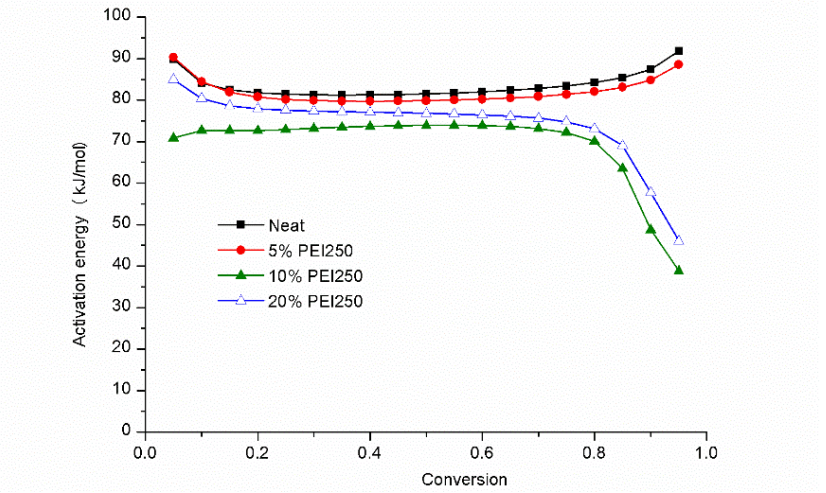

Figure 3. Activation energy during curing of neat and PEI250 formulations obtained by using the Kissinger-Akahira-Sunose method

Table 2 summarizes the results of the linear fitting and other kinetic parameters. The linear regression coefficients get close to one and the similarity between fitted and isoconversional activation energies evidence the quality of the fitting and the suitability of the kinetic model chosen. All formulations show similar kinetic parameters, an indication of the fact that the curing mechanism is not significantly affected by the presence of the star polymer modifier. The values of $d\alpha/dt$ and k, calculated using Arrhenius equation and the kinetic parameters, activation energy and pre-exponential factor obtained by adjustment, agree with the reactivity of the different formulations and with the experimental calorimetric curves (Figure 2). On increasing the content of star polymer up to 5%, the curing accelerates (k and $d\alpha/dt$ increase), but gradually decelerates (k and $d\alpha/dt$ decrease) at higher modifier contents. The kinetic effects of the modifier are more relevant when PEI250 is used, showing greater differences between the values of k and $d\alpha/dt$ and those of the neat formulation.

Table 2. Kinetics parameters of curing process

Formulation	E [a] (kJ/mol)	ln A [a] (min^{-1})	n [a]	m [a]	r [a]	$k_{150ºC}$ [b] (min^{-1})	$(d\alpha/dt)_{0.5}$ [c] (min^{-1})	E_{iso} [d] (kJ/mol
Neat	82	22.92	1.58	0.42	0.999	0.66	0.165	83
5% PEI8	76	21.39	1.53	0.47	0.999	0.69	0.174	77
10% PEI8	77	21.42	1.54	0.46	0.999	0.65	0.161	77
20% PEI8	67	18.48	1.53	0.47	0.999	0.50	0.125	69
5% PEI250	81	22.64	1.55	0.45	0.999	0.75	0.187	82
10% PEI250	70	18.95	1.57	0.43	0.992	0.38	0.095	71
20% PEI250	75	20.95	1.57	0.43	0.999	0.45	0.113	75

[a] Kinetic parameters obtained by model-fitting using an autocatalytic model with $n+m=2$
[b] Values of rate constant at 150ºC using the Arrhenius equation and the parameters E and ln A
[c] Values of reaction rate at 150ºC obtained using the equation rate $d\alpha/dt=k\cdot f(\alpha)=k\cdot(1-\alpha)^n\cdot\alpha^n$ at 50% conversion
[d] Average isoconversional activation energy.

The curing kinetics of all formulations were studied with FTIR spectroscopy at 100ºC in order to identify the main reactions taking place during curing and compared with the curing kinetics obtained by non-isothermal procedure. **Figure 4** shows FTIR spectra recorded during isothermal curing of neat formulation at 100ºC. The general features of the epoxy-anhydride curing reaction can be observed: the decrease of the anhydride groups (bands at 1780 and 1860 cm^{-1}) that react giving rise to ester groups (1735 cm^{-1}). The disappearance of epoxy groups was also observed but not quantified because of the difficulty to separate its contribution from the different overlapping signals in the region around 910 cm^{-1}.

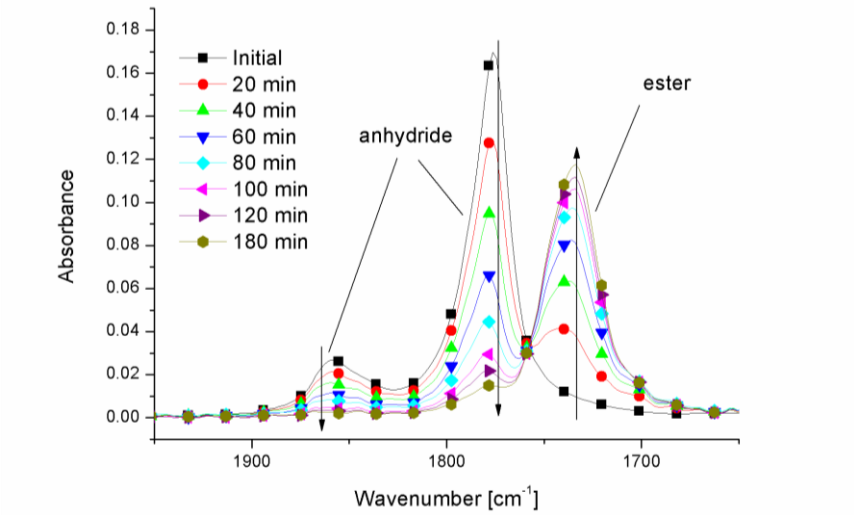

Figure 4. FTIR spectra recorded during curing of neat formulation at 100ºC

Figure 5 shows the evolution of ester and anhydride groups against time recorded during curing for the 10%PEI250 formulation at 100 ºC in the spectrometer. It can be observed that the formation of ester and the disappearance of anhydride groups take place almost at the same time up to 0.6 of conversion, showing little discrepancies at higher conversion. This result agrees with the fact the curing mainly follows an alternating epoxy-anhydride mechanism catalyzed by tertiary amines. The inset in Figure 5 plots the ester **c**onversion with respect to the anhydride conversion at 100ºC for neat and all the PEI250 formulations. It can be observed that the evolution of both groups follows the diagonal line, indicating again an alternating copolymerization mechanism. Figure 5 shows the conversion of epoxy groups determined by using equation (4) from the non-isothermal isoconversional kinetic parameters obtained by DSC. It can be observed that the conversions are similar to those obtained by FTIR. The slight differences between the evolutions of the different reactive species observed at high conversions can be related with the activation of a second curing mechanism that takes place during non-isothermal curing in DSC (Figure 5) at higher temperatures, uncatalyzed epoxy-anhydride reaction or epoxy homopolymerization, a process that is not activated during isothermal curing at moderate temperatures. FTIR and DSC simulation of PEI8 formulations showed similar trends than those observed for PEI250.

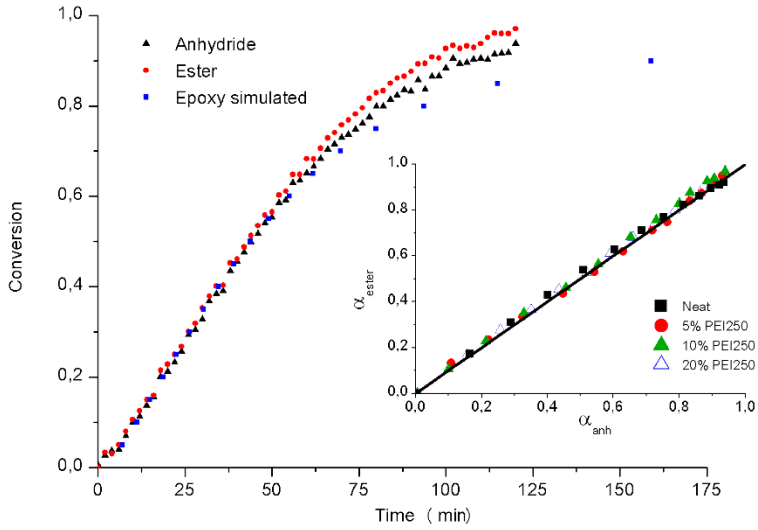

Figure 5. Conversion of the ester groups, α_{ester}, and reacted anhydride, α_{anh}, during curing of 10% PEI250 formulation at 100ºC in FTIR. Epoxy conversion simulated using non-isothermal isoconversional DSC. Inset: conversion of the ester groups against reacted anhyidride for neat and PEI250 formulations.

It can be concluded that curing of epoxy-anhydride formulations containing PEI8 and PEI250 proceeds mainly by anionic alternating copolymerization catalyzed by tertiary amines. Rocks *et al.*[28] studied the curing of epoxy-anhydride formulations catalyzed by tertiary amines by Raman spectroscopy and concluded that, in spite of the complexity of the curing mechanism, the overall curing profile corresponded to an alternating epoxy-anhydride copolymerization. However, epoxy-amine condensation may take place, thus permitting the covalent linkage between the modifier and the matrix. The quantification of this process is not possible, since it may take place to a very low extent. The other processes, occurring at higher temperatures, as observed by DSC, may not be relevant depending on the isothermal curing schedule selected in the processing.

Table 3 shows the experimental heats of polymerization, Δh, calculated as the average heat of the experiments at different heating rates. On increasing the proportion of modifier Δh (J/g) decreases due to the lower content of reactive epoxy and anhydride groups, whereas Δh (kJ/ee) remains almost constant and similar to the values reported for other similar epoxy systems.[29] FTIR spectra of both isothermal and non-isothermal cured samples showed that the absorbance bands of oxirane and anhydride groups disappeared completely. Moreover, no residual heat was observed after a second dynamic scan made up to 250ºC to determine T_g. These results indicate that all formulations reacted almost completely.

Table 3. Calorimetric data, α_{gel}, thermal stability data and dynamomechanical properties of the formulation studied in this work

Formulation	Δh [a] (J/g)	Δh [b] (kJ/ee)	$T_{g\infty}$ [c] (ºC)	$T_{g\infty,Fox}$ [d] (ºC)	α_{gel} [e]	T_{max} [f] (ºC)	Tan δ [g] peak (ºC)	Tan δ [h] FWHM (ºC)	E_r' [i] (MPa)
Neat	288	103	132	132	0.47	406	143	14	28
5% PEI8	272	103	126	115	0.55	406	139	17	24
10% PEI8	258	103	118	99	0.49	405	130	25	20
20% PEI8	249	112	111	71	0.52	405	124	32	16
5% PEI250	257	97	118	115	0.45	405	127	16	23
10% PEI250	255	102	111	99	0.45	404	124	25	18
20% PEI250	230	103	103	71	0.48	403	114	32	13

[a] Enthalpies per gram of mixtures
[b] Enthalpies per equivalent of epoxy groups
[c] Glass transition temperature after isothermal curing
[d] Calculated glass transition temperature, using DSC data and Fox equation
[e] Degree of conversion at gelation determined as the conversion reached by non-isothermal TMA and DSC tests at 2ºC/min
[f] Temperature of the maximum rate of weight loss calculated by thermogravimetry
[g] Temperature of maximum of tan δ
[h] FWHM stands for full width at half maximum of tan δ
[i] Storage modulus in the rubbery state determined at tan δ peak + 50ºC

The T_g of the isothermally cured samples, determined by DSC, decreases progressively on increasing the proportion of star polymer in the formulation, but this decrease is more evident when PEI250 is used. The different flexibility of both modifiers, the amount of physical entanglement and croslinking density and the existence of separated phases of different size and structure could be the responsible of this behaviour. In order to understand the effect of the star on the matrix, the Fox equation was applied to predict the T_g of the fully cured thermosets. Up to 5% of PEI250 content, the thermosets have an experimental value of T_g similar to the predicted by this equation, whereas formulations containing 10% and 20% of both modifiers show experimental T_g's significantly higher than the theoretical ones. These results could be explained by a phase separation of the star polymer due to the incompatibility produced during the curing reaction, which was further confirmed by electron microscopy.

The results of the gelation tests are summarized in Table 3. The conversion at the gelation point α_{gel} is only little affected by the addition of both star polymers, and in all cases the obtained values are within the range commonly observed for epoxy-anhydride systems, around 0.3-0.5.[24,30,31] This scattering of values can be explained not only by the differences and accuracy of the measuring techniques but from the presence of protic impurities or the occurrence of initiator regeneration reactions that tend to increase α_{gel}.[30-32]

Figure 6 shows the thermogravimetric curves for neat and PEI250 formulations. It can be observed that the degradation takes place in only one step, indicating random breaking of bonds. Formulations containing PEI8 show similar TGA traces (not shown). The results of the thermogravimetric analysis of all formulations are summarized in Table 3. Although modified formulations contain C-N bonds that are less stable than the C-C bonds of the epoxy matrix, all formulations show similar thermal stability (T_{max}). This is in agreement with previously reported results using poly(ε-caprolactone) modified polymers.[17,20] This can be explained by the low proportion of hyperbranched core in the modifier structure (even lower in the formulation), the similar thermal stability of the ester bonds in the poly(ε-

caprolactone) arms and the epoxy-anhydride polyester network structure, and the possible covalent linkage between the matrix and the modifier.

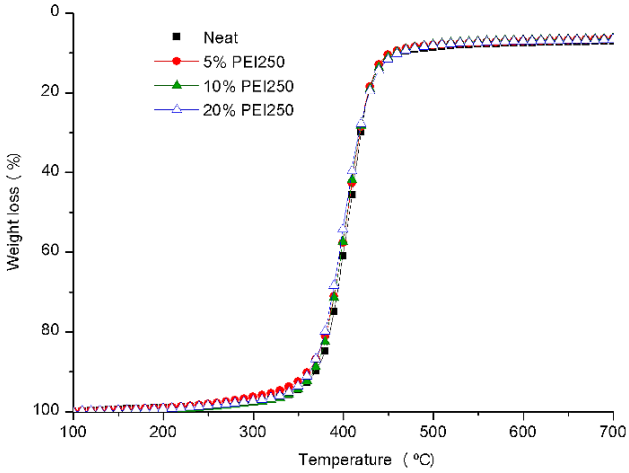

Figure 6. Thermogravimetric curves at 10ºC/min in nitrogen atmosphere of the neat and PEI250 formulations

Thermomechanical properties and thermal stress

Table 3 collects the results of the DMA characterization of all the samples prepared. **Figures 7** and **8** plot the evolution of tan δ and storage modulus of PEI250 and PEI8 formulations, respectively. In agreement with the calorimetric data, when the proportion of modifier increases, the network relaxation curves are shifted towards lower temperatures, indicating that T_g decreases on adding modifier, as seen with DSC. The effect is more remarkable in PEI250 formulations, probably due to an increase in the plasticization caused by the longer poly(ε-caprolactone) arms or a decrease in the crosslinking density. It can also be observed that the α-relaxations (related to the T_g) of all formulations are unimodal, indicating that all thermosets have homogeneous network structures, but modifier-rich formulations show a more disperse network, as seen from the broader α-relaxation and higher FWHM values. Meng and coworkers[33,34] observed the contrary trend using hyperbranched polyethers as toughening agents for epoxy/amine systems, but their materials showed a homogeneous morphology. Table 3 and Figures 7 and 8 show a decrease in the rubbery modulus and in the height of α-relaxation upon addition of the modifier. According to the rubber elasticity theory, the relaxed modulus is proportional to the crosslinking density, but deviations from the ideal network behaviour are likely to occur for a variety of reasons.[26,35,36] The decrease in rubbery modulus is not proportional to the modifier content, suggesting an additional decrease in the crosslinking density connected with the participation of the star polymer in the curing process.

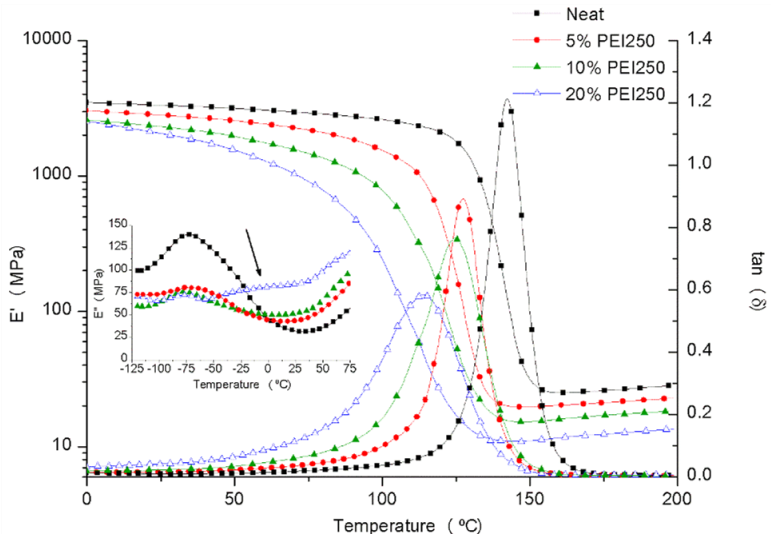

Figure 7. Storage modulus and tan δ curve against temperature for neat and PEI250 modified materials. The inset shows a detail of loss modulus curves at low temperatures.

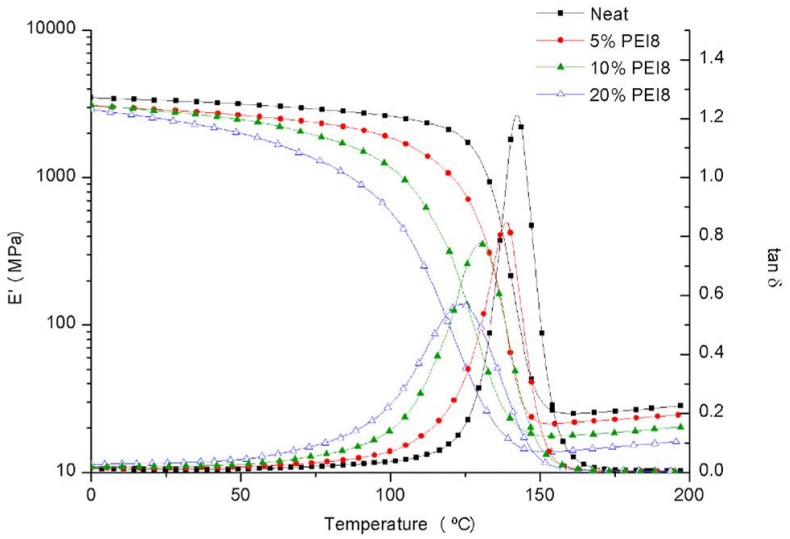

Figure 8. Storage modulus and tan δ curve against temperature for neat and PEI8 modified materials

The inset in Figure 7 shows a detail of loss modulus curves in the region of low temperature. It can be seen that the β-relaxation (attributed to glyceryl or diphenylpropane groups) decreases but it broadens on increasing the modifier content. This can be tentatively attributed to a new star polymer-rich phase formed during curing and to a restricted mobility of the matrix structure due to the additional bonding with star-polymer.

In order to determine the potential application of the prepared materials as coatings, the generation of thermal stress during cooling of neat and PEI250 and PEI8 formulations on steel as a rigid substrate were studied using the Benabdi and Roche methodology described in the experimental section.[23] In a previous work, we demonstrated that the

intrinsic stress generated during curing of an epoxy system, due to rearrangement of molecular structure, and the thermal stress generated in the rubbery state, are much lower than the thermal stress generated on cooling down from the T_g to room temperature,[14,20] therefore in the present work we only calculate the thermal stress originated on cooling.

Table 4 collects the thermal stress values, σ_{th}, calculated using equations (7) and (8) and the following experimental data of epoxy/anhydride/PEIX coating: CTE_c in the glassy state determined by TMA, elastic modulus determined by DMA at room temperature (40ºC), E_c, and stress free temperature, *SFT*, taken as the glass transition temperature determined by TMA. It can be observed as σ_{th} decreases significantly on increasing the modifier content, due to a decreasing of some of these three parameters: CTE_c, E_c and *SFT*. In general, E_c and *SFT* regularly decrease on increasing PEIX content, according to the high flexibility and low crosslinking density of modified thermosets, whereas CTE_c does not follow a clear trend. While the CTE_c of PEI8 formulations hardly varies, CTE_c of PEI250 formulations increases slightly. Although this increase tends to increase the stresses, the lower E_c and *SFT* values of PEI250 formulations compensate this effect leading to significant reduction of thermal stress. This reduction is higher for PEI250 formulations than for PEI8 formulations and the highest reduction of σ_{th} is achieved by adding a 20% of PEI250. These results agree, again, with the higher flexibility and lower crosslinking density induced by the presence of PEI250 and its possible participation in the curing process.

Table 4. Thermal data of the materials and thermal stresses generated during cooling for the different formulations

Formulation	E_c [a] (MPa)	α [b]	*SFT* [c]	CTE_c [d]	$1/R$ [e] (mm^{-1})	σ_{th} [f] (MPa)
Neat	3241	0.018	125	87	0.0169	16.4
5% PEI8	2796	0.016	119	83	0.0146	12.5
10% PEI8	2626	0.015	113	85	0.0137	11.2
20% PEI8	2203	0.012	104	92	0.0129	9.1
5% PEI250	2687	0.015	109	93	0.0145	12.1
10% PEI250	2505	0.014	105	95	0.0139	10.9
20% PEI250	1782	0.010	96	102	0.0123	7.4

[a] Elastic modulus determined by DMTA.
[b] Ratio of coating and substrate module $\alpha = E_c/E_s$.
[c] Stress free temperature taken as the transition glass transition temperature determined by TMA.
[d] Thermal expansion coefficient in the glassy state determined by TMA.
[e] Curvature determined using eq. (6)
[f] Thermal stress determined using eq. (7).

Mechanical characterization and morphology

The toughness behaviour of all cured formulations was investigated by impact test and the morphology was analyzed by SEM on the impacted fracture. **Figure 9** shows that both PEI250 and PEI8 produce a significant increase in the impact strength of the cured materials, proportional to the amount of modifier used. This increase is more than 100% with respect to the neat formulation, for thermosets containing a 20% of both modifiers. This result is consistent with a phase-separated morphology, where soft particles of modifier adhered to the epoxy/anhydride matrix absorb energy during impact test, although

the DMA and DSC results showing a decrease in the T_g of the cured material suggest also some enhancement in the matrix shear yielding. The degree of interfacial adhesion between the soft phase and the matrix is critical in toughening. Effective toughening is believed to occur with an intermediate interfacial bonding, since an excessive adhesion can deteriorate the interfacial adhesion between the toughener phase and the matrix.[36] In previous works we observed that polymeric modifiers with excessive physical-chemical compatibility with the matrix led to their covalent incorporation into the network structure, preventing phase separation and producing very little toughness enhancement, whereas polymers that phase-separate during curing but with certain physical-chemical compatibility with the matrix led to the highest increase in impact strength.[14] Although it is not possible to know the amount of amine groups that react during curing, it is reasonable assuming the formation of some covalent bonds between the remaining amine groups at the core of the star polymer and the epoxy groups. Although the addition of both stars increases toughness characteristics the improvement achieved with PEI250 is higher. The amount of covalent bonds formed between matrix and modifier, the higher flexibility of PEI250 and the resulting polymer matrix and the lower thermal stress in PEI250 formulations can justify the differences observed between PEI250 and PEI8 thermosets.

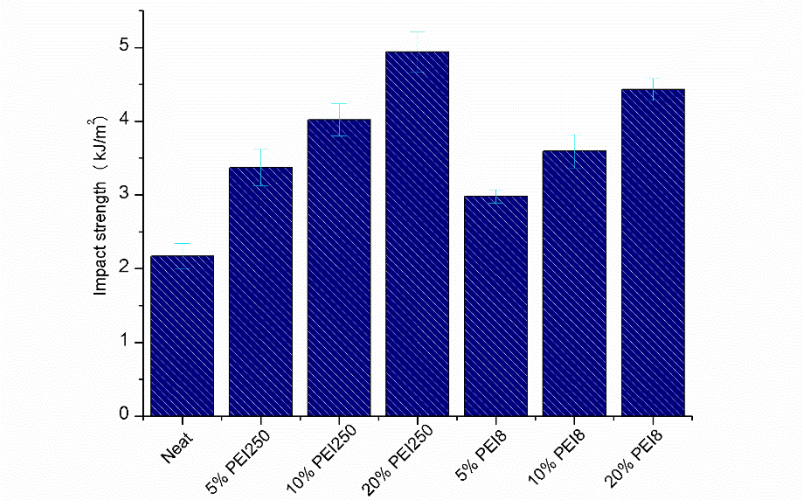

Figure 9. Impact strength for neat DGEBA/anhydride and thermosets with PEI250 and PEI8

Figure 10 shows some SEM micrographs of the fractured surfaces of materials after impact tests. In previous works it was observed that the fracture of the neat DGEBA/anhydride formulation is relatively smooth and glassy and does not show any significant morphological features, due to the formation of a homogeneous material.[20,37] On the contrary, materials containing PEI8 and PEI250 (Figure 7) show a characteristic morphology completely different from that of the neat formulation. PEI8 micrographs present nanograined morphology with nanosized grains. This nanopatterned organization can be attributed to the presence of amino groups, which can react during curing with epoxides changing the morphology in the surrounding of the star polymer. In a previous study[20] on the modification of DGEBA/anhydride thermosets with star polymers we could observe that the presence of reactive groups in the star led to homogeneous materials, whereas the blocking of these reactive groups produced nanograined morphology. In the present case, PEI8 has a high content of blocked groups and a low content of amine reactive groups, leading to the nanostructure observed by SEM inspection. PEI250

thermosets show a phase-separated morphology with nano-sized (75 to 150 nm) fine particles well adhered to the epoxy/anhydride matrix. It can be hypothesized that these particles are formed by PEI250 surrounded by epoxy/anhydride matrix covalently bonded to PEI250 but some aggregation of star polymers cannot be discarded. The differences between two morphologies can be attributed to the different molecular weight of the star polymer and to the amount of amine groups of star polymer that reacts during curing. Although both morphologies lead to significant toughness enhancement in the materials, phase-separated morphology produces a slightly higher improvement than nanograined morphology.

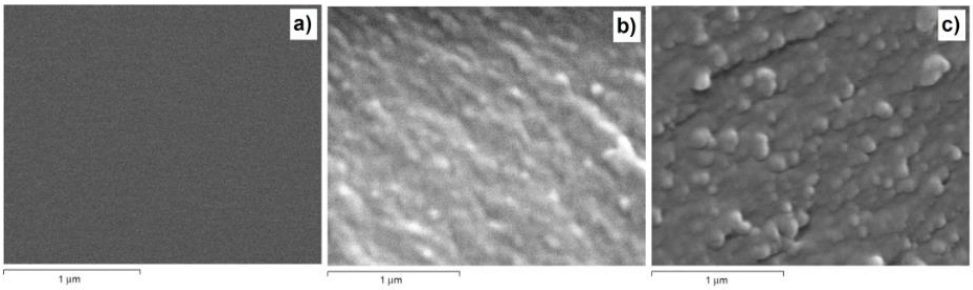

Figure 10. SEM micropgraphs at 50000 magnifications of the fractured surfaces of the materials obtained from a) neat, b) 10% PEI8 and c) 10% PEI250 formulations

Conclusions

The curing of epoxy/anhydride systems in the presence of PEI8 and PEI250 and tertiary amines mainly proceeds by anionic alternating copolymerization catalyzed by tertiary amines, although the uncatalyzed epoxy-anhydride polycondensation and the epoxy-amine reaction can take place to some extent.

The addition of star polymers with poly(ethyleneimine) cores and blocked poly(ε-caprolactone) arms to epoxy/anhydride formulations allows to obtain thermosets with significant improved toughness and low thermal stress generation during cooling, with only a slight reduction on glass transition temperature and croslinking density.

The flexibility and molecular weight of the star modifiers used, as well as the amount of amino reactive groups in the modifier affect the morphology of the resulting thermosets but only slightly their thermomechanical properties and curing process. The use of high molecular weight modifier with blocked terminal groups leads to phase-separated morphologies with nano-sized fine particles well adhered to the epoxy/anhydride matrix by the presence of unreacted amine groups.

References

[1] May C. A.: Introduction to epoxy resins, in 'Epoxy resins. Chemistry and technology' (ed.: May C. A.) Marcel Dekker, New York, 1-8 (1988).
[2] Bauer R. S.: Epoxy resin chemistry. American Chemical Society, Washington, Vol 114, (1979).
[3] Pascault J. P., Williams R. J. J.: Epoxy polymers: new materials and innovations. Wiley-VCH, Weinheim, (2010).
[4] Lange J., Toll S., Manson J.-A.E.: Residual stress build-up in thermoset films cured above their ultimate glass transition temperature. Polymer, **36**, 3135-3141 (1995).

[5] Thomas R., Durix S., Sinturel C., Omonov T., Goossens S., Groeninckx G., Moldenaers P., Thomas S.: Cure kinetics, morphology and miscibility of modified DGEBA-based epoxy resin-Effects of a liquid rubber inclusion. Polymer, **48**, 1695-1710 (2007).
[6] Mijovic J., Shen M., Sy J.W., Mondragón I.: Dynamics and morphology in nanostructured thermoset network/block copolymer blends during network formation. Macromolecules, **33**, 5235-5244 (2000).
[7] Choi J., Yee A.F., Laine R.M.: Toughening of Cubic Silsesquioxane Epoxy Nanocomposites Using Core−Shell Rubber Particles: A Three-Component Hybrid System. Macromolecules, **37**, 3267-3276 (2004).
[8] Mezzenga R., Boogh L., Månson J. A. E.: A review of dendritic hyperbranched polymer as modifiers in epoxy composites. Composites Science and Technology, **61,** 787-795 (2001).
[9] Morell M., Ramis X., Ferrando F., Serra A.: Effect of polymer topology on the curing process and mechanical characteristics of epoxy thermosets modified with linear or multiarm star poly(ε-caprolactone). Polymer, **52**, 4694-4702 (2011).
[10] Ratna D., Varley R., Simon G. P.: Toughening of trifunctional epoxy using an epoxy-functionalized hyperbranched polymer. Journal of Applied Polymer Science, **89**, 2339-2345 (2003).
[11] Flores M., Fernández-Francos X., Ferrando F., Ramis X., Serra A.: Efficient impact resistance improvement of epoxy/anhydride thermosets by adding hyperbranched polyesters partially modified with undecenoyl chains. Polymer, **53**, 5232-5241 (2012).
[12] Lagunas C., Fernández-Francos X., Ferrando F., Flores M., Serra A., Morancho J.M. Salla J.M., Ramis X.: New epoxy thermosets modified with amphiphilic multiarm star polymers as toughness enhance. Reactive & Functional Polymers, **83**, 132-143 (2014).
[13] Tomuta A., Ramis X., De la Flor S., Serra A.: Influence of end groups in hyperbranched polyesters used as modifiers in the characteristics of epoxy thermosets cured by adipic dihydrazide. Express Polymer Letters, **7**, 595-606 (2013).
[14] Luo L., Meng Y., Qui Y., Li X.: An epoxy-ended hyperbranched polymer as a new modifier for toughening and reinforcing in epoxy resin. Journal of Applied Polymer Science, **130**, 1064-1073 (2013).
[15] Zhang D., Chen Y., Jia D.: Toughness and reinforcement of diglycidyl ether of bisphenol-A by hyperbranched poly(trimellitic anhydride-butanediol glycol) ester epoxy resin. Polymer Composites, **30**, 918-925 (2009)
[16] Liu T., Nie Y., Chen R., Zhang L., Meng Y., Li X.: Hyperbranched polyether as an all-purpose epoxy modifier: controlled synthesis and toughening mechanisms. Journal of Materials Chemistry A, **3**, 1188-1198 (2015)
[17] Acebo C., Fernández-Francos X., Ferrando F., Serra A., Salla J.M., Ramis X.: Multiarm star with poly(ethyleneimine) core and poly(ε-caprolactone) arms as modifiers of diglycidylether of bisphenol A thermosets cured by 1-methylimidazole. Reactive & Functional Polymers, **73**, 431-441 (2012).
[18] Acebo C., Fernández-Francos X., Ferrando F., Serra A., Ramis X.: New epoxy thermosets modified with multiarm star poly(lactide) with poly(ethyleneimine) as core of different molecular weight. European Polymer Journal, **49**, 2316-2326 (2013).
[19] Morell M., Erber M., Ramis X., Ferrando F., Voit B., Serra A.: New epoxy thermosets modified with hyperbranched poly(ester-amide) of different molecular weight. European Polymer Journal, **46**, 1498-1509 (2010).
[20] Acebo C., Picardi A., Fernández-Francos X., De La Flor S., Ramis X., Serra A.: Effect of hydroxyl ended and end-capped multiarm star polymers on the curing process and mechanical characteristics of epoxy/anhydride thermosets. Progress in Organic Coatings, **77**, 1288-1298 (2014).
[21] Gonzalez S., Fernández-Francos X., Salla J.M., Serra A., Mantecón A., Ramis X.: New thermosets obtained by cationic copolymerization of DGEBA with γ-caprolactone with improvement in the shrinkage. II. Time–temperature–transformation (TTT) cure diagram. Journal of Applied Polymer Science, **104**, 3406-3416 (2007).
[22] Flores M., Fernández-Francos X., Ramis X., Serra A.: Novel epoxy-anhydride thermosets modified with a hyperbranched polyester as toughness enhancer. I. Kinetics study. Thermochimica Acta, **544**, 17-26 (2012).
[23] Benabdi M., Roche A.A.: Mechanical properties of thin and thick coatings applied to various substrates. Part I, An elastic analysis of residual stresses within coating materials. Journal of Adhesion Science and Technology, **11**, 281-299 (1997).

[24] Fernández-Francos X., Rybak A., Sekula R., Ramis X., Serra A.: Modification of epoxy–anhydride thermosets using a hyperbranched poly(ester-amide): I. Kinetic study. Polymer International, **61**, 1710-1725 (2012).
[25] Santiago D., Fernández-Francos X., Ramis X., Salla J.M., Sangermano M.: Comparative curing kinetics and thermal–mechanical properties of DGEBA thermosets cured with a hyperbranched poly(ethyleneimine) and an aliphatic triamine, Thermochimica Acta, **526**, 9-21 (2011).
[26] Fernández-Francos X., Santiago D., Ferrando F., Ramis X., Salla J.M., Serra A., Sangermano M.: Network structure and thermomechanical properties of hybrid DGEBA networks cured with 1-methylimidazole and hyperbranched poly(ethyleneimine)s, Journal of Polymer Science Part B: Polymer Physics, **50**, 1489-1503 (2012).
[27] Mauri A.N., Riccardi C.C.: The effect of epoxy excess on the kinetics of an epoxy–anhydride system, Journal of Applied Polymer Science, **85**, 2341-2349 (2002).
[28] Rocks J., Rintoul L., Vohwinkel F., George G.: The kinetics and mechanism of cure of an amino-glycidyl epoxy resin by a co-anhydride as studied by FT-Raman spectroscopy, Polymer **45**, 6799-6811 (2004).
[29] Leonard J.: Heats and entropies of polymerization ceiling temperatures, equilibrium monomer concentrations and polymerizability of heterocyclic compounds. in 'Polymer Handbook' (ed(s).: Brandrup J., Immermut E. H., Grulke E. A.), Wiley-Intersecience, New York, Vol 1, II/363-II/407 (1999).
[30] Dušek K., Luňák S., Matějka L.: Gelation in the curing of epoxy resins with anhydrides, Polymer Bulletin **7**, 144-152 (1982).
[31] Mauri A.N., Galego N., Riccardi C.C., Williams R.J.J.: Kinetic Model for Gelation in the Diepoxide−Cyclic Anhydride Copolymerization Initiated by Tertiary Amines, Macromolecules **30**, 1616-1620 (1997).
[32] Fernandez-Francos X., Ramis X., Serra A. Journal of Polymer Science Part A: Polymer Chemistry **52**, 61-75 (2014).
[33] Liu, T., Nie Y., Zhang L., Chen R., Meng Y., Li X.: Dependence of epoxy toughness on the backbone structure of hyperbranched polyether modifiers, RCS Advances **5**, 3408-3416 (2015).
[34] Miao X., Meng Y., Li X.: A novel all-purpose epoxy-terminated hyperbranched polyether sulphone toughener for an epoxy/amine system, Polymer **60**, 88-95 (2015).
[35] Pascault J.P., Sautereau H., Verdu J., Williams R.J.J.: Thermosetting polymers. Marcel Dekker, New York (2002).
[36] Sue H.-J., Garcia-Meitin E.I., Pickelman D.M.: Fracture behavior of rubber-modified high performance epoxies. in 'Polymer toughening' (ed.: Arends C.B.) Marcel Dekker, New York, 131-174 (1996).
[37] Tomuta A., Fernández-Francos X., Ferrando F., Serra A., Ramis X.: New epoxy-anhydride thermosets modified with multiarm stars with hyperbranched polyester cores and poly(ε-caprolactone) arms, Polymer-Plastics Technology and Engineering, **53**, 645-654 (2014).

UNIVERSITAT ROVIRA I VIRGILI
HYPERBRANCHED POLY(ETHYLENEIMINE) DERIVATIVES AS MODIFIERS IN EPOXY NETWORKS
Cristina Acebo Gorostiza

UNIVERSITAT ROVIRA I VIRGILI
HYPERBRANCHED POLY(ETHYLENEIMINE) DERIVATIVES AS MODIFIERS IN EPOXY NETWORKS
Cristina Acebo Gorostiza

UNIVERSITAT ROVIRA I VIRGILI
HYPERBRANCHED POLY(ETHYLENEIMINE) DERIVATIVES AS MODIFIERS IN EPOXY NETWORKS
Cristina Acebo Gorostiza

5. Synthesis of hyperbranched ethoxysilylated poly(ethyleneimine) and their use in the preparation of hybrid thermosets

5

UNIVERSITAT ROVIRA I VIRGILI
HYPERBRANCHED POLY(ETHYLENEIMINE) DERIVATIVES AS MODIFIERS IN EPOXY NETWORKS
Cristina Acebo Gorostiza

5.1 Introduction

Demands for epoxy resins are extremely strong because of their wide applications as adhesives, coatings and as advanced composites in aerospace and electronic industries.[1] However, epoxy thermosets have several limitations mainly related to their low mechanical properties and high thermal expansion coefficient (CTE) compared with inorganic materials. Thus, when applied as protective coatings on metal substrates, they are quite fragile, and the variation in the temperature leads to a mismatch between the substrate and the coating leading to the loss of adhesion and to the apparition of cracks. These limitations can be overcome by using inorganic/epoxy materials.[2] Inorganic fillers are the most common additives used in epoxy formulations to improve mechanical properties, such as modulus, strength and scratch resistance.[3]

These materials can be obtained by different routes: (a) by the addition of peformed nanoparticles or nanoclusters[4] or (b) by in situ generation of an inorganic phase through a conventional sol-gel process.[5] The in situ sol-gel polymerization of metal precursors in a polymeric (or monomeric) matrix is a better approach in front of the addition of silica fillers since makes possible a very fine dispersion of the inorganic phase in the polymeric matrix.

Sol-gel process consists in two different reactions on metal oxide precursors: hydrolysis and condensation, which occur in aqueous solutions, or in the liquid state, or in organic solutions in a highly humid atmosphere, producing polymeric inorganic metal oxide particles. As inorganic precursors, Si derivatives, Al, Ti, Zr, Sn, and V salts can be used.[6] However, Si derivatives are the most used.The formation of silica structures is represented in **Scheme 5.1**.

Hydrolysis

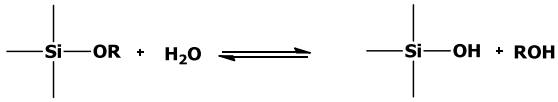

Condensation

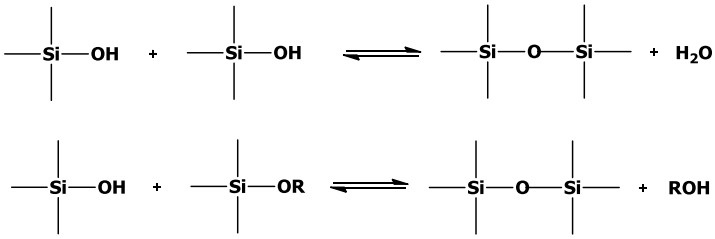

Scheme 5.1 Sol-gel reaction of silicon inorganic precursors

[1] E. M. Petrie, *Epoxy Adhesive Formulations*, McGraw-Hill, New York, **2006**.
[2] J. J. Chruściel, E. Leśniak, *Progress in Polymer Science*, **2015**, *41*, 67-121.
[3] A. C Pierre, *New Types of Sol-Gel Derived Materials*, in *Introduction to Sol-Gel Processing*, Kluver Academic: Norwell, **1998**.
[4] F. Gröhn, G. Kim, B. J. Bauer, E. J. Amis, *Macromolecules*, **2001**, *34*, 2179-2185.
[5] L. Matejika, O. Dukh, J. Kolarik, *Polymer*, **2000**, *41*, 1449-1459.
[6] J. Wen, G. L. Wilkes, *Chemistry of Materials*, **1996**, *8*, 1667-1681.

Hydrolysis is a reversible process in which there is the possibility that alcohol attacks the silanol leading to the formation of an alkoxide. This process is known as re-esterification and is favored at high content of alcohol as the solvent or in the presence of other hydroxylic species.[7]

Another reaction that can occur during a sol-gel process is the transesterification, which is the reaction of an alcohol with a silylalkoxide with the corresponding formation of a different silylalkoxide (**see Scheme 5.2**).

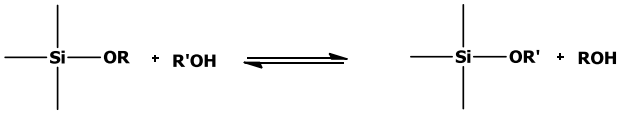

Scheme 5.2 Transesterification reaction

This reaction occurs when the alcohol used as the solvent is different from that formed in the hydrolysis reaction but can also be used to link poly(hydroxylic) compounds to silica structures or to functionalize hydroxylated surfaces.

The sol–gel process is acid or base catalyzed and the silica structure is determined mainly by the catalytic conditions. Thus, acid catalysis favors a faster hydrolysis of the precursor, finally leading to an open weakly branched polymer-like structure. On the contrary, in a basic medium the hydrolysis occurs slower but the polycondensation is faster producing compact colloidal particles.[8,9] In **Scheme 5.3** the effect of the catalyst in the morphology of the network is depicted.

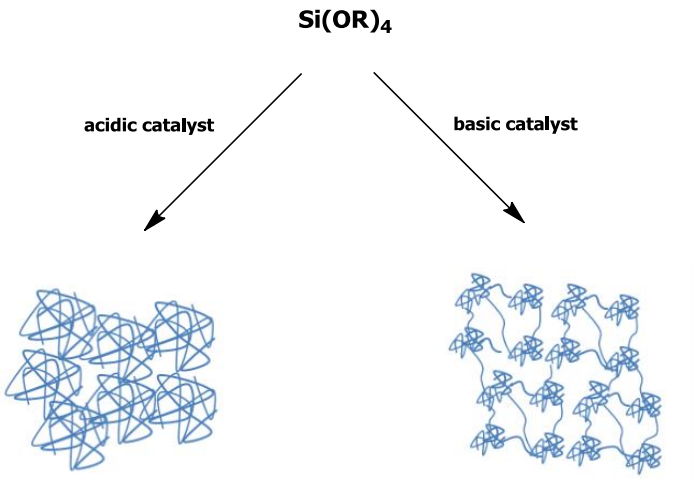

Scheme 5.3 Catalyst influence in the formation of the inorganic network by sol-gel

The formation of the inorganic silica network depends on the condensation reaction of the previously-formed silanol structures that leads to new Si–O–Si bonds. Generally, the precursors have three (trialkoxysilane, T_n) or four (tetraalkoxysilane, Q_n) hydrolyzable

[7] N. Georgieva, R. Bryaskova, R. Tzoneva, *Material Letters*, **2012**, *88*, 19-22.
[8] L. Matějka, J. Pleštil, K. Dušek, *Journal of Non-Crystalline Solids,* **1998**, *226*, 114-121.
[9] C. R. Silva, C. Airoldi, *Journal of Colloid and Interface Science*, **1997**, *195*, 381–387.

groups. The subscript *n* indicates the number of silanol groups condensed to siloxane bonds. In **Scheme 5.4** the chemical structures of silanols and the possible structures produced in the condensation are represented. From ^{29}Si NMR experiments it is possible to determine the details on the degree of hydrolysis and polycondensation.

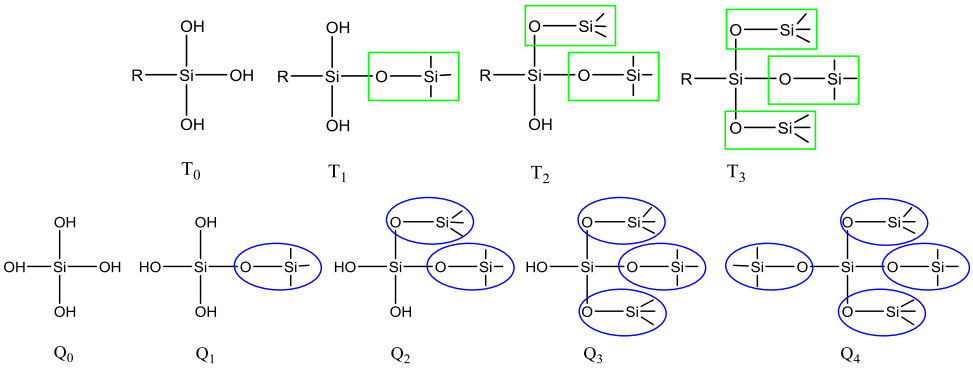

Scheme 5.4 Structure of the possible condensed forms during the sol-gel process

The formation of the inorganic silica structure in epoxy hybrids can take place before or after the curing process. Many sol-gel hybrid materials have been prepared by different curing methodologies.[10] In order to obtain good mechanical properties, the compatibility of organic and inorganic structures by the formation of covalent bonding is an essential condition and for this reason, the use of coupling agents is needed.[11,12] Usually, commercially available trialkoxysilyl compounds with organic reactive groups are applied as coupling agents in epoxy hybrids being the (3-glycidyloxypropyl)trimethoxysilane (GPTMS) the most used.[13,14] Moreover, the addition of tetraethyl orthosilicate (TEOS) to the formulation containing organoalkoxysilane precursors usually aims to increase the SiO_2 content and the size of the particles formed. The organic-inorganic networks can be tailored by combining the addition of TEOS and the type of the coupling agent[15] and the size of the particles formed are related with the mechanical properties of the final material.[16]

The cyclization of alkoxysilanes by intramolecular polycondensation allow to form polyhedral functional silsesquioxanes (POSS) with random, ladder cage or semi-cage structures. Octasilsesquioxane T_8 (**Scheme 5.5**) has been observed in sol-gel processes starting from trialkoxysilanes under some particular synthetic conditions.[17]

[10] A. Serra, X. Ramis, X. Fernández-Francos, *Coatings*, **2016**, *6*, 8.
[11] F. Branda, F. Tescione, V. Ambrogi, D. Sannino, B. Silvestri, G. Luciani, A. Costantini, *Polymer Bulletin*, **2011**, *66*, 1286-1300.
[12] H. Beneš, J. Galy, J.-F. Gérard, J. Pleštil, L. Valette, *Journal of Applied Polymer Science*, **2012**, *125*, 1000-1011.
[13] F. Pisticelli, M. Lavorgna, G. G. Buonocore, L. Verdolotti, J. Galy, L. Mascia, *Macromolecular Materials and Engineering*, **2013**, *298*, 896-909.
[14] S. R. Davis, A. R. Brough, A. Atkinson, *Journal of Non-Crystal Solids*, **2003**, *315*, 197-205.
[15] L. Prezzi, L. Mascia, *Advances in Polymer Technology*, **2005**, *24*, 91-102.
[16] S. Palraj, M. Selvaraj, K. Maruthan, G. Rajagopal, *Progress in Organic Coatings*, **2015**, *81*, 132-139.
[17] Y. Kaneko, M. Shoirikia, T. Mizumob, *Journal of Materials Chemistry*, **2012**, *22*, 14475-14478.

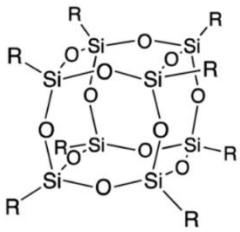

Scheme 5.5 Chemical structure of octameric cage (POSS)

The cage-like structures of POSS can allow the construction of the materials with precise control of the nanoarchitecture. For this reason POSS reagents, monomers and polymers are emerging as a new chemical technology for the nano-reinforced organic–inorganic hybrids and the polymers incorporating POSS are becoming the focus of many studies due to the simplicity in processing and the excellent comprehensive properties of this class of hybrid materials.[18,19]

As it has been said before, HBPs are advantageous modifiers to enhance the properties of epoxy thermosets. Taking all of this into account, some authors combined the strategy of the generation of silica particles by sol-gel procedure with the use of hyperbranched structures to improve some characteristics of thermosetting materials.[20-22]

Since the use of coupling agents is highly advisable, the preparation of multifunctional coupling agents by silylation of the final groups of hyperbranched polymers can be greatly advantageous to improve epoxy resins by generation of silica particles by sol-gel process from the alkoxysilanes at the end groups of the hyperbranched structures.[23] As an alternative, the use of epoxy-terminated hyperbranched polymer as epoxy component has also been proposed.[24]

Taking into account that amino groups are reactive with isocyanates, in this study a modification of poly(ethyleneimine) with (3-isocyanatopropyl) triethoxysilane has been done. The triethoxysilylated hyperbranched poly(ethyleneimine) has been used to prepare different hybrid organic-inorganic materials with different silica content and different inorganic structures. An advantage of the amino groups in the PEI structure is that the amines cannot react with silanol groups in contrast with hydroxyl groups, avoiding the gelation during the preparation of the modifier or during the storage, which is an undesired side-reaction in OH-terminated hyperbranched.

The aim of our studies has been the improvement of scratch characteristics in coatings by the implementation of the sol-gel methodology to anionically cured epoxy resins. The mechanical characteristics have been rated by scratch test. Depth sensing indentation was also used to go deeply in the mechanical characterization of the sol-gel hybrid materials

[18] J. J. Chruściel, E. Leśniak, *Progress in Polymer Science*, **2015**, *41*, 67-121.
[19] J. Choi, J. Harcup, A. F. Yee, Q. Zhu, R. M. Laine, *Journal of American Chemical Society*, **2001**, *123*, 11420-11430.
[20] M. Sangermano, M. Messori, M. Martin Galleco, G. Rizza, B. Voit, *Polymer*, **2009**, *50*, 5647-5652.
[21] A. Houel, J. Galy, A. Charlot, J.-F. Gérard, *Journal of Applied Polymer Science*, DOI: 10.1002/app.39830, **2014**.
[22] V. Geiser, Y. Letterrier, J.-A.E. Månson, *Macromolecular Materials and Engineering*, **2012**, *297*, 155-166.
[23] M. Sangermano, H. El Sayed, B. Voit, *Polymer*, **2011**, 52, 2103-2109.
[24] S. Allauddin, M. K. A. Chandran, K. K. Jena, R. Narayan, K. V. S. N. Raju, *Progress in Organic Coatings*, **2013**, *76*, 1402-1412.

prepared by us. [25] However, these lasts studies have not been included in the PhD report, since it falls out of the scope.

The work herein presented has been published in the following articles

- Novel epoxy-silica hybrid coatings by using ethoxysilyl-modifed hyperbranched poly(ethyleneimine)with improved scratch resistance. *Polymer* **2014**, *55*, 5028-5035.
- Hybrid epoxy networks from ethoxysilyl-modified hyperbranched poly(ethyleneimine) and inorganic reactive precursors. *European Polymer Journal* **2015***, 70,* 18-27.

[25] V. Lorenzo, C. Acebo, X. Ramis, A. Serra, *Progress in Organic Coatings*, **2016**, *92*, 16-22.

UNIVERSITAT ROVIRA I VIRGILI
HYPERBRANCHED POLY(ETHYLENEIMINE) DERIVATIVES AS MODIFIERS IN EPOXY NETWORKS
Cristina Acebo Gorostiza

5.2 Novel epoxy-silica hybrid coatings by using ethoxysilyl-modifed hyperbranched poly(ethyleneimine)with improved scratch resistance

Cristina Acebo, Xavier Fernández-Francos, Massimo Messori, Xavier Ramis, Àngels Serra

Polymer **2014***, 55,* 5028-5035

UNIVERSITAT ROVIRA I VIRGILI
HYPERBRANCHED POLY(ETHYLENEIMINE) DERIVATIVES AS MODIFIERS IN EPOXY NETWORKS
Cristina Acebo Gorostiza

Polymer **2014**, *55*, 5028-5035

Novel epoxy-silica hybrid coatings by using ethoxysilyl-modified hyperbranched poly(ethyleneimine) with improved scratch resistance.

Abstract

A new hyperbranched poly(ethyleneimine) with ethoxysilyl groups at the chain ends has been synthesized and characterized and then used in epoxy formulations to generate new organic/inorganic hybrid materials. Formulations of different proportions of diglycidylether of bisphenol A and the prepared ethoxysilylated hyperbranched poly(ethyleneimine) were maintained in a thermostatized controlled humidity chamber to form the inorganic silica network by a sol-gel process and then the epoxy resin was cured at higher temperature using 1-methylimidazole as anionic initiator.

Transparent hybrid materials were prepared and characterized by thermal tests and their fine morphology was observed by transmission electron microscopy. The formation of the silicon structure was confirmed by ^{29}Si-NMR studies. Thermal stability was evaluated by thermogravimetry. Improvement of the mechanical coating performance was confirmed by scratch measurements.

Keywords

Hyperbranched polymers, epoxy resin, sol-gel process, coatings.

Introduction

Nowadays, there is a great interest in organic/inorganic hybrid materials because of the applications that this type of materials have in the aeronautic and automobile industry, as coatings, in circuit boards, etc.[1,2] The characteristics usually improved by the formation of the inorganic network, typically silica-like structures, in the epoxy matrix, are hardness, solvent resistance, barrier properties, optical appearance, corrosion resistance and even self-healing and fire retardancy abilities.[3-6]

Sol-gel processes are advantageous in front of the more conventional addition of nanoparticles or nanoclays, mainly because of the fine dispersion of the inorganic phase reached into the epoxy matrix. Moreover, the addition of a small amount of nanoparticles drastically increases the viscosity, which is always an important issue in coatings applications whereas the formulation applied before the sol-gel process has a still low viscosity.[7]

Hyperbranched polymers (HBP)s are advantageous polymeric modifiers to increase toughness in epoxy thermosets.[8-10] They have been extensively used in the last years because they help to keep the viscosities of the formulations at a reduced value without compromising other thermomechanical properties, due to their densely branched and globular structure and their multifunctionality, in contrast to what happens on adding linear polymers or rubbers as toughness additives. As a result, the use of solvents in coatings formulations can be reduced or even avoided. The high number of functional groups and the possibility of their functionalization allows to tailor the compatibility of the HBPs in the resin, thus achieving homogeneous or phase separated structures at will in the cured material.[11,12] Taking into account the above mentioned advantages, some authors combined the strategy of the generation of inorganic silicon particles by sol-gel procedure

with the use of hyperbranched structures to improve some characteristics of thermosets.[13-15]

The use of organoalkoxy silanes as coupling agents to incorporate polymerizable organic substituents such as epoxide or amine has been applied since Si-C bonds are stable and allow the covalent linkage between the inorganic structures formed and the polymer matrix.[16,17] Moreover, phase separation in organic and inorganic domains can be prevented by the use of coupling agents.[18] Thus, it seems that the preparation of multifunctional coupling agents by silylation of the final groups of hyperbranched polymers can be greatly advantageous to improve epoxy resins by generation of silica particles by sol-gel process from the alkoxysilanes at the end groups of the hyperbranched structure. This approximation has been reported previously in the UV curing of cycloaliphatic epoxy resins with hyperbranched polyesters.[13] In that study, a hyperbranched aromatic-aliphatic polyester was modified in different extents at the final phenol groups by reacting with 3-(triethoxysilyl)propyl isocyanate and added to cycloaliphatic epoxy formulations cationically polymerized. In some cases, tetraethoxysilane (TEOS) was also added to the formulation. The presence of unmodified phenol groups in the chain end of the HBP allowed the covalent bonding of inorganic and organic networks, because of their participation in the homopolymerization mechanism. In all the studies the proportion of HBP was kept at 20%. The dual cure procedure started with the photoirradiation to perform the curing of the epoxide resin, followed by the sol-gel process. The authors could clearly demonstrate that the use of the hyperbranched silylated polymer was advantageous in the formation of transparent films in contrast to what occurred by applying the same curing procedure without silylated hyperbranched but adding TEOS as source of silica particles.[13] The reason for that was the larger particle size obtained with TEOS as demonstrated by TEM analysis.

It is known that rigid inorganic structures in epoxy matrices sometimes do not produce an ideal toughening effect due to the weak interface interaction between the organic and inorganic phases. The addition of rubbery materials can induce a cooperative effect between soft and rigid particles and in this way, toughness enhancement of thermosets can be established with no loss of strength, modulus or glass transition temperature.[19] According to that, the use of a low T_g HBP functionalized at the chain ends with triethoxysilyl groups can lead to interesting materials from the point of view of the mechanic behavior.

Hyperbranched poly(ethylene imine)s are commercially available polymers with the trade name Lupasol®. They have a high number of primary and secondary amines in their structure in reference to their molecular weight, because of the small structural units. Thus, the modification of primary or secondary amines with triethoxysilyl groups rends a high proportion of inorganic structure after sol-gel process. The inorganic network formed is connected to the polymer matrix through a highly soft structure that can make possible the rearrangement of the rigid particles.

In the present work, we have studied the synthesis and characterization of the triethoxy silylated hyperbranched poly(ethylene imine) and its use in diglycidylether of bisphenol A (DGEBA) formulations using 1-methylimidazole as anionic initiator. The formulations prepared have been cured by a dual process, being the first one the sol-gel and the second the thermal homopolymerization of DGEBA. Since the sol-gel process leads to a higher shrinkage than homopolymerization of epoxides, the choice of this cure schedule seems to be more promising form the point of view of the low generation of internal stresses during curing.[14]

The advantage of our system in reference to other sol-gel processes before described is the possibility to improve the proportion of inorganic structures by the only increase of silylated HBP. The modified HBP prepared has a higher content of Si than other described previously[13] and has a soft structure. In this way, the rigid particles formed will be interconnected by flexible structures that should enhance mechanical characteristics. Because of the high proportion of silicon in the HBP no tetra ethyl orthosilicate (TEOS) has been added to the mixtures and therefore the formation of cage-like structures can be expected.

To confirm that sol-gel process was complete we registered ^{29}Si NMR spectra in solid state of the thermosets and the homogeneous dispersion of inorganic domains in the hybrid was visualized by TEM microscopy. The formation of a very homogeneous hybrid material could be confirmed with the presence of nanometric inorganic particles.

One of the peculiarities of the hybrid coatings is the increase in surface hardness due to the presence of inorganic domains in the epoxy matrix.[15] Since the hardness increase is usually related to the improvement in the scratch resistance we have evaluated this property to characterize the materials obtained.[20] The improvements achieved were confirmed by optical examination after scratch test. The materials showed the capacity of self-repairing when the amount of the silylated HBP was increase.

Experimental

Materials

Poly(ethyleneimine) (PEI) Lupasol®FG (PEI800, 800 g/mol, BASF) was dried under vacuum before use. 3-(Triethoxysilyl)propyl isocyanate (TESPI), diethylenetriamine (DETA) and 1-methylimidazole (1-MI) were purchased from Sigma-Aldrich and used without further purification. Chloroform was purchased from Scharlab, dried under $CaCl_2$ and distilled before used. Diglycidylether of bisphenol A (DGEBA) Araldite GY 240 (EEW = 182 g/eq) was provided by Huntsman. Ammonium dihydrogen phosphate from Acros Organics was used for the controlled humidity chamber.

Preparation of tris(3-triethoxysilyl propylenecarbamoyl) diethylene triamine

Diethylenetriamine (0.5 g, 4.84 mmol) was dissolved in dry chloroform, cooled at 0ºC and the equivalent amount of TESPI (3.6 g, 14.51 mmol) was added drop-wise. The mixture was kept at room temperature overnight. The solvent was eliminated in vacuum.

^{1}H NMR (400 MHz, $CDCl_3$, δ in ppm): 3.8 (-Si-O-C**H**$_2$-), 3.3-3.1 (-C**H**$_2$- from diethylenetriamine and NH-CO-NH-C**H**$_2$-), 1.6 (-CH_2-C**H**$_2$-CH_2-), 1.2 (-CH_2-C**H**$_3$) and 0.6 (-C**H**$_2$-Si-). ^{29}Si NMR spectrum is represented in **Figure 1**.

Preparation of triethoxysilyl modified hyperbranched poly(ethyleneimine) (PEI-Si) (Scheme 1)

In a three necked flask equipped with magnetic stirring, funnel addition and argon inlet PEI (2 g, 34.32 meq of NH) was dissolved in 20 mL of dry chloroform. The solution was brought to 0ºC and TESPI (8.5 g, 34.32 mmol) was added drop-wise. After the addition the mixture was left at room temperature overnight. The solvent was eliminated in the rotavap and then the oil obtained was dried in vacuum overnight.

^{1}H NMR (400 MHz, CDCl3, δ in ppm): 3.78 (-Si-O-C**H**2-, e), 3.5-2.5 (PEI core and NH-CO-NH-C**H**2-, a) 1.6 (-CH2-C**H**2-CH2-, b) 1.2 (-CH2-C**H**3, d) and 0.6 (-C**H**2-Si-, c) (see **Figure 2**). ^{29}Si NMR spectrum is represented in Figure 1**.**

Sample preparation

The PEI-Si was added to the epoxy resin at a content of 20, 30, 50 and 80 wt% and a 2% in wt. in reference to the DGEBA of 1-MI was added and stirred mechanically until the mixture became clear. The formulations were coated on glass slides by means of a wire-wound applicator. The sol-gel process was carried out by thermal treatment at 80ºC for one day in a controlled high humid atmosphere (95-98% relative humidity controlled by a saturated solution of aqueous $NH_4H_2PO_4$) and was followed by a thermal curing process at 180ºC during 2 h in an oven.

Characterization techniques

Solution ^{1}H NMR measurements were carried out in a Varian Gemini 400 spectrometer using $CDCl_3$ as the solvent. For ^{1}H and ^{29}Si NMR measurements TMS was used as the reference. For ^{29}Si NMR measurements the conditions used were d_1=0.4s acquisition time = 0.7 s, a number of scans of 3000 and applying an inverse gated decoupling pulse sequence.

Solid-state ^{29}Si NMR spectra (^{29}Si CPMAS-NMR) were recorded at 25ºC for the cured hybrid samples on a Bruker Advance III 400MHz at a frequency of 79.4950 MHz on a ceramic probe CP/MAS of 4 mm. NMR spectra were obtained from 40000 scans using the following parameters: rotor spin rate 10000 Hz, recycling time 5 s, contact time 2.0 ms and acquisition time 18.4 ms. In the processing of the data, exponential apodization with line broadening 50 Hz, FT and manual phasing and baseline correction were used.

FTIR Spectroscopy. A Bruker Vertex FTIR spectrometer equipment (resolution of 4 cm-1) with an attenuated-total-reflectance accessory with a diamond crystal (Golden Gate heated single-reflection diamond ATR, Specac-Teknokroma) was used to confirm the functionalization of PEI.

Calorimetric analyses were carried out on a Mettler DSC-822e thermal analyzer. Samples of approximately 10 mg were placed in aluminum pans under nitrogen atmosphere. The calorimeter was calibrated using an indium standard (heat flow calibration) and an indium-lead-zinc standard (temperature calibration). The glass transition temperature of PEI-Si was determined, by means of a heating scan at 10 ºC/min, as the temperature of the half-way point of the jump in the heat capacity when the material changed from glassy to the rubbery state under N_2 atmosphere and the error is estimated to be approximately ± 1 °C. T_g*s* of the hybrid materials were determined at a heating rate of 30ºC/min after a first scan from 0 to 180ºC followed by a cooling at 10 ºC/min from 180 to 0ºC.

Thermogravimetric analyses were carried out in a Mettler TG50 thermobalance. Samples with an approximate mass of 8 mg were degraded between 40 and 800 ºC at a heating rate of 10 ºC/min in air (100 cm^3/min measured in normal conditions).

The morphology of the different hybrids was analyzed by imaging ultrafine pieces from the samples. These pieces had a thickness of 60 µm, in a transmission electron microscope (TEM, JEOL model 1011) with a 0.2 nm resolution.

Scratch test was carried out on a CSM Micro-Combi Tester by using Rockwell C diamond scratch indenter (tip radius 0.1 mm) and progressively increasing the normal force (F_n) from 0.01 to 5.0 N for a scratch length of 3 mm and at a scratch rate of 60 mm/min. Both penetration depth during scratching (Pd) and residual depth after scratching (D_p) have been detected for at least four scratch tests for each sample.

Results and discussion

Synthesis and characterization of triethoxysilylated hyperbranched poly(ethyleneimine) (PEI-Si)

The silylation of poly(ethyleneimine) (PEI) was performed by reacting the previously dried PEI with (3-isocyanatopropyl) triethoxysilane (TESPI) at low temperature as represented in **Scheme 1**. The modification procedure was similar to the used in the partial silylation of an aromatic-aliphatic polyester previously reported.[13] However, in the present case the complete modification was desired and the proportion of isocyanate used was one to one in reference to the total number of primary and secondary amines in the PEI structure. It should be noted that Lupasol®FG with an average molecular weight of 800 g/mol has an average of 6.4 secondary amines and 7.9 primary amines per molecule. Amines are advantageous in reference to hydroxyl groups in the functionalization with triethoxysilylated moieties, because amines cannot react with silanol groups, in contrast with hydroxylic groups,[21] and therefore, gelation during the modification process or during storage can be avoided.

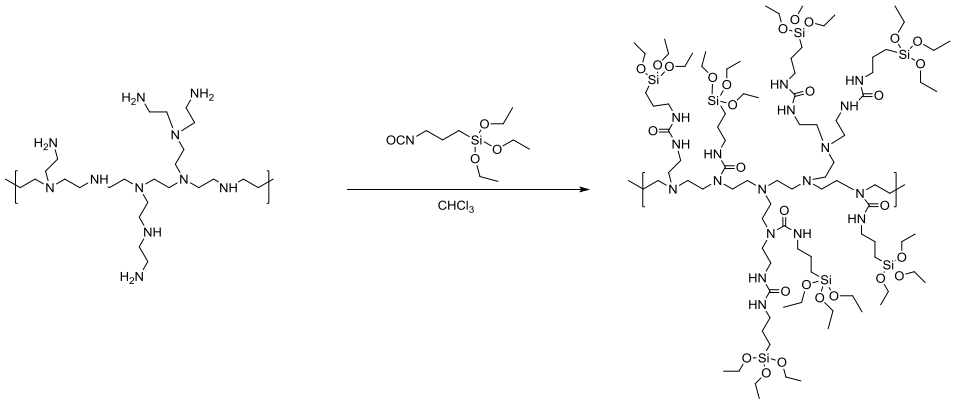

Scheme 1. Synthetic route to PEI-Si

In the synthesized PEI-Si we could observe by FTIR analysis the complete disappearance of the isocyanate band at 2271 cm^{-1} and the new urea groups formed that gives absorptions at 3321 cm^{-1} (N-H st) and at 1623 cm^{-1} (C=O st), confirming the modification achieved.

The polymer synthesized was also characterized by NMR spectroscopy, being the most interesting spectroscopic data the chemical shifts of ^{29}Si atoms. Figure 1 shows the spectrum obtained for the silylated PEI prepared. It was quite surprising to find the presence of two overlapping broad Si signals. The broadening of these signals is originated by the short relaxation times of the silicon atoms in the polymer and the different chemical environments of the silicon atoms in the hyperbranched structure. To confirm the

assignment of these different silicon signals, we synthesized a model compound and then investigated it by ^{29}Si NMR spectroscopy. Because PEI has secondary and primary amines that can react with isocyanate, we selected as the model compound the triethoxysilylated diethylenetriamine, because of the similar structure. The ^{29}Si spectrum of this model compound is also included in Figure 1.

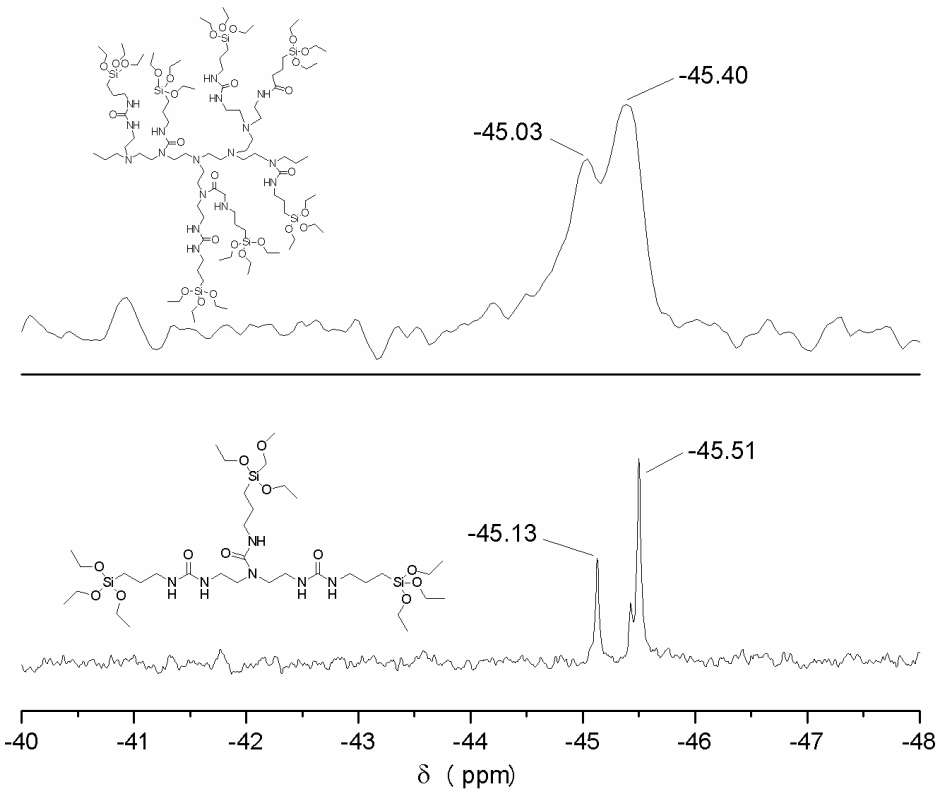

Figure 1. ^{29}Si NMR spectrum in $CDCl_3$ of triethoxysilyl hyperbranched poly(ethyleneimine) (PEI-Si) and (3-triethoxysilyl propylenecarbamoyl) diethylenetriamine

As we can see, two well defined signals at a similar chemical shift to those of PEI-Si appear in the spectrum, which confirms that the splitting of the signals is due to the attachment of TESPI to both primary and secondary amines in the PEI structure. Thus, ^{29}Si signals are sensitive to the characteristics of the urea group formed by reacting TESPI with primary or secondary amines. Although these spectra are not fully quantitative, taking into account the peak size, we could assign the peaks at 45.40 and 45.51 ppm to the silyl group attached to the primary amine and the peaks at 45.03 and 45.13 to the silicon attached to the secondary amine.

In Figure 2 the ^{1}H NMR spectrum of the silylated PEI is represented. As we can see, in addition to the protons of the core structure (denoted as PEI), the propylene and the ethoxy protons can be clearly appreciated. Small traces of ethanol from slight hydrolysis of ethoxy groups could be also detected.

The polymer was thermally characterized by DSC and TGA. The *Tg* of the PEI-Si was -44ºC. By thermogravimetry a complex degradative pattern could be observed but the temperature of maximum rate of degradation is 274 ºC.

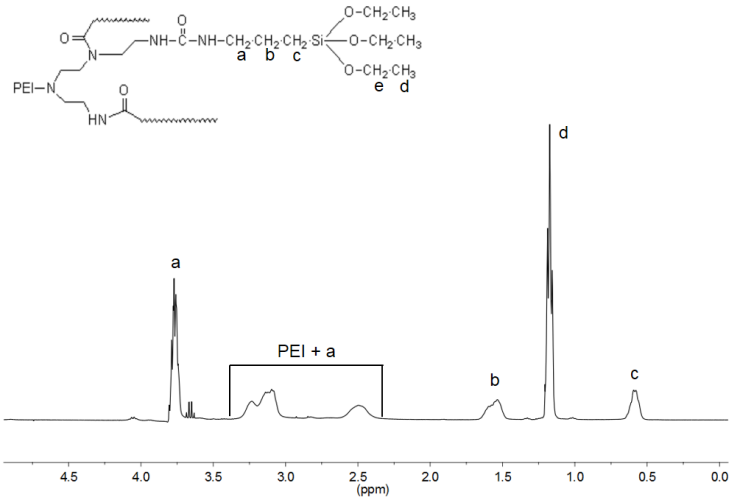

Figure 2. ^{1}H NMR spectrum in $CDCl_3$ of the triethoxysilyl hyperbranched poly(ethyleneimine)(PEI-Si)

Preparation of films from DGEBA and PEI-Si mixtures

The preparation of the hybrid coatings is based in two well-known processes: sol-gel and epoxy anionic homopolymerization, which takes place in this order but with some overlapping due to the easy thermal homopolymerization of epoxides initiated by 1-MI, even at moderate temperatures.

The sol-gel process of the triethoxysilyl groups at the chain end of the hyperbranched PEI consist in a hydrolysis step followed by the condensation of the silanol groups formed in the presence of an acidic or basic catalyst.[4] In our study, the presence of the PEI structure prevents the use of acidic catalyst and therefore 1-methylimidazole (1-MI) was selected as a basic catalyst for this process. In addition, 1-MI can play the role of initiator in the anionic homopolymerization of the resin. This homopolymerization is responsible for the formation of the organic network. Tertiary amine groups in the PEI structure can also act as a basic catalyst in the sol-gel process.

Under basic conditions, water dissociates to produce nucleophilic hydroxyl anions in a quick first step. The hydroxyl anions lead to an SN_2 substitution on silicon atom to produce the corresponding silanol.[22]

The sol-gel hybrid films were prepared by mixing different proportions of DGEBA and PEI-Si with 2 phr of 1-MI obtaining homogeneous mixtures (named as x:y, being x and y the percentages of DGEBA and PEI-Si, respectively). The homogenized mixtures were coated on glass slides and then heated for one day at 80ºC in a controlled high humidity atmosphere. After this step, the coatings were solid and transparent and the curing of epoxide and condensation reaction was completed in an oven at 180ºC during 2 h. This schedule should lead to materials with a low internal stress and without voids or cracks because the hydrolysis of ethoxysilyl groups and ulterior condensation, resulting in large

shrinkage, occurs when the mobility of the organic phase is still high.[14] The curing of the epoxy resin, although initiated in the first step, is completed at high temperature and takes place with much less shrinkage because of the ring-opening mechanism adopted.[23]

All the coatings obtained were hard, with a good appearance and completely transparent (see **Figure 3**), regardless of the proportion of PEI-Si added. This can be the evidence that the organic-inorganic phase separation is on a scale smaller than 400 nm.

Figure 3. Photograph of one of the hybrid samples obtained showing the transparency of the coating

To confirm the formation of inorganic silicon structures by condensation of silanols, NMR studies of the cured samples were registered. **Figure 4** shows the ^{29}Si CPMAS-NMR spectrum of the hybrid material obtained from a formulation 50:50 PEI-Si/DGEBA. No remaining signals corresponding to the silylated hyperbranched or the hydrolyzed forms could be appreciated, but several overlapped signals in the region between -55 and -75 ppm, corresponding to the T species, are formed.

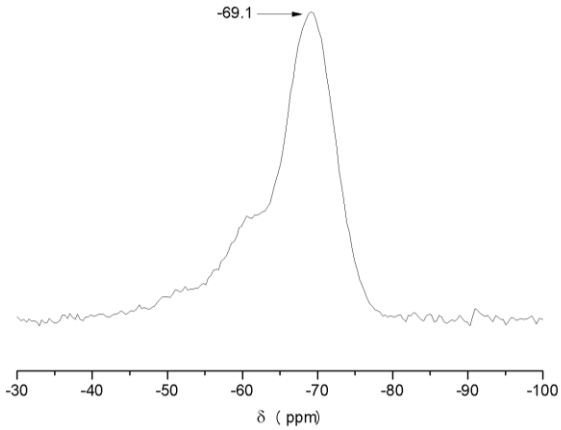

Figure 4. 29Si CPMAS-NMR spectrum of the hybrid thermoset obtained from the formulation 50:50 DGEBA/PEI-Si

According to Matejka et al.,[24] cage-like and branched polysilsesquioxanes, $RSiO_{3/2}$, can be formed from trifunctional monomers, since cyclization is a typical feature of the polymerization of alkoxysilanes. This cyclization process explains the large deviation in conversion at gelation between calculated and experimental values in case of using a triethoxysilane as sol-gel precursor.[25,26] However, in this study monomeric organo trialkoxysilanes were reacted and identified by NMR spectroscopy in solution and therefore thin peaks were registered and could be assigned to defined structures. In contrast, in our study the complex hyperbranched structure of PEI-Si with a high multifunctionality and the formation of the organic network should affect the formation of well-defined structures because of topological restrictions and steric hindrance giving rise to open cage-like structures, to some degree of branching or even to linear non-fully reacted silicon

structures. In addition, if there are two different signals in the ^{29}Si-NMR spectrum of the pure PEI-Si, it is predictable that some splitting in the spectrum of the hybrid material could also appear, due to the different chemical environments. Finally, it should be considered that solid state NMR spectroscopy usually does not show good resolution and therefore it is quite difficult from the spectrum in Figure 4 to elucidate the structure of the inorganic part.

In previous literature reports,[27] the signals between -66.4 and -69.2 ppm were attributed to T_3 units of cubic cage structures and even higher field signals were observed and assigned to higher member cages. It was reported that T_2 units (with an uncondensed silanol) appear in the region of -60 ppm.[22,24] As we can see in Figure 4, the shoulder in the T_2 region is small, which indicates a low proportion of linear non-cage structures in the silica part and therefore, silsesquioxane structures seem to predominate. To summarize, regardless of the characteristics of the cage-like structures formed, it can be assured that inorganic particles has been formed and it is connected to the organic matrix by the hyperbranched polyethylene imine. This organic structure could be also partially connected to the epoxy network because amine groups are able to act as nucleophiles in front of epoxides, and therefore initiate homopolymerization of epoxy groups. Also, hydrogen bond interactions between PEI structure and epoxy network are foreseeable. A good interaction between inorganic and organic phase is required to improve mechanical performance of hybrid materials.

Thermal characterization

By calorimetry the T_g of all the hybrid materials were investigated but they were difficult to detect by the low mobility of the network structure. **Table 1** collects the data measured.

Table 1 Composition and properties of hybrid samples.

Formulation (DGEBA/PEI-Si)	$T_{5\%}$ [a] (ºC)	$T_{1st\ peak}$ [b] (ºC)	T_{max} [c] (ºC)	$T_{3rd\ peak}$ [d] (ºC)	*Char yield* [e] (wt%)	T_g [f] (ºC)
Neat	319	-	381	553	-	198
80:20	273	260	358	523	1.4	83
70:30	254	262	357	528	2.5	81
50:50	253	267	361	540	6.9	82
20:80	243	273	353	568	14.2	

[a] Temperature of the onset decomposition on TGA data at 10ºC/min taken as the 5% weight loss.
[b] Temperature of the maximum rate of the first degradation peak
[c] Temperature of the maximum descompsition rate
[d] Temperature of the maximum rate of the third degradation peak
[e] Residue at 750ºC
[f] Glass transition temperature of the hybrid materials

Although in a first scan the T_g of the hybrid materials could not be detected, after a controlled program of heating and cooling to eliminate the aging and humidity uptake the T_g of the hybrids could be measured at around 80ºC, which is considerably lower than the T_g of the neat material. No much difference among them could be appreciated and in the scan of the material with a higher proportion of PEI-Si, and therefore higher proportion of rigid inorganic particles, no change in the calorific capacity could be detected.

Thermogravimetric studies were performed for all the hybrid materials. **Figure 5** shows the curves of weight loss and its derivative against temperature. Table 1 shows the main data obtained by this technique.

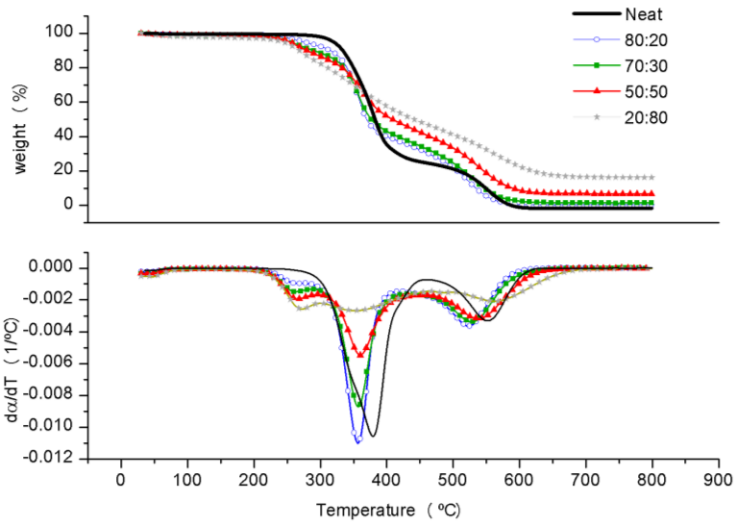

Figure 5. Thermogravimetric traces of the neat and the different hybrid materials at 10ºC/min in air atmosphere

First of all it should be commented that no loss of volatiles is observed at temperatures below 200 ºC, confirming that the condensation of silanol groups during curing was complete. As we can see in the figure, there are three main degradation processes. The degradation at lower temperature increases with the proportion of PEI-Si in the formulation and can be related to the degradation process of the PEI structure. In a previous study using PEI and 1-MI in the curing of DGEBA we could see a similar behavior: the higher the proportion of PEI the more important this degradation process was.[28] From the values collected in Table 1 we can see that this process leads to a decrease of the temperature of the initial weight loss (denoted as $T_{5\%}$). Some authors described that on increasing the proportion of silica particles in the hybrid material the initial decomposition temperature increases.[16,21] This behavior is not observed in our case, because of the presence of the poly(ethyleneimine) structure that degrades at lower temperature. There is also a decrease of the temperature of maximum rate of weight loss on adding PEI-Si to the formulation, but its proportion does not affect the temperature but only the degradation rate. This degradation process should be related to the thermal breakage of the organic matrix. Thus, the silica content affects the rate of degradation of the epoxy matrix. The third degradation process is the oxidative degradation that leads to the loss of organic residues giving rise to the char yield related to silica content. As we can see from the values of the table char yield reflects the increased proportion of silica in the material.

TEM analysis

Figure 6 shows TEM micrographs of two hybrid materials with different content of silica (from formulations DGEBA/PEI-Si 80:20 and 20:80).

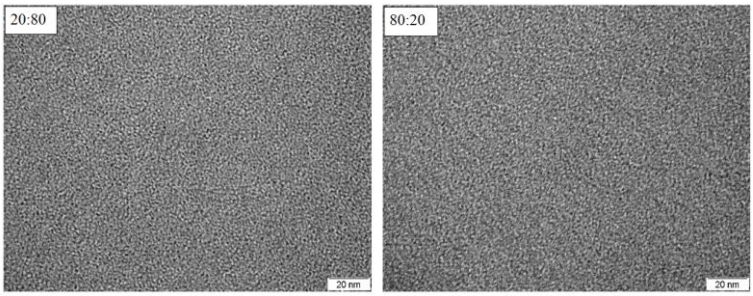

Figure 6. TEM micrographs of hybrid materials obtained from formulations DGEBA/PEI-Si 20:80 and 80:20 catalyzed by 2phr of 1-MI

A homogeneous dispersion of fine particles of silica can be observed, without any appreciable aggregates or macroscopic phase separation. The silica particles are embedded in the organic matrix on nanometric scale < 10 nm. Similar silica nanodomains were obtained by using a partially silylated aromatic-aliphatic hyperbranched polyester as coupling agent.[13] Thus, it can be confirmed that hyperbranched coupling agents are adequate to prepare homogeneous hybrid materials and that strong chemical-bond interaction between organic and inorganic domains, is crucial to avoid macroscopic phase separation.

Scratch tests

Typical penetration depth (P_d) *vs.* normal force (F_n) curves are reported in **Figure 7** for the investigated samples. The P_d values can be considered as an indication of the resistance to penetration (rigidity and hardness) of the cured coatings which are influenced by several factors such as chemical composition, degree of cross-linking, etc.

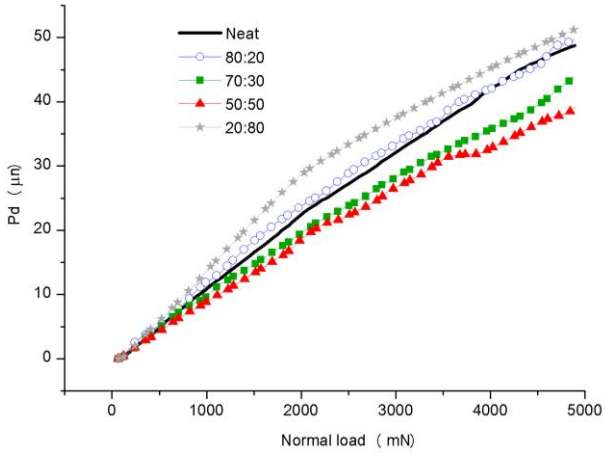

Figure 7. Penetration depth (P_d) as a function of normal force (F_n) for the neat and the different hybrid materials.

Figure 7 shows that P_d values increase monotonically by increasing the normal force without significant changes of slope due to the integrity of the material. The slopes of the

curves are clearly influenced by the chemical composition with the lowest values of P_d (that is the highest resistance to penetration during scratching) exhibited by the formulations with intermediate PEI-Si content (DGEBA/PEI-Si 70:30 and 50:50). An excessive amount of PEI-Si (DGEBA/PEI-Si 20:80 sample) leads to a worsening of P_d behavior also with respect to the neat material. It should be taken into account the structure of PEI-Si. On increasing its proportion in the formulation more inorganic network is formed increasing the resistance to the penetration. However, the soft character of the flexible hyperbranched PEI leads to a resistance reduction. Because both facts affect in contrary sense the maximum in this property is reached at an intermediate proportion.

Typical residual depth (R_d) vs. scratch length curves are reported in **Figure 8** for the investigated samples.

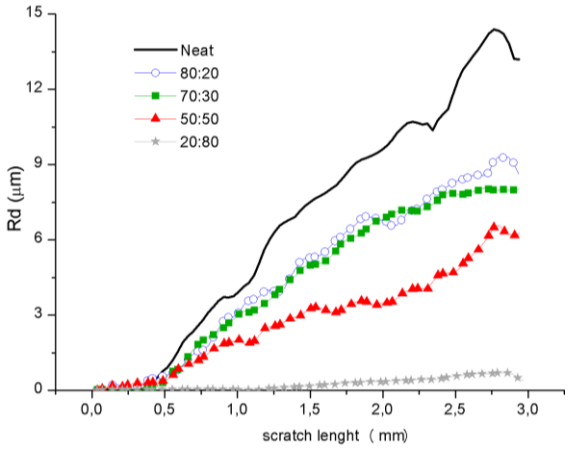

Figure 8. Residual depth (Rd) as a function of scratch length for the neat and the different hybrid materials

The R_d values can be considered as an indication of the elastic recovery after scratching and they are much more related to the ultimate scratch resistance than P_d values. The slope of R_d curves is relatively high for the neat material and progressively decreases by increasing the amount of PEI-Si modifier as indicated by the values of R_d measured at the end of the scratch (3 mm), that is about 13 μm for the neat materials down to 1 μm for DGEBA/PEI-Si 20:80 sample. The increased scratch resistance due to the presence of PEI-Si modifier is also clearly evident from the optical micrographies of samples surface after scratching (**Figure 9**). Again, the flexibility of the PEI structure, in addition to the crosslinks produced by the silica network constitutes the basis to explain the elastic recovery observed.

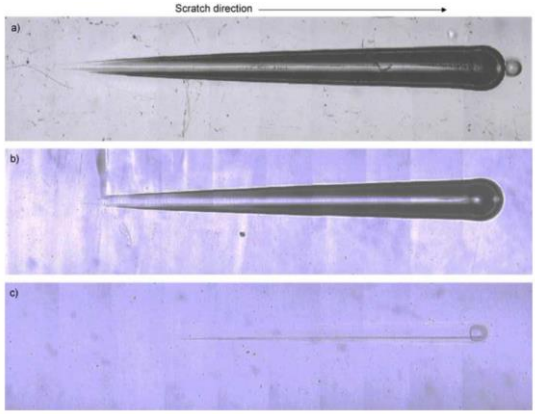

Figure 9. Optical micrographies after scatching for a)neat, b)DGEBA/PEI-Si 80:20 and c)DGEBA/PEI-Si 20:80 materials

Conclusions

The silylation of a commercial hyperbranched polyethyleneimine has been successfully performed without gelation. The silylation of primary and secondary has been confirmed by ^{1}H and ^{29}Si NMR spectroscopy.

The use of 1-methylimidazole has allowed obtaining hybrid materials, since it catalyzed both sol-gel and epoxy homopolymerization, which took place at two different temperatures, 80 and 180 ºC, respectively.

The occurrence of the sol-gel condensation with formation of cage-like and branched silicon structures was confirmed by solid-state ^{29}Si NMR spectroscopy, because of the presence of T_3 signals.

TEM analysis allowed confirming the homogeneous morphology of the hybrid material with nanometric silicon particles embedded in the organic matrix without aggregates.

Scratch tests of the hybrid films showed that the highest resistance to penetration during scratching was exhibited by the formulations with intermediate PEI-Si content (DGEBA/PEI-Si 70:30 and 50:50). The elastic recovery after scratching increased with the proportion of silylated polyethyleneimine in the formulation and the materials showed the capacity of self-repairing.

To increase the size of the inorganic particles, the addition of little amounts of tetraethyl orthosilicate (TEOS) will be of interest. Also, to improve the interaction between inorganic particles and organic matrix the introduction of epoxy ethoxysilylated coupling agent to the formulation could lead to enhance mechanical and thermomechanical characteristics.

References

[1] Piscitelli F, Lavorgna M, Buonocore GG, Verdolotti L, Galy J, Masci L. Plasticizing and reinforcing features of siloxane domains in amine-cured epoxy/silica hybrids. Macromol Mater Eng 2013;298:896-909.
[2] Ponyrko S, Kobera L, Brus J, Matejka L, Epoxy-silica hybrids by nonaqueous sol-gel process. Polymer 2013;54:6271-6282.
[3] Schottner G, Hybrid sol-gel-derived polymers: Applications of multifunctional materials. Chem Mater 2001;13:3422-3435.

[4] Judeinstein P, Sanchez C. Hybrid organic–inorganic materials: a land of multidisciplinarity. J Mater Chem 1996;6:511-525.
[5] Wang D, Bierwagen GP. Sol–gel coatings on metals for corrosion protection. Prog Org Coat 2009;64:327-338.
[6] Shuyu L, Matthias NN, Sabyasachi G. Recent developments in flame retardant polymeric coatings. Prog Org Coat 2013;76:1642-1665.
[7] Goertzen WK, Sheng X, Akinc M, Kessler MR. Rheology and curing kinetics of fumed silica/cyanate ester nanocomposites. Polym Eng Sci 2008;48:875-883.
[8] Boogh L, Pettersson B, Månson J-A E. Dendritic hyperbranched polymers as toughеners for epoxy resins. Polymer 1999; 40:2249-2261.
[9] Ratna D, Varley R, Simon GP. Toughening of trifunctional epoxy using an epoxy-functionalized hyperbranched polymer. J Appl Polym Sci 2003;89:2339-2345.
[10] Xu G, Shi W, Gong M, Yu F, Feng J. Curing behavior and toughening performance of epoxy resins containing hyperbranched polyester. Polym Adv Tech 2004;15:639-644.
[11] Foix D, Serra A, Amparore L, Sangermano M. Impact resistance enhancement by adding epoxy ended hyperbranched polyester to DGEBA photocured thermosets. Polymer 2012;53:3084-3088.
[12] Flores M, Fernández-Francos X, Ferrando F, Ramis X, Serra A. Efficient impact resistance improvement of epoxy/anhydride thermosets by adding hyperbranched polyesters partially modified with undecenoyl chains. Polymer 2012;53:5232-5241.
[13] Sangermano M, El Sayed H, Voit B. Ethoxysilyl-modified hyperbranched polyesters as mulitfunctional coupling agents for epoxy-silica hybrid coatings. Polymer 2011;52:2103-2109.
[14] Geiser V, Leterrier Y, J-A E. Månson. Low-stress hyperbranched polymer/silica nanostructures produced by UV curing, sol/gel processing and nanoimprint lithography. Macromol Mater Eng 2012;297:155-166.
[15] Sangermano M, Messori M, Martin Galleco M, Rizza G, Voit B. Scratch resistant tough nanocomposite epoxy coatings based on hyperbranched polyesters. Polymer 2009;50:5647-5652.
[16] Bi Y-T, Li Z-J, Liang W, Preparation and characterization of epoxy/SiO_2 nano-composites by cationic photopolymerization and sol-gel process. Polym Adv Technol 2014;25:173-178.
[17] Nazir T, Afzal A, Siddiqi HM, Ahmad Z, Dumon M. Thermally and mechanically superior hybrid epoxy-silica polymer films via sol-gel method. Prog Org Coat 2010;69:100-106.
[18] Mascia L, Prezzi L, Haworth B. Substantiating the role of phase bicontinuity and interfacial bonding in epoxy-silica nanocomposites. J Mater Sci 2006;41:1145-1155.
[19] Le Q-H, Kuan H-C, Dai J-B, Zaman I, Luong L, Ma J. Structure-property relations of 55 nm particle-toughened epoxy. Polymer 2010; 51:4867-4879.
[20] Sangermano M, Messori M, Scratch resistance enhancement of polymer coatings. Macromol Mater Eng 2010; 295: 603–612.
[21] Houel A, Galy J, Charlot A, Gerard J-F. Synthesis and characterization of hybrid films from hyperbranched polyester using a sol–gel process. J Appl Polym Sci 2014, DOI: 10.1002/APP.39830.
[22] Beneš H, Galy J, Gérard J-F, Pleštil J, Valette L. Solvent-free synthesis of reactive inorganic precursors for preparation of organic/inorganic hybrid materials. J Sol-Gel Sci Technol 2011;59:598-612.
[23] Sadhir R. K., Luck M. R. Expanding Monomers: Synthesis, Characterization and Applications; Eds.; CRC: Boca Raton, FL, 1992.
[24] Matejka L, Dukh O, Brus J, Simonsick Jr WJ, Meissner B. Cage-like structure formation during sol-gel polymerization of glycidyloxypropyl trimethoxysilane J. Non-Cryst Solids 2000;270:34-47.
[25] Devreux F, Boilot JP, Chaput F, Lecomte A. Sol-gel condensation of rapidly hydrolyzed silicon alkoxides: A joint ^{29}Si NMR and small-angle X-ray scattering study. Phys Rev A 1990;41: 6901-6909.
[26] Pascault JP, Sautereau H, Verdu J, Williams RJJ. Thermosetting Polymers. Marcel Dekker: New York; 2002.
[27] Crivello JV, Malik R. Synthesis and photoinitiated cationic polymerization of monomers with the silsesquioxane core. J Polym Sci Part A Polym Chem 1997;35: 407-425.
[28] Fernández-Francos X, Santiago D, Ferrando F, Ramis X, Salla JM, Serra A, Sangermano M. Network Structure and Thermomechanical Properties of Hybrid DGEBA Networks Cured with 1-Methylimidazole and Hyperbranched Poly(ethyleneimine)s. J Polym Sci Part B Polym Phys 2012;50:1489-1503.

5.3 Hybrid epoxy networks from ethoxysilyl-modified hyperbranched poly(ethyleneimine) and inorganic reactive precursors

Cristina Acebo, Xavier Fernández-Francos, José-Ignacio Santos, Massimo Messori, Xavier Ramis, Àngels Serra

European Polymer Journal **2015***, 70,* 18-27

UNIVERSITAT ROVIRA I VIRGILI
HYPERBRANCHED POLY(ETHYLENEIMINE) DERIVATIVES AS MODIFIERS IN EPOXY NETWORKS
Cristina Acebo Gorostiza

European Polymer Journal **2015**, *70*, 18-27

Hybrid epoxy networks from ethoxysilyl-modified hyperbranched poly(ethyleneimine) and inorganic reactive precursors

Abstract

New epoxy-silica hybrid coatings were prepared by a dual process consisting of a sol-gel process using tetraethoxysilane (TEOS) or 3-glycidyloxypropyl trimethoxysilane (GPTMS) in the presence of hyperbranched poly(ethyleneimine) with ethoxysilyl groups at the chain ends (PEI-Si) followed by a homopolymerization of diglycidylether of bisphenol A (DGEBA) using 1-methylimidazole (1-MI) as anionic initiator. The influence of the amount of TEOS and GPTMS in the characteristics of the coating was examined.

Thin transparent films were obtained and their morphology was observed by transmission electron microscopy (TEM). The hydrolytic condensation was confirmed by ^{29}Si-NMR studies. Cage-like nanometric structures were formed in case of adding GPTMS and bigger silica particles on adding TEOS to the formulation. Thermal stability was evaluated by thermogravimetry and the scratch resistance properties were also investigated, showing an improvement in resistance to break and to detachment in all the coatings containing GPTMS.

Keywords

Hyperbranched polymers, epoxy resin, sol-gel, coatings, hybrids.

Introduction

Hybrid organic/inorganic nanomaterials have attracted a great deal of attention in the field of polymer research as well as in industrial applications because their advanced properties like abrasion and scratch resistance, toughness, mechanical properties, self-healing or corrosion resistance attributed to the formation of the inorganic particles in the polymer matrix, while keeping transparency.[1-4]

Hybrid materials are usually obtained by the addition of preformed nanoparticles, the most significant examples being layered silicates, silica nanoparticles or polyhedral oligomeric silsesquioxane (POSS).[5-7] In these cases, the homogenous dispersion of the silica filler in the organic matrix may represent a challenge. An alternative route to incorporate silica into the polymer matrix is the sol-gel process involving a series of hydrolysis and condensation reactions under mild conditions starting from hydrolyzable multifunctional alkoxysilanes as inorganic precursors for forming inorganic domains, being tetraethoxysilane (TEOS) the most typical one.[8-12] Using this route it is possible to grow an inorganic phase into an organic matrix allowing a fine dispersion of the inorganic phase even at molecular level. Another advantage of the *in situ* generation of the inorganic phase is that the addition of a small amount of nanoparticles drastically increases the viscosity, which is always an important issue in coatings applications whereas the formulation applied before the sol-gel process still has a low viscosity.[13]

Hyperbranched polymers (HBP)s have been applied as modifiers in epoxy thermosets to improve toughness.[14-16] In the last years, they have been extensively used because of their special architectures present some advantages over conventional toughening agents. HBPs help to keep the viscosity of the formulations at a reduced value due to the lower entanglement caused by the branching, whereas they do not produce any appreciable

decrease in thermomechanical parameters. The highly branched structures gives access to a large number of functional end groups and thus allows tailoring the compatibility/reactivity of the HBPs in the resin resulting in homogeneous or phase separated materials.[17,18] Due to the enhancement of the thermomechanical properties that can be achieved by adding HBPs and the improvement in nanocomposite processing reached through sol-gel procedures, the strategy of combining both methodologies was adopted by several authors.[19-21]

Inorganic domains can be generated from organoalkoxy silane precursors with functional groups (epoxy, amine, etc.), which are used as coupling agents, to react with organic matrices enabling a good incorporation of inorganic structures into an organic phase.[22,23] In this way, phase separation in organic and inorganic domains can be prevented by the use of these compounds, being one of the most used in epoxy matrices 3-glycidoxypropyltrimethoxysilane (GPTMS).[24] Thus, it seems that the preparation of multifunctional coupling agents by silylation of the end groups of hyperbranched polymers can be greatly advantageous to improve the properties of epoxy resins by generation of silica-like particles by sol-gel process from the alkoxysilane end groups. Sangermano et al.[19] prepared epoxy-silica materials using as inorganic precursor hyperbranched aromatic-aliphatic polyester modified to different extents at the final phenol groups by reacting with 3-isocyanatepropyl triethoxysilane. The addition of ethoxysilyl-modified HBP as a coupling agent allowed the covalent bonding of inorganic and organic networks. In some cases, TEOS was also added to the formulation. The authors could clearly demonstrate that the use of the silylated hyperbranched polymer was advantageous in the formation of transparent films in contrast to what occurred by applying the same curing procedure without silylated hyperbranched but adding TEOS as source of silica particles.

In our group, we synthesized a triethoxy silylated hyperbranched poly(ethylene imine) (PEI-Si) which was used in different proportions as inorganic precursor in diglycidylether of bisphenol A (DGEBA) formulations using 1-methylimidazole as anionic curing agent.[25] The materials obtained were highly transparent and no particles could be observed by TEM analysis. However, ^{29}Si NMR spectra demonstrated that the sol-gel processes occurred with the formation of cage-like structures (POSS) with particle size <10 nm. One of the peculiarities of these hybrid coatings was the increase in surface hardness due to the presence of silica domains well dispersed in the epoxy matrix and formulations with intermediate PEI-Si had the highest resistance to penetration. It has been reported that the incorporation of POSS cages into polymers improves several properties such as thermal stability, glass transition temperature, flame and heat resistance and modulus.[26]

In spite of the good characteristics of the hybrid materials obtained in our previous study, there was not a clear evidence of a real covalent linkage between PEI-Si structure (and the POSS cages formed by sol-gel) with the epoxy matrix, which is usually required to achieve the best mechanical performance in sol-gel thermosets. Because of that, in the present work we have taken the formulation with DGEBA/PEI-Si 50:50 w/w as the neat material and we have studied the effect of adding different proportions of TEOS or GPTMS. The addition of TEOS aims at increasing the particle size and the addition of GPTMS to enhance the interaction between organic and inorganic phases. In addition, the presence of a single epoxy group in the GPTMS structure would produce a looser epoxy network structure. We have also tested if there is a synergistic effect of adding both silicon precursors to the selected formulation. The characterization of the materials has been performed by ^{29}Si NMR spectroscopy in solid state and the morphology of the hybrid was

visualized by TEM microscopy. The mechanical properties of the films were rated by scratch tests.

Experimental

Materials

Poly(ethyleneimine) (PEI) Lupasol®FG (PEI800, 800 g/mol, BASF) was dried under vacuum before use. 1-Methylimidazole (1-MI) and tetraethyl orthosilicate (TEOS) were purchased from Sigma-Aldrich and used without further purification. Chloroform was purchased from Scharlab, dried under $CaCl_2$ and distilled before used. Diglycidylether of bisphenol A (DGEBA) Araldite GY 240 (EEW = 182 g/eq) was gently provided by Huntsman. Ammonium dihydrogen phosphate ($NH_4H_2PO_4$), 3-isocyanatepropyl triethoxysilane (TESPI) and 3-glycidoxypropyl trimethoxysilane (GPTMS) were purchased from Acros Organics. Triethoxysilyl modified hyperbranched poly(ethyleneimine) (PEI-Si) was prepared as described previously[25] by reacting Lupasol and TESPI in chloroform.

Sample preparation

In all the samples the weight proportion of PEI-Si/DGEBA was 50:50 and 2 phr of 1-MI in reference to the DGEBA were added. The inorganic precursors TEOS and GPTMS were added to the formulations in the range between 10 and 40 wt%. The formulations were coated on glass slides by means of a wire-wound applicator. The sol-gel process was carried out by thermal treatment at 80ºC for one day in a controlled highly humid atmosphere (95-98% relative humidity controlled by a saturated solution of aqueous $NH_4H_2PO_4$) and was followed by a thermal curing process at 150ºC during 2 h in an oven.

Characterization techniques

Solution NMR spectra were carried out in a Varian Gemini 400 spectrometer using $CDCl_3$ as the solvent. For ^{29}Si NMR measurements tetramethylsilane (TMS) was used as the reference. For ^{29}Si NMR measurements the conditions used were d_1=0.4 s acquisition time = 0.7 s, a number of scans of 3000 and applying an inverse gated decoupling pulse sequence.

Solid-state ^{29}Si CPMAS NMR spectra were recorded on a Bruker AVANCE III 400 MHz spectrometer WB equipped with wide bore 9.4 T superconducting magnet in Larmor frequencies of 79.5 MHz. Powdered samples were packed into 4 mm ZrO2 rotors. Chemical shifts are given relative to TMS. NMR spectra were registered using a CP MAS pulse sequence with an acquisition time of 0.0184 s and 34432 scans using the following parameters: rotor spin rate 10000 Hz and recycling delay of 5 s. In the processing of the data exponential apodization with line broadening 40 Hz, FT and manual phasing and baseline correction were used.

Calorimetric analyses were carried out on a Mettler DSC-822e thermal analyzer. Samples of approximately 10 mg were placed in aluminum pans under nitrogen atmosphere. The calorimeter was calibrated using an indium standard (heat flow calibration) and an indium-lead-zinc standard (temperature calibration). T_gs of the hybrid materials were determined at a heating rate of 30ºC/min after a first scan from 0 to 180ºC followed by cooling at 10ºC/min from 180ºC/min to 0ºC. The error is estimated to be approximately ± 1 °C.

Thermogravimetric analyses were carried out in a Mettler TGA/SDTA 851e thermobalance. Samples with an approximate mass of 8 mg were degraded between 30 and 900 ºC at a heating rate of 10 ºC/min in air (100 cm^3/min measured in normal conditions).

The morphology of the different hybrids was analyzed by imaging thin pieces from the samples. These pieces had a thickness of 60 µm, in a transmission electron microscope (TEM, JEOL model 1011) with a 0.2 nm resolution.

Scratch test was carried out on a CSM Micro-Combi Tester by using Rockwell 0.1 mm diameter spherical diamond indenter. Progressive scans increasing the normal load from 10 to 5000 mN were made for a scratch length of 3 mm and at a scratch rate of 60 mm min^{-1}, according to an adaptation of the Test Mode A described by the technical standard ASTM D 7027. A prescan with a constant and very low load (10 mN) was carried out in order to record the starting surface profile. At least 5 progressive scans were performed for each sample with penetration depth (P_d) recording. First and second critical load values (Lc_1 and Lc_2) were determined by optical microscopy after scratch test evaluating the occurrence of the first visible crack on the coating surface and the detachment of the coating from the glass substrate, respectively.

Results and discussion

The synthesis of the triethoxysilylated hyperbranched poly(ethyleneimine) (PEI-Si) was conducted following the procedure described in a previous work.[25] All the primary and secondary amines were modified by using TESPI. By ^{29}Si NMR spectroscopy two signals were observed at -45.4 and -45.0 ppm attributable to the silyl groups attached to the primary and to the secondary amines at the HBP structure. **Scheme 1** shows the idealized structure of the PEI-Si together with the other compounds used in the formulations.

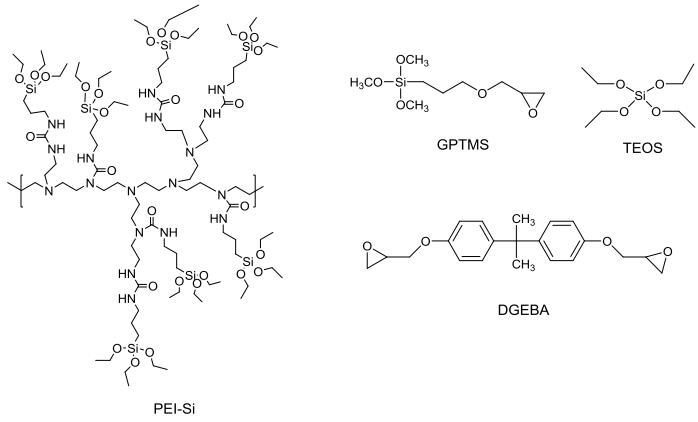

Scheme 1. Idealized structure of the ethoxysilylated poly(ethyleneimine) prepared and structure of the compounds used in the preparation of the hybrid thermosets

Preparation of films from DGEBA and PEI-Si and TEOS or GPTMS mixtures

The hybrid materials were prepared using the same protocol as the previous work,[25] which is based in two well-known processes: sol-gel and epoxy anionic homopolymerization. Both processes partially overlapped because of the easy thermal homopolymerization of epoxides initiated by 1-MI, even at moderate temperatures. 1-MI

also acts as basic catalyst in the sol-gel process together with tertiary amine groups located in the PEI-Si structure. The use of acidic conditions is prevented by the basic character of the HBP.[2] It has been reported that sol-gel processes under basic conditions lead to the formation of particulate inorganic domains, due to the fast rates of condensation reactions that leads to separation by nucleation and growth mechanism.[24] Water dissociates to produce nucleophilic hydroxyl anions in a quick first step. The hydroxyl anions lead to an SN_2 substitution on silicon atom to produce the corresponding silanol.[12]

While sol-gel process produces inorganic structures, epoxy homopolymerization originates the networked organic matrix. The interaction between PEI-Si and the organic matrix could not be confirmed in the previous study, since all the primary and secondary groups of PEI were transformed into ureas by reaction with TESPI. Neither urea groups nor tertiary amines are sufficiently nucleophilic to attack epoxides in an extensively way. However, a partial interaction by hydrogen bonding was foreseeable. To increase the interaction between both domains, in the present study we have added GPTMS, which has an epoxy group that can homopolymerize and a methoxysilylated group that can participate in the formation of cage-like particles with ethoxysilyl groups from PEI-Si. The addition of TEOS has the aim to create bigger inorganic particles and to increase the proportion of Si in the materials, reducing the proportion of cage-like structures, since the higher functionality of TEOS can lead to networked silica particles and bicontinuous nanocomposites. The addition of TEOS and GPTMS at the same time aims at obtaining larger particles covalently linked to the epoxy network. **Table 1** collects the composition of all the formulations studied in weight percentages.

Table 1. Notation and compositions of the formulations studied. All the formulations have 2 phr of 1-MI in reference to DGEBA.

Formulation	DGEBA		PEI-Si		TEOS		GPTMS	
	wt (%)	mol (%)	wt (%)	mol (%)	wt (%)	mol (%)	wt (%)	mol (%)
Neat	50	96	50	4	-	-	-	-
10% TEOS	45	80.4	45	3.5	10	16.1	-	-
20% TEOS	40	67.5	40	3.1	20	29.4	-	-
30% TEOS	35	56.2	35	2.4	30	41.4	-	-
40% TEOS	30	45	30	2	40	53	-	-
10% GPTMS	45	82.5	45	3.5	-	-	10	14
20% GPTMS	40	71.1	40	3	-	-	20	25.9
30% GPTMS	35	58	35	2.5	-	-	30	39.5
40% GPTMS	30	47.4	30	2	-	-	40	50.6
20% TEOS/ 20% GPTMS	30	48	30	2	20	24	20	26

The sol-gel hybrid films were easily prepared by mixing the different proportions of the components of the formulation and adding 2 phr of 1-MI (parts of amine per hundred parts of DGEBA) obtaining in all cases homogeneous mixtures. The viscous mixtures were coated on glass slides and then heated for one day at 80 ºC in a controlled high humidity atmosphere. After sol-gel process the coatings were solid and transparent and the condensation reaction and the curing of DGEBA were then performed in an oven at 150 ºC during 2 h. The films obtained after this schedule were hard and transparent with a light

color and without any visible particle at the naked eye (see **Figure 1**). The optical quality based on the transparency of the materials prepared accounts for the formation of small inorganic domains with sizes lower than 400 nm. Although some shrinkage stress should occur due to the significant volume change caused by the loss of alcohol and water, no cracks, voids or debonding were observed.

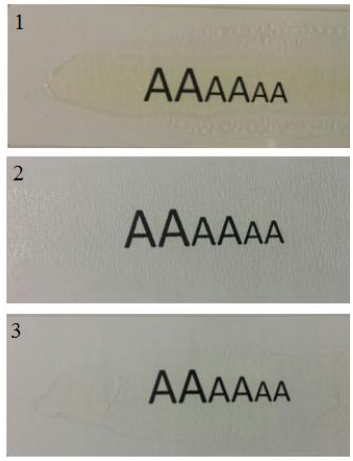

Figure 1. Photographs of the films prepared showing the transparency and appearance. 1 (Neat material); 2 (40% TEOS) and 3 (40% GPTMS)

Characterization of sol-gel condensed films

To confirm the formation of inorganic structures by condensation of silanols, ^{29}Si NMR studies of the cured samples were registered in the solid state. **Figure 2** shows the ^{29}Si CPMAS NMR spectra of the material obtained from formulations 30% GPTMS and 30%TEOS.

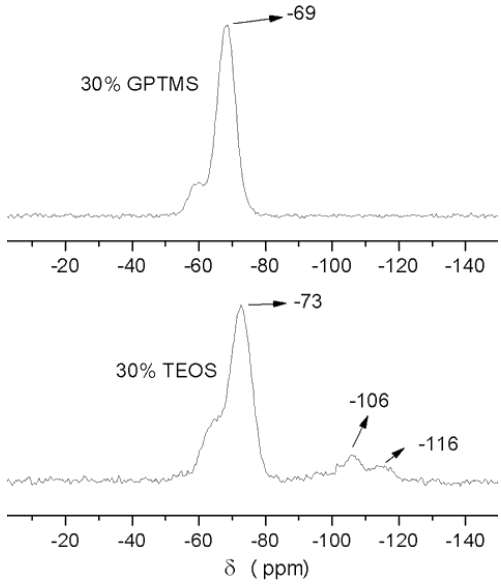

Figure 2. ^{29}Si CPMAS-NMR spectra of the hybrid thermosets obtained from formulations 30% GPTMS and 30% TEOS

It should be commented that no signals corresponding to the silicon precursors were observed in any spectra. Both spectra containing GPTMS or TEOS show peaks in the region of T_i units. For the sample 30% GPTMS the maximum of the *T* peak is -69 ppm which can be assigned to T_3 of cubic cage-like structures according to the reported by Matejka et al.,[27] for sol-gel processes from compounds having trialkoxysilyl groups. They described that cyclization is a typical feature of the polymerization of alkoxysilanes. The trifunctionality of the PEI-Si in the 30% TEOS sample also contributes to the formation of T_3 units in addition to the Q_i units produced according to the tetrafunctionality of TEOS. However, in the sample with TEOS the maximum of the peak is shifted to high field in 4 ppm. This fact could be explained by the formation of linear T_3 structures or cages with a high number of silicon atoms per structure because of the reaction with TEOS. Cubic cage-like structures reduce the valence angles of Si atoms and consequently the density of positive charge diminishes. Thus, in linear structures or in bigger cages the internal tension is reduced and the signal would be high-field shifted.[27]

The apparition of a shoulder at higher chemical shift in both spectra can be attributed to the presence of T_2 units, with uncondensed silanols or to the incompletely condensed POSS cages. This shoulder seems to be proportionally more intense for the TEOS sample. In the spectrum of the material containing TEOS, *Q* signals can be observed in the region of 100-120 ppm. The signals are broad and have a bad resolution but Q_3 signals at –106 ppm are more intense than Q_4 at -116 ppm, indicating that the condensation of TEOS has not been completed. The assignment of signals is based on previously reported results.[27,28]

Thermal characterization

Calorimetric studies allowed determining the T_g of the hybrid materials. The values are collected in **Table 2**.

Table 2. Thermal data of the hybrid materials prepared obtained by TGA and DSC

Formulation (DGEBA/PEI-Si)	T_g [a] (ºC)	$T_{5\%}$ [b] (ºC)	$T_{1st\ peak}$ [c] (ºC)	T_{max} [d] (ºC)	$T_{3rd\ peak}$ [e] (ºC)	*Residue* [f] (wt%)	*Residue* [g] (wt%)
Neat	89	254	267	371	562	8.41	9.10
10% TEOS	83	254	268	372	562	10.1	10.27
20% TEOS	82	255	267	371	557	11.08	11.74
30% TEOS	78	254	267	373	562	12.84	13.1
40% TEOS	75	254	266	375	570	13.5	14.24
10% GPTMS	73	252	263	364	560	9.36	9.67
20% GPTMS	68	254	262	365	574	10.26	10.75
30% GPTMS	68	256	258	366	610	11.62	12.30
40% GPTMS	67	259	259	367	610	12.30	13.62
20% TEOS/20% GPTMS	68	257	268	368	576	12.49	13.24

[a] Glass transition temperature of the hybrid materials
[b] Temperature of the onset decomposition on TGA data at 10ºC/min taken as the 5% weight loss.
[c] Temperature of the maximum rate of the first degradation peak
[d] Temperature of the maximum decomposition rate
[e] Temperature of the maximum rate of the third degradation peak
[f] Experimental residue at 900ºC in air atmosphere
[g] Theoretical residue

The T_g of the neat formulation, obtained only from the ethoxysilyl-modified HBP and DGEBA is of 89 ºC. Assuming that the organic phase consists mainly of homopolymerized DGEBA, this is a rather low value in comparison with those reported in the literature.[29,30] One must take into account that, during the sol-gel process, the sample is exposed to a highly humid environment, and that ethanol and water are released by the hydrolysis and condensation of ethoxysilyl groups. Both ethanol and water can participate in the anionic homopolymerization of DGEBA as chain-transfer agents, reducing the crosslinking density and consequently the T_g.[31] The hyperbranched structure of the ethoxysilyl modifier is flexible, but it is assumed that it is mainly embedded and immobilized into the inorganic domains. However, it might be that some flexible segments resulting from incomplete hydrolysis and condensation might have an effect on the organic phase.

On increasing the proportion of TEOS in the formulation the T_g values slightly decrease. This result follows the opposite trend to that reported by Sangermano et al.[19] They observed an increase of 20 to 45ºC on adding a 30% of TEOS to hyperbranched silylated modified HBP epoxy formulations. However, a decrease in the T_g was reported by Matejka et al.[32] on adding TEOS to an epoxy-amine formulation. These authors attributed the reduction in T_g to a non-efficient immobilization of the epoxy network by silica, due to the low extent of the covalent interfacial bonding. As we will demonstrate by TEM, the addition of a high proportion of TEOS to the formulation leads to a clear separation into large inorganic domains, which do not influence greatly the mobility of the organic network. Finally, as we saw by ^{29}Si-NMR spectroscopy, TEOS is not fully condensed, since Q_3 signals seems to be predominant to Q_4. The low conversion in the sol-gel process results in the formation of undercured soft flexible silica/siloxane domains leading to plasticization of the material resulting in a decrease in the T_g.[32]

The addition of GPTMS to the formulation also leads to a reduction of the T_g values much noticeable than on adding similar proportions of TEOS. The replacement of DGEBA by the monofunctional epoxide GPTMS leads to a decrease in the average epoxide functionality and a reduction of the epoxy network crosslinking density. In addition, the flexible structure of GPTMS can cause a certain plasticization. Such effects lead to the corresponding diminution of the T_g as it was reported previously.[32] Sun et al.[33] compared the effect of adding micro or nanofillers in epoxy composites and observed that on increasing the proportion of nanoparticles the T_g of the nanocomposite is reduced whereas the contrary trend was observed for microparticles. This observation helps to understand how the formation of a higher proportion of inorganic nanostructures reduces the T_g as observed. The material obtained from a mixture with a 20% of TEOS and a 20% of GPTMS shows the same T_g than the one measured for the 20% GPTMS material, without any further reduction for the presence of TEOS in the sample.

The thermal stability of the materials prepared was studied by thermogravimetry. In **Figure 3** the weight loss and the derivative of the degradation curve are represented for the material 20% TEOS.

It should be commented that all the degradation curves of the materials showed a similar shape, with three defined processes, but no loss of volatiles was observed at low temperature which indicates that the condensation of silanol groups was practically complete. The first degradation peak corresponds to the degradation of poly(ethyleneimine) structure,[30] the second peak to the degradation of the epoxy network, whereas the third corresponds to the oxidative degradation leading to the loss of organic matter giving rise to the silicon residue.[25]

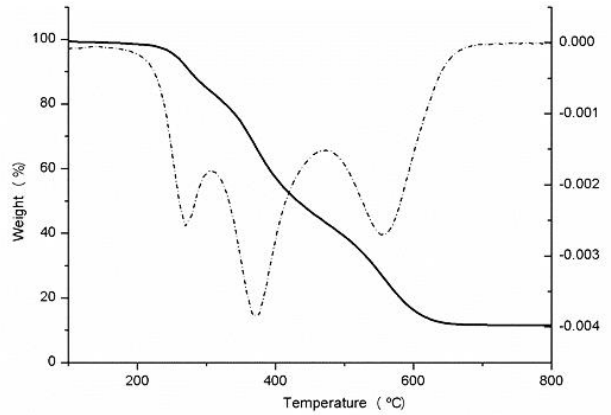

Figure 3. TGA and DTG curves of the material obtained from the formulation with a 20%TEOS in air atmosphere.

The data obtained from the degradation curves are collected in Table 2. As we can see, the addition of TEOS or/and GPTMS to the formulation does not lead to any effect in the initial temperature of degradation, taken as the 5% of weight loss. The temperatures of the maximum of the three degradative processes are very similar with the exception of the temperature of the third peak for samples with GPTMS that shifts to higher temperatures with the increasing amount of this coupling agent. That could be explained by the increase in the covalent bonding between organic and inorganic structures. The residue at 900 ºC as expected increases with the amount of Si in the material. On comparing the calculated Si content with the experimental residue we can see that there are not great differences, but the experimental values are slightly lower than those calculated. It can be related to an incomplete hydrolysis of alkoxide groups that was reflected in the presence of T_2 and Q_3 signals in the ^{29}Si NMR spectroscopy.

TEM analysis

Figure 4 shows the TEM micrographs of some of the hybrid materials prepared. In the micrographs the difference in the electronic transmission between organic and inorganic phases allows assign the dark area to the Si particles, covalently connected to the organic matrix. As in the previous paper,[25] in the micrograph of the neat material we cannot see any appreciable aggregation between inorganic particles in the matrix by the presence of the cage-like structures obtained by sol-gel from ethoxysilylated PEI and DGEBA. The POSS particles formed are embedded in the epoxy matrix with sizes < 10 nm that rends transparency to the hybrid coating.

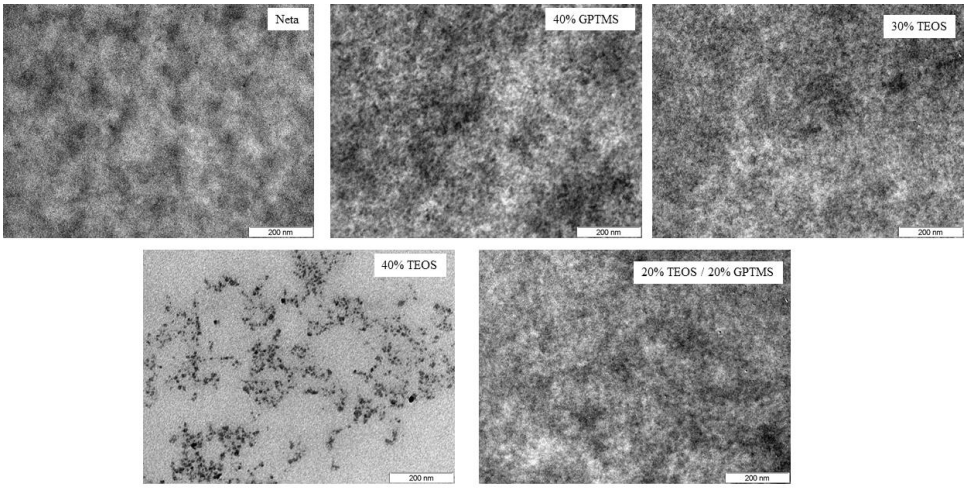

Figure 4. TEM micrographs of hybrid materials obtained from different formulations at a magnification of 120K

On increasing the proportion of POSS structures the nanodomains become interconnected and a bicontinuous nanophase-separated morphology can be observed in the micrograph of the sample 40% of GPTMS which shows a more inhomogeneous morphology with less-defined boundaries between domains. A similar behavior was observed in epoxy thermosets modified with POSS end-capped polyesters.[34]

On adding a proportion of TEOS up to 30% to the formulation, the material obtained presented no clear evidence of the formation of silica particles and a morphology similar to the 40%GPTMS material is observed in Figure 4. However, on increasing the proportion of TEOS up to 40% clear aggregates of silica particles with particle sizes less than 40 nm can be observed. The material containing 20% of TEOS and 20 % of GPTMS shows a similar morphology that the one commented for 40% GPTMS. Although the generation of particles with TEOS or GPTMS is different because of the tetrafunctionality of the former and the trifunctionality of the latter, the Si content for both formulations is similar. Thus, it seems that in our systems the morphology of the material is more dependent on the Si content than on the structure of the silica precursor. However, the presence of the PEI-Si structure in all those materials helps dispersing the particles in the matrix, leading to a more homogeneous distribution.

Scratch resistance analysis

One of the main ways to improve scratch resistance in organic coatings is to reinforce them by embedding fillers in the organic matrix. To reach significant improvements the regular distribution and the dispersion of the particles into the matrix is crucial. Therefore, to increase scratch resistance, the *in situ* formation of the inorganic nanodomains through sol–gel processes has been demonstrated as one of the best strategies.[35] Some of the data extracted from scratch test are collected in **Table 3**.

Table 3. Data from scratch tests of the hybrid coatings prepared

Formulation	P_d 1N[a] (μm)	P_d 4N[a] (μm)	Lc_1[b] (mN)	Lc_2[c] (mN)
Neat	10.1 ± 0.3	31.6 ± 0.2	670	3530
10% TEOS	10.1 ± 0.9	30.7 ± 2.5	800	3000
20% TEOS	10.9 ± 1.7	35.9 ± 6.7	560	3740
30% TEOS	9.8 ± 1.7	28.8 ± 0.7	260	3840
40% TEOS	10.5 ± 1.2	30.5 ± 0.8	430	3730
10% GPTMS	16.3 ± 2.7	46.2 ± 2.2	650	not detected
20% GPTMS	12.4 ± 0.4	39.8 ± 2.6	680	not detected
30% GPTMS	16.1 ± 1.0	45.1 ± 1.1	620	not detected
40% GPTMS	16.2 ± 1.6	48.9 ± 4.1	820	not detected
20% TEOS/20% GPTMS	11.9 ± 3.6	36.3 ± 8.2	450	not detected

[a] Penetration depth values recorded at 1N and 4N of normal load
[b] First critical load
[c] Second critical load

Penetration depth values (P_d) can be considered as an indication of the resistance to penetration which includes rigidity (modulus) and hardness. These values can be affected by structural parameters of the organic network structure and inorganic domains and the lowest values represent the highest resistance to penetration during scratching. From both series of results detected at 1N and 4N of normal load reported in the table we can see that the presence of TEOS in the hybrid coating keeps the resistance to penetration in reference to the neat material whereas the addition of GPTMS reduces this characteristic. The lower functionality of GPTMS could explain this behavior, since the flexibility increases (that is the modulus decreases) due to a reduction of crosslinking density as it was noted by the decrease in the T_g.

The scratch behavior of coatings is the result of a complex interrelation among several parameters and factors such as modulus, strength, friction coefficient, thickness and viscoelasticity of the coating and its adhesion to the specific substrate.[36] The scratch resistance properties of the hybrid coatings here investigated can be evaluated by first and second critical load values (Lc_1 and Lc_2, respectively) reported in Table 3. Lc_1 (normal load at which the first crack appears on the surface) can be seen as an indirect indication of cohesive forces (strength and deformability) in the coating material and represents the main parameter for the evaluation of the scratch resistance. Lc_2 (normal load at which the detachment of coating from substrate occurs) is an indirect indication of adhesive forces between coating and substrate. In the present case Lc_1 and Lc_2 values are affected by very high values of standard deviation (not reported in table but up to 300 mN in some cases) suggesting a general inhomogeneity of the coating from a mechanical point of view. In this view, Lc_1 values indicate a comparable resistance to scratch for all the coatings investigated (with the negative exception of 30% TEOS sample). It has to be noticed that the addition of GPTMS to the formulation leads to more reliable Lc_1 values (lower standard deviation values), which seems to indicate a more homogeneous material. An optimum Lc_1 is achieved with 40 % of GPTMS. More interestingly, Lc_2 values offer a significant differentiation among the different series of coatings. The presence of TEOS induces a slight improvement of the detachment resistance of the coatings (with the exception of 10% TEOS sample) while the presence of GPTMS in the formulation produces an extremely

adhesive coating with absence of detectable second critical load values in the experimental conditions used for the test.

Some representative optical micrographs after scratch test are collected in **Figure 5**. The presence of a second critical load Lc_2 is well evident in the case of Neat and 20% TEOS coating formulations (Figures 5a and b, respectively) as indicated by the arc tensile cracks shown to the right part of the scratch. On the contrary, a second critical load Lc_2 is not shown by the system containing GPTMS (Figure 5c).

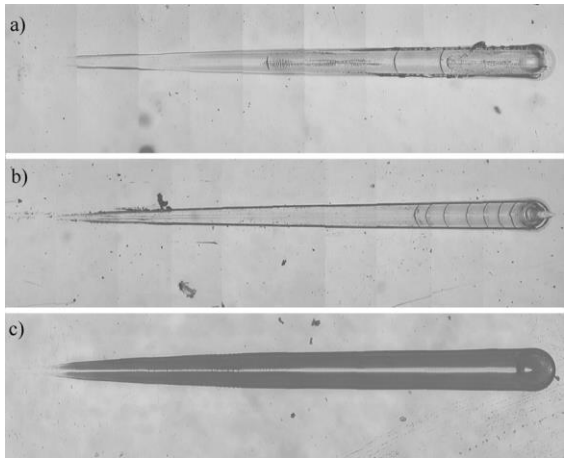

Figure 5. Optical micrographs after scratch test of a) Neat, b) 20% TEOS and c) 20% GPTMS materials

Conclusions

The addition of GPTMS to the formulation led to materials with a high transparency by the formation of cage-like structures that also incorporates the final groups of the PEI-Si structure. This was confirmed by CPMAS ^{29}Si NMR spectroscopy. The materials obtained showed a slightly lower T_g due to a reduction in the crosslinking density of the organic domain. The modified materials presented a similar thermal stability than the neat formulation although the last thermo oxidative process is delayed, which was attributed to the covalent linkage of inorganic particles to the epoxy matrix. The observation of these materials by TEM revealed that nanodomains became interconnected with the formation of a bicontinuous nanophase-separated morphology. The penetration depth, measured by scratch tests, increased on increasing the proportion of GPTMS in the formulation according to a lower rigidity by the reduction in crosslinking density.

When TEOS was added to the formulation, the ^{29}Si NMR spectra showed, in addition to *T* signals, corresponding to cubic-like structures, broad and unresolved *Q* signals attributed to complete and incomplete TEOS condensation. T_g values are slightly reduced by the addition of TEOS. In TEM microscopy the presence of 40% TEOS in the hybrid material led to the observation of well separated silica particles.

The addition of GPTMS or TEOS to the formulation did not increase the overall scratch characteristics in reference to the neat material, since cage-like structures were already produced by the sol-gel condensation of ethoxysilylated PEI. However, the scratch tests confirmed the higher homogeneity of the materials modified with GPTMS due to its compatibilizing effect, and showed a clear increase in resistance to break and detachment

upon addition of GPTMS. The incorporation of GPTMS to TEOS containing formulations allowed to prepare non-detachable coatings.

References

[1] G. Schottner, Hybrid sol-gel-derived polymers: applications of multifunctional materials, Chem. Mater. 13 (10) (2001) 3422-3435.
[2] P. Judeinstein, C. Sanchez, Hybrid organic–inorganic materials: a land of multidisciplinarity, J. Mater. Chem. 6 (1996) 511-525.
[3] D. Wang, G.P. Bierwagen, Sol–gel coatings on metals for corrosion protection, Prog. Org. Coat. 64 (4) (2009) 327–338.
[4] S. Liang, N.N. Matthias, S. Gaan, Recent developments in flame retardant polymeric coatings. Prog. Org. Coat. 76 (11) (2013) 1642-1665.
[5] E. Jacquelot, J. Galy, J.-F. Gérard, A. Roche, E. Chevet, E. Fouissac, D. Verchère, Morphology and thermo-mechanical properties of new hybrid coatings based on polyester/melamine resin and pyrogenic silica. Prog. Org. Coat. 66 (1) (2009) 86-92.
[6] S.-W. Kuo, F.-C. Chang, POSS related polymer nanocomposites. Prog. Polym. Sci. 36 (12) (2006) 1649-1696.
[7] S. Bizet, J. Galy, J.-F. Gérard, Structure−Property Relationships in Organic−Inorganic Nanomaterials Based on Methacryl−POSS and Dimethacrylate Networks. Macromolecules 39 (7) (2006) 2574-2583.
[8] J.C. Brinker, G.W. Scherer, Sol–gel science: the physics and chemistry of sol–gel processing; Academic Press: New York, 1990.
[9] U. Schubert, N. Huesing, A. Lorenz, Hybrid inorganic-organic materials by sol-gel processing of organofunctional metal alkoxides. Chem. Mater. 7 (11) (1995) 2010-2027
[10] J. Wen, G.-L. Wilkes, Organic/inorganic hybrid network materials by the sol−gel approach. Chem. Mater. 8 (8) (1996) 1667-1681
[11] L. Matějka, O. Dukh, B. Meissner, D. Hlavatá, J. Brus, A. Strachota. Block copolymer organic−inorganic networks. Formation and structure ordering. Macromolecules 36 (21) (2003) 7977-7985
[12] H. Beneš, J. Galy, J.-F. Gérard, J. Pleštil, L. Valette, Solvent-free synthesis of reactive inorganic precursors for preparation of organic/inorganic hybrid materials. J. Sol–Gel Sci. Technol. 59 (2011) 598-612.
[13] W.K. Goertzen, X. Sheng, M. Akinc, M.R. Kessler. Rheology and curing kinetics of fumed silica/cyanate ester nanocomposites. Polym. Eng. Sci. 48 (5) (2008) 875-883.
[14] L. Boogh, B. Pettersson, J.-A.E. Månson, Dendritic hyperbranched polymers as toughеners for epoxy resins. Polymer 40 (9) (1999) 2249-2261.
[15] D. Ratna, R. Varley, G.P. Simon, Toughening of trifunctional epoxy using an epoxy-functionalized hyperbranched polymer. J Appl. Polym. Sci. 89 (9) (2003) 2339-2345.
[16] G. Xu, W. Shi, M. Gong, F. Yu, J. Feng. Curing behavior and toughening performance of epoxy resins containing hyperbranched polyester. Polym. Adv. Technol. 15 (11) (2004) 639-644.
[17] D. Foix, A. Serra, L. Amparore, M. Sangermano, Impact resistance enhancement by adding epoxy ended hyperbranched polyester to DGEBA photocured thermosets. Polymer 53 (15) (2012) 3084-3088.
[18] M. Flores, X. Fernández-Francos, F. Ferrando, X. Ramis, A. Serra, Efficient impact resistance improvement of epoxy/anhydride thermosets by adding hyperbranched polyesters partially modified with undecenoyl chains. Polymer 53 (23) (2012) 5232-5241.
[19] M. Sangermano, H. El Sayed, B. Voit, Ethoxysilyl-modified hyperbranched polyesters as multifunctional coupling agents for epoxy-silica hybrid coatings. Polymer 52 (10) (2011) 2103-2109.
[20] V. Geiser, Y. Leterrier, J.-A.E. Månson, Low-Stress Hyperbranched polymer/silica nanostructures produced by UV curing, sol/gel processing and nanoimprint lithography. Macromol. Mater. Eng. 297 (2) (2012) 155-166.
[21] M. Sangermano, M. Messori, M. Martin Galleco, G. Rizza, B. Voit, Scratch resistant tough nanocomposite epoxy coatings based on hyperbranched polyesters. Polymer 50 (24) (2009) 5647-5652.

[22] Y.-T. Bi, Z.-J. Li, W. Liang, Preparation and characterization of epoxy/SiO_2 nano-composites by cationic photopolymerization and sol-gel process. Polym. Adv. Technol. 25 (2) (2014) 173-178.
[23] T. Nazir, A. Afzal, H.M. Siddiqi, Z. Ahmad, M. Dumon, Thermally and mechanically superior hybrid epoxy-silica polymer films via sol-gel method. Prog. Org. Coat. 69 (1) (2010) 100-106.
[24] L. Mascia, L. Prezzi, B. Haworth, Substantiating the role of phase bicontinuity and interfacial bonding in epoxy-silica nanocomposites. J. Mater. Sci. 41 (4) (2006) 1145-1155.
[25] C. Acebo, X. Fernàndez-Francos, M. Messori, X. Ramis, A. Serra, Novel epoxy-silica hybrid coatings by using ethoxysilyl-modified hyperbranched poly(ethylenimine) with improved scratch resistance. Polymer 55 (20) (2014) 5028-5035
[26] J.J. Chruściel, E. Leśniak. Modification of epoxy resins with functional silanes, polysiloxanes, silsesquioxanes, silica and silicates. Prog. Polym. Sci. 41 (2015) 67-121.
[27] L. Matejka, O. Dukh, J. Brus, W.J. Simonsick Jr., B. Meissner, Cage-like structure formation during sol-gel polymerization of glycidyloxypropyl trimethoxysilane J. Non-Cryst. Solids 270 (2000) 34-47.
[28] F. Piscitelli, M. Lavorgna, G.G. Buonocore, L. Verdolotti, J. Galy, L. Mascia. Plasticizing and reinforcing features of siloxane domains in amine-cured epoxy/silica hybrids. Macromol. Mater. Eng. 298 (2013) 896-909
[29] M.S. Heise, G.C. Martin, Curing mechanism and thermal properties of epoxy- imidazole systems. Macromolecules 22 (1989) 99-104.
[30] X. Fernandez-Francos, D. Santiago, F. Ferrando, X. Ramis, J.M. Salla, A. Serra, M. Sangermano, Network structure and thermomechanical properties of hybrid DGEBA networks cured with 1-methylimidazole and hyperbranched poly(ethyleneimine)s. J. Polym. Sci., Part B: Polym. Phys. 50 (21) (2012) 1489-1503.
[31] X. Fernandez-Francos, Theoretical modeling of the effect of proton donors and regeneration reactions in the network build-up of epoxy thermosets using tertiary amines as initiators. Eur. Polym. J. 55 (2014) 35-47.
[32] S. Ponyrko, L. Kobera, J. Brus, L. Matejka, Epoxy-silica hybrids by nonaqueous sol-gel process. Polymer 54 (2013) 6271-6282.
[33] Y. Sun, Z. Zhang, K. Moon, C.P. Wong, Glass transition and relaxation behavior of epoxy nanocomposites. J. Polym. Sci., Part B. Polym. Phys. 42 (2004) 3849-3858.
[34] Y. Ni, S. Zheng, Nanostructured thermosets from epoxy resin and an organic-inorganic amphiphile. Macromolecules 40 (2007) 7009-7018.
[35] M. Sangermano, E. Gaspari, L. Vescovo, M. Messori. Enhancement of scratch-resistance properties of methacrylated UV-cured coatings. Prog. Org. Coat. 72 (2011) 287- 291.
[36] M. Sangermano, M. Messori, Scratch resistance enhancement of polymer coatings. Macromol. Mater. Eng. 295 (2010) 603-612.

UNIVERSITAT ROVIRA I VIRGILI
HYPERBRANCHED POLY(ETHYLENEIMINE) DERIVATIVES AS MODIFIERS IN EPOXY NETWORKS
Cristina Acebo Gorostiza

UNIVERSITAT ROVIRA I VIRGILI
HYPERBRANCHED POLY(ETHYLENEIMINE) DERIVATIVES AS MODIFIERS IN EPOXY NETWORKS
Cristina Acebo Gorostiza

6. The use of modified hyperbranched poly(ethyleneimine) as macromonomer in the preparation of thermosets by a two-stage click-chemistry process

UNIVERSITAT ROVIRA I VIRGILI
HYPERBRANCHED POLY(ETHYLENEIMINE) DERIVATIVES AS MODIFIERS IN EPOXY NETWORKS
Cristina Acebo Gorostiza

6.1 Introduction

"Click Chemistry" is a term that was introduced by K. B. Sharpless and co-workers in 2001 to describe reactions that are high yielding, wide in scope, stereospecific, simple to perform and can be conducted in easily removable or benign solvents.[1] Sharpless defined click chemistry early on as the generation of complex substances by bringing together smaller units via heteroatoms. This chemistry is not limited to a specific type of reaction and the most commonly used click reactions that have been adapted to fulfill the above criteria are: a) pericyclic reactions commonly Huisgen type [3+2] cycloadditions and diels–Alder reaction,[2,3] b) ring-opening of strained molecules such as epoxides, aziridines, and aziridiniumions,[4] c) non-aldol carbonyl chemistry (involving amines, oximes and hydrazones),[5] d) addition reactions especially thiol-ene/yne chemistry, and Michael additions (**Scheme 6.1)**.[6] Nowadays, the characteristics of click reactions include a) high yields, b) regiospecificity and stereospecificity, c) insensitivity to oxygen or water, d) mild, solventless (or aqueous) reaction conditions, e) orthogonality with other common organic synthesis reactions, and f) amenability to a wide variety of readily available starting compounds.[7,8]

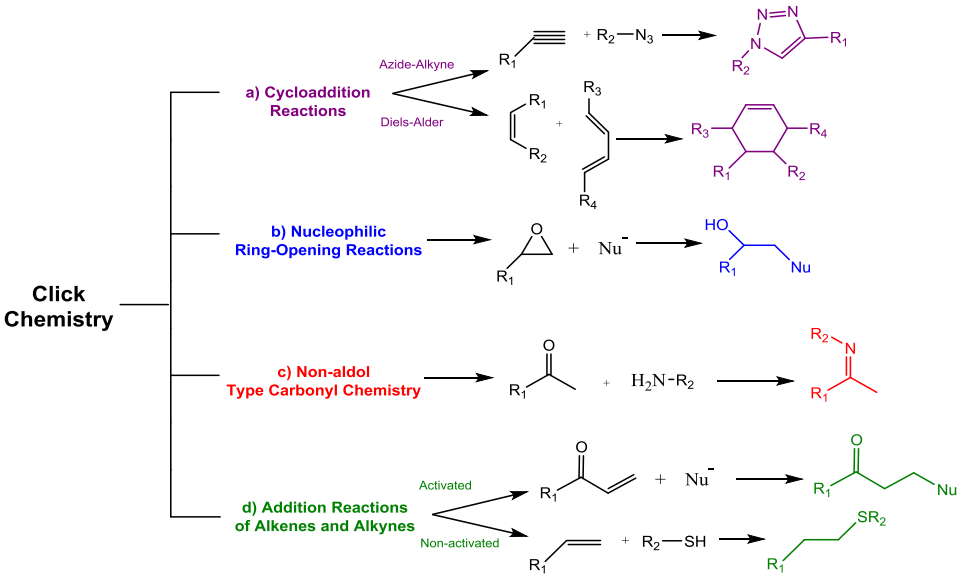

Scheme 6.1 Selection of click reactions

Since the foundation of click chemistry, there has been an explosive growth in publications of this practical and sensible chemical approach and over the years, the

[1] H. C. Kolb, M. G. Finn, K. B. Sharpless, *Angewandte Chemie International Edition*, **2001**, *40*, 2004-2021.
[2] G. Franc, A. K. Kakkar, *Chemistry A European Journal*, **2009**, *15*, 5630-5639.
[3] B. Voit, *New Journal of Chemistry*, **2007**, *31*, 1139-1151.
[4] G. Kumaraswamy, K. Ankamma, A. Pitchaiah, *The Journal of Organic Chemistry*, **2007**, *72*, 9822–9825.
[5] K. L. Heredia, Z. P, Tolstyka, H. D. Maynard, *Macromolecules*, **2007**, *40*, 4772-4779.
[6] C. E. Hoyle, A. B. Lowe, C. N. Bowman, *Chemical Society Reviews*, **2010**, *39*, 1355-1387.
[7] M. A. Tasdelena, B. Kiskanb, Y. Yagci, *Progress in Polymer Science*, **2016**, *52*, 19-78.
[8] C.-H. Wong, S. C. Zimmerman, *Chemical Communications*, **2013**, *49*, 1679-1695.

developments in the area of click chemistry have been considerable. As a consequence of its simplicity, this chemistry has a significant impact in applications such as bioconjugation,[9] materials science[10] and drug systems.[11]

Click chemistry provides powerful and versatile tools for materials synthesis owing to its simplicity, selectivity, efficiency, and tolerance of various functional groups. Consequently, a wide range of controlled-architecture materials have been synthesized through various click reactions, including block copolymers, micelles, dendrimers, gels and networks.[12,13]

In materials science, the aim is to achieve performance and a set of desired characteristics in the final material and/or device in as simple and effective manner as possible. These performances include specifications on mechanical and physical behavior as well as chemical characteristics. This is related with the goal of click chemistry wherein it argues that the focus of chemical process selection should be directed towards the identification, optimization, and simplification of an overall process.[1] For this reason, click chemistry is used in materials development as an effective tool to modify polymers or materials with a variety of functional components and to prepare polymer networks.[14-16] Moreover, by different click methodologies stimuli-responsive materials have been synthesized[17] and nanoscale materials have been prepared due to its efficiency and selectivity.[18]

In this chapter, we will introduce some of these click reactions used in our studies in the preparation of new materials. These reactions are the Huisgen cycloaddition, the Michael addition and the reaction of thiols with non-activated unsaturated compounds and with highly strained heterocycles (thiol-yne/thiol-ene/thiol-epoxy reaction) and will be explained in detail in the following sections.

6.1.1 Huisgen cycloaddition

To date, the most popular click reaction that has been adapted to fulfill these criteria is the 1,3-dipolar cycloaddition, also known as Huisgen cycloaddition, between an azide and a terminal alkyne affording the 1,2,3-triazole moiety (Scheme 6.1).[19] The potential of this reaction is very high, since alkyne and azide components can be incorporated into a wide range of substrates.[20] For more than 40 years, this reaction suffered from a lack of selectivity yielding a mixture of the 1,4- and the 1,5-regioisomers (**Scheme 6.2 a**).[19] In 2002, it was reported that copper (I) salts were able to accelerate this reaction by up to 10

[9] J.-F. Lutz, H. G. Börner, K. Weichenhan, *Macromolecules*, **2006**, *39*, 6376-6383.
[10] R. K. Iha, K. L. Wooley, A. M. Nyström, D. J. Burke, M. J. Kade, C. J. Hawker, *Chemical Reviews*, **2009**, *109*, 5620-5686.
[11] H. C. Kolb, K. B. Sharpless, *Drug Discovery Today*, **2003**, *8*, 1128-1137.
[12] W. Xi, T. F. Scott, C. J. Kloxin, C. N. Bowman, *Advanced Functional Materials*, **2014**, *24*, 2572-2590.
[13] P. Thirumurugan, D. Matosiuk, K. Jozwiak, *Chemical Reviews*, **2013**, *113*, 4905-4979.
[14] G. J. Chen, L. Tao, G. Mantovani, V. Ladmiral, D. P. Burt, J. V. Macpherson, D. M. Haddleton, *Soft Matter,* **2007**, *3*, 732-739.
[15] I. Nischang, O. Brueggemann, I. Teasdale, *Angewandte Chemie International Edition,* **2011**, *50*, 4592-4596.
[16] C. A. De Forest, K. S. Anseth, *Nature Chemistry,* **2011**, *3*, 925-931.
[17] Q. Zhang, Z. J. Ning, Y. L. Yan, S. X. Qian, H. Tian, *Macromolecular Rapid Communications*, **2008**, *29*, 193-201.
[18] H. M. Li, F. O. Cheng, A. M. Duft, A. Adronov, *Journal of the American Chemical Society*, **2005**, *127*, 14518-14524.
[19] R. Huisgen, S. Guenter, M. Leander, *Chemische Berichte*, **1967**, *100*, 2494-2507.
[20] L. Liang, D. Astruc, *Coordination Chemistry Reviews*, **2011**, *255*, 2933-2945.

million times.[21,22] More importantly, at room temperature or with only moderate heating, the copper catalyst directs the formation of only one of the two regioisomers, namely the 1,4-regioisomer (**Scheme 6.2 b**). Nowadays, this reaction is known as a CuI-catalyzed azide/alkyne cycloaddition (CuAAC).

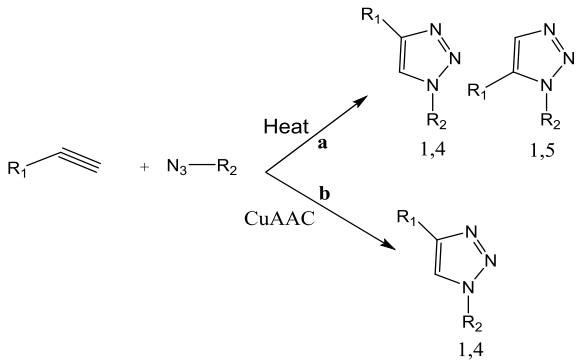

Scheme 6.2 1,3-Dipolar cycloaddition between azides and alkynes, a) un-catalyzed and b) Cu(I) catalyzed

Usually, the reaction is catalyzed by the reduction of Cu (II) salts using ascorbic acid or/and sodium ascorbate as a reducing agent, but Cu(I) species that are either added directly as cuprous salts can also be used.[21]

The application of the CuAAC reaction is very broad and the expansion of this chemistry is considerable.[23] The CuAAC in the polymer field have been extensively used and may be divided into two categories: the use for derivatization and functionalization of linear and branched polymers and the preparation of polymers based on triazole formation.

The functionalization of polymers with triazole groups has been quite popular. As an example, when performing atom transfer radical polymerization, the terminal of the polymer is a good leaving group, e.g. Br, which can easily be substituted with azide. The azide terminated polymers have been used to add functionality to polymers by CuAAC.[18,24] The peripheral functionalization or “decoration” of dendritic polymers by this click reaction is extremely useful for applications to many fields. It allows the molecule to carry a large number of molecular fragments of interest for their physical, catalytic or biomedical properties.[25]

Polymerization by CuAAC to prepare dendrimer-based drug delivery systems[26] and bioconjugation of dendrimers using click chemistry[27] is a very promising reaction since triazole bridge is considered to be biologically stable.[28] The potential given by the

[21] V. V. Rostovtsev, L.G. Green, V.V. Fokin, K.B. Sharpless, *Angewandte Chemie International Edition*, **2002**, *41*, 2596-2599.
[22] C. W. Tornøe, C. Christensen, M. Meldal, *The Journal of Organic Chemistry*, **2002**, *67*, 3057-3064.
[23] M. Meldal, C. W. Tornøe, *Chemical Reviews*, **2008,** *108,* 2952-3015.
[24] J. F. Lutz, H.G. Börner, K. Weichenhan, *Macromolecules* **2006**, *39*, 6376-6383.
[25] D. Astruc, E. Boisselier, C. Ornelas, *Chemical Reviews*, **2010**, *110*, 1857-1959.
[26] C. Ornelas, J. Ruiz, E. Cloutet, S. Alves, D. Astruc, *Angewandte Chemie International Edition*, **2007**, *46*, 872-877.
[27] H. R. Marsden, A. Kros, *Macromolecular Bioscience*, **2009**, *9*, 939-951.
[28] P. Wu, V.V. Fokin, *Aldrichimica Acta*, **2007**, *40*, 7-17.

combination of click chemistry and dendritic structures allows to build up dendrons of different generations by a convergent and a divergent approach (**Scheme 6.3**).[29]

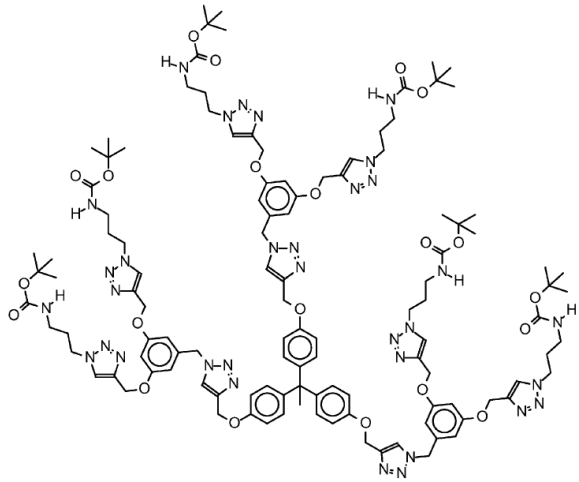

Scheme 6.3 End-functionalized poly(triazole) dendrimer prepared by click chemistry

Furthermore, three-dimensional polymer networks were produced by polymerization of mixtures of small bis-azide and tris- and quad-alkyne monomers.[30,31] Additionally, polymerization through triazole linkages have been reported. Thermosetting materials can be prepared by anionic homopolymerization due to the catalytic effect of the triazole groups in the ring opening polymerization of epoxy groups (**Scheme 6.4**).[32,33]

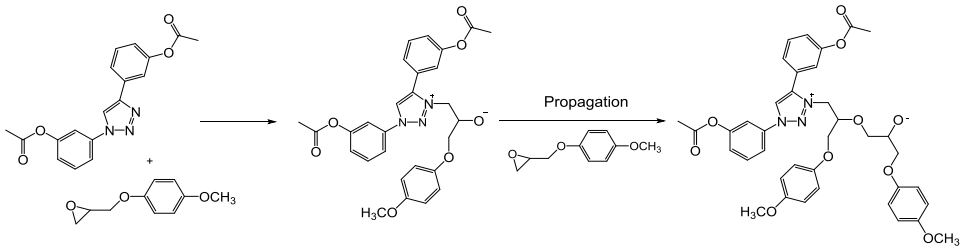

Scheme 6.4 Reaction between triazole moieties and epoxide groups

Taking into account the last application, in the present thesis the use of triazole moieties as anionic initiator in the homopolymerization of diglycidyl ether of bisphenol A has been proposed. For this study a modification of hyperbranched poly(ehyleneimine) (PEI) with

[29] P. Wu, A. K. Feldman, A. K. Nugent, C. J. Hawker, A. Scheel, B. Voit, J. Pyun, J. M. J. Fréchet, K. B. Sharpless, V. V. Fokin, *Angewandte Chemie International Edition*, **2004**, *43*, 3928-3932.
[30] D. D. Díaz, S. Punna, P. Holzer, A. K. Mcpherson, K. B. Sharpless, V. V. Fokin, M. G. Finn, *Journal of Polymer Science, Part A: Polymer Chemistry,* **2004**, *42*, 4392-4403.
[31] N. L. Baut, D. D. Díaz, S. Punna, M. G. Finn, H. R. Brown, *Polymer*, **2007**, *48*, 239-244.
[32] B-Y. Ryu, T. Emrick, *Macromolecules*, **2011**, *44*, 5693-5700.
[33] M. Ghaemy, S. Shabzendedar, M. Taghavi. *Chinese Journal of Polymer Science*, **2015**, *33*, 301-317.

azide and alkyne moieties has been done for the preparation of a triazole macromonomer that is used as a multifunctional crosslinking agent.

The preparation of azides from primary aliphatic amines via diazotransfer reaction with triflyl azide (TfN_3) as a diazo donor it was reported (**Scheme 6.5**).[34] This procedure requires the previous preparation of the triflyl azide using triflic anhydride and sodium azide (NaN_3). By this synthetic pathway, the modification of the primary amino groups of commercially available PEI (Lupasol® FG, 800 g/mol) was tried to prepare multifunctional azide macromonomer. From the degree of polymerization of PEI, the proportion of NH_2/NH/N and the equivalent number of primary amines by molecule we calculated the number of reactive groups capable of being modified (NH_2), which resulted to be in average 8 per PEI molecule. From this number it could be possible to know the number of equivalents of the triflyl azide needed for the conversion of amino groups into azide.

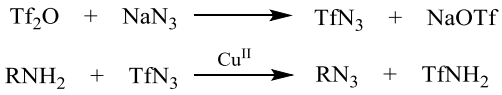

Scheme 6.5 Diazotransfer reaction between azide and amines

It should be said that by this procedure it was not possible to prepare the azide-terminated PEI. In the presence of water, triflic anhydride hydrolyzes and this can be the reason for which the reaction did not proceed since the PEI structure has a high hydrophilic character.

This unsuccessful result led us to undertake the modification of PEI with alkyne moieties for the preparation of triazole macromonomer by the CuAAc methodology. The propargyl groups were introduced as end groups in the PEI structure by two different methodologies. Once obtained the modified PEI, the condensation with a simple alkyl azide was performed in the presence of the Cu catalyst.

6.1.2 Michael addition

Michael addition reactions, which are also commonly termed conjugate additions, are widely used in polymer synthesis for tailored macromolecular architectures due to their click nature. In biological applications such as protein derivatization the mild Michael addition reaction conditions are favorable since high temperatures, oxidizing radicals, and organic solvents are not feasible.[35] Furthermore, the Michael addition has been used for the synthesis of crosslinked polymers such as hydrogels, thermoset resins and coatings, where rapid cure and high conversions are necessary for performance.[36,37]

Michael addition is an easy reaction between nucleophiles (Michael donors) and activated electrophiles (Michael acceptors), usually *α,β*-unsaturated carbonylic compounds, in which the nucleophile adds across a carbon–carbon multiple bond (**Scheme 6.6**). Although, the Michael addition is generally considered the addition of enolate nucleophiles to activated olefins, a wide range of functional groups such as amines, thiols, and phosphines possess sufficient nucleophilicity to perform as Michael donors. As

[34] R.-B. Yan, F. Yang, Y. Wu, L.-H. Zhang, X.-S. Ye, *Tetrahedron Letters*, **2005**, *46*, 8993-8995.
[35] D. L. Elbert, A.B. Pratt, M.P. Lutolf, S. Halstenberg, J.A. Hubbell, *Journal of Controlled Release*, **2001**, 76, 11-25.
[36] B. D. Mather, K. Viswanathan, K. M. Miller, T. E. Longa, *Progress in Polymer Science*, **2006**, *31*, 487-531.
[37] G. González, X. Fernández-Francos, A. Serra, M. Sangermano, X. Ramis, *Polymer Chemistry*, **2015**, *6*, 6987-6997.

an example, when the nucleophile is a basic nitrogen compound the reaction is named as an aza-Michael addition.

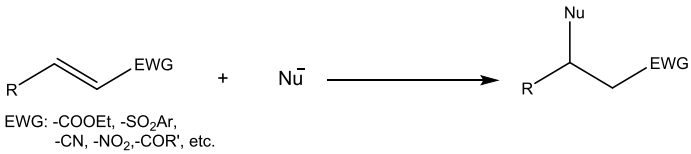

Scheme 6.6 Michael addition reaction

Aza-Michael addition is an excellent way of forming C–N bonds and is of tremendous significance in asymmetric synthesis.[38,39] In our group, aza-Michael reactions were used to prepare thermosetting polymers based in amino-acrylate systems.[37] In the present thesis, this reaction was used to introduce alkyne moieties at the end groups in the PEI structure by reaction of propargyl acrylate and the commercially available PEI. Then the propargyl-ended hyperbranched poly(ethyleneimine) was used as a alkyne macromoner in the CuAAc reaction for the preparation of the triazole macroinitiator.

6.1.3 Thiol chemistry

Among all the click reactions, thiol chemistry has attracted a great deal of attention due to its efficiency and versatility.[40] The reactivity of the thiol gives rise to an advantage of the thiol-click reactions in that they proceed, under appropriate conditions, more rapidly than many other click processes in some cases, with reaction times necessary to achieve high conversions less than 1–10 seconds.

Thiol chemistry can be divided into two categories: the base-catalyzed nucleophilic reactions associated with the thiol–epoxy, thiol–isocyanate and thiol Michael addition reactions and radical-mediated reactions related to the thiol–ene and thiol–yne reactions (**Scheme 6.7**).[41]

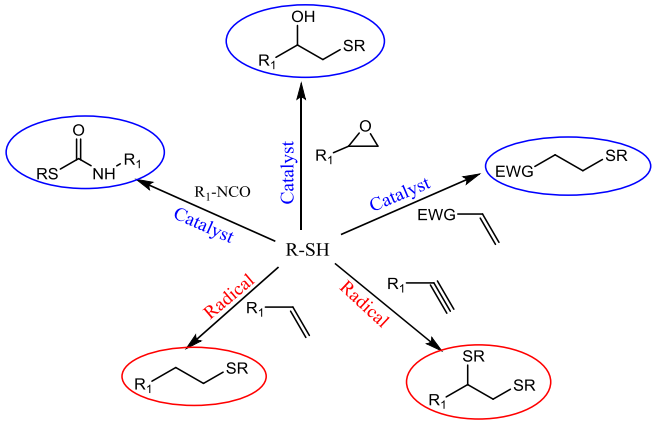

Scheme 6.7 Different thiol-click reactions

[38] P. R. Krishna, A. Sreeshailam, R. Srinivas, *Tetrahedron*, **2009**, *65*, 9657-9672.
[39] D. Enders, C. Wang, J. X. Liebich, *Chemistry-A European Journal*, **2009**, *15*, 11058-11076.
[40] C. E. Hoyle, A. B. Lowe, C. N. Bowman, *Journal of Materials Chemistry C*, **2013**, *1*, 4481-4489.
[41] C. E. Hoyle, A. B. Lowe, C. N. Bowman, *Chemical Society Reviews*, **2010**, *39*, 1355-1387.

In this study, the focus was to use the thiol-epoxy reaction as a nucleophilic thiol chemistry and both thiol-ene and thiol-yne radical reactions in the preparation of thermosets by new methodologies.

Thiol-epoxy reaction

The thiol–epoxide reaction has been implemented in many important biosynthetic and biomedical applications.[42] In addition, the ring-opening reaction involving thiols and epoxides is industrially important and involved in the formation of adhesives, high performance coatings and composites.[43]

The basic thiol–epoxy reaction mechanism is a simple nucleophilic ring-opening reaction by the thiolate anion followed by protonation of the alkoxide anion via the quaternary ammonium (**Scheme 6.8 a**) originally formed via reaction of the base catalyst and thiol to generate the initial thiolate or by proton exchange between the formed alkoxide and another thiol (**Scheme 6.8 b**). This mechanism was proposed to describe the curing of thiol-epoxy systems catalyzed by bases.[44]

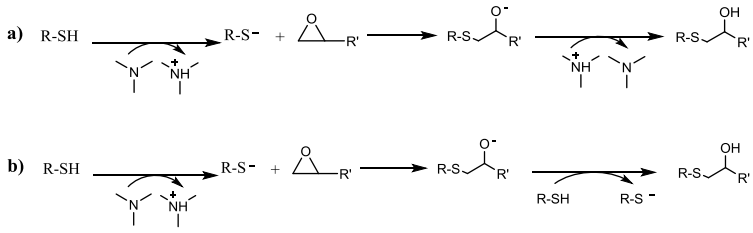

Scheme 6.8 Catalyzed thiol-epoxy ring opening polymerization

However, the low basicity of some tertiary amines that can be used as catalyst for the thiol–epoxy reaction makes the proton exchange leading to the formation of a thiolate anion highly unlikely. An alternative reaction mechanism was recently proposed to model successfully the thiol–epoxy curing catalyzed by a moderately basic tertiary amine.[45] First of all, there is a nucleophilic attack of the tertiary amine on the epoxy ring, with the assistance of a proton donor such as an alcohol to facilitate ring-opening (**Scheme 6.9 a**), followed by proton exchange between the thiol and the alkoxide to produce the thiolate anion and a hydroxyl ammonium compound. The thiolate anion propagates the reaction by nucleophilic attack on the epoxy ring and the regeneration of the thiolate anion by proton exchange of the formed alkoxide with another thiol (**Scheme 6.9 b**). Usually, this reaction occurs under thermal conditions and the reaction kinetics and the mechanism of the curing process are determined by the base used.

[42] S. De, A. Khan, *Chemical Communications*, **2012**, *48*, 3130-3132.
[43] Y. C. Yuan, M. Z. Rong, M. Q. Zhang, J. Chen, G. C. Yang, X. M. Li, *Macromolecules*, **2008**, *41*, 5197-5202.
[44] K. Jin, W. H. Heath, J. M. Torkelson, *Polymer*, **2015**, *81*, 70-78.
[45] X. Fernández-Francos, A.-O. Konuray, A. Belmonte, S. De la Flor, A. Serra, X. Ramis, *Polymer Chemistry*, **2016**, *7*, 2280-2290.

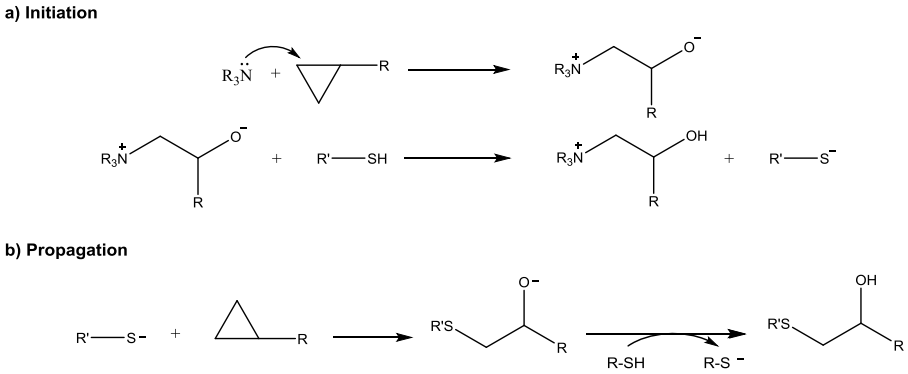

Scheme 6.9 Proposed curing mechanism of thiol-epoxy condensation catalyzed by tertiary amine

Thiol-ene/thiol-yne reactions

Thiol-ene and thiol-yne processes take place by the stoichiometric reaction of alkynes with thiols via a radical step growth mechanism that can be initiated by light, peroxides, thermal initiators or any systems whereby radicals are generated.[46] However, these reactions are commonly initiated photochemically.[47] It should be said that one of the distinct features between thiol-ene and thiol-yne is that in thiol-ene each ene functional group reacts only once with a thiol group whereas in thiol-yne each yne group react twice. The utilization of these thiol reactions ranges from high performance protective polymer networks to processes that are important in the optical, biomedical, sensing, and bioorganic modification fields.[48]

Both reactions are efficient tools for the post-polymerization modification of well-defined reactive precursor (co)polymers[49] and for the construction of complex (macro)molecules, such as poly(thioether) dendrimers (**Scheme 6.10**).[50] Due to their fast reaction kinetics and high yield, thiol-ene and thiol-yne reactions are highly used for the bioconjugation of polymers, for tissue engineering applications, for the production of degradable polymers and for the preparation of high quality soft imprint lithographic stamps, among others.[48]

In the thermosetting field, thiol-ene and thiol-yne step growth processes are widely used since allows to obtain uniform networks with low shrinkage and stress. Moreover, the incorporation of tioether networks permits a higher refractive index than comparable organic networks.[51,52]

[46] C. E. Hoyle, C. N. Bowman, *Angewandte Chemie International Edition*, **2010**, *49*, 1540 -1573.
[47] C. E. Hoyle, T. Y. Lee, T. Roper, *Journal of Polymer Science, Part A: Polymer Chemistry*, **2004**, *42*, 5301-5338.
[48] A. B. Lowe, C. N. Bowman, *Thiol-X Chemistries in Polymer and Material Science*, Croydon, RSC Publishing, **2013**.
[49] J. K. Sprafke, J. M. Spruell, K. M. Mattson, D. Montarnal, A. J. McGrath, R. Pötzsch, D. Miyajima, J. Hu, A. A. Latimer, B. Voit, T. Aida, C. J. Hawker, Journal of Polymer Science, Part A: Polymer Chemistry **2015**, *53*, 319-326.
[50] K. L. Killops, L. M. Campos, C. J. Hawker, *Journal of American Chemical Society*, **2008**, *130*, 5062-5064.
[51] J. W. Chan, Hui Zhou, C. E. Hoyle, A. B. Lowe, *Chemistry of Materials*, **2009**, 21, 1579-1585.
[52] Q. Wei, R. Pötzsch, X. Liu, H. Komber, A. Kiriy, B. Voit, P.-A. Will, S. Lenk, S. Reineke, *Advanced Functional Materials*, **2016**, DOI: 10.1002/adfm.201504914

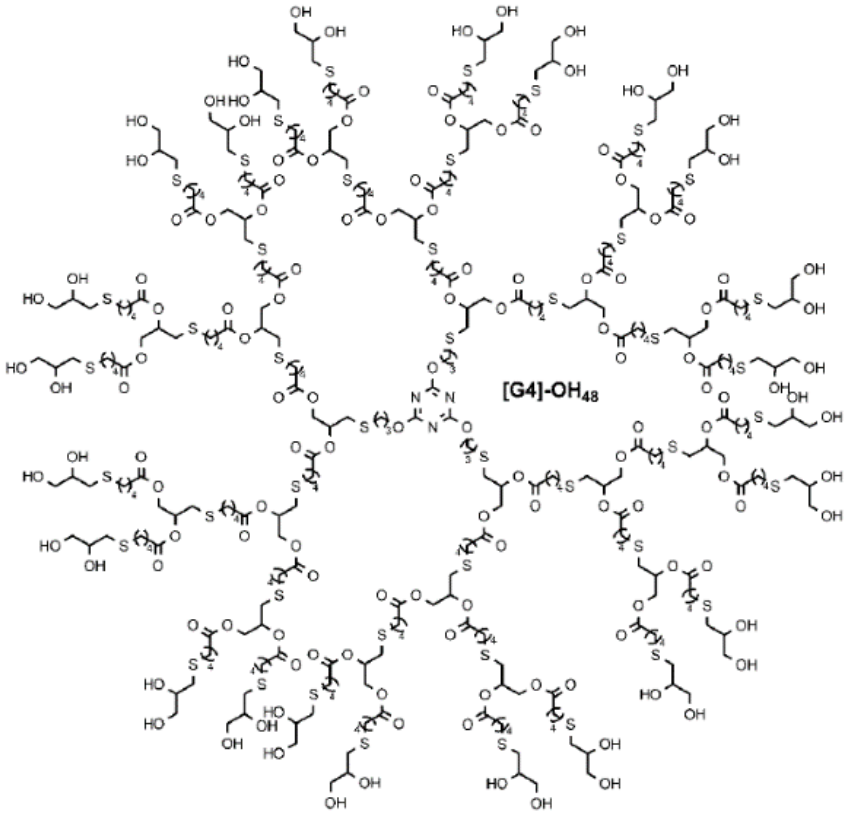

Scheme 6.11 Dendrimer via radical thiol-ene reaction

By thiol-ene and thiol-yne methodologies, polysulfide networks have been prepared.[53,54] However, the materials obtained are limited by their poor mechanical and physical properties due to the flexibility of the thiol monomers. To overcome this disadvantage, several authors combine thiol-ene systems with a network structure derived from thiol-acrylate or thiol-epoxy reaction.[55,56,57] As an alternative, the use of a multifunctional monomer to increase the functionality of the reactive mixture to enhance the thermomechanical characteristics of the final materials has been reported.[58]

Taking into account this new alternative, in this thesis, the preparation of allyl and propargyl terminated hyperbranched poly(ethyleneimine) as multifunctional macromonomers for thiol-ene and thiol-yne polymerizations was carried out. Different materials were obtained by combination of the thiol-ene or thiol-yne networks, obtained by the addition of the HBP synthesized and a tetrathiol, with thiol-epoxy curing systems to tailor the final properties of the thermosets.

[53] N. B. Cramer, J. P. Scott, C. N. Bowman, *Macromolecules*, **2002**, *35*, 5361-5365.
[54] A. B. Lowe, *Polymer*, **2014**, *55*, 5517-5549.
[55] M. Sangermano, I. Roppolo, R. Acosta Ortiz, A. G. Navarro Tovar, A. E. García Valdez, L. Berlanga Duarte. *Progress in Organic Coatings*, **2015**, *78*, 244-248.
[56] J. A. Carioscia, J. W. Stansbury, C. N. Bowman, *Polymer*, **2007**, 48, 1526-1532.
[57] Y. Jian, Y. He, Y. Sun, H. Yang, W. Yang, J. Nie, *Journal of Materials Chemistry C*, **2013**, *1*, 4481-4489.
[58] T. Yoshimura, T. Shimasaki, N. Teramoto, M. Shibata, *European Polymer Journal*, **2015**, *67*, 397-408.

6.1.4 Dual curing systems

Dual curing is a processing methodology based on the combination of two different and compatible polymerization reactions taking place simultaneously or sequentially, in a well-controlled way. Sequential dual-curing processing makes possible to obtain stable materials after the first curing stage that maintain the ability, upon application of a second stimulus, to activate the second curing stage and complete the processing leading to a fully-cured material with the desired final properties.[59]

One goal of click chemistry is the potential of combining multiple click reactions, either performed simultaneously or in tandem, to synthesize complex structures and materials. In recognition of this task, several recent examples of sequential processes involving two thiol reactions, or even more interestingly, thiol-click and alkyne–azide click reactions are considered.[41] An advantage coming from the first combination is that the thiol component can participate in both processes and therefore the networks arising from thiol-ene and thiol-epoxy reactions are covalently interconnected. Another advantage comes from the fact that both thiol-ene and thiol-epoxy reactions are step-wise so that relevant network build-up parameters during both curing stages such as gel point conversion, gel fraction or crosslinking density can be easily calculated using well-established methods.[60] Thus, it is possible to tailor the curing process and the material properties in the intermediate stage and at the end of it in order to fit different processes and material requirements in a flexible way.

Recently, in our group, sequential dual curing systems have been reported using different methodologies. Thermosets by two-stage sequential aza-Michael addition and free-radical polymerization of amine-acrylate systems have been prepared.[37] Furthermore, the strategy of combining two thiol-click reactions has been studied in our group.[45,61] Thermosetting materials have been obtained by combining sequential thiol-ene/thiol-epoxy reactions in which the first stage is a radical thiol-ene reaction initiated by a photoinitiator and the second one is a base-catalyzed thiol-epoxy reaction initiated by a tertiary amine.[61] Since the first process is activated by UV-light and the second one is thermal, the aim of this methodology was to define a dual-curing system with a controlled curing sequence, with no overlapping between both curing reactions, and with sufficient stability in the intermediate stage.

Taking into account this strategy, in this chapter different thermosetting materials have been prepared by combining, firstly thiol-ene or thiol-yne reactions and secondly a thiol-epoxy reaction. The objective is to investigate on the separation or overlapping of both processes in order to obtain sequential dual curing systems for the preparation of these new thermosets.

The work herein presented has been published in the following articles that compose this chapter:

- Synthesis of 1,2,3-triazole ended functionalized hyperbranched poly(ethyleneimine) and its use as multifunctional anionic macroinitiator for DGEBA curing. *European Polymer Journal.* Submitted

[59] D. P. Nair, N. B. Cramer, J. C. Gaipa, M. K. McBride, E. M. Matherly, R. R. McLeod, R. Shandas, C. N. Bowman, *Advanced Functional Materials*, **2012**, 22, 1502-1510.
[60] D. R. Miller, E. M. Valles, C. W. Macosko, *Polymer Engineering & Science*, **1979**, *19*, 272-283.
[61] D. Guzmán, X. Ramis, X. Fernández-Francos, A. Serra, *RSC Advances*, **2015**, *5*, 101623-101633.

- Multifunctional allyl-terminated hyperbranched poly(ethyleneimine) as component of new thiol-ene/thiol-epoxy materials.
  Reactive & Functional Polymers **2016**, *99*, 17-25
- Thiol-yne/thiol-epoxy crosslinked materials based on propargyl modified poly(ethyleneimine) and diglycidylether of bisphenol A resins.
  RSC Advances. Submitted

UNIVERSITAT ROVIRA I VIRGILI
HYPERBRANCHED POLY(ETHYLENEIMINE) DERIVATIVES AS MODIFIERS IN EPOXY NETWORKS
Cristina Acebo Gorostiza

6.2 Synthesis of 1,2,3-triazole functionalized hyperbranched poly(ethyleneimine) and its use as multifunctional anionic macroinitiator for diglycidyl ether of bisphenol A curing

Cristina Acebo, Albena Lederer, Dietmar Appelhans, Xavier Ramis, Àngels Serra

European Polymer Journal. Submitted

UNIVERSITAT ROVIRA I VIRGILI
HYPERBRANCHED POLY(ETHYLENEIMINE) DERIVATIVES AS MODIFIERS IN EPOXY NETWORKS
Cristina Acebo Gorostiza

Synthesis of 1,2,3-triazole functionalized hyperbranched poly(ethyleneimine) and its use as multifunctional anionic macroinitiator for diglycidyl ether of bisphenol A curing

Abstract

Hyperbranched poly(ethyleneimine) (PEI) has been modified by the addition of propargyl acrylate following a Michael addition reaction. On this polymer (PEI-yne) a copper (I)-catalyzed azide alkyne cycloaddition (CuAAC) has been performed to obtain a multifunctional triazole initiator (PEI-TA). After structural and thermal characterization this polymer has been used in different proportions as anionic multifunctional macroinitiator in diglycidyl ether of bisphenol A (DGEBA) homopolymerization. The curing process has been studied by calorimetry and the thermosets obtained have been thermally characterized and compared with thermosets prepared by using 1-methylimidazole (1-MI) as standard initiator. The electron microscopy inspection of the fracture surfaces of the new materials prepared shows the formation of submicrometer particles that should enhance toughness characteristics, changing smooth fracture surfaces in 1-MI initiated materials to multi-planar surface with tortuous and thicker cracks.

Keywords

Epoxy resins; hyperbranched polymer; anionic homopolymerization; click reaction; azide-yne.

Introduction

Epoxy resins are widely used in coatings, adhesives, molding compounds and polymer composites. These materials present good thermomechanical properties and excellent processability. The crosslinked epoxy polymers can be obtained by polycondensation reaction of epoxy monomers with amines, anhydrides or thiols, among others.[1]

Epoxy resins can also be crosslinked by ring-opening homopolymerization. This process requires the presence of an initiator. Among them, tertiary amines as imidazoles are extensively applied in anionic curing mechanisms.[2,3]

Recently, Ryu *et al.*[4] reported the synthesis of diglycidylether of bisphenol-1,2,3-triazoles (DGE-BPTs) and studied their self-catalyzed curing behavior. They found that DGE-BPT could be used alone to form a networked structure due to the catalytic effect of the triazole groups in the molecule. Non-isothermal differential scanning calorimetry analysis (DSC) showed large exotherms between 195 and 250ºC in all samples tested. Following a similar approach, nanocomposites of poly(triazole-ether-imidazole)s with epoxy-functionalized Fe_3O_4 nanoparticles were prepared with a strong interfacial interaction between inorganic particles and the polymer matrix. The presence of triazole and imidazole in the polymer structure led to crosslinked materials with enhanced thermal and mechanical properties.[5] The formation of thermosets by azide-yne reaction has been explored by Diaz et al.[6,7] They reported that high T_gs were obtained while the adhesion to copper substrates was highly enhanced. It was postulated that 1,2,3-triazoles have a good affinity to metallic surfaces and are far more stable than 1,2,4-triazoles to the attack by other chemicals.

Following these precedents, the aim of the present study was the synthesis of a multifunctional crosslinker with 1,2,3-triazole groups in its structure to prepare improved epoxy thermosets by anionic homopolymerization reaction. The multifunctionality of hyperbranched polymers (HBP) with a large amount of terminal groups will bring an advantageous approach to reach improved epoxy thermosets at convenient curing conditions. The use of hyperbranched polymers as multifunctional crosslinking agents has been previously explored by us.[8] An important improvement in mechanical and thermomechanical characteristics by adding these HBP modifiers to epoxy thermosets are also foreseeable from our previous experience with 10-undecenoyl Boltorn modified HBPs or end-capped poly(ε-caprolactone) multiarm stars, among others.[9,10]

1,2,3-Triazoles were firstly prepared by Huisgen 1,3-dipolar cycloadditions.[11] Since then, several synthetic methodologies have been developed.[12-14] Click chemistry affords the [3 + 2] cycloaddition reaction between alkynes and azides leading to the formation of 1,2,3-triazoles moieties. Nowadays, the most used "click" reaction is the Cu^{I}-catalyzed azide/alkyne cycloaddition (CuAAC)[15,16] and a large variety of copper catalysts can be used as the catalyst. Usually, the reaction is performed with a Cu^{II} salt together with a reducing agent (usually sodium ascorbate) or a Cu^{I} compound. CuAAC reaction is fairly general with a broad range of alkynes and azides as starting materials. A wide variety of azides can be synthesized by SN_2 reactions from organic halides or arylsulfonates and sodium azide[17] and propargylic compounds can be easily prepared by different conventional methodologies.

To be used as a multifunctional crosslinking agent, in the present study, we have synthesized and characterized 1,2,3-triazole terminated poly(ethyleneimine) (PEI-TA), by the CuAAC reaction of an azide on propargyl functionalized poly(ethyleneimine) (PEI-yne), previously prepared by Michael addition reaction of commercially available poly(ethyleneimine) (PEI) on propargyl acrylate. In the Michael addition reaction, amines can be added to activated carbon–carbon double bonds under mild conditions.[18]

The catalytic effect of the synthesized PEI-TA in the anionic curing of DGEBA resins has been studied by adding different proportions of this HBP to the formulations by monitoring the curing evolution by DSC. The materials prepared have been characterized by thermogravimetry (TGA), thermomechanical analysis (DMTA) and scanning electron microscopy (SEM) and compared to the conventional DGEBA thermosets obtained by using 1-MI as initiator.

Experimental section

Materials

Hyperbranched poly(ethyleneimine) (PEI) Lupasol G100 (M_w = 5000 g/mol, M_n = 3600 g/mol) was kindly donated by BASF SE (Ludwigshafen, Germany) and used without further purification. From the molecular weight of the polymer and of the repeating unit an average degree of polymerization of 84 was calculated.[19] The equivalent number of primary, secondary and tertiary amines per mol of PEI is 27.2, 31.4 and 25.4, respectively.[19]

1-Methylimidazole (1-MI), 1-bromopentane, methyl acrylate, sodium azide, propargyl acrylate and CuI from Sigma-Aldrich were used without further purification. Solvents were purchased from Scharlab. Diglycidylether of bisphenol A (DGEBA) Araldite GY 240 was kindly provided by Huntsman (EEW = 182 g/eq).

Synthesis of propargyl-terminated hyperbranched poly(ethylenimine) (PEI-yne) (Scheme 1)

In a 100 mL two neck round-bottomed flask provided with magnetic stirrer, addition funnel and argon inlet, 1 g of PEI (Lupasol G100, 0.2 mmol, 11.7 meq of reactive amine, NH and NH_2) and 1.29 g of propargyl acrylate (11.7 mmol) were dissolved in a mixture of MeOH/H_2O (50:1 v/v). The reaction mixture was stirred at 40ºC for one day. The solvents were evaporated and the yellow oil was dried under vacuum during two days.

Tg (by DSC) = -41 ºC

Thermal stability determined by TGA in N_2 atmosphere. $T_{5\%}$= 285 ºC and T_{max}= 378ºC.

Elemental analysis: 50.37 %C, 8.30 %H, 9.60 %N. On basis of this result 92% of modification was calculated, taking into account that both primary and secondary amino groups in PEI react only once.

M_w (g/mol) = 22,100 and M_n (g/mol) = 17,100 both determined by SEC-MALLS in DMAc; M_w/M_n = 1.29; M_w (g/mol) = 10,936 calculated taking into account the modification degree obtained by elemental analysis $M_w = M_w$ PEI + (58.6 x 0.92 x 110.1).

^{1}H-NMR (400 MHz, $CDCl_3$, δ in ppm): 3.7 (-COO-C**H**$_2$-C≡C-), 2.8 (-NH-C**H**$_2$-C**H**$_2$-COO-), 2.7-2.4 (broad signal of PEI methylene protons) and 2.45 (**H**-C≡C) (see **Figure 1**).

^{13}C-NMR (100.6 MHz, DMSO-d_6, δ in ppm): 172.4 (-**C**OO-), 84.1 (-**C**≡CH), 74.7 (-C≡**C**H), 54-50 (broad signal of PEI methylene carbons), 51.1 (-COO-**C**H$_2$-C≡C-), 48.9 (-NH-**C**H$_2$-CH$_2$-COO-) and 32.0 (-NH-CH$_2$-**C**H$_2$-COO-).

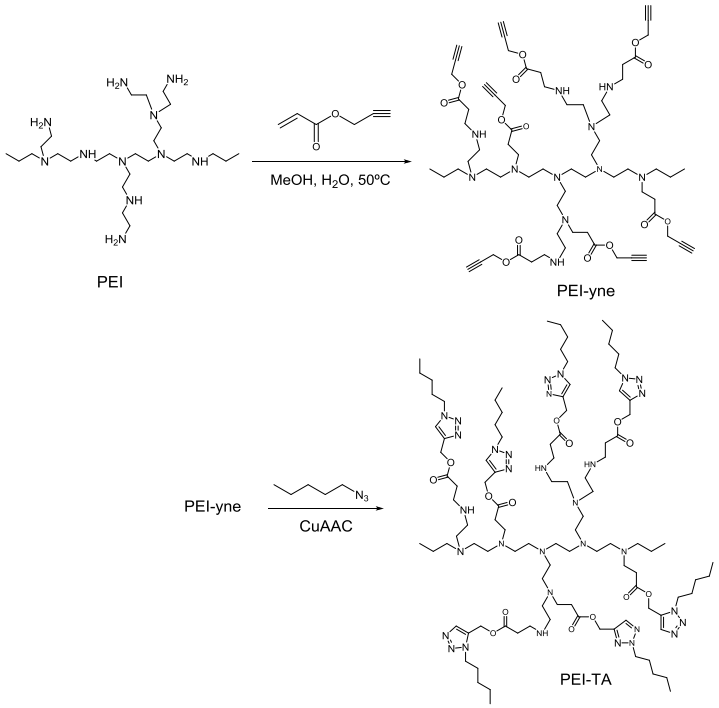

Scheme 1. Synthetic pathway to the preparation of the multifunctional macroinitiator

Synthesis of 1-azide pentane

The organic azide was synthesized from the corresponding bromide.[20] In a 100 mL two neck round-bottomed flask provided with magnetic stirrer and argon inlet, 1-bromopentane (5 g, 33 mmol) was dissolved in 40 mL of DMSO. Sodium azide (2.15 g, 33 mmol) was added in one batch and the solution was stirred overnight at room temperature and then water was added slowly. The product was extracted with diethyl ether, which was then washed with brine, dried over sodium sulfate and the solvent removed producing a clear liquid.

^{1}H-NMR (400 MHz, $CDCl_3$, δ in ppm): 3.09 (-C**H**$_2$-N_3), 1.46 (-C**H**$_2$-CH_2-N_3), 1.15 (-C**H**$_2$-) and 0.76 (C**H**$_3$-).

^{13}C-NMR (100.6 MHz, $CDCl_3$, δ in ppm): 48.2 (-**C**H_2-N3), 30.0-29.4 (-**C**H_2-), 22.4 (CH_3-**C**H_2-) and 14.1 (**C**H_3-).

Synthesis of triazole hyperbranched poly(ethylenimine) (PEI-TA) (Scheme 1)

The click reaction was performed according to a reported procedure.[21] PEI-yne (0.5 g, 0.046 mmol, 2.5 meq) and 1-azide pentane (0.28 g, 2.5 mmol) were dissolved into 10 mL of dry DMF. To the resulting mixture 0.48 g (2.55 mmol) of CuI was added. The mixture was stirred for 24 h under argon atmosphere at room temperature. FT-IR spectroscopy allowed us to confirm that the reaction was completed by the disappearance of the azide stretching peak around 2100 cm^{-1}. Finally, the product was collected after evaporating the solvent as a viscous green liquid (92% of modification, 22% w/w of triazole content).

T_g = -27 ºC (determined by DSC)

Thermal stability determined by TGA in N_2 atmosphere. $T_{5\%}$= 302 ºC; T_{max}= 337 ºC.

^{1}H-NMR (400 MHz, $CDCl_3$, δ in ppm): 7.6 (triazole proton), 4.8 (O-C**H**$_2$-triazole) 4.3 (-C**H**$_2$-N triazole), 3.6 (-NH-C**H**$_2$-C**H**$_2$-COO-), 2.7-2.4 (broad signal of PEI methylene protons), 2.0 (-C**H**$_2$-CH_2-triazole), 1.2 (-C**H**$_2$-) and 0.9 (C**H**$_3$-).

^{13}C-NMR (100.6 MHz, DMSO-d_6, δ in ppm): 172.2 (-**C**OO-), 147.8 (quaternary C of triazole), 122.2 (tertiary carbon of triazole), 54.7 (-COO-**C**H_2-triazole), 54-50 (broad signal of PEI methylene carbons), 51.2 (**C**H_2-N triazole), 49.1 (-NH-**C**H_2-CH_2-COO-), 35.8 (-NH-CH_2-**C**H_2-COO-), 31.9 and 30.8 (-**C**H_2-), 21.5 (**C**H_3-**C**H_2-) and 13.8 (-**C**H_3).

Preparation of epoxy thermosets

Mixtures of DGEBA and PEI-TA or 1-MI were prepared by adding the required amount of the initiator to the epoxy resin and gently heating until it was dissolved and the solution became transparent. The compositions of the formulations studied are summarized in **Table 1.**

Table 1. Notation and compositions of the formulation prepared

Sample	DGEBA (g)	PEI-TA (g)	Triazole (phr)[b]	1-MI (g)	1-MI (phr)[b]	Eq_{epo}/Eq_{ini}[a]
1-MI-5.6	0.5	-	-	0.027	5.6	7.9
1-MI-11.2	0.5	-	-	0.055	11.2	3.9
PEI-TA-2	0.5	0.045	2	-	-	18.6
PEI-TA-5	0.5	0.11	5	-	-	7.9
PEI-TA-10	0.5	0.23	10	-	-	3.9

a. Ratio between equivalents of epoxy to equivalents of initiator (imidazole or triazole units)
b. Parts of initiator by hundred parts of resin in weight

Characterization

^{1}H-NMR (400 MHz) and ^{13}C-NMR (100.6 MHz) measurements were carried out in a Varian Gemini 400 spectrometer. $CDCl_3$ and DMSO-d_6 were used as the solvent. For internal calibration TMS was used as standard.

The determination of the molecular weight of the polymers was performed on an Agilent 1200 pump system (US) equipped with a multi-angle light scattering (MALS) detector (Tristar MiniDawn, Wyatt Technology, DE) and refractive index (RI) detector (Knauer, DE) using LiCl(3g/L)-DMAc as an eluent in a PolarGel-M-column (Polymer Laboratories, UK).

Elemental analysis was performed on a vario MICRO CHNSO and Cl Elemental Analysis (ELEMENTAR Analysensysteme GmbH, DE)

FTIR-680PLUS spectrometer from JASCO with a resolution of 4 cm^{-1} in the absorbance mode, equipped with an attenuated total reflection accessory (ATR) with thermal control and a diamond crystal (Golden Gate heated single-reflection diamond ATR from Specac-Teknokroma).

Raman spectroscopy was performed using the RAMAN Imaging Microscope System alpha300R (WITec GmbH, Ulm, Germany) with a laser wavelength of 532 nm. The laser power was 10 mW and the objective used had a magnification of 20x. The integration time was of 0.5 s for one single spectrum with 500 accumulations. All spectra were smoothed by the Savitzky-Golay method.

Calorimetric analyses were carried out on a Mettler DSC-822e thermal analyzer. Samples of approximately 10 mg were placed in aluminum pans under nitrogen atmosphere. The calorimeter was calibrated using an indium standard (heat flow calibration) and an indium-lead-zinc standard (temperature calibration).

Non-isothermal curing of prepared mixtures was performed from 30 to 400 ºC at heating rate of 10 ºC/min. Isothermal experiments were done to determine the thermal curing treatment required for preparing the materials in the oven.

The glass transition temperatures (T_gs) of the completed cured materials were determined, by means of a second heating scan at 10 ºC/min after the isothermal curing selected, as the temperature of the half-way point of the jump in the heat capacity when the material changed from glassy to the rubbery state under N_2 atmosphere.

Thermogravimetric analyses were carried out in a Mettler TGA-SDTA 851E thermobalance. Samples with an approximate mass of 8 mg were heated from 30 ºC to 800 ºC at 10 ºC/min in N_2 (100 cm^3/min measured in normal conditions).

Dynamic mechanical thermal analyses were carried out with a TA Instruments DMA Q800. The samples were cured isothermally in a mold (5 mm width and 3 mm thick) at 120 ºC for 2 h, 150 ºC for 1 h and 200ºC for 30 min. The samples were carefully polished to ensure constant dimensions in as much as little variations of dimensions lead to erroneous measurements. The samples were analyzed in three-point bending mode with a support span of 10 mm. The viscoelastic properties of the cured materials were determined by means of a temperature ramp at 3 ºC/min from 35 to 250 ºC and with a frequency of 1 Hz.

The cryofracture area of the specimens was metalized with gold and observed with a scanning electron microscope (SEM) Jeol JSM 6400 with a resolution of 3.5 nm.

Results and Discussion

Synthesis and characterization of PEI-yne

Michael addition reaction has been used to build polymers with different topologies, because of its efficiency and selectivity derived from its *click* nature.[22,23]As detailed in the experimental part, the average number of active amines per molecule (27.2 primary and 31.4 secondary amines) in the PEI structure is globally 58.6. To investigate the degree of modification achievable by Michael addition reaction a first study using 85.8 mol of methyl acrylate per mol of PEI was done, since the hyperbranched character and the different reactivity of primary and secondary amines could reduce the expected modification. Once the reaction was finished, we could prove that the consumption of methyl acrylate was not complete, which was an evidence of the lower global functionality of the PEI molecule. It was reported for Michael addition reactions[24] that secondary amines formed by this process were unable to further react with acrylic compounds and therefore they remain unreacted. Taking this into account, it should be considered that both primary and secondary amines act as monofunctional units and the number of acrylate groups attached by the Michael addition process at the PEI structure can be in average a maximum of 58.6 per molecule.

According to the above results, the synthesis of propargyl terminated PEI (PEI-yne) was carried out using propargyl acrylate as a Michael acceptor and commercially available poly(ethyleneimine) (Lupasol G100) as a Michael donor as it is represented in Scheme 1. The reaction was performed at 50ºC overnight in a mixture MeOH/water to compatibilize both reactants, since it is known that water is an efficient promoter.[25]

The presence of the triple bond in the synthesized PEI-yne was confirmed by Raman spectroscopy (absorption at 2125 cm^{-1}) since the low content of alkyne moieties in the PEI structure did not give an adequate signal in the FTIR spectrum.

The structure of the PEI-yne was determined by ^{1}H and ^{13}C-NMR and Raman spectroscopy. In the ^{1}H-NMR spectrum represented in **Figure 1** we can see the presence of the methylene protons (**a** and **b**), appearing as an unresolved signal at ≈ 2.8 ppm in addition to the propargylic methylene (**c**) and methine (**d**) protons at δ = 3.7 and 2.45 ppm, respectively. Acetylenic proton overlaps with signals of the PEI nucleus. The signals in the ^{13}C-NMR spectrum (detailed in the experimental part) also agree with the

ones expected for the modified structure with two significant signals at δ = 84.1 and 74.7 ppm, attributed to the acetylenic carbons.

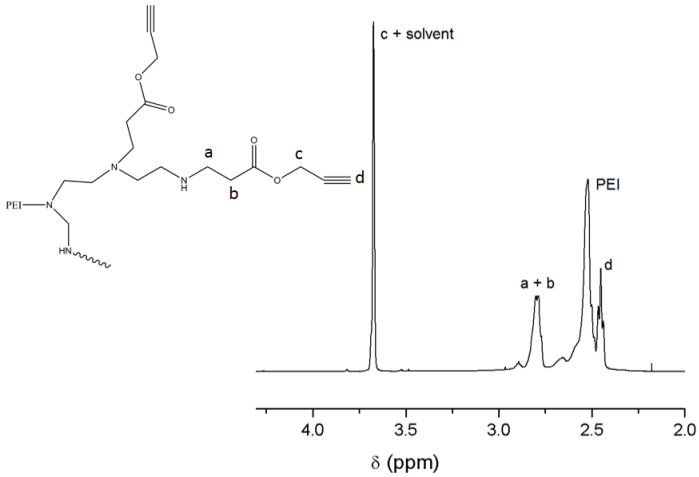

Figure 1. ^{1}H-NMR spectrum of PEI-yne in $CDCl_3$ as the solvent

Although in previous synthetic studies based in PEI structures the degree of modification achieved was calculated by ^{1}H NMR spectroscopy, in the present study it was not accurate enough.[10,26] The higher molecular weight of the starting PEI polymer leads to the broadening of the signals together with the overlapping of the nucleus signals with acetylenic protons. This prevents the calculation of the achieved degree of modification. For this reason, the degree of modification of the PEI was calculated by elemental analysis following a reported procedure and resulted to be 92%.[27] The molecular weight of the PEI-yne synthesized was determined by SEC chromatography using a MALLS detector as detailed in the experimental part.

Synthesis and characterization of PEI-TA

The transformation of acetylenic groups of the previously synthesized PEI-yne to 1,2,3-triazole (PEI-TA) was done by the well-known CuAAC reaction.[12-15] It is reported that polar solvents favor the heterocyclic bond formation step and the solubility of the catalyst.[15] In the case of the CuI as the catalyst the formation of a cluster has been reported.[28] In the present case, PEI-yne was reacted with 1-azide pentane in the presence of CuI in solution of DMF at room temperature in an inert atmosphere. After 24 h, the reaction was stopped since by FTIR measurements the total disappearance of the azide stretching peak at 2100 cm^{-1} was observed (**Figure 2**).[21,29,30]

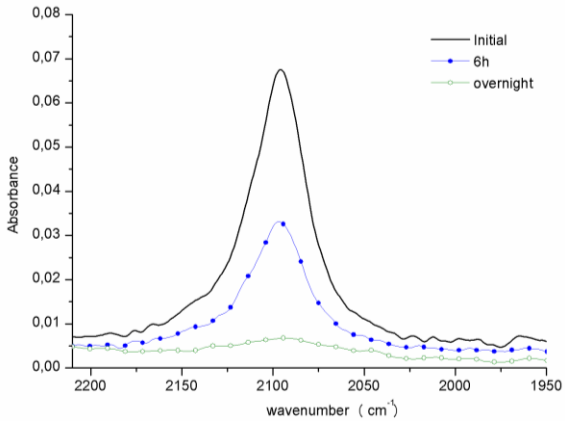

Figure 2. FTIR azide absorptions region taken from the reaction mixture at different reaction times

Since the acetylene group was not detected by FTIR, Raman spectra of the initial azide, PEI-yne and PEI-TA samples were registered. **Figure 3** shows the region of the spectra between 2040 and 2160 cm^{-1} in which the absorption of acetylenic band at 2130 cm^{-1} and of the azide band at 2100 cm^{-1} appear. In the spectrum of PEI-TA both bands are not detected, which confirms that the complete reaction was achieved.

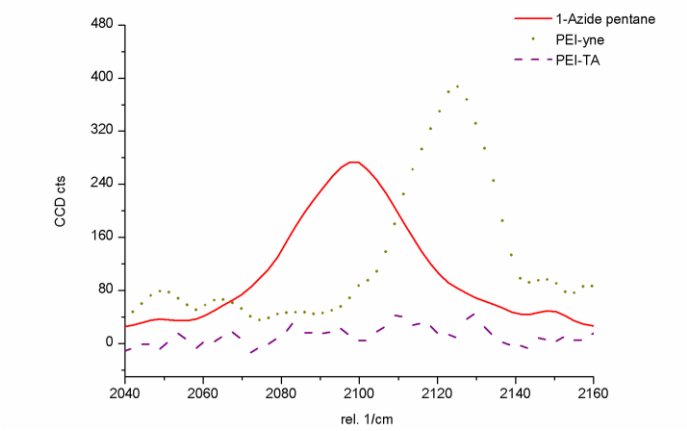

Figure 3. Acetylene and azide absorptions region of the Raman spectra taken for azide, PEI-yne and PEI-TA samples.

The structural characterization of the 1,2,3-triazole containing HBP (PEI-TA) was done by NMR spectroscopy. **Figure 4** presents the ^{1}H-NMR spectrum of this polymer. The most significant signal corresponds to the triazole proton (**d**) appearing at 7.6 ppm. In addition, some signals have been shifted significantly in reference to the starting products. Protons in **c** position are shifted from 3.7 in PEI-yne to 4.8 ppm and protons in **e** position, appearing at 3.09 in the 1-azide pentane shift to 4.3 ppm in the spectrum of this polymer. It should be noted the total absence of the most significant signals of the starting material PEI-yne (Figure 1), which accounts for a complete modification by azide-yne click reaction.

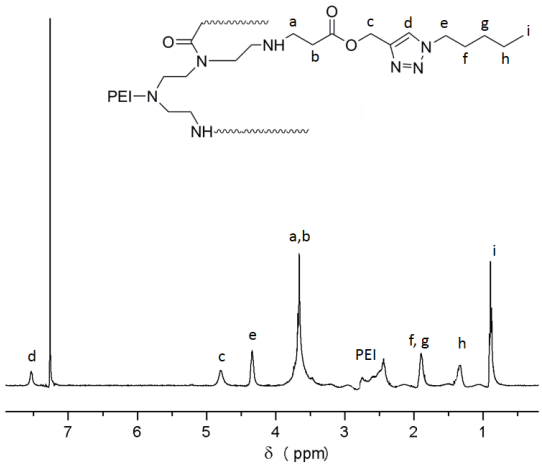

Figure 4. ^{1}H-NMR spectrum of PEI-TA in $CDCl_3$ as the solvent

Study of the curing process

As reported, the nucleophilic character of imidazoles is able to promote anionic homopolymerization of epoxides.[31] In previous studies, 1-MI was used as initiator and 5 phr were needed to complete the cure of DGEBA formulations.[32,33] According to that, we selected this proportion of triazole groups in DGEBA formulations (Table 1) to investigate the initiating ability of the triazole in the PEI-TA structure. A lower and a higher proportion of PEI-TA were also tested to better understand their effect on the kinetics. Table 1 presents the composition of the formulations studied. **Figure 5** shows the non-isothermal DSC curves at 10ºC/min of the formulations containing the different proportions of PEI-TA.

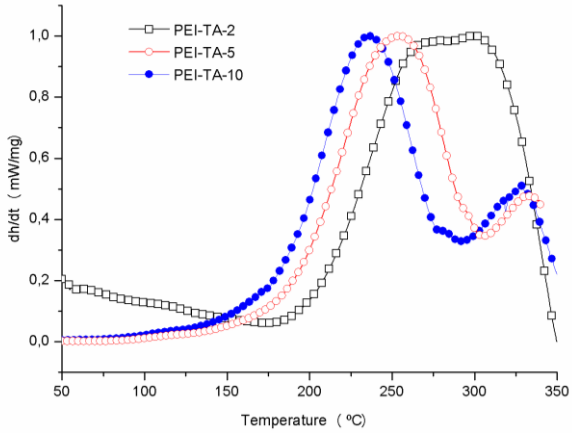

Figure 5. Calorimetric curves registered at 10ºC/min in N_2 atmosphere of the different formulations studied with 2, 5 and 10 phr of triazole groups

The formulation containing 5 phr of triazole groups (PEI-TA-5) presents the maximum of the peak at 250ºC. In previous papers,[32,33] we reported that on using 5 phr of 1-MI the maximum of the peak was at 125ºC. On increasing the proportion of triazole to 10 phr (sample PEI-TA-10) only a slight acceleration was observed and the maximum of the

peak is shifted to 220ºC, higher than the temperature at which the curing takes place using 1-MI. The high viscosity of PEI-TA prevents to increase the proportion of this HBP in the reactive mixture and therefore the highest proportion leading to homogeneous mixtures is 10 phr. In a previous study on self-curable epoxy resins with triazole in their structure,[4] temperatures of the maximum of the exotherm between 200 and 240ºC could be measured. However, in that case 18 phr of triazole groups were present in the reactive formulation. All these results suggest a lower reactivity of triazole, with a lower nucleophilicity than imidazole. This fact can be rationalized on the basis of the lower electronic density of triazole nitrogen than of imidazole. It should also be noticed that in contrast to previously published results,[4] the calorimetric curves are bimodal with a noticeable exotherm above 300ºC (Figure 5). This exotherm could be due to an uncatalyzed thermal homopolymerization of epoxides. The reason could be searched in the topological restrictions to the attack of the nucleophilic species (triazoles) to the oxirane ring. However, a partial degradation of the network structure cannot be discarded, since PEI derivatives are degraded at temperatures about 300ºC.[26] As we can see in Figure 5, reducing the proportion of triazole in the reactive mixture (sample PEI-TA-2) the exotherm at higher temperature is clearly enhanced and the maximum of the first exotherm is shifted to higher temperatures as expected. The growing of the second exotherm on decreasing the proportion of PEI-TA in curing reaction is an indication that thermal homopolymerization of epoxides plays an important role in these curing processes. Taking these results into account, only the samples PEI-TA-5 and 10 were selected to follow up the study.

It should be considered that unreacted secondary amine groups were also present in the PEI-TA structure and they could react with epoxy groups. This reaction was taking place before 150 ºC in a previous study on the reaction of unmodified PEI with DGEBA.[34] From DSC curves it is not clear if this reaction occurs, but in any case it will contribute to the increase in the crosslinking density.

Although it is convenient to determine the enthalpies from the curing exotherms to confirm that a complete conversion of epoxides is achieved, the complex shape of the DSC curves for these formulations prevents an accurate determination of these enthalpies.

Isothermal experiments were carried out to find out the adequate cure schedule to reach materials without any degradation, by looking at the highest T_g value reached. The curing schedule which was selected to prepare the materials for their characterization was the following: 120ºC for 2h, 150ºC for 1h and 200ºC for 30 min.

Characterization of thermosets

The thermomechanical characteristics of the thermosets were determined by DMTA and compared with those of neat thermosetting polymers prepared by using 1-MI as initiator in comparable proportions as shown in Table 1. **Figure 6** shows the variation of tan δ and the storage modulus (E') plots against temperature for all the materials prepared and **Table 2** collects the main data extracted from these analyses.

As it can be observed, the shape of the tan δ curves in the temperature range studied is in all cases unimodal indicating homogeneous characteristics of these materials. It can also be seen that the addition the PEI-TA to the formulation in comparison to 1-MI thermosets decreases the temperatures of the maximum of tan δ and the storage

modulus in the rubbery region in comparison to 1-MI materials, according to the higher flexibility of PEI structure and to the lower content of rigid DGEBA in PEI-TA formulations.

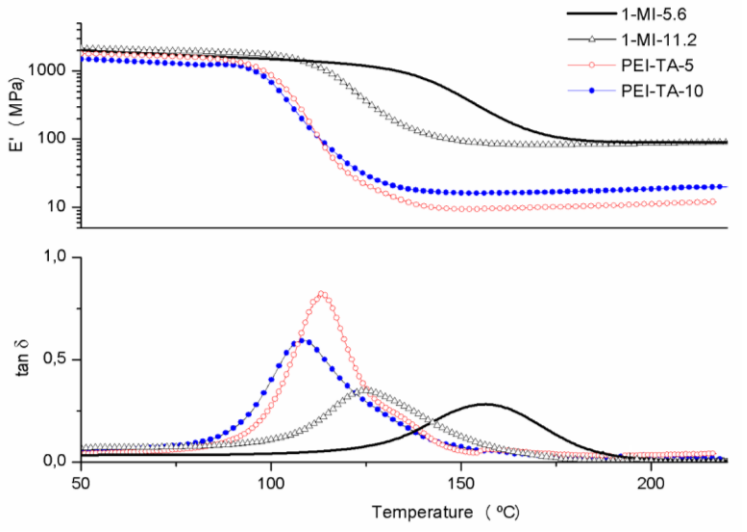

Figure 6. Storage modulus and tan δ evolution against temperature for the materials prepared

On increasing the proportion of PEI-TA in the formulation the tan *δ* temperature shifts to lower values, whereas the storage modulus in the rubbery region slightly increases. A similar behavior was observed in thiol-ene/thiol-epoxy materials obtained from allyl terminated hyperbranched PEI.[26] These effects were rationalized on the basis of the higher flexibility of the PEI structure and the lower amount of rigid aromatic moieties coming from DGEBA that leads to a reduction of the transition temperature (tan *δ*). On the other hand, the small repeating units in the PEI structure lead to a higher number of crosslinking points. Therefore, with increasing the proportion of PEI-TA in the formulation the molecular weight between crosslinks decreases and the storage modulus in the rubbery region increases according to the ideal rubber theory.[35]

Table 2. Thermomechanical and thermogravimetric data for the materials prepared

Formulation	DMTA				TGA	
	$T_{tan\,\delta}$ [a] (˚C)	*FWHM* [b] (˚C)	*Tan δ* [c]	E_r [d] (MPa)	$T_{5\%}$ [e] (˚C)	T_{max} [f] (˚C)
1-MI-5.6	157	39	0.26	80	393	437
1-MI-11.3	125	31	0.35	84	378	437
PEI-TA-5	113	18	0.78	8	320	411
PEI-TA-10	108	30	0.59	16	313	408

[a] Temperature of maximum of tan *δ*
[b] FWHM stands for full width at half maximum
[c] Maximum value of tan *δ*
[d] Storage modulus in the rubbery state determined at tan *δ* peak + 50ºC
[e] Temperature of the onset decomposition on TGA data at 10ºC/min calculated for a 5% weight loss
[f] Temperature of the maximum decomposition rate based on the TGA data at 10ºC/min

It should be noted that the damping characteristics, related to the height of the tan *δ* curves, are much higher for the novel materials prepared than for standard 1-MI materials

in a quite broad range of temperatures, which is valuable from the point of view of toughness enhancement.

The thermal stability of the thermosets has been evaluated by thermogravimetric analysis and compared to the materials obtained with 1-MI as initiator. **Figure 7** shows the degradation curves and the derivatives obtained and the main data are collected in Table 2.

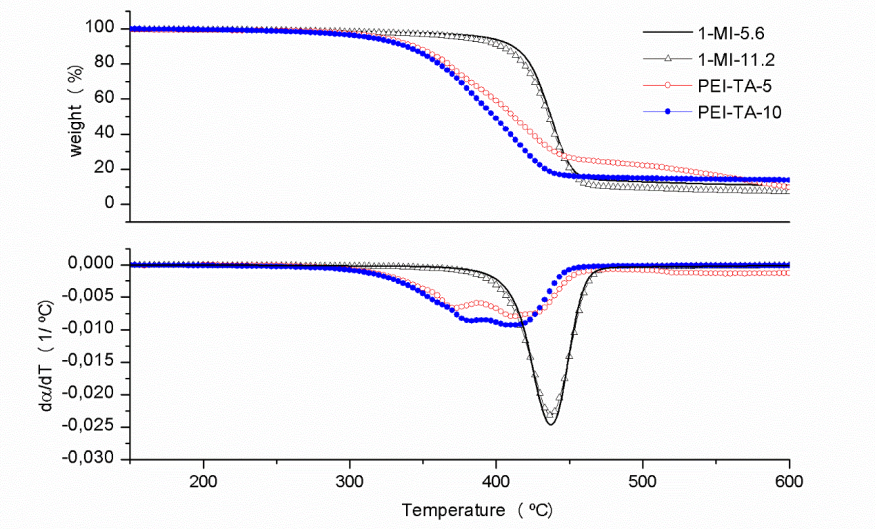

Figure 7. Thermogravimetric curves for the materials prepared

As we can see, the materials prepared by PEI-TA formulations present a lower stability than 1-MI thermosets and the initial degradation occurs about 70 ºC below than the materials obtained with 1-MI. In addition, the degradative process is much complex, as extracted from the complex shape of the degradation curves. The presence of PEI structure in the materials, with a lower stability than homopolymerized DGEBA is responsible for the decrease in the thermal stability and the prompt degradation of the material.[26] From these thermal studies it can be inferred that curing temperatures should be lower than 300ºC and the curves at high temperature in the non-isothermal DSC scans in PEI-TA-5 and PEI-TA-10 formulations are mainly due to degradation.

The morphology of the materials prepared was examined by SEM from cryofractured samples. The type of fracture is related to the toughness and therefore by examining the fracture surface information about this characteristic can be extracted. **Figure 8** collects the micrographs of the fracture surfaces at different magnifications.

Whereas the conventional 1-MI initiated material, Figure 8 (A), shows a smooth and fragile fracture with some cracks with little evidence of deformation which accounts for its poor impact resistance, the fracture surfaces of materials containing PEI-TA (Figure 8 B and C up) show a multi-planar nature with tortuous and thicker cracks resulting from plastic deformation and cavitation upon fracture. At higher magnifications (Figure 8 B and C down) it can be appreciated the formation of rubbery particles of submicrometer sizes. These particles help to improve toughness through deviation of cracks and through cavitation mechanisms, increasing the energy absorbed during fracture. The fact that the PEI structure is covalently linked to the DGEBA matrix by the triazole units, acting as

initiators, can cause this cavitation effect. In previous studies of our group, phase separation and cavitation have demonstrated good toughness improvements in DGEBA thermosets.[9] The formation of the particles observed could be due to the separation of PEI moieties, which in the present study are derived from PEI with molecular weight of 5,000 D, with a more polar character than homopolymerized DGEBA. In previous studies on the preparation of PEI modified thermosets, the molecular weight of the initial PEI was only 800 D and separation was observed only when PEI modifiers were not covalently linked to the epoxy matrix.[10,36]

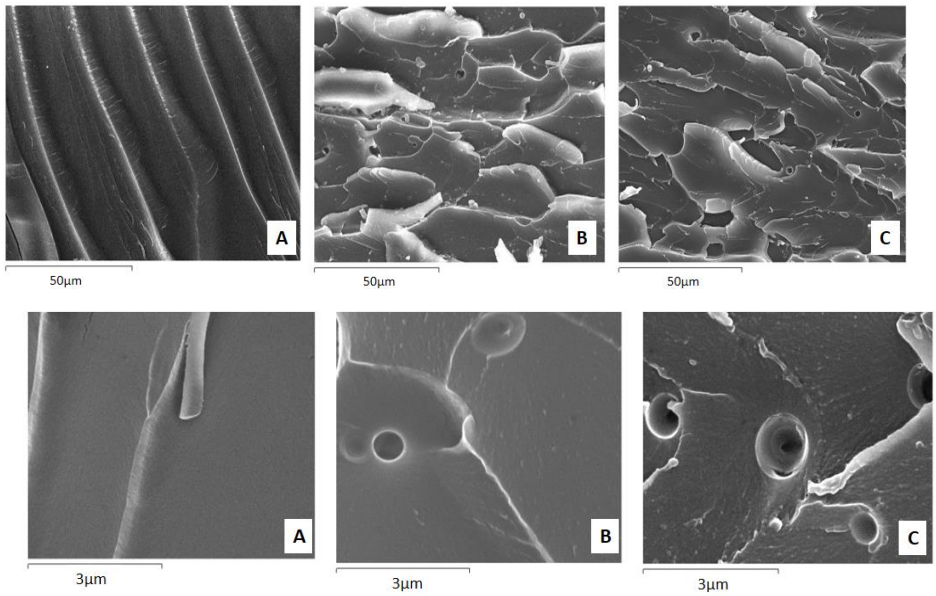

Figure 8. SEM micrographs at 1,000 (up) and 18,000 (down) magnifications of the fracture surfaces of the thermosets obtained from formulations: 1-MI-5.6 (A); PEI-TA-5 (B) and PEI-TA-10 (C)

Conclusions

Michael addition reaction of poly(ethyleneimine) (PEI) to propargyl acrylate was selected to prepare a propargyl modified hyperbranched polymer (PEI-yne), which was reacted with 1-azide pentane following a CuAAC azide-yne click reaction. The structure of the 1,2,3-triazole decorated hyperbranched polymer (PEI-TA) obtained was confirmed by NMR, FTIR and Raman spectroscopy.

PEI-TA was used in different proportions as anionic initiator in the curing of diglycidyl ether of bisphenol A (DGEBA) formulations and calorimetric studies showed a lower reactivity of triazole units in comparison to 1-methylimidazole (1-MI). However, DGEBA/PEI-TA formulations could be cured following an optimized schedule avoiding thermal degradation.

The novel thermosets obtained were thermally characterized and compared to thermosets obtained by using 1-MI as standard anionic initiator. The thermal stability of the novel materials was lower due to the presence of PEI structures that degrades at temperatures about 300ºC. Tan δ and storage modulus are lower than 1-MI materials, but the damping characteristics are better. On increasing the proportion of PEI-TA in the

formulation the tan δ decreases due to the flexibility introduced in the network structure by PEI moieties and the reduction of aromatic DGEBA structures.

SEM inspection of the cryofracture surfaces shows the formation of submicron particles in the PEI-TA modified thermosets that leads to a tough fracture with tortuous and thick cracks and presence of cavitation, which should enhance toughness in comparison to the one of the thermosets initiated by 1-MI.

References

[1] May C.A., Epoxy Resins Chemistry and Technology, 2nd edition. Marcel Dekker, New York, 1988.
[2] Fernández-Francos X., Salla J.M., Mantecón A., Serra A., Ramis X. Crosslinking of mixture of DGEBA with 1,6-dioxaspiro[4,4]nonan-2,7-dione initiated by tertiary amines. I. Study of the reaction and kinetic analysis. Journal of Applied Polymer Science 2008, 109, 2304-2315.
[3] Liu L., Li M. Curing mechanisms and kinetic analysis of DGEBA cured with a novel imidazole derivative curing agent using DSC techniques, Journal of Applied Polymer Science, 2010, 117, 3220–3227.
[4] Ryu B.-Y., Emrick T. Bisphenol-1,2,3-triazole (BPT) epoxies and cyanate esters: synthesis and self-catalyzed curing. Macromolecules, 2011, 44, 5693-5700.
[5] Ghaemy M., Shabzendedar S., Taghavi M. Synthesis and characterization of heterocyclic functionalized polymers by click reaction: preparation of magnetic nanocomposites and studies on their thermal, mechanical, photophysical and metal ions removal properties, Chinese Journal of Polymer Science, 2015, 33, 301-317.
[6] Le Baut N., Díaz D.D., Punna S., Finn M.G., Brown H.R. Study of high glass transition temperature thermosets made from the copper(I)-catalyzed azide-alkyne cycloaddition reaction. Polymer 2007, 48, 239-244.
[7] Díaz D.D., Punna S., Holzer P., Mcpherson A.K., Sharpless K.B., Fokin V.V., Finn M.G. Click chemistry in materials synthesis. 1. Adhesive polymers from copper-catalyzed azide-alkyne cycloaddition. Journal of Polymer Science: Part A: Polymer Chemistry 2004, 42, 4392–4403.
[8] Foix D., Jiménez-Piqué E., Ramis X., Serra A., DGEBA thermosets modified with an amphiphilic star polymer. Study on the effect of the initiator on the curing process and morphology, Polymer, 52, 2011, 5009-5017.
[9] Flores M., Fernández-Francos X., Ferrando F., Ramis X., Serra A. Efficient impact resistance improvement of epoxy/anhydride thermosets by adding hyperbranched polyesters partially modified with undecenoyl chains. Polymer 2012, 53, 5232-5241.
[10] Acebo C., Picardi A., Fernández-Francos X., De la Flor S., Ramis X., Serra A. Effect of hydroxyl ended and end-capped multiarm star polymers on the curing process and mechanical characteristics of epoxy/anhydride thermosets. Progress in Organic Coatings, 2014, 77, 1288-1298.
[11] Huisgen, R. 1,3 – Dipolar cycloadditions: past and future, Angewandte Chemie, International Edition, 1963, 2, 565-632.
[12] Tornøe C., Christensen C., Meldal M. Peptidotriazoles on solid phase: [1,2,3]-triazoles by regiospecific copper(I)-catalyzed 1,3-dipolar cycloadditions of terminal alkynes to azides, Journal of Organic Chemistry, 2002, 67, 3057–3064.
[13] Rostovtscv V.V., Green L.G., Fokin V.V., Sharpless K.B., A stepwise Huisgen cycloaddition process: copper(I)-catalyzed regioselective “ligation” of azides and terminal alkynes, Angewandte Chemie, International Edition, 2002, 41, 2596-2599.
[14] Katrizky A.R., Singh S.K., Synthesis of *c*-carbamoyl-1,2,3-triazoles by microwave-induced 1,3-dipolar cycloaddition of organic azides to acetylenic amides, Journal of Organic Chemistry, 2002, 67, 9077-9079
[15] Liang L., Astruc D., The copper(I)-catalyzed alkyne-azide cycloaddition (CuAAC) “click” reaction and its applications. An overview. Coordination Chemistry Reviews, 2011, 255, 2933–2945.
[16] Valentin O.R., Fokin V.V., Finn M.G., Mechanism of the ligand-free Cu^{I}-catalyzed azide–alkyne cycloaddition reaction, Angewandte Chemie International Edition, 2005, 44, 2210 – 2215.
[17] Bräse S., Gil C., Kerstin K., Zimmermann V. Organic Azides: An exploding diversity of a unique class of compounds, Angewandte Chemie International Edition, 2005, 44, 5188 – 5240.

[18] Mather B.D., Viswanathan K., Miller K.M., Long T.E., Michael addition reactions in macromolecular design for emerging technologies, Progress in Polymer Science, 2006, 31, 487-531.
[19] Appelhans D., Komber H., Quadir M.A., Richter S., Aigner A., Loos K., Müller M., Seidel J., Arndt K.-F., Haag R., Voit B., Hyperbranched PEI with various oligosaccharide architectures: Synthesis, characterization, ATP complexation and cellular uptake properties, Biomacromolecules, 2009, 10, 1114-1124.
[20] O'Neil E.J., DiVittorio K.M., Smith B.D. Phosphatidylcholine-derived bolaamphiphiles via click chemistry, Organic Letters, 2007, 9, 199-202.
[21] Sykam K., Donempudi S. Novel multifunctional hybrid diallyl ether monomer via azide alkyne click reaction as crosslinking agent in protective coatings, Polymer , 2015, 62, 60-69.
[22] Retailleau M., Ibrahim A., Croutxé-Barghorn C., Allonas X., Ley C., Le Nouen D. One-pot three-step polymerization system using double click Michael addition and radical photopolymerization, ACS Macro Letters, 2015, 4, 1327−1331.
[23] González G., Fernández-Francos X., Serra A., Sangermano M., Ramis X. Environmentally-friendly processing of thermosets by two-stage sequential aza-Michael addition and free-radical polymerization of amine–acrylate mixtures, Polymer Chemistry, 2015, 6, 6987-6997.
[24] Wu D., Liu, Y., He, C., Chung, T., Goh, S. Effects of chemistries of trifunctional amines on mechanisms of michael addition polymerizations with diacrylates, Macromolecules, 2004, 37, 6763-6770.
[25] Ranu B.C., Banerjee S., Significant rate acceleration of the aza-Michael reaction in water, Tetrahedron Letters, 2007, 48, 141-143.
[26] Acebo C., Fernández-Francos X., Ramis X., Serra A., Multifunctional allyl-terminated hyperbranched poly(ethyleneimine) as component of new thiol–ene/thiol–epoxy materials, Reactive and Functional Polymers, 2016, 99, 17-25.
[27] Appelhans D., Komber H., Quadir M.A., Richter S., Aigner A., Loos K., Müller M., Seidel J., Arndt K.-F., Haag R., Voit B. Hyperbranched PEI with various oligosaccharide architectures: Synthesis, characterization, ATP complexation and cellular uptake properties, Biomacromolecules, 2009, 10, 1114-1124.
[28] Meldal M., Tornøe C.W. Cu-Catalyzed Azide-Alkyne Cycloaddition, Chemical Reviews, 2008, 108, 2952-3015.
[29] Crescenzi V., Cornelio L., Di Meo C., Nardecchia S., Lamanna R., Novel hydrogels via click chemistry: synthesis and potential biomedical applications, Biomacromolecules, 2007, 8, 1844-1850.
[30] Li H., Zheng Q., Han C. Click synthesis of podand triazole-linked gold nanoparticles as highly selective and sensitive colorimetric probes for lead(II) ions, Analyst, 2010, 135, 1360–1364.
[31] Fernández-Francos X., Cook W.D., Salla J.M., Serra A., Ramis X., Crosslinking of mixture of DGEBA with 1,6-dioxaspiro[4,4]nonan-2,7-dione initiated by tertiary amines. III. Effect of hydroxyl groups on the network formation. Polymer International 2009, 58, 1401-1410.
[32] Acebo C., Fernández-Francos X., Ferrando F., Serra A., Salla J.M., Ramis X., Multiarm star with poly(ethyleneimine) core and poly (ε-caprolactone) arms as modifiers of diglycidyl ether of bisphenol A thermosets cured by 1-methylimidazole. Reactive and Functional Polymers, 2013, 73, 431-441.
[33] Acebo C., Fernández-Francos X., Ferrando F., Serra A., Ramis X, New epoxy thermosets modified with multiarm star poly(lactides) with poly(ethyleneimine) as core of diferent molecular weight. European Polymer Journal, 2013, 49, 2316-2326.
[34] Santiago D., Fernández-Francos X., Ramis X., Salla J.M., Sangermano M. Comparative curing kinetics and thermal–mechanical properties of DGEBA thermosets cured with a hyperbranched poly(ethyleneimine) and an aliphatic triamine Thermochimica Acta 2011, 526, 9-21.
[35] Sperling L.H. Introduction to Physical Polymer Science, John Wiley & Sons: New York, 2005.
[36] Acebo C., Fernández-Francos X., De la Flor S., Ramis X., Serra A. New anhydride/epoxy thermosets based on diglycidyl ether of bisphenol A and 10-undecenoyl modified poly(ethyleneimine) with improved impact resistance. Progress in Organic Coatings 2015, 85, 52-59.

UNIVERSITAT ROVIRA I VIRGILI
HYPERBRANCHED POLY(ETHYLENEIMINE) DERIVATIVES AS MODIFIERS IN EPOXY NETWORKS
Cristina Acebo Gorostiza

6.3 Multifunctional allyl-terminated hyperbranched poly(ethyleneimine) as component of new thiol-ene/thiol-epoxy materials

Cristina Acebo, Xavier Fernández-Francos, Xavier Ramis, Àngels Serra

Reactive & Functional Polymers **2016**, *99*, 17-25

UNIVERSITAT ROVIRA I VIRGILI
HYPERBRANCHED POLY(ETHYLENEIMINE) DERIVATIVES AS MODIFIERS IN EPOXY NETWORKS
Cristina Acebo Gorostiza

Reactive & Functional Polymers **2016**, *99*, 17-25

Multifunctional allyl-terminated hyperbranched poly(ethyleneimine) as component of new thiol-ene/thiol-epoxy materials

Abstract

A new allyl terminated hyperbranched poly(ethyleneimine) was synthesized and characterized and then used in different proportions as multifunctional macromonomer in tetrathiol-diglycidyl ether of bisphenol A formulations. The curing process had a two-stage character and was composed by two click reactions: a first photoinduced thiol-ene addition followed by a thermal thiol-epoxy reaction. The thiol-ene reaction was catalyzed by a radical initiator and the thiol-epoxy curing by tertiary amines. The evolution of the first part of the curing was studied by photo-DSC and FTIR and the results compared with those obtained in a photoirradiation chamber, which was used to prepare samples for thermomechanical tests. These studies showed that the thermal thiol-epoxy process prematurely began during the photoirradiation because the presence of amines in the PEI structure accelerated this process. The thiol-epoxy reaction was more extensively produced when the proportion of the poly(ethyleneimine) increased in the formulation. The overlapping between both processes was greater in the photoirradiation chamber than in the photo-DSC. The intermediate material was completely cured by thermal treatment in an oven. The need of adding 1-methylimidazole as catalyst to complete the thiol-epoxy reaction was derived from the calorimetric studies. The materials prepared were characterized by thermogravimetry and thermomechanical analysis.

Keywords

Photopolymerization; thiol-epoxy; thiol-ene; dual curing; hyperbranched poly(ethyleneimine).

Introduction

In the last years, thiol chemistry has attracted a great deal of attention due to its efficiency and versatility in numerous thiol reactions commonly regarded as *click* reactions.[1, 2] Thiol click chemistry can be divided in two categories which are the base catalyzed nucleophilic reactions: thiol-epoxy,[3,4] thiol-isocyanate[5,6] and thiol-Michael[7,8] and radical-mediated reactions: thiol-ene[9,10] and thiol-yne.[11,12]

Recently, thiol-ene photoinitiated polymerization has attracted a significant interest due to their features. Firstly, a wide range of -ene compounds, including activated and non-activated double bonds as well as multiply-substituted olefins can serve as the substrates and any thiol can be employed, including highly functional compounds. Secondly, such reactions are generally extremely rapid and can be completed in a matter of seconds, are tolerant to the presence of air/oxygen and moisture and proceed with (near) quantitative formation of the corresponding thioether. Finally, the thiol-ene reaction can be employed in combination with living polymerization such as ring opening polymerization (ROP),[13] ring-opening metathesis polymerization (ROMP),[14] cationic polymerization[15] or controlled radical vinyl polymerization.[16] Besides, thiol-ene processes exhibit reduced polymerization shrinkage and stress and show high uniformity in crosslinking density.[17]

It has been reported that polysulfides derived from thiol-ene polymerization present some limitations in their physical/mechanical properties, particularly those related to modulus and attainment of high glass transition temperature due to the flexible core of the

commercially available thiol monomers.[18,19] Many different strategies for achieving these improvements have been followed in the literature, as for example the incorporation of significant amounts of inorganic fillers, particularly nano-sized inorganic structures[20] and the formation of inorganic domains using a sol–gel process.[21, 22]

Another approach proposed to enhance these mechanical characteristics is the combination of the photo-curable thiol-ene formulation with an epoxy resin that can be polymerized. This approach was followed by several authors. Carioscia *et al.*[23] combine the properties of polyethers derived from epoxy resins with the polysulfides derived from the thiol-ene polymerization. They developed a thiol-ene/thiol-epoxy system by combining an epoxy resin with a multifunctional thiol and an unsaturated compound in the presence of a tertiary amine as a catalyst. It was found that in addition to thiol-ene photopolymerization, anionic polymerization of the epoxy resin proceeded as a side reaction of the thiol-epoxy process. Saharil *et al*.[24] proposed the use of off-stoichiometric thiol-ene-epoxy mixtures in which a rapid curing of thiol-ene occurs to a simultaneously initiated slow thiol-epoxy reaction. On adding epoxy resins to thiol-ene formulations, the ability to directly react with almost any dry surface is gained, and the two-stage curing facilitates bonding, by providing a compliant bond surface after the first stage of cure that is subsequently hardened fully upon the second cure. This curing system was well suited for self-gluing of micropatterned parts for microfluidics[24] and adhesive wafer bonding.[25] Sangermano *et al*.[26] proposed the use of a pentaallylic triamine curing agent which can react with multifunctional thiols to produce polysulfides *in situ*, and at the same time has the ability to initiate the anionic polymerization of an epoxy resin. Combining the network structure derived from the epoxy curing process with a thiol-ene system an important toughening effect was achieved due to the presence of the flexible polysulfide moieties. In that study, the exothermicity of the thiol-ene UV polymerization activates the amine-epoxy polymerization and during the irradiation time (300 s) the epoxy conversion reached 41%.

In the last years, mechanical and thermomechanical characteristics have also been improved by adding hyperbranched polymers to curing formulations because of their high number of end groups able to participate in the network formation. Moreover, such dendritic structures can be considered as toughness modifiers without drawbacks in the processability, because of the low entanglement that leads to the low viscosity of the reactive mixture.[27,28]

Taking all of this into account, the aim of the present work is the preparation of new materials by the combination of thiol-ene and thiol-epoxy reactions, using an allyl modified hyperbranched poly(ethyleneimine) (PEIene) as a multifunctional comonomer.

In previous studies, we applied the thiol-ene reactions to prepare a hyperbranched polymer with thioether and ester groups in its structure which was used in a photo/thermal epoxy cationic homopolymerization.[29] Moreover, a two-stage thiol-ene/epoxy homopolymerization was employed in another study taking advantage of the multifunctionality of allyl terminated hyperbranched polyesters.[30] In both cases, the high functionality of hyperbranched polymers allowed us to reach a glass transition temperature higher than expected due to the tighter network structure.

In the present paper, we describe the synthesis and characterization of the allyl-terminated hyperbranched poly(ethyleneimine) (PEIene) used as a multifunctional ene-macromonomer in the thiol-ene photoinitiated process. Hyperbranched poly(ethyleneimine) has been extensively used after modification, mainly in encapsulation and molecular transport[31,32] but also in the improvement of thermosets.[33,34] The amine

groups in its structure allow attaching different moieties[35] or even grow different polymeric branches.[34] The polymer synthesized, PEIene, was mixed in different proportions with diglycidylether of bisphenol A (DGEBA) and the corresponding stoichiometric proportion of pentaerythritol tetrakis (3-mercaptopropionate) (PETMP) and then cured in a photo/thermal two stage consecutive process. On changing the PEIene/DGEBA proportion the contribution of each polymerization mechanism varies and subsequently the properties of the final materials. The presence of tertiary amine in the PEI-ene structure can catalyze the thiol-epoxy reaction which is the second step of the curing. Due to this fact the curing conditions have been deeply studied by FTIR/DSC-UV and in a photoirradiation chamber to know about the separation or overlapping of both processes. The materials obtained were characterized by TGA and DMTA.

Experimental Part

Materials

Poly(ethyleneimine) (PEI) Lupasol®FG (800 g/mol) was kindly donated by BASF and used without further purification. From the molecular weight of the polymer and of the repeating unit an average degree of polymerization of 18.6 was calculated. According to the data sheet, the relationship (NH_2/NH/N) was (1/0.82/0.53) and thus by calculations the equivalent number of primary, secondary and tertiary amines resulted to be 0.010, 0.00837, and 0.0053 eq/g. Allyl glycidyl ether, pentaerythritol tetrakis (3-mercaptopropionate) (PETMP), 1-methylimidazole (1-MI) and 2,2-dimethoxy-2-phenylacetophenone (DMPA) were all purchased from Sigma-Aldrich. Isopropanol was purchased from Scharlab. Diglycidylether of bisphenol A (DGEBA) Araldite GY 240 (EEW = 182 g/eq) was provided by Huntsman.

Synthesis of allyl-terminated hyperbranched poly(ethylenimine) (PEIene) (Scheme 1)

In a 50 mL two neck round-bottomed flask provided with magnetic stirrer, addition funnel and Ar inlet, 2 g of PEI (2.5 mmol) were dissolved in 10 mL of i-PrOH. Then, the stoichiometric quantity of allyl glycidyl ether (6.63 g, 58.1 mmol) was added. The reaction mixture was kept at 50ºC for a day. The crude product (yellowish oil) was dried at 50ºC under vacuum during two days.

^{1}H-NMR ($CDCl_3$, δ in ppm) (see **Figure 1**): 5.87 ppm (-C**H**=CH_2, **5**), 5.2 (-CH=C**H**$_2$, **6**), 3.98 ppm (-O-C**H**$_2$-CH=, **4**), 3.82 (-C**H**-OH)-, **2**), 3.38 (-CH-OH-C**H**$_2$-O-, **3**) and 2.7-2.4 ppm ((-**C**H_2-N(CH_2)-, **1** and PEI).
^{13}C-NMR ($CDCl_3$, δ in ppm): 134.7 ppm (-**C**H=CH_2), 117.9 ppm (-CH=**C**H_2), 77.5 ppm (-CH(OH)-**C**H_2-O-), -76.8 ppm (-O-**C**H_2-CH=), 72.5 ppm (-**C**H-OH-) and 70-50 ppm (-**C**H_2-N and PEI nucleus).
T_g, determined by DSC = - 55ºC.
Thermal stability, determined by TGA in N_2, $T_{5\%}$= 311ºC, T_{max}= 345ºC.

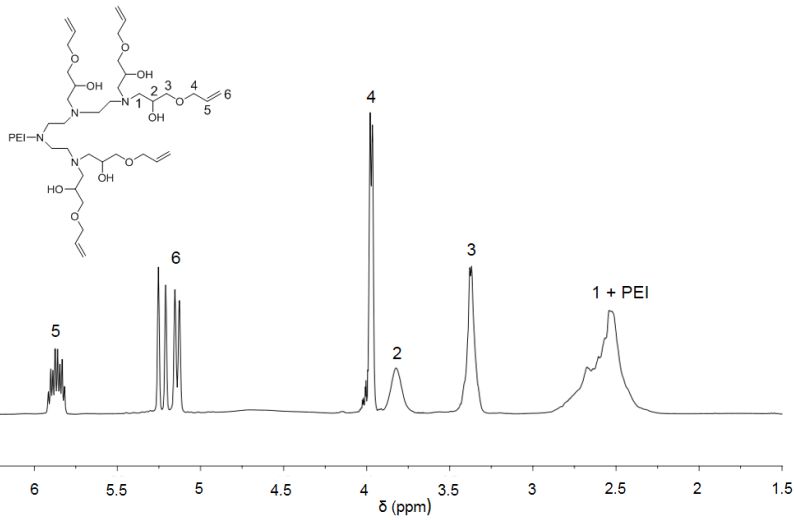

Figure 1. ^{1}H NMR spectrum of allyl-terminated hyperbranched poly (ethyleneimine) in $CDCl_3$

Preparation of formulations and samples

The formulations were prepared by beating at room temperature different amounts of PETMP-PEIene and PETMP-DGEBA stoichiometric mixtures, taking into account that the functionalities of the different reactants are: 4 for PETMP, 2 for DGEBA and 22 for PEIene. Compositions of 20, 40, 60 and 80% w/w of PETMP-PEIene/PETMP-DGEBA, neat PETMP-PEIene and neat PETMP-DGEBA formulations were tested. The formulations were named as x thiol-ene, being x the proportion of the mixture PETMP-PEIene in the formulation. The mixture PETMP-PEIene contained 1 phr of DMPA (parts of initiator for 100 parts of mixture). The photoinitiator was dissolved into the formulation by heating at 70ºC until the mixture became clear. PETMP-DGEBA formulation contained 2 phr of 1-MI (parts of amine by 100 parts of DGEBA). The composition of the mixtures is detailed in **Table 1**.

Table 1. Composition of the formulations per gram of mixture

Sample	PEIene		DGEBA		PETMP	
	(mmol)	(g)	(mmol)	(g)	(mmol)	(g)
0 thiol-ene	-		1.65	0.60	0.82	0.40
20 thiol-ene	0.037	0.12	1.30	0.46	0.86	0.41
40 thiol-ene	0.065	0.22	0.99	0.36	0.86	0.42
60 thiol-ene	0.101	0.33	0.68	0.25	0.88	0.42
80 thiol-ene	0.13	0.44	0.33	0.12	0.90	0.44
100 thiol-ene	0.16	0.55	-	-	0.91	0.45

Rectangular samples (40 mm x 10 mm x 1.5 mm) were obtained in a Teflon mold covered with a poly(propylene) film by irradiation under light-curing equipment (Dymax ECE 2000 UV light-curing flood lamp system) during 2 min (in intervals of 30 s with 5 min among them, 1 min for each face of the sample) (UV-intensity of 105 mW/cm^2, 365 nm) and then thermally treated at 100ºC for 1 h and 120 ºC for 30 min in an oven.

Characterization techniques

^{1}H NMR and ^{13}C NMR measurements were carried out in a Varian Gemini 400 spectrometer. $CDCl_3$ was used as the solvent. For internal calibration the solvent signal corresponding to $CDCl_3$ was used: δ (^{1}H) = 7.26 ppm, δ (^{13}C) = 77.16 ppm.

Photocalorimetric experiments were performed in order to study the thiol-ene stage of the dual curing. The samples were photocured at 30ºC using a Mettler DSC-821e calorimeter (Mettler-Toledo, Schwerzenbach, Switzerland) appropriately modified to permit irradiation with a Hamamatsu Lightningcure LC5 (HgeXe lamp) with two beams, one for the sample side and the other for the reference side. Samples weighing *ca.* 5 mg were cured in open aluminum pans in a nitrogen atmosphere. Two scans were performed on each sample in order to substract the thermal effect of the UV irradiation from the photocuring experiment, each one consisting of 2 min of temperature conditioning, 6 min of irradiation and finally 2 more minutes without UV light. A light intensity of 30 mW/cm^2 (calculated by irradiating graphite-filled pans on only the sample side) was employed.

Dynamic postcuring experiments were carried out in a Mettler 822e calorimeter with a TSO801RO robotic arm (Mettler-Toledo, Schwerzenbach, Switzerland), from -100ºC to 250ºC, under a nitrogen atmosphere at 10ºC/min. The degree of conversion, X_{UV}, during the photocuring stage was calculated in the basis of the heat evolved during the postcuring as follows:

$$X_{UV} = 1 - \frac{\Delta H_{post}}{\Delta H_{tot}} \quad (1)$$

where ΔH_{post} is the heat released during the postcuring process and ΔH_{tot} corresponds to the heat evolved during complete cure of the formulation.

A Bruker Vertex FTIR spectrometer equipment (resolution of 4 cm^{-1}) with an attenuated-total-reflectance accessory with a diamond crystal (Golden Gate heated single-reflection diamond ATR, Specac-Teknokroma) was used to monitor the UV curing. All the measurements were performed at room temperature. An irradiation lamp (Hamamatsu Lightningcure LC5 (HgeXe lamp)) was used to induce the photopolymerization (light intensity of 30 mW/cm^2). The samples were irradiated for 2 min and IR spectra were collected before and after irradiation. The UV process was followed by the thiol band at 2570 cm-^{1} and allyl band at 1643 cm^{-1}.

Thermogravimetric analyses were carried out in a nitrogen atmosphere with a Mettler TGA/SDTA 851e thermobalance. Samples with an approximate mass of 8 mg were degraded between 30 and 800 ºC at a heating rate of 10 ºC/min in N_2 (100 cm^3/min measured in normal conditions).

Dynamic mechanical thermal analyses were carried out with a TA Instruments DMA Q800 device. The samples were prepared as described before. Single cantilever bending at 1 Hz and amplitude 10μm was performed at 3 ºC/min from 50 ºC below T_g to 50ºC after T_g for each sample.

Results and discussion

Synthesis and characterization of the allyl-terminated hyperbranched poly(ethylenimine) (PEIene)

In this work we synthesized an allyl-terminated hyperbranched poly(ethylenimine) (PEIene) by reacting PEI with a molecular weight of 800 g/mol with allyl glycidyl ether at 50ºC in isopropanol, taking advantage of the nucleophilicity of amines of PEI which react with the oxirane ring. The synthetic pathway is depicted in **Scheme 1**.

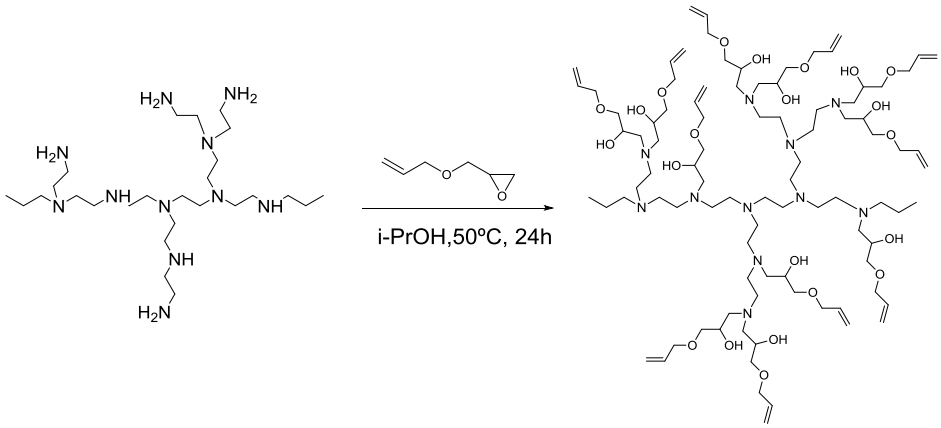

Scheme 1. Synthetic route of allyl-terminated hyperbranched poly(ethyleneimine) (PEIene)

From the degree of polymerization of PEI and the relationship (NH_2/NH/N) (1/0.82/0.53) published in the data sheet, we calculated the average number of active groups per molecule, NH and NH_2, which resulted to be 6.4 secondary amines and 7.9 primary amines in average per molecule.[34] From this number and taking into account that the secondary amines can react twice in front of the epoxide group the quantity of allyl glycidyl ether was calculated. By ^{1}H-NMR (**Figure 1**) we confirmed that the practical complete reaction was achieved because of the disappearance of epoxy group signals and the appearance of signal 2, corresponding to the methine group formed by the attack of the amine to the epoxide. Following the procedure previously reported[36] we calculated the degree of modification from the integration of the signals coming from the methine proton (signal 2) and the protons of PEI structure (subtracting the area of signal 3) and applying the following equation:

$$x = \frac{I(2)}{[I(PEI+1) - I(3)]/4} \quad (2)$$

where, *I(x)* is the integration of the group of protons assigned in Figure 1. From *x* and the relationship between primary amine end groups (*T*), secondary amine linear units (*L*), and tertiary amine dendrimeric units (D) and taking into account that primary amines can react twice with oxiranes it is possible to calculate the degree of modification (*DM*) by using the next equation:

$$DM = x(L + 2T + D)x\ 100/(L + 2T) \quad (3)$$

In this way, a modification degree of 100.2 % was calculated which falls in the range of error for a complete modification. The knowledge of the degree of modification and the average number of allyl groups in the PEI ene structure is essential to calculate the composition of the curing formulations.

Study of the photopolymerization and thermal process

Dual curing thermosets are formulations that can be partially cured, with a controlled advancement of the intermediate curing, as an initial stage after being applied onto a substrate and then later completely cured under heat. Usually, they combined two different curing methodologies, photocuring and thermal curing. Dual curing also offers the possibility of tailoring the material properties by changing the monomer and initiator concentrations and curing conditions[23] which can be understood by the mechanism of each reaction. Click reactions are very valuable to be applied for dual curing thermosets because of their orthogonality and selectivity and the high yields without elimination of volatiles.

Thiol-ene polymerization, in which a thiol adds to a carbon-carbon double bond, uses radical species as initiator and is often photochemically induced as represented in **Scheme 2.**[37] DMPA was used as photoinitiator and cleaved by absorbing a photon of light, whereupon it abstracts a hydrogen atom from a thiol monomer, generating a thiyl radical that further reacts.

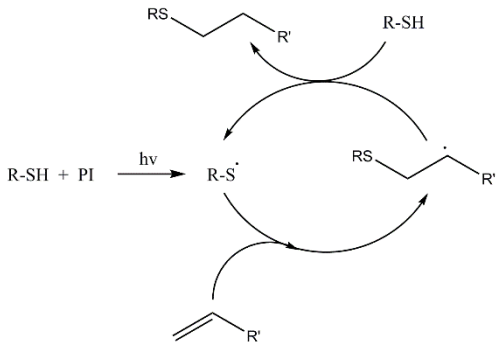

Scheme 2. Mechanism of the radical thiol–ene reaction

On the basis of this mechanism, it is generally assumed that, given an initial stoichiometric mixture of thiol and ene functional groups, the thiol and ene components will be consumed at identical rates.

To confirm the completion of thiol-ene reaction between PETMP and PEIene, FTIR spectra of the samples were registered during UV-irradiation. **Figure 2** represents the FTIR of the 100 thiol-ene sample, before and after irradiation. Before irradiation, the spectrum of the liquid film presents the –SH band at 2576 cm^{-1} and -C=C- band at 1643 cm^{-1}, since the reaction mixture consists of stoichiometric amounts of thiol and ene supplemented with a small percentage of photoinitiator. As we can see, after 2 min of irradiation, the absorptions due to the thiol monomer and the double bond have disappeared completely which evidences that the thiol-ene reaction has been completed. It should be commented, that the FTIR spectra during irradiation were taken for all the formulations but the monitoring of the thiol-ene reaction was not always possible, firstly by the presence of the peaks from DGEBA which overlaps the -C=C- band and secondly

because unreacted thiol groups are still present in the mixture to react with epoxy monomers.

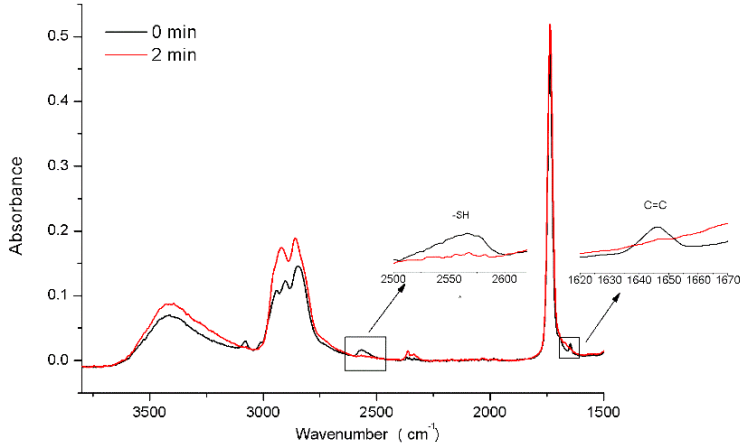

Figure 2. FTIR-UV spectra of the 100 thiol–ene formulation before and after UV-irradiation

The second process in the proposed dual curing is the thiol-epoxy reaction, which consists in a simple nucleophilic ring-opening reaction by a thiolate anion, formed by hydrogen abstraction with amine. The alkoxide anion formed is protonated by proton transfer from a quaternary ammonium salt formed in the activation of thiol or by the thiol itself, as depicted in **Scheme 3**. This mechanism puts in evidence the role of tertiary amine as catalyst.

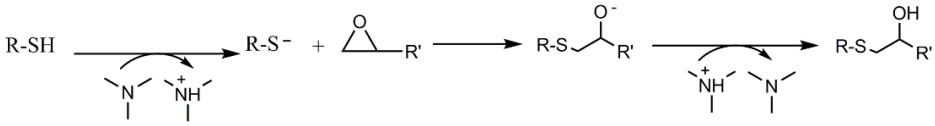

Scheme 3. Mechanism for the thiol–epoxy reaction

In our case, PEIene has several tertiary amines in the structure which can act like a base and promote the thiol-epoxy curing by opening of the oxirane rings. This could be an advantage since no amine should be added but it can be also a drawback because of it can lead to the partial overlapping of thiol-ene and thiol-epoxy reactions, suppressing the dual character of the curing process. Since the concentration of amine (acting as a basic catalyst) is an important issue in the catalysis of the thiol-epoxy process, the composition of the formulation, in which the PEIene proportion is varied, is one of the main factors affecting the kinetics of both processes and the characteristics of the materials after the first stage and after complete curing.

First of all, the effect of the basicity of the amines in the PEIene structure on the thiol-epoxy reaction was evaluated by DSC experiments. The enthalpy per epoxy equivalent was calculated for each non-irradiated formulation and compared with values reported in the literature[38] to verify that the thiol-epoxy reaction took place completely. Only in formulations containing 60% or 80% of PETMP-PEIene the total conversion of epoxy groups was achieved. When the proportion of PETMP-PEIene was lower, we realized that the thiol-epoxy reaction was not completed. As an example, in formulation 20 thiol-ene an

only 45% of epoxide conversion was evaluated. These results suggest that the basicity of the medium, due to the amines in PEIene is not enough to fully catalyze the thiol-epoxy reaction. Taking this into account, 1-methyl imidazole (1-MI) was added to all the formulations and the thiol-epoxy reaction was completed in all of them. Calorimetric curves for the previously irradiated 20 thiol-ene formulation with and without 2 phr of 1-MI are represented in **Figure 3**.

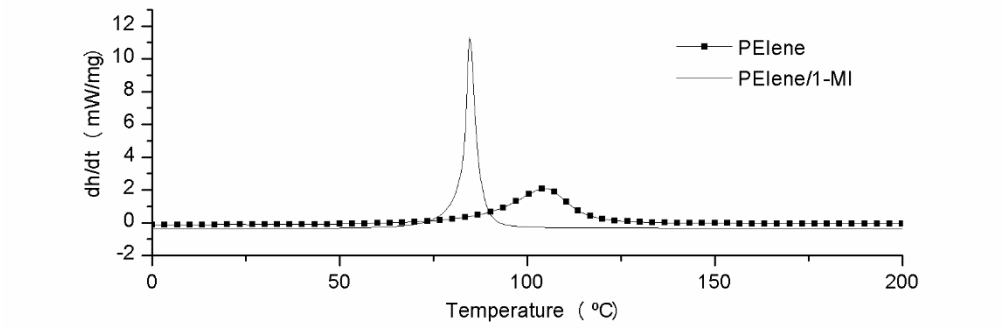

Figure 3. Calorimetric curves of the previously irradiated 20 thiol–ene sample

As we can see, on comparing the curves, different shapes can be observed. The addition of 1-MI to the sample produces a faster curing at lower temperatures and in a narrower range. Moreover, whereas the heat evolved in the sample containing 1-MI is 126 kJ/ee, the heat for the non-catalyzed formulation is only 52 kJ/ee, which indicates that when the proportion of PEIene in the formulation is low the epoxy reaction cannot be completed in the absence of added 1-MI. For this reason, 2 phr of 1-MI (in reference to DGEBA) was added to all formulations.

Carioscia et al.[23] reported that epoxy homopolymerization occurred in thiol-ene/thiol epoxy formulations and this competitive process became more important when the epoxy concentration was decreased. This was attributed to the reduced mobility of the unreacted thiol group in the materials, greater when the vinyl group concentration increased. As a base, the authors selected 2,4,6-tris(dimethylaminomethyl)phenol, which could initiate the homopolymerization process. To investigate if in our system the homopolymerization was a competitive process we could not follow the evolution of both thiol and epoxy bands in the FTIR spectra, but thiol absorptions have disappeared completely in the spectrum of the final material, which indicates that thiol reacts stoichiometrically with the epoxide groups and therefore no appreciable homopolymerization competes.

Once the individual reactions were characterized the combination of a first photochemical reaction followed by the thermal polymerization in the dual curing was studied.

The photoinduced thiol-ene polymerization was investigated by photo-DSC at 30ºC. The photocalorimetry experiment was done first of all in an isothermal irradiation curing during 6 min to register the complete exothermal curve. These studies were carried to find out the minimum time necessary to reach the maximum conversion of thiol groups during the irradiation, which was determined to be 2 min. The heat flow per double bond equivalent for all the formulations is reported in **Table 2.** As we can see, the 100 thiol-ene formulation rends an enthalpy per double bond equivalent of 60 kJ. Similar results were obtained for all the formulations, which indicate that in the photocalorimeter the thiol-ene reaction has

been completed in all of them. Since 2 min of irradiation were enough to reach the complete thiol-ene reaction, we registered a dynamic scan after 2 min of isothermal photocuring and the T_gs of these materials were determined. As we can see, on increasing the proportion of PEIene in the formulation the T_g also increases, as the result of the crosslinking by thiol-ene reaction on the hyperbranched structure of the multifunctional PEI.

Table 2. Calorimetric data of the different formulations studied

Sample	DSC data after irradiation in photo-DSC			DSC data after irradiation in the chamber			Final material
	ΔH^a (kJ/C=Ceq)	X^b (%)	$T_g{}^c$ (ºC)	ΔH^d (kJ/ee)	X^e (%)	$T_g{}^f$ (ºC)	$T_g{}^g$ (ºC)
0 thiol-ene	-	-		125	-	-	55
20 thiol-ene	60	0	-26	124	2	-26	50
40 thiol-ene	59	0	-18	114	9	-11	42
60 thiol-ene	62	7	-5	70	40	5	30
80 thiol-ene	64	14	0.5	57	54	10	20
100 thiol-ene	60	-	7	-	-	7	7

[a] Heat released per ene equivalent during irradiation in the photo-DSC during 6 min at 30 ºC.
[b] Epoxy group conversion after 2 min of irradiation in the photo-DSC determined by Eq. 1
[c] Glass transition of the material after 2 min of irradiation in photo-DSC determined in a second dynamic scan.
[d] Heat released by epoxy equivalent after irradiation during 2 min in the irradiation chamber, determined in a dynamic scan at 10ºC/min.
[e] Epoxy group conversion after irradiation in the chamber determined from DSC data and Eq. 1.
[f] Glass transition of the intermediate material after irradiation during 2 min in the chamber determined by DSC .
[g] Glass transition determined in a second scan in the DSC, of the final material after irradiation and a first dynamic scan at 10ºC/min.

We also investigated if both processes overlap during photocuring in the DSC. To know about this overlapping, the irradiated samples were subjected to a dynamic scan to determine the heat released by the epoxy-thiol reaction. From this value and the enthalpy per epoxy equivalent in the 0 thiol-ene formulation we can determine by eq. 1, the degree of conversion achieved by thiol-epoxy thermal process. In this way, a partial conversion of epoxides (7 and 14%) could be detected for formulations 60 and 80 thiol-ene, as collected in the table. Thus, by photo-DSC we could determine that the process has a dual character only in formulations 20 and 40 thiol-ene, in which the proportion of amines is low. The explanation to the overlapping between thiol-ene and thiol-epoxy processes can be found in the heat evolved during the thiol-ene process, higher when the extension of this reaction is also higher. It should be taken into account that although the heat evolved by C=C equivalent are quite similar the heat by gram increases on increasing the PEIene content in the formulation. The heat evolved in the thiol-ene photopolymerization was also attributed as the responsible of the overlapping with epoxide homopolymerization in case of using pentallylamine as -ene monomer.[18] However, the extent of epoxide homopolymerization was even larger and could be detected when the proportion of allylic compound was only 10%.

The preparation of films by the present two-stage process requires the use of a UV chamber to perform the first stage of curing. To see if the data and conclusions obtained by photo-DSC were reproducible in a bigger scale, we prepared samples in a mold and they were irradiated for 2 min as described in the experimental part. As we can see in Table 2, the thiol-epoxy reaction overlaps in all the formulations, being this overlapping more evident on increasing the proportion of PEIene in the formulation. The overlapping of the two reactive processes was also confirmed by comparing the T_g values obtained for the

irradiated formulations. Only 20 thiol-ene sample has similar T_g values despite the irradiation system applied and the 40 and 60 thiol-ene samples have a higher T_g when the materials were irradiated in the chamber than in the photo-DSC. It was quite surprising that the 80 thiol-ene sample shows a higher T_g than the 100 thiol-ene, but it can be rationalized by the DGEBA-thiol reaction which cannot occur in 100 thiol-ene formulation. This also confirms that thiol-epoxy reaction is a competitive process occurring during photoirradiation. As we can see, the conversion of thiol-epoxy reaction in this sample was determined to be 54% by measuring enthalpies.

The differences between photo-DSC and chamber can be attributed not only to the different radiation conditions but also to the size of the sample, which diffuse the heat in a different manner. Thus, the presence of amine groups in the formulation which catalyze the thiol-epoxy process, together with the heat evolved in the thiol-ene reaction avoid a pure dual-curing process to occur on preparing samples in the irradiation chamber. Sangermano et al.[18] studied by pyrometry the temperature reached during photoirradiation in thiol-ene/epoxy reactions. Although the systems and irradiation conditions were not exactly the same, temperatures of 78ºC could be measured, which are enough to start thiol-epoxy reaction.

All the samples prepared were submitted to a post-thermal treatment to complete the epoxy group conversion. The temperature of the cure and post-cure process was chosen taking into account the experiments performed by DSC. The irradiated samples were thermally treated for 1h at 100ºC and 30 min at 120ºC. Table 2 collects the T_g values determined by DSC of the materials after the thermal stage. On increasing the PEIene content in the formulation the T_gs decreased by the presence of the flexible structure of the polysulfide formed and the lower proportion of aromatic moieties, coming from DGEBA. The aliphatic structure of thiol limits the T_g value up to 55ºC for the 0 thiol-ene sample.

Characterization of the materials

The thermal stability of the complete cured materials was determined by TGA. **Figure 4** shows the thermogravimetric curves and the derivatives of the materials in N_2 atmosphere. As we can see, whereas the neat 0 thiol-ene and 100 thiol-ene present a main degradative process at different temperatures in the derivative curves, the other materials show both processes with contributions depending on the composition of the initial formulation. The main degradative process that appears in the 100 thiol-ene sample occurs at lower temperature than the process of the 0 thiol-ene sample. Moreover, a shoulder appears in all the samples at temperatures higher than 400ºC.

The most typical data extracted from TGA studies are collected in **Table 3**. As we can see, the materials begin to degrade at higher temperature when the proportion of PEIene in the formulation is lower, and the highest stability was observed by the thiol-epoxy neat material (0 thiol-ene). $T_{2\%}$ has been taken as the temperature at which the mechanical characteristics of the material usually begin to fail and from the point of view of the behavior of the material at high temperature is more meaningful than T_{max}. $T_{2\%}$ is reduced in 65ºC in the neat thiol-ene sample in comparison to the neat thiol-epoxy material. In previous studies we observed the low thermal stability of PEI containing thermosets.[33] The higher the proportion of PEI in the material the more important is the degradation at lower temperature, because of the breakage of the poly(ethyleneimine) structure. The same behavior is observed by looking at the T_{max} and $T_{shoulder}$ in which the degradative processes

of the PEI structure leads to a reduction of these temperatures on increasing the proportion of PEI in the material.

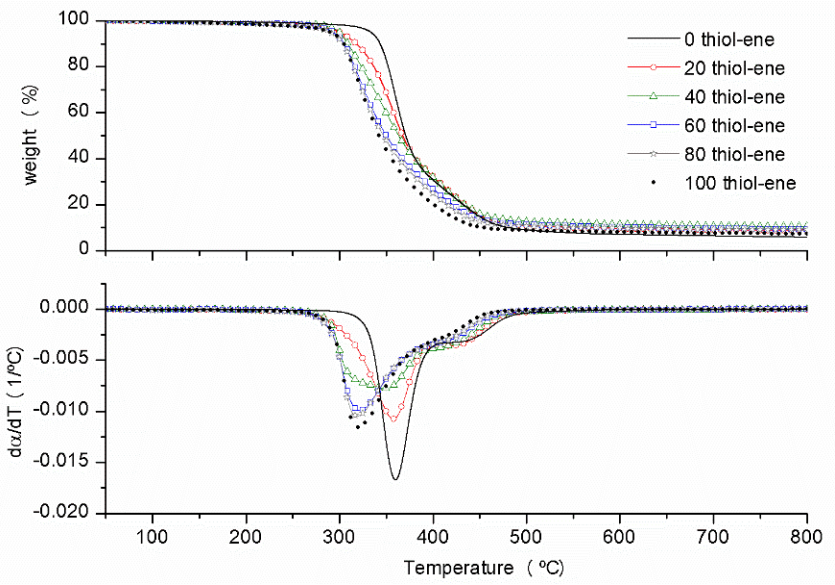

Figure 4. Thermogravimetric curves at 10 °C/min in N2 atmosphere of cured materials

Table 3. Thermal stability and thermomechanical characteristics of the cured materials

	TGA			DMTA	
Sample	$T_{2\%}$[a] (ºC)	T_{max}[b] (ºC)	$T_{shoulder}$[c] (ºC)	E_r[d] (MPa)	$T_{tan\,\delta}$[e] (ºC)
0 thiol-ene	304	360	441	12	58
20 thiol-ene	281	357	436	11	53
40 thiol-ene	270	348	428	19	40
60 thiol-ene	265	334	423	24	30
80 thiol-ene	252	318	422	26	24
100 thiol-ene	239	318	420	28	14

[a] Temperature of the 2% of weight loss in N_2 atmosphere.
[b] Temperature of the maximum decomposition rate.
[c] Temperature of the maximum rate of degradation in the last process.
[d] Storage modulus in the rubbery state.
[e] Temperature of maximum of *tan δ* curve.

Thermomechanical analysis of the materials prepared was performed. **Figure 5** collects the evolution of storage modulus and tan *δ* against temperature. As we can see, the material transforms from the glassy to the rubbery state at lower temperature on increasing the amount of PEIene in the formulation, because the higher flexibility of this structure and the lower amount of rigid aromatic structures coming from DGEBA. However, the modulus in the rubbery state tends to increase. The explanation to this fact can be found in the lower molecular weight between crosslinks on increasing the amount of PEI structures, since the structural unit in the HBP is rather short. Thiol-DGEBA polymerization leads to a network structure with a high molecular weight between crosslinking points.

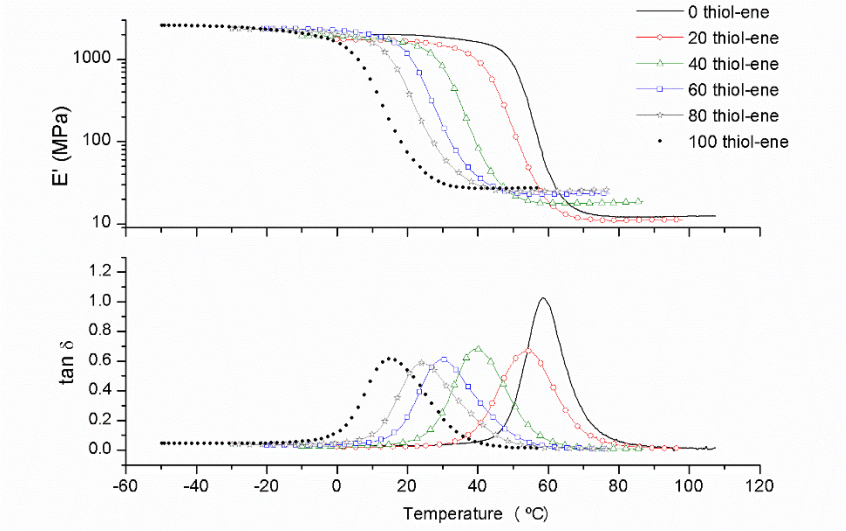

Figure 5. Storage modulus and tanδ evolution against temperature for the materials obtained

The shape of the tan *δ* curves (Figure 5) is in all cases unimodal indicating a complete homogeneous material. The temperatures of the maximum of tan *δ* decrease on increasing the proportion of PEIene in the formulation, similarly as the decrease in T_g observed by DSC.

Figure 6 shows the flexibility and appearance of one of the materials obtained, which are pale yellow and somewhat transparent.

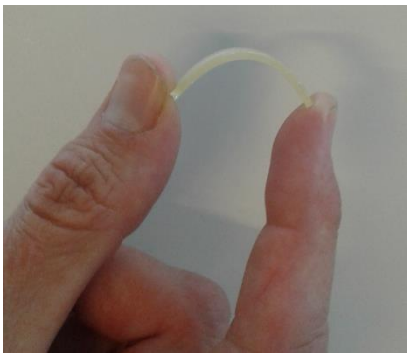

Figure 6. Photograph of the material prepared from 60 thiol–ene formulation

Conclusions

A new allyl terminated hyperbranched poly(ethyleneimine) (PEIene) was synthesized by reaction of PEI with allyl glycidyl ether. This multifunctional macromonomer has been used as -ene component in thiol-ene/thiol-epoxy curing formulations.

Different formulations of PEIene/DGEBA with stoichiometric amounts of pentaerythritol tetrakis (3-mercaptopropionate) were cured by a two-stage process consisting of a first photoirradiation and a second thermal treatment. To catalyze both processes a photoinitaitor (DMPA) and a base (1-MI) were necessary.

The presence of amines in the PEIene structure together with the heat evolved in the thiol-ene process led to an early initiation of the thiol-epoxy reaction during photocuring. The overlapping of both processes is greater on increasing the amount of PEIene in the formulation. This overlapping occurs in different proportions in the photo-DSC and in the photoirradiation chamber, because of the different irradiation conditions and size of the sample.

The materials are thermally more stable by increasing the proportion of DGEBA in the formulation, since the PEIene structure begins to degrade at lower temperatures.

The T_gs of the final materials decrease on increasing the proportion of PEIene in the formulation, due to the high flexibility of this hyperbranched structure. However, the storage modulus in the rubbery state increases, because of the lower molecular weight between crosslinks in rich PEIene materials.

References

[1] C. E. Hoyle, A. B. Lowe, C. N. Bowman. Thiol-click chemistry: a multifaceted toolbox for small molecule and polymer synthesis. Chem. Soc. Rev. 39 (2010) 1355-1387.
[2] M. H. Stenzel. Bioconjugation using thiols: Old chemistry rediscovered to connect polymers with nature's building blocks. ACS Macro. Lett. 2 (2013) 14-18.
[3] A. Brändle, A. Khan. Thiol-epoxy 'click' polymerization: efficient construction of reactive and functional polymers. Polym. Chem. 3 (2012) 3224-3227.
[4] S. De, A. Khan. Efficient synthesis of multifunctional polymers via thiol-epoxy ''click'' chemistry. Chem. Commun. 48 (2012) 3130-3132.
[5] R. M. Hensarling, S. B. Rahane, A. P. LeBlanc, B. J. Sparks, E. M. White, J. Locklin, D. L. Patton. Thiol–isocyanate ''click'' reactions: rapid development of functional polymeric surfaces. Polym. Chem. 2 (2011) 88-90.
[6] X. K. D. Hillewaere, R. F. A. Teixeira, L-T.T. Nguyen, J. A. Ramos, H. Rahier, F. E. Du Prez. Autonomous self-healing of epoxy thermosets with thiol-isocyanate chemistry. Adv. Funct. Mater. 24 (2014) 5575–5583.
[7] D. P. Nair, M. Podgorski, S. Chatani, T. Gong, W. Xi, C. R. Fenoli, C. N. Bowman. The thiol-Michael addition click reaction: A powerful and widely used tool in Materials Chemistry. Chem. Mater. 26 (2014) 724-744.
[8] B. D. Mather, K. Viswanathan, K. M. Miller, T. E. Long. Michael addition reactions in macromolecular design for emerging technologies. Prog. Polym. Sci. 31 (2006) 487–531.
[9] A. B. Lowe. Thiol-ene 'click' reactions and recent applications in polymer and materials synthesis. Polym. Chem. 1 (2010) 17-36.
[10] C. E. Hoyle, T. Y. Lee, T. Roper. Thiol–enes: Chemistry of the past with promise for the future. J. Polym. Sci. Part A: Polym. Chem. 42 (2004) 5301-5338.
[11] A. B. Lowe. Thiol-yne 'click'/coupling chemistry and recent applications in polymer and materials synthesis and modification. Polymer 55 (2014) 5517-5549.
[12] R. Hoogenboom. Thiol–yne chemistry: A powerful tool for creating highly functional materials. Angew. Chem. Int. Ed. 49 (2010) 3415-3417.
[13] Z. Beyazkilic, M. U. Kahveci, B. Aydogan, B. Kiskan, Y. Yagci. Synthesis of polybenzoxazine precursors using thiols: Simultaneous thiol–ene and ring-opening reactions. J. Polym. Sci. Part A: Polym. Chem. 50 (2012) 4029-4036.
[14] T. Griesser, A. Wolfberger, U. Daschiel, V. Schmidt, A. Fian, A. Jerrar, C. Teicherte, W. Kernac. Cross-linking of ROMP derived polymers using the two-photon induced thiol–ene reaction: towards the fabrication of 3D-polymer microstructures. Polym. Chem. 4 (2013) 1708-1714.
[15] M. Bednarek. Application of cationic polymerization by activated monomer mechanism and click reactions for the synthesis of functionalized polylactide. Polimery 57 (2012) 501-509.
[16] H. Liu, S. Li, M. Zhang, W. Shao, Y. Zhao. Facile synthesis of ABCDE-type H-shaped quintopolymers by combination of ATRP, ROP, and click chemistry and their potential applications as drug carriers. J. Polym. Sci. Part A: Polym. Chem. 50 (2012) 4705-4716.

[17] H. Lu, J. A. Carioscia, J. W. Stansbury, C. N. Bowman. Investigations of step-growth thiol-ene polymerizations for novel dental restoratives. Dent. Mater. 21 (2005) 1129-1136.
[18] M. Sangermano, M. Cerrone, G. Colucci, I. Roppolo, R. Acosta Ortiz. Preparation and characterization of hybrid thiol-ene/epoxy UV–thermal dual-cured systems. Polym. Int. 59 (2010) 1046-1051.
[19] T. Yoshimura, T. Shimasaki, N. Teramoto, M. Shibata. Bio-based polymer networks by thiol–ene photopolymerizations of allyl-etherified eugenol derivatives. Eur. Polym. J. 67 (2015) 397-408.
[20] P. M. Ajayan, L. S. Schadler, P. V. Braun. Nanocomposite Science and Technology. Wiley-VCH, Weinheim, 2003.
[21] K. Zou, M.D. Soucek. UV-Curable Organic-Inorganic Hybrid Film Coatings Based on Epoxidized Cyclohexene Derivatized Linseed Oil. Macromol. Chem. Phys. 205 (2004) 2032-2039.
[22] M. Sangermano, G. Colucci, M. Fragale, G. Rizza. Hybrid organic inorganic coatings based on thiol-ene systems. React. Funct. Polym. 69 (2009) 719-723.
[23] J. A. Carioscia, J. W. Stansbury, C. N. Bowman. Evaluation and control of thiol-ene/thiole-epoxy hybrid networks. Polymer 48 (2007) 1526-1532.
[24] F. Saharil, F. Forsberg, Y. Liu, P. Bettotti, N. Kumar, F. Niklaus, T. Haraldsson, W. van der Wijngaart, K. B. Gylfason. Dry adhesive bonding of nanoporous inorganic membranes to microfluidic devices using the OSTE(+) dual-cure polymer. J. Micromech. Microeng, 23 (2013) 025021.
[25] F. Forsberg, F. Saharil, T. Haraldsson, N. Roxhed, G. Stemme, W. Wijngaart, F. van der; Niklaus. A comparative study of the bonding energy in adhesive wafer bonding J. Micromech. Microeng. 23 (2013) 085019.
[26] M. Sangermano, I. Roppolo, R. Acosta Ortiz, A. G. Navarro Tovar, A. E. García Valdez, L. Berlanga Duarte. Interpenetrated hybrid thiol-ene/epoxy UV-cured network with enhanced impact resistance. Prog. Org. Coat. 78 (2015) 244-248.
[27] M. Morell, M. Erber, X. Ramis, F. Ferrando, B. Voit, A. Serra. New epoxy thermosets modified with hyperbranched poly(ester-amide) of different molecular weight. Eur. Polym. J. 46 (2010) 1498-1509.
[28] Boogh L, Pettersson B, Månson J. A. E. Dendritic hyperbranched polymers as toughening for epoxy resins. Polymer 40 (1999) 2249-2261.
[29] D. Foix, X. Ramis, A. Serra, M. Sangermano. UV generation of a multifunctional hyperbranched thermal crosslinker to cure epoxy resins. Polymer 52 (2011) 3269-3276.
[30] M. Flores, A. M. Tomuta, X. Fernández-Francos, X. Ramis, M. Sangermano, A. Serra. A new two-stage curing system: Thiol-ene/epoxy homopolymerization using an allyl terminated hyperbranched polyester as reactive modifier. Polymer 54 (2013) 5473-5481.
[31] P.-F. Cao, Z. Su, A. de Leon, R. C. Advincula. Photoswitchable Nanocarrier with Reversible Encapsulation Properties. ACSMacroLett. 4 (2015) 58-62.
[32] M. Adeli, R. Haag. Multiarm Star Nanocarriers Containing a Poly(ethylene imine) Core and Polylactide Arms. J. Polym. Sci: Part A: Polym. Chem. 44 (2006) 5740–5749.
[33] X. Fernández-Francos, D. Santiago, F. Ferrando, X. Ramis, J.M. Salla, A. Serra, M. Sangermano. Network structure and thermomechanical properties of hybrid DGEBA networks cured with 1-methylimidazole and hyperbranched poly(ethyleneimine)s. J. Polym. Sci. Part B: Polym. Phys. 50 (2012) 1489-1503.
[34] C. Acebo, X. Fernández-Francos, F. Ferrando, A. Serra, J.M. Salla, X. Ramis. Multiarm star with poly(ethyleneimine) core and poly(ε-caprolactone) arms as modifiers of diglycidylether of bisphenol A thermosets cured by 1-methylimidazole. React. Funct. Polym. 73 (2013) 431-441.
[35] C. Acebo, X. Fernández-Francos, M. Messori, X. Ramis, A. Serra. Novel epoxy-silica hybrid coatings by using ethoxysilyl-modified hyperbranched poly(ethyleneimine) with improved scratch resistance. Polymer 55 (2014) 5028-5035.
[36] H. Liu, Y. Chen, Z. Shen. Thermoresponsive hyperbranched polyethylenimines with isobutyramide functional groups. J. Polym. Sci: Part A: Polym. Chem. 45 (2007) 1177-1184.
[37] M. S. Kharasch, A. T. Read, F. O. R. Mayo. The Peroxide Effect in the Addition of Reagents to Unsaturated Compounds. XVI. The Addition of Thioglycolic Acid to Styrene and Isobutylene. Chem. Ind. (London) 57 (1938) 752
[38] D. Guzmán, X. Ramis, X. Fernández-Francos, A. Serra. New catalysts for diglycidylether of bisphenol A curing based on thiol-epoxy click reaction. Eur. Polym. J. 59 (2014) 377-386.

UNIVERSITAT ROVIRA I VIRGILI
HYPERBRANCHED POLY(ETHYLENEIMINE) DERIVATIVES AS MODIFIERS IN EPOXY NETWORKS
Cristina Acebo Gorostiza

6.4 Thiol-yne/thiol-epoxy hybrid crosslinked materials based on propargyl modified hyperbranched poly(ethyleneimine) and diglycidylether of bisphenol A resins

Cristina Acebo, Xavier Fernàndez-Francos, Xavier Ramis, Àngels Serra

RSC Advances. Submitted

UNIVERSITAT ROVIRA I VIRGILI
HYPERBRANCHED POLY(ETHYLENEIMINE) DERIVATIVES AS MODIFIERS IN EPOXY NETWORKS
Cristina Acebo Gorostiza

Thiol-yne/thiol-epoxy hybrid crosslinked materials based on propargyl modified hyperbranched poly(ethyleneimine) and diglycidylether of bisphenol A resins

Abstract

A novel curing methodology based in the combination of thiol-yne and thiol-epoxy click reactions has been developed. The curing process consists in a first photoinitiated thiol-yne reaction, followed by a thermal thiol-epoxy process. As alkyne substrate a new propargyl terminated hyperbranched poly(ethyleneimine) (PEIyne) has been synthesized from the reaction of commercial poly(ethylenimine) (PEI) and glycidyl propargyl ether.

The evolution of the curing of different mixtures of PEIyne and diglycidylether of bisphenol A (DGEBA) with the stoichiometric amount of tetrathiol (PETMP) has been monitored by DSC.

The new hybrid materials have been characterized by thermomechanical analysis, thermogravimetry and by electronic microscopy inspection and compared with neat thiol-yne and thiol-epoxy materials. The T_gs of the complete cured materials increase with the proportion of epoxide in the formulation. The thiol-yne network improves the plasticity of the fracture of the materials.

Keywords

Click reaction; thiol; epoxy resin; photocuring; hyperbranched.

Introduction

Crosslinked polymeric materials are extensively used in industrial applications.[1] In the last years more requirements has been put to get materials for advanced technologies, and a growing interest in fully organic hybrid polymer networks has emerged. These hybrid polymeric materials can be obtained from the combination of two or more polymerization mechanisms of different reactive precursors. Usually, one of these mechanisms is initiated by photoirradiation and the other occurs by thermal treatment.[2-4] Alternatively, two different photochemical processes can be combined[5,6] or even two thermal polymerization steps.[7] By combining polymerization mechanisms, it is possible to tailor the characteristics of the materials either by concurrent or sequential polymerization steps. The use of monomers or macromonomers with functionalities capable of participating in both polymerization mechanisms constitutes an advantage in the compatibilization of both polymeric structures that could have different polarity or miscibility.

Thiol monomers can be used in a broad range of efficient synthetic processes with a great variety of reactive substrates like epoxides, acrylates, isocyanates, acetylenes and vinyl groups. Some of these reactions are radical-mediated, such as the photoinitiated thiol-ene and thiol-yne reactions or thermal nucleophilic processes, such as base-catalyzed thiol-epoxy, thiol-isocyanate and thiol-Michael additions. These reactions have been used, alone or combined, to prepare networked polymers in a fast and efficient manner due to advantages of the click character of these reactions (fast, high conversion, solvent-free, oxygen-tolerant, etc.).[8-10] In combined processes, multifunctional thiols, that can react in both stages of curing, play the role of coupling agents, connecting two types of polymeric structures, which hinders macrophase separation to occur.

The combination of thiol-ene and thiol-epoxy reactions to prepare crosslinked materials with tailored characteristics has been reported, but the networks formed are quite flexible and have a low crosslinking density, which leads to low glass transition temperatures.[11-13]

Recently, we reported the crosslinking of thiol-epoxy formulations containing allyl-terminated hyperbranched poly(ethyleneimine) (PEIene), used as a macromonomer, in thiol-ene/thiol-epoxy processes. The curing methodology consists in an initial photoinduced thiol-ene reaction followed by a thermal base catalyzed thiol-epoxy process.[14] The advantage of using PEIene as a reactive component is to increase the functionality of the reactive mixture and enhance the thermomechanical characteristics of the intermediate material, since thiol-ene materials are generally highly flexible.[15-17] Additionally, the use of hyperbranched polymers in epoxy thermosets modification has been reported to be advantageous to improve toughness and other mechanical characteristics.[18,19]

Thiol-yne reaction is a radical mediated click reaction which takes place in a two-step process: the addition of thiol to the carbon-carbon triple bond to yield an intermediate vinyl thioether, and a thiol-ene reaction with remaining thiol, yielding the 1,2 double-addition species. This reaction is well-documented in organic chemistry, but it has been seriously overlooked in the thermosets field. Recently, thiol-yne reaction has been used in the preparation of polyfunctional materials via sequential thiol-Michael/thiol-yne strategy. High refractive index optical networks suitable for diverse applications were obtained with high yield.[20,21]

To increase the functionality in comparison with similar formulations based on thiol-ene reactive mixture and explore the feasibility of combined thiol-epoxy and thiol-yne click processes, we have prepared propargyl terminated poly(ethyleneimine) (PEIyne) and added in different proportions to thiol-epoxy formulations. The change from allyl to propargyl groups in the PEI structure should lead to an increase in the thermomechanical characteristics of the intermediate and final materials. The addition of two thiol groups to the propargyl moiety results in the double hydrothiolation of the triple bond and therefore the thiol-yne chemistry allows doubling the crosslinking density as compared with thiol-ene systems.[22]

It is worth to note that the thiol-yne reaction, as it has been stated, has emerged as a useful tool for material synthesis for advanced applications specially because of their good optical characteristics.[23-27] However, to the best of our knowledge, there are no reported studies in the formation of hybrid networks from the combination of thiol-yne and thiol-epoxy processes.

In the present study, mixtures in different proportions of diglycidyl ether of bisphenol A (DGEBA), PEIyne and tetrafunctional thiol (PETMP), catalyzed by a photoinitiator and a base, were photoirradiated and subsequently thermally cured. The evolution of the reaction was monitored by calorimetry in order to investigate if the two-stage curing process is sequential or both processes overlap. The materials prepared were characterized by thermomechanical analysis (DMTA), thermogravimetry (TGA) and their morphology visualized by electronic microscopy (SEM) and they were compared with neat thiol-yne and thiol-epoxy materials.

Experimental Part

Materials

Poly(ethyleneimine) (PEI) Lupasol®FG (800 g/mol) was kindly donated by BASF and used without further purification. From the molecular weight of the polymer and of the repeating unit, an average degree of polymerization of 18.6 was calculated. According to the data sheet, the relationship (NH_2/NH/N) was (1/0.82/0.53) and thus by calculations the equivalent number of primary, secondary and tertiary amines resulted to be 10, 8.37 and 5.3 meq/g. Glycidyl propargyl ether (GPE), pentaerythritol tetrakis (3-mercaptopropionate) (PETMP), 1-methylimidazole (1-MI) and 2,2-dimethoxy-2-phenylacetophenone (DMPA) were all purchased from Sigma-Aldrich. Ethanol was purchased from Scharlab. Diglycidylether of bisphenol A (DGEBA), Araldite GY 240 (EEW = 182 g/eq) was provided by Huntsman.

Synthesis of propargyl-terminated hyperbranched poly(ethyleneimine) (PEIyne) (Scheme 1)

In a 50 mL two neck round-bottomed flask provided with magnetic stirrer, addition funnel and Ar inlet, 1 g of PEI (1.25 mmol, 27.5 meq) were dissolved in 10 mL of ethanol. Then, the stoichiometric quantity of glycidyl propargyl ether (3.08 g, 27.5 mmol) was added. The reaction mixture was kept at 50ºC for a day. The crude product (yellowish oil) was dried at 50ºC under vacuum during two days.

^{1}H-NMR ($CDCl_3$, δ in ppm) (see **Figure 1**): 4.17 ppm (-O-C**H**$_2$-C≡C, **4**), 3.85 (-C**H**$_2$-OH, **2**), 3.48 ppm (-CH(OH)-C**H**$_2$-O-, **3**), 2.8-2.3 ppm (-C≡C**H**, **5**; -C**H**$_2$-N-, **1** and PEI nucleus).

^{13}C-NMR ($CDCl_3$, δ in ppm): 80.3 (-**C**≡CH), 78.9 ppm (-CH(OH)-**C**H$_2$-O-), 76.5 ppm (-O-**C**H$_2$-CH≡), 75.2 (-C≡**C**H), 72.5 ppm (-**C**H-OH-) and 70-50 ppm (-**C**H$_2$-N and PEI nucleus).

T_g, determined by DSC = - 40ºC.

Thermal stability, determined by TGA in N_2, $T_{5\%}$= 321ºC, T_{max}= 352ºC.

Preparation of the formulations and samples

PETMP-PEIyne in stoichiometric proportions were prepared and 1 phr of DMPA (1 part of photoinitiator for 100 parts of mixture) was added. The mixture was put in a bath at 70ºC until the solution became clear. PETMP-DGEBA stoichiometric mixture, containing 2 phr of 1-MI (parts of amine by 100 parts of DGEBA), was prepared by beating at room temperature. The curing formulations were prepared by beating at room temperature different amounts of the previously prepared PETMP-PEIyne and PETMP-DGEBA. Compositions of 20/80, 40/60, 60/40 and 80/20 w/w of PETMP-PEIyne/PETMP-DGEBA, neat PETMP-PEIyne and neat PETMP-DGEBA formulations were tested. The formulations were named as x thiol-yne, being x the proportion of PETMP-PEIyne mixture in the formulation.

It has been taken into account to prepare the stoichiometric formulations that the functionalities of the different reactants are: 4 for PETMP, 2 for DGEBA and 22 for PEIyne. The composition of the mixtures is detailed in **Table 1**.

Table 1. Composition of the formulations per gram of reactive mixture

Sample	PEIyne		DGEBA		PETMP	
	(mmol)	(g)	(mmol)	(g)	(mmol)	(g)
0 thiol-yne	-	-	1.65	0.60	0.82	0.40
20 thiol-yne	0.023	0.08	1.32	0.48	0.91	0.44
40 thiol-yne	0.046	0.15	0.98	0.36	0.99	0.49
60 thiol-yne	0.069	0.23	0.66	0.24	1.08	0.53
80 thiol-yne	0.092	0.30	0.32	0.12	1.17	0.58
100 thiol-ene	0.116	0.38	-	-	1.26	0.62

Rectangular samples of the crosslinked materials (40 mm x 10 mm x 1.5 mm) were obtained in a Teflon mold by irradiation under light-curing equipment (Dymax ECE 2000 UV light-curing flood lamp system) during 2 min (in intervals of 30 s with 5 min among them, 1 min for each face of the sample) (UV-intensity of 105 mW/cm^2, 365 nm) and then thermally treated at 100ºC for 1 h and 120 ºC for 30 min in an oven.

Characterization techniques

^{1}H NMR and ^{13}C NMR measurements were carried out in a Varian Gemini 400 spectrometer. $CDCl_3$ was used as the solvent. For internal calibration the solvent signal corresponding to $CDCl_3$ was used: δ (^{1}H) = 7.26 ppm, δ (^{13}C) = 77.16 ppm.

Photocalorimetric experiments were performed in order to study the thiol-yne stage of the curing process. The samples were photocured at 30ºC using a Mettler DSC-821e calorimeter (Mettler-Toledo, Schwerzenbach, Switzerland) appropriately modified to permit irradiation with a Hamamatsu Lightningcure LC5 (HgeXe lamp) with two beams, one for the sample side and the other for the reference side. Samples weighing *ca.* 5 mg were cured in open aluminum pans in a nitrogen atmosphere. Two scans were performed on each sample in order to subtract the thermal effect of the UV irradiation from the photocuring experiment, each one consisting of 2 min of temperature conditioning, 6 min of irradiation and finally 2 more minutes without UV light. A light intensity of 30 mW/cm^2 (calculated by irradiating graphite-filled pans on only the sample side) was employed.

The glass transition temperatures of the intermediate (after irradiation) and final material were determined by a dynamic scan from -100ºC to 250ºC, under a nitrogen atmosphere at 10ºC/min in a Mettler 822e device.

Dynamic postcuring experiments were carried out in a Mettler 822e calorimeter with a TSO801RO robotic arm (Mettler-Toledo, Schwerzenbach, Switzerland), from -100ºC to 250ºC, under a nitrogen atmosphere at 10ºC/min. The degree of conversion, X_{UV}, during the photocuring stage was calculated in the basis of the heat evolved during the postcuring as follows:

$$X_{UV} = 1 - \frac{\Delta H_{post}}{\Delta H_{tot}} \quad (1)$$

where ΔH_{post} is the heat released during the thermal postcuring process and ΔH_{tot} corresponds to the heat evolved during complete cure of the formulation.

A Jasco FTIR spectrometer equipment (resolution of 4 cm^{-1}) with an attenuated-total-reflectance accessory with a diamond crystal (Golden Gate heated single-reflection diamond ATR, Specac-Teknokroma) was used to monitor the UV curing. All the measurements were performed at room temperature. An irradiation lamp (Hamamatsu Lightningcure LC5 (HgeXe lamp)) was used to induce the photopolymerization (light intensity of 30 mW/cm^2). The samples were irradiated for 2 min and IR spectra were collected before and after irradiation. The UV process was followed by the thiol band at 2570 cm^{-1} and propargyl band at 2109 cm^{-1}.

Thermogravimetric analyses (TGA) were carried out in a nitrogen atmosphere with a Mettler TGA/SDTA 851e thermobalance. Samples with an approximate mass of 8 mg were degraded between 30 and 800 ºC at a heating rate of 10 ºC/min in N_2 (100 cm^3/min measured in normal conditions).

Dynamic mechanical thermal analyses (DMTA) were carried out with a TA Instruments DMA Q800 device. The samples were prepared as described before. Single cantilever bending at 1 Hz and amplitude 10 μm was performed at 3 ºC/min from 50 ºC below T_g to 50ºC after T_g for each sample.

The cryofracture of the specimens was metalized with gold and observed with a scanning electron microscopy (SEM) Jeol JSM 6400 with a resolution of 3.5 nm.

Results and discussion

Synthesis and characterization of the propargyl-terminated hyperbranched poly(ethyleneimine) (PEIyne)

In a previous work,[28] we synthesized a propargyl-terminated poly (ethylenimine) of higher molecular weight (Lupasol® G100, 5000 g/mol) by reaction of PEI with propargyl acrylate. In that case, we proved that the functionality in propargyl units achieved was only 58.6 in average, what means that NH_2 and NH react only with one acrylate group. Since in the present study we aim to increase the functionality of the components of the mixture to achieve higher T_gs, we modified PEI following a similar synthetic procedure that the one used in the preparation of allyl terminated PEI,[14] that is, through the reaction of PEI with propargyl glycidyl ether as shown in **Scheme 1**. Using this methodology, NH_2 reacts twice with glycidyl groups and NH once, reaching a practically complete modification. In the present study, we started from PEI with lower molecular weight because of viscosity issues, since the first reaction in the curing process is a photoinitiated thiol-yne at room temperature without any solvent.

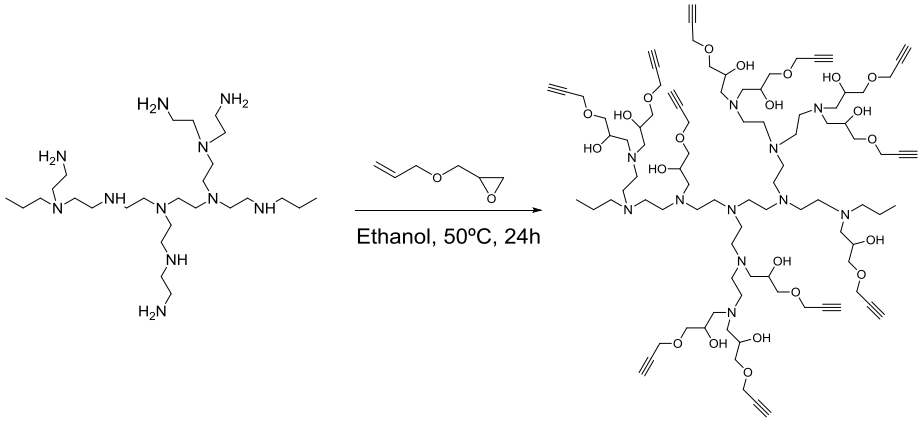

Scheme 1. Synthetic route to propargyl terminated hyperbranched poly(ethyleneimine)

The characterization of the PEIyne synthesized was performed by FTIR and NMR spectroscopy. By FTIR the propargyl group produced a characteristic band at 2110 cm^{-1} and the presence of hydroxyl groups was put in evidence by a broad adsorption centered at 3300 cm^{-1}.

Figure 1 shows the ^{1}H-NMR spectrum of PEIyne in $CDCl_3$. As we can see, methylene and methine protons of the new unit appear as separate signals at 4.17, 3.85 and 3.48 ppm, but acetylenic protons (5) appear overlapped with the signals corresponding to methylene protons linked to N of the PEI structure.

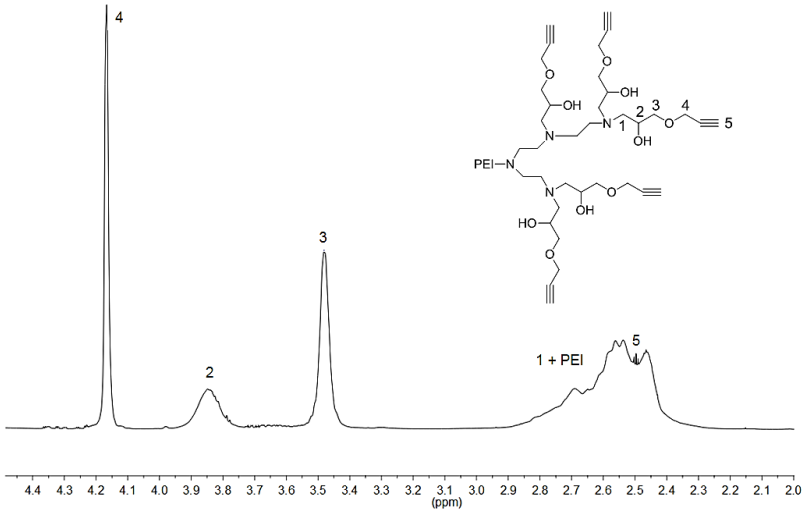

Figure 1. ^{1}H NMR spectrum of propargyl-functionalized poly(ethyleneimine) PEIyne

The degree of modification was calculated by ^{1}H-NMR spectroscopy, similarly as described in a previous paper[14] but taking into account that the signals corresponding to the propargyl proton overlapped with the signals of the core and should be subtracted. The modification degree calculated by this methodology was approximately 100%, taking into account the range of error attributable to the determination procedure.

Study of the photopolymerization process

Thiol-yne reaction takes place by a radical-mediated step-growth mechanism initiated by photoirradiation. The reaction proceeds under mild conditions, rapidly and achieve a high yield, without side-reactions, similarly to what happens in thiol-ene reaction, but with a double addition of thiol groups to triple bond.[8] Type II photoinitiators, like benzophenone derivatives, can be used to initiate this process. The initiator absorbs UV light and goes to the triplet state, where it abstracts hydrogen from the thiols forming thiyl radicals. Both, thiol-ene and thiol-yne reactions proceed by the addition of a thiyl radical to the substrate. As illustrated in **Scheme 2**, after the first addition, a carbon-centered radical is produced that subsequently abstracts a hydrogen from another thiol, generating a vinyl sulfide moiety and regenerating a thiyl radical. The vinyl sulfide is capable of undergoing further reaction through the addition of a second thiyl radical to the vinyl sulfide. Each yne moiety reacts with two thiol groups to form an 1,2-dithioether structure.[20,22] The reaction proceeds at high rates under ambient humidity and atmospheric oxygen conditions to high conversion, thereby providing an extremely efficient methodology for fabricating high-performance cross-linked polymer networks and films in a facile and convenient fashion.

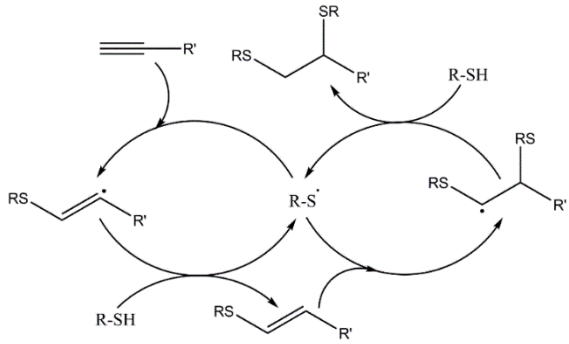

Scheme 2. Reaction mechanism proposed for the addition of thiols to alkynes

From the kinetics point of view, the rate of alkyne disappearance is equal to the rate of thiol loss and vinyl creation. The formed vinyl sulfides are consumed immediately upon creation and therefore alkyne acts as a difunctional in thiol-yne step-growth polymerizations.[22] Bowman's group demonstrated that thiol-yne materials have a higher crosslink density, glass transition temperature and modulus as compared to an analogous thiol-ene network.[22]

The monitoring of thiol-yne reaction was performed by FTIR and photocalorimetry. A mixture in stoichiometric proportions of PEIyne and PETMP and 1 phr of DMPA was irradiated in the UV chamber during 120 s (in intervals of 30 s with 5 min between them, 60 s irradiation on each face of the sample). The material obtained was studied by FTIR. **Figure 2** shows the FTIR spectra before and after irradiation. The typical signals of thiol groups (at 2576 cm^{-1}) and acetylene units (at 2110 cm^{-1}), which are magnified, disappear completely, indicating that the fully reaction has been achieved. No absorptions of vinyl sulfide groups can be detected.

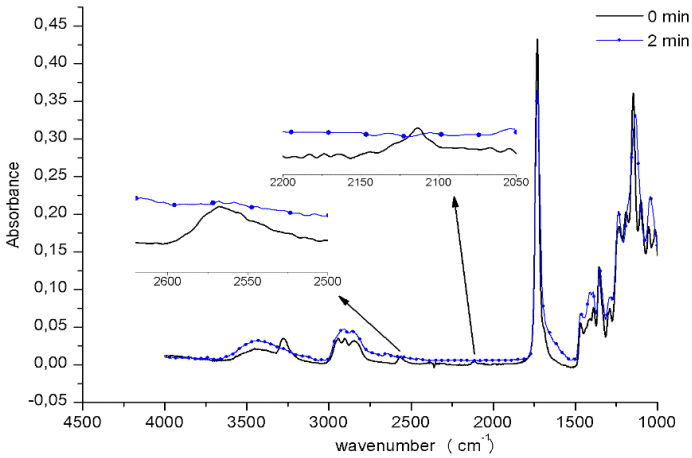

Figure 2. FTIR spectra of the 100thiol-yne formulation, before and after UV irradiation

The UV irradiation of this mixture in the photocalorimeter at 30ºC produces an enthalpy of about 122 kJ/eq of triple bond, just twice the enthalpy released in the thiol-ene polymerization system previously studied by us.[14] The T_gs after scanning in the photo-DSC and after irradiation in the chamber were determined and the value of 25ºC was obtained for both materials (see **Table 2**). The multifunctionality of the PEIyne structure allows to reach Tgs higher than described for networks prepared from simple tetrafunctional thiols and alkyne formulations.[29] Once the conditions to perform thiol-yne reaction were achieved the curing of the complex mixtures was undertook.

Table 2. Calorimetric data of the different formulations studied

Sample	DSC data after irradiation in photo-DSC			DSC data after irradiation in the chamber			Final material
	ΔH [a] (kJ/C≡Ceq)	X [b] (%)	T_g [c] (ºC)	ΔH [d] (kJ/ee)	X [e] (%)	T_g [f] (ºC)	T_g [g] (ºC)
0 thiol-yne	-	-		125	-	-	56
20 thiol-yne	122	3	-27	120	4	-27	53
40 thiol-yne	121	5	-26	118	6	-23	35
60 thiol-yne	121	17	-6	102	18	-4	29
80 thiol-yne	124	33	-2	80	36	2	27
100 thiol-yne	122	-	25	-	-	25	25

[a] Heat released per yne equivalent during irradiation in the photo-DSC during 6 min at 30 ºC.
[b] Epoxy group conversion after 2 min of irradiation in the photo-DSC determined by Eq. 1
[c] Glass transition of the material after 2 min of irradiation in photo-DSC determined in a second dynamic scan.
[d] Heat released by epoxy equivalent after irradiation during 2 min in the irradiation chamber, determined in a dynamic scan at 10ºC/min.
[e] Epoxy group conversion after irradiation in the chamber determined from DSC data and Eq. 1.
[f] Glass transition of the intermediate material after irradiation during 2 min in the chamber determined by DSC
[g] Glass transition determined in a second scan in the DSC at 10ºC/min, of the final material after irradiation in the chamber.

Study of combined photo-thermal processes

To establish a new sequential photo/thermal dual curing process, it is desired that both reactions occur independently in a controlled manner, with a stable intermediate

material.[3,13] Up to now, no description on the use of thiol-yne/thiol-epoxy sequences in thermoset preparation has been reported, but the procedure must be parallel to thiol-ene/thiol-epoxy two step curing.

The main issue in the combination of both click reactions in a two-step curing process is that the initial thiol-yne reaction, which is photoinitiated, releases heat. Thus, some thiol-epoxy reaction could occur during this photoirradiation, because of the presence of tertiary amines in the PEI structure and the added 1-MI which can catalyze the thermal process, as depicted in Scheme 3. In the previous study with PEIene it was put in evidence that 1-MI must be added to the formulation to reach the complete thiol-epoxy reaction.

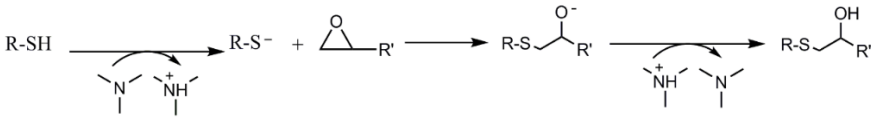

Scheme 3. Mechanism of epoxy-thiol reaction catalyzed by tertiary amines

In the previous study, based on the thiol-ene/thiol-epoxy process with PEIene, both reactions partially overlap and therefore the intermediate material is not only consequence of the thiol-ene, but also thiol-epoxy contributes to the formation of the network.[14] Therefore, in the present case, it is also required the investigation of the possible overlapping. To do that, different PEIyne/DGEBA mixtures in different proportions with the stoichiometric proportion of PETMP were studied by photo-DSC. The enthalpy released was measured and the enthalpy per alkyne equivalent calculated. The values obtained are collected in Table 2. As we can see, the values of enthalpy are similar, which could indicate that the thiol-yne process reached the completeness, even when a high proportion of epoxide is present in the formulation. By thermal dynamic DSC scans performed from each irradiated mixture, the heat evolved in the thiol-epoxy thermal process was evaluated. From these values we were able to calculate the conversion of epoxide groups during irradiation by using equation 1 and taking into account the enthalpy of the neat epoxy-thiol formulation (0 thiol-yne) and its proportion in the combined curing process. As we can see in Table 2, the conversion in epoxide during the UV stage increases with the proportion of thiol-yne reaction and it is even higher than the one calculated in PEIene/DGEBA/PETMP formulations.[14] This fact seems to support that the heat released during the UV-process, initiates the thermal reaction. In the previous study, we could determine that formulations with 20 and 40 of thiol-ene reaction behave in the photocalorimeter as dual curing systems, in a sequential and well controlled manner. This does not happen in the present thiol-yne/thiol-epoxy formulations.

FTIR studies gave us no more insight in the chemistry of this process, since the mixtures were rather complex and the most typical bands weak.

The preparation of the samples to be further characterized was performed by irradiating in the UV chamber in molds. After irradiation, the samples were investigated by dynamic DSC to determine the extent in which the epoxy conversion has occurred in these conditions by measuring the remaining enthalpy. The values of enthalpy determined are collected in Table 2, together with the conversion of epoxide calculated as explained before. As we can see, the extent of epoxy-thiol reaction is similar in the UV chamber to the one determined in the photocalorimeter, which is different from that we obtained in PEIene/DGEBA formulations.

The T_gs of the intermediate materials, after irradiation in photoDSC and UV chamber were determined and they are collected in Table 2. As it can be seen, they increase with the amount of PEIyne in the formulation, as the result of the higher crosslinking by thiol-yne reaction on the hyperbranched structure of the multifunctional PEIyne and are similar in both cases. However, not only the thiol-yne network is the responsible of the Tg achieved, but the competitive thiol-epoxy reaction also contributes to the increase of this value. If we look at the Tg of the completely cured material we can appreciate a tendency of increasing on increasing the proportion of epoxide in the formulation until reaching similar values of 54-56ºC for both 20 thiol-yne and 0 thiol-yne samples. The Tgs of the final materials prepared with the contribution of thiol-yne reaction are slightly higher than the ones obtained by thiol-ene, when the proportion of radical mediated process is predominant.[14] It should be taken into account that thiol-yne formulations are richer in PETMP than thiol-ene, which is the more flexible structure participating in the global network and therefore the increase in T_g is limited.

Characterization of the photo-thermal cured materials

The thermal stability of the materials obtained after irradiation in the UV chamber and thermally cured at 100ºC for 1 h and 120 ºC for 30 min in an oven was studied by thermogravimetry. **Figure 3** shows the weight-loss curves and their derivatives.

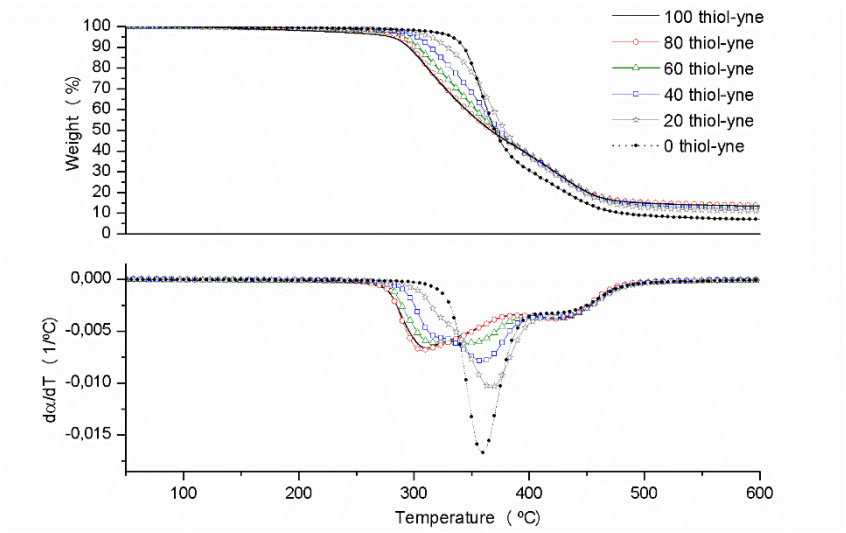

Figure 3. Thermogravimetric curves at 10ºC/min in N_2 atmosphere of cured materials

From the thermogravimetric curves we can see that the addition of PEIyne to the formulations leads to more degradable materials, since the neat DGEBA/PETMP (0 thiol-yne) thermoset begins to degrade at the highest temperature with a more simple shape of the derivative curve. When PEIyne was in the formulation the initial decomposition temperature diminishes, the range of decomposition temperatures broadens, and the mechanism of degradation becomes more complex. This behavior changes accordingly to the composition of the materials. This behavior was the one expected, since we have previously observed the lower thermal stability of thermosets modified with PEI derivatives, because of the breakage of C-N bonds.[14,30]

The temperature-dependent viscoelastic properties of the materials prepared were characterized by DMTA. The mechanical spectra, including plots of *E'*, *E''* and tan δ against temperature for all materials are shown in **Figure 4**.

The addition of PEIyne to the formulation leads to a reduction of the temperature of the tan δ maximum and to the broadening of the curve indicating a higher flexibility and a less homogeneous character of the network, according to the contribution of the hyperbranched poly(ethyleneimine) to the network structure.

From the loss modulus plots, the peaks corresponding to the T_gs can be observed. The evolution of this parameter clearly reflects the composition of the formulation. The higher the proportion of PEI-yne the lower the T_g of the materials because of the flexibility introduced, although the reduction of this value in the 20 thiol-yne material in reference to the neat 0 thiol-yne is scarce, such as obtained from DSC studies.

Storage modulus plots show a broad relaxation for the materials with thiol-yne proportions higher than 40%. Usually, *E'* values reach a plateau at a temperature about 50ºC higher than the main relaxation temperature. The values of moduli at this plateau decrease with decreasing cross-link density of the networks, consistent with the prediction of the thermodynamic equation of state for ideal rubber elasticity.[31] However, in the present case the complexity of the network with thiol-yne, thiol-epoxy and poly(ethyleneimine) structures does not lead to any regular variation in the storage moduli in the rubbery region. However, neat thiol-epoxy (0 thiol-yne) materials, with a high molecular weight between crosslinks show the lowest value of relaxed modulus in comparison to the hybrid formulations. Accordingly, 100 thiol-yne, with the lowest molecular weight between crosslinks leads to the highest value.

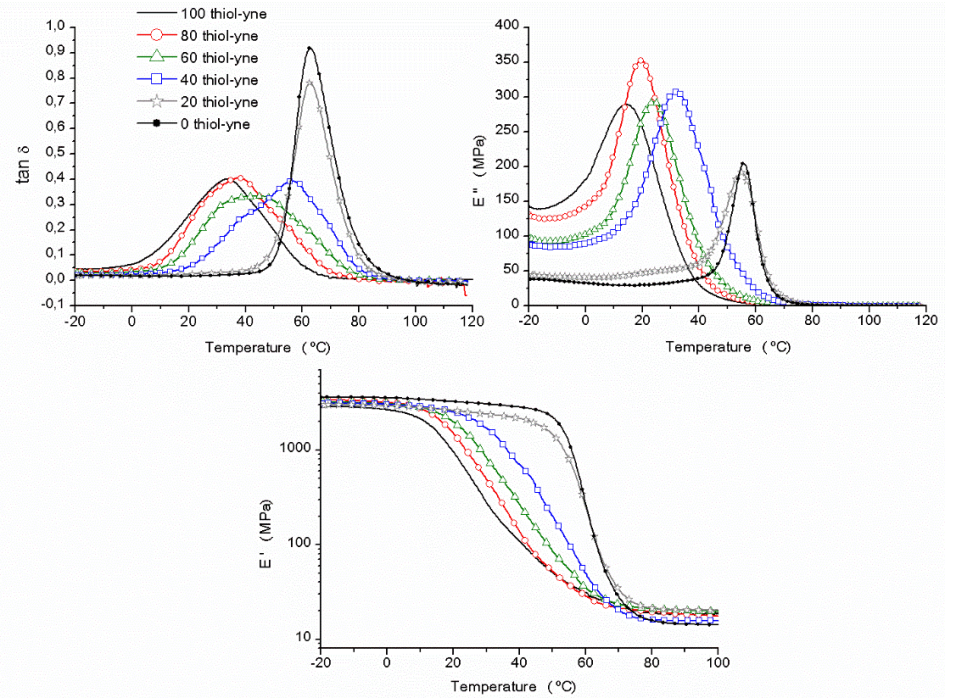

Figure 4. Tan δ evolution, loss and storage moduli against the temperature for the materials obtained

The morphologies of the cryofractured materials were visualized by scanning electron microscopy (SEM). **Figure 5** shows the most representative micrographs of the samples.

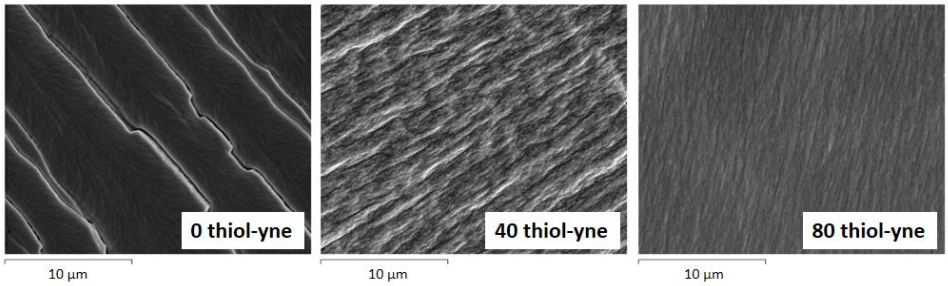

Figure 5. SEM micrographs of the cryofractured surfaces of some of the cured materials prepared

As we can observe, whereas the neat thiol-epoxy material presents a quite fragile fracture with a little evidence of deformation, the samples containing PEIyne show a highly plastic fracture, which must enhance the toughness of the materials. The SEM micrograph at higher magnification of the sample 20 thiol-yne in **Figure 6** shows a nanograined morphology produced by the hybrid character of the network structure. The other hybrid samples also showed some type of nanophase separation.

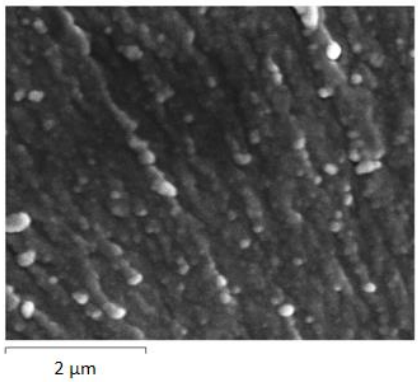

Figure 6. SEM micrograph showing the morphology of the 20 thiol-yne sample

Conclusions

Propargyl units were introduced at the chain ends of hyperbranched poly(ethyleneimine) by reaction of this polymer with glycidyl propargyl ether, achieving a nearly complete modification, as evaluated by ^{1}H NMR spectroscopy. This propargyl terminated HBP, PEIyne, was used as a macromonomer in a thiol-yne photopolymerization reaction.

Different formulations of PEIyne and DGEBA in different proportions with the stoichiometric amount of PETMP were firstly photoirradiated and then thermally cured to obtain hybrid organic materials. The curing process was a combination of a photoinitiated thiol-yne and a thermally induced thiol-epoxy click reaction, catalyzed by a photoinitiator (DMPA) and 1-MI as a base, respectively.

The study of this curing process allowed us to confirm that in the photoirradiation step, in which thiol-yne reaction occurred, thiol-epoxy reaction competed, due to the heat evolved in the thiol-yne coupling and the presence of tertiary amines in the formulation.

The double addition of thiol groups to the alkyne moieties allowed reaching higher glass transition temperatures in the materials in comparison to similar formulations based on thiol-ene reactions, accordingly to their higher crosslinking densities.

The T_gs of the cured materials increased on decreasing the proportion of PEIyne in the formulation, because of the more rigid structure of DGEBA.

The thermal stability is decreased on increasing the proportion of PEIyne in the formulation due to the presence of PEI structures.

The addition of PEIyne to the materials increased the plastic character of the fracture, which must enhance the toughness of these materials.

References

[1] M. Chanda, S.K. Roy, S.K., *Industrial Polymers, Specialty Polymers and Their Applications*, CRC Press, Boca Raton, USA, 2007.
[2] M. Adachi, H. Okamura, M. Shirai. *Chem. Lett*., 2013, **42**, 1056-1058.
[3] G. González, X. Fernández-Francos, À. Serra, M. Sangermano, X. Ramis. *Polym. Chem.,* 2015, **6**, 6987-6997.
[4] C.-H. Park, S.-W. Lee, J.-W. Park, H.-J. Kim. *React. Funct. Polym.,* 2013, **73**, 641–646.
[5] B. de Ruiter, A. El-ghayoury, H. Hofmeier, U. S. Schubert, M. Manea. *Prog. Org. Coat.,* 2006, **55** 154-159.
[6] R. Acosta Ortiz, A.E. Garcia Valdéz, L. Berlanga Duarte, R. Guerrero Santos, L.R.O. Flores, M. D. Soucek. *Macromol. Chem. Phys.*, 2008, **209**, 2157-2168.
[7] X. Fernández-Francos, A-O. Konuray, A. Belmonte, S. De la Flor, À. Serra, X. Ramis. *Polym. Chem.,* 2016, **7**, 2280-2290.
[8] A. B. Lowe, C.N. Bowman. Eds. *Thiol-X Chemistries in Polymer and Materials Science*. RSC Publishing, Croydon, UK, 2013.
[9] C.E. Hoyle, A.B. Lowe, C.N. Bowman. *Chem. Soc. Rev.*, 2010, **39**, 1355-1387.
[10] C.E. Hoyle, C.N. Bowman, *Angew. Chem. Int*., 2010, **49**, 1540-1573.
[11] F. Saharil, F. Forsberg, Y. Liu, P. Bettotti, N. Kumar, F. Niklaus, T. Haraldsson, W. van der Wijngaart, K.B. Gylfason, *J. Micromech. Microeng.* 2013, **23**, 025021.
[12] J.A. Carioscia, J.W. Stansbury, C.N. Bowman, *Polymer,* 2007, **48**, 1526-1532.
[13] D. Guzmán, X. Ramis, X. Fernández-Francos, A. Serra, *RSC Adv.* 2015, **5**, 101623-101633.
[14] C. Acebo, X. Fernández-Francos, X. Ramis, A. Serra, *React. Funct. Polym.* 2016, **99**, 17-25.
[15] T. Yoshimura, T. Shimasaki, N. Teramoto, M. Shibata, *Eur. Polym. J.* 2015, **67**, 397-408.
[16] B. G. Rutherglen, R. A. McBath, Y. L. Huang, D. A. Shipp, *Macromolecules,* 2010, **43**, 10297-10303.
[17] D. A. Shipp, C. W. McQuinn, B. G. Rutherglen, R. A. McBath, *Chem. Commun.,* 2009, 6415-6417.
[18] L. Boogh, B. Pettersson, J.A.E. Månson, *Polymer* 1999, **40**, 2249-2261.
[19] M. Flores, X. Fernández-Francos, F. Ferrando, X. Ramis, A. Serra. *Polymer*, 2012, **53**, 5232-5241.
[20] A. B. Lowe, C. E. Hoyle, C. N. Bowman, *J. Mater. Chem.,* 2010, **20**, 4745-4750.
[21] J. W. Chan; C. E. Hoyle, A. B. Lowe, *J. Am. Chem. Soc.*, 2009, **131**, 5751-5753.
[22] D. B. Fairbanks, T. F. Scott, C. J. Kloxin, K. S. Anseth, C. N. Bowman. *Macromolecules*, 2009, **42**, 211-217.
[23] A.B. Lowe, *Polymer*, 2014, **55**, 5517-5549.
[24] J.W. Chan, H. Zhou, C.E. Hoyle, A B. Lowe. *Chem. Mater.* 2009, **21**, 1579-1585.
[25] Q. Wei, R. Pötzsch, X. Liu, H. Komber, A. Kiriy, B. Voit, P-A. Will, S. Lenk, S. Reineke. *Adv. Funct. Mater.* 2016, **26**, 2545-2553.
[26] R. Hoogenboom. *Angew. Chem. Int. Ed.* 2010, **49**, 3415-3417.

[27] R. Pötzsch, H. Komber, B. C. Stahl, C. J. Hawker, B. Voit. *Macromol. Rapid Commun.* 2013, **34**, 1772-1778.
[28] C. Acebo, A. Lederer, D. Appelhans, X. Ramis, A. Serra, Send to revision
[29] J.W. Chan, J. Shin, C.E. Hoyle, C.N. Bowman, A.B. Lowe, *Macromolecules* 2010, **43**, 4937-4942.
[30] X. Fernández-Francos, D. Santiago, F. Ferrando, X. Ramis, J.M. Salla, A. Serra, M. Sangermano. *J. Polym. Sci. Part B: Polym. Phys.* 2012, **50**, 1489-1503.
[31] L.H. Sperling, *Introduction to Physical Polymer Science*. John Wiley & Sons: New York, USA, 2005.

UNIVERSITAT ROVIRA I VIRGILI
HYPERBRANCHED POLY(ETHYLENEIMINE) DERIVATIVES AS MODIFIERS IN EPOXY NETWORKS
Cristina Acebo Gorostiza

UNIVERSITAT ROVIRA I VIRGILI
HYPERBRANCHED POLY(ETHYLENEIMINE) DERIVATIVES AS MODIFIERS IN EPOXY NETWORKS
Cristina Acebo Gorostiza

7. Conclusions

7

UNIVERSITAT ROVIRA I VIRGILI
HYPERBRANCHED POLY(ETHYLENEIMINE) DERIVATIVES AS MODIFIERS IN EPOXY NETWORKS
Cristina Acebo Gorostiza

Conclusions

1. The suitability of hyperbranched poly(ethyleneimine) as basic structure to be easily modified has been demonstrated. Its industrial availability, the high proportion of reactive amine groups and the low molecular weight of the repeating unit are the key points allowing it to reach multifunctional macromonomers with tailored structure which could be used as modifiers of thermosetting materials.

2. The addition of poly(ethyleneimine) partially modified with 10-undecenoyl units to diglycidylether of bisphenol A/anhydride formulations led to improve impact resistance of these epoxy thermosets, keeping high glass transition temperatures. The toughness increase depended on the morphology of the materials, resulting from the proportion of reactive and unreactive groups in the modifier.

3. The use of poly(ethyleneimine) as a multifunctional core allowed us to prepare a series of multiarm stars with different number and length of poly(ε-caprolactone) arms. It was demonstrated the goodness of these structures as epoxy impact modifiers, leading to better rheological properties when the arms were shorter. When hydroxyl ends were blocked by acetylation, toughness was enhanced as the result of the nanostructuration, which varied with the molecular weight of the modifier.

4. The addition of multiarm stars with poly(ethyleneimine) core and poly(lactide) arms to epoxy formulations led to improvements in reworkability by the presence of secondary ester groups in the network. The molecular weight of the core scarcely affected the rheology of the reactive formulation, the evolution of the curing and the final properties of the modified thermosets.

5. Triethoxysilylated poly(ethyleneimine) was prepared and used as inorganic sol-gel precursor in epoxy hybrid materials. ^{29}Si NMR spectroscopy demonstrated the formation of cage-like structures that were embedded in the epoxy matrix. Some of the hybrid materials obtained showed improved scratch resistance and they exhibited a recovery capacity which depended on the proportion of modifier. The hybrid material with the highest content of silicon precursor showed a self-repairing behaviour. The addition of tetraethyl orthosilicate to the previous formulation led to the formation of silica nanodomains which did not increase the scratch characteristics. However, the addition of 3-(glycidyloxypropyl) trimethoxysilane to the formulation led to achieve improved resistance to break and to non-detachable coatings.

6. The reaction of poly(ethyleneimine) with allyl or propargyl glycidyl ether led to the preparation of allyl or propargyl multifunctional macromonomers. These hyperbranched structures were used in the preparation of organic hybrid materials through thiol click curing reactions. By combining a first photoinitiated thiol-ene or thiol-yne reaction with a second thiol-epoxy thermal process and changing the contribution of both reactions in the global curing process a series of tailored materials were obtained. The presence of amines in the poly(ethyleneimine) structure hindered the possibility to reach true sequential dual curing processes because of their catalytic effect in the epoxy-thiol reaction.

7. A new multifunctional 1,2,3-triazole macroinitiator was prepared by the aza-Michael addition of poly(ethyleneimine) on propargyl acrylate and subsequent 1,3-cycloaddition reaction with 1-azide pentane. This multifunctional initiator was used in the anionic thermal curing of diglycidylether of bisphenol A formulations and compared to 1-methylimidazole, which is a well-known anionic initiator. The lower reactivity of the new 1,2,3-triazole macroinitiator was observed. Although, the temperature of the maximum of tan δ and storage moduli were lower by the flexible structure of this macroinitiator, the damping characteristics were higher and the fracture behavior better, since by electronic microscopy nanophase separation that led to cavitation effects was visualized.

UNIVERSITAT ROVIRA I VIRGILI
HYPERBRANCHED POLY(ETHYLENEIMINE) DERIVATIVES AS MODIFIERS IN EPOXY NETWORKS
Cristina Acebo Gorostiza

UNIVERSITAT ROVIRA I VIRGILI
HYPERBRANCHED POLY(ETHYLENEIMINE) DERIVATIVES AS MODIFIERS IN EPOXY NETWORKS
Cristina Acebo Gorostiza

8. Appendices

UNIVERSITAT ROVIRA I VIRGILI
HYPERBRANCHED POLY(ETHYLENEIMINE) DERIVATIVES AS MODIFIERS IN EPOXY NETWORKS
Cristina Acebo Gorostiza

List of abbreviations

1-MI	1-methylimidazole
%wt	weight percentage
α	degree of conversion
α_{gel}	conversion at gelation
δ	chemical shift (ppm) or gap between tension and deformation
ε-CL	ε-caprolactone
σ_R	residual stress
σ_{th}	thermal stress
η*	complex viscosity
Δh_m	fusion enthalpy
Δh_t	heat released
Δh_{theor}	theorical reaction heat
Δh_{TOT}	total reaction heat
A	pre-exponential factor
BDMA	N,N-benzyldimethylamine
CDI	1,1′-carbonyldiimidazole
CIPS	chemical induced phase separation
CuAAC	copper(I)-catalyzed alkyne-azide cycloaddition
CTE	coefficient of thermal expansion
$d\alpha/dt$	reaction rate
DB	degree of branching
DGEBA	diglycidyl ether of bisphenol A
DM	degree of modification
DMF	N,N-dimethylformamide
DMAP	N,N-dimethylaminopyridine
DMPA	2,2-dimethoxy-2-phenylacetophenone
DMTA	dynamic mechanical thermal analysis
DMSO	dimethylsulfoxide

$\overline{DP}$	degree of polymerization
DSC	differential scanning calorimetry
E	energy loss of the pendulum with sample
E'	storage modulus
E"	loss modulus
E_0	energy loss of the pendulum without sample
E_a	activation energy
ee	epoxy equivalent
EtOH	ethanol
F_n	normal force
FTIR-ATR	fourier transformed infrared spectroscopy-attenuated total reflectance
FHWM	full width at half maximum of tan δ
G'	storage modulus
G"	loss modulus
GPC	gas permeation chromatography
GPTMS	3-(glycidoxypropyl)trimethoxymethylsilane
HBP	hyperbranched polymer
HKN	hardness knoop number
I	intensity
I.S.	impact strength
i-PrOH	isopropanol
KAS	Kissinger-Akahira-Sunose
k	rate constant
LA	lactide
L_{C1}	first critical load
L_{C2}	second critical load
MeCN	acetonitrile
MTHPA	methyltetrahydrophthalic anhydride
$\overline{M_n}$	number average molecular weight
$\overline{M_w}$	weight average molecular weight

$\frac{\overline{M_w}}{\overline{M_n}}$	molecular weight dispersity (PDI)
NMR	nuclear magnetic resonance
PEI	poly(ethyleneimine)
PCL	poly(ε-caprolactone)
P_d	penetration depth
phr	parts per hundred
PLA	poly(lactide)
PI	photoinitiator
PETMP	pentaerythritol tetrakis(3-mercaptopropionate)
R_d	residual depth
ROP	ring opening polymerization
SEC	size exclusion chromatography
SEM	scanning electron microscopy
SFT	stress free temperature
Sn(Oct)$_2$	tin (II) 2-ethylhexanoate
T	temperature
$T_{x\%}$	temperature of the lost of x% of weight
T_g	glass transition temperature
$T_{g\infty}$	glass transition temperature after isothermal curing
t_{gel}	gel time
T_m	melting temperature
T_{max}	temperature of the maximum degradation rate
$T_{shoulder}$	temperature of the shoulder in TGA
$T_{tan\ \delta}$	temperature of maximum of *tan δ* curve
t_{vitr}	vitrification time
tan δ	loss factor
TEA	triethylamine
TEM	transmission electron microscopy
TEOS	tetraethyl orthosilicate
TESPI	3-(triethoxysilyl)propyl isocyanate

TGA	thermogravimetric analysis
THF	tetrahydrofurane
TMA	thermal mechanical analysis
UV	ultraviolet
X	conversion degree
X_{gel}	gel point conversion

List of publications

Publications from the thesis

Cristina Acebo, Xavier Fernández-Francos, Francesc Ferrando, Àngels Serra, Josep M. Salla, Xavier Ramis. "Multiarm star with poly(ethyleneimine) core and poly(ε-caprolactone) arms as modifier of diglycidylether of bisphenol A thermosets cured by 1-methylimidazole". *Reactive & Functional Polymers* **2013**, *73*, 431-441.

Cristina Acebo, Xavier Fernández-Francos, Francesc Ferrando, Àngels Serra, Xavier Ramis. "New epoxy thermosets modified with multiarm star poly(lactide) as core of diferent molecular weight". *European Polymer Journal* **2013**, *49*, 2316-2326.

Cristina Acebo, Annamaria Picardi, Xavier Fernández-Francos, Silvia De la Flor, Xavier Ramis, Àngels Serra. "Effect of hydroxyl ended and end-capped multiarm star polymers on the curing process and mechanical characteristics of epoxy/anhydride thermosets". *Progress in Organic Coatings* **2014**, *77*, 1288-1298.

Cristina Acebo, Xavier Fernández-Francos, Massimo Messori, Xavier Ramis, Àngels Serra. "Novel epoxy-silica hybrid coatings by using ethoxysilyl-modified hyperbranched poly(ethyleneimine) with improved scratch resistance". *Polymer* **2014**, *55*, 5028-5035.

Cristina Acebo, Xavier Fernández-Francos, Silvia De la Flor, Xavier Ramis, Àngels Serra. "New anhydride/epoxy thermosets based on diglycidyl ether of bisphenol A and 10-undecenoyl modified polyethyleneimine with improved impact resistance". *Progress in Organic Coatings* **2015**, *85*, 52–59.

Cristina Acebo, Miquel Alorda, Francesc Ferrando, Xavier Fernández-Francos, Àngels Serra, Josep M. Morancho, Josep M. Salla, Xavier Ramis. "Epoxy/anhydride thermosets modified with end-capped star polymers with poly(ethyleneimine) cores of different molecular weight and poly(ε-caprolactone) arms". *eXPRESS Polymer Letters* **2015**, *9*, 809-823.

Cristina Acebo, Xavier Fernández-Francos, Jose-Ignacio Santos, Massimo Messori, Xavier Ramis, Àngels Serra. "Hybrid epoxy networks from ethoxysilyl-modified hyperbranched poly(ethyleneimine) and inorganic reactive precursors". *European Polymer Journal* **2015**, *70*, 18-27.

Cristina Acebo, Xavier Fernández-Francos, Xavier Ramis, Àngels Serra. "Multifunctional allyl-terminated hyperbranched poly(ethyleneimine) as component of new thiol-ene/thiol-epoxy materials". *Reactive & Functional Polymers*, **2016**, *99*, 17-25.

Cristina Acebo, Albena Lederer, Dietmar Appelhans, Xavier Ramis, Àngels Serra, "Synthesis of 1,2,3-triazole ended functionalized hyperbranched poly(ethyleneimine) and its use as multifunctional anionic macroinitiator for diglycidyl ether of bisphenol A curing". *European Polymer Journal*. Submitted

Cristina Acebo, Xavier Fernández-Francos, Xavier Ramis, Àngels Serra, "Thiol-yne/thiol-epoxy crosslinked materials based on propargyl modified poly(ethyleneimine) and diglycidylether of bisphenol A resins". *RSC Advances.* Submitted

Collaborations in other publications

Josep M. Morancho, Xavier Fernàndez-Francos, **Cristina Acebo**, Josep M. Salla, Àngels Serra. “Thermal curing of an epoxy-anhydride system modified with hyperbranched poly(ethylene imine)s with different terminal groups”. *Journal of Thermal Analysis and Calorimetry* DOI 10.1007/s10973-016-5376-z.

Vicente Lorenzo, **Cristina Acebo**, Xavier Ramis, Àngels Serra. “Mechanical characterization of sol–gel epoxy-silylated hyperbranched poly(ethyleneimine) coatings by means of Depth Sensing Indentation methods”. *Progress in Organic Coatings* **2016**, 92, 16-22.

Oleksandra Korychenska, **Cristina Acebo**, Mykola Bezuglyi, Àngels Serra, Juozas V. Grazulevicius, “Epoxy thermosets modified by carbazole decorated hyperbranched poly(ethyleneimine) with enhanced optical characteristics”. *Reactive & Functional Polymers*. Submitted

Meeting contributions and stages

Meeting contributions

Cristina Acebo, Xavier Fernández-Francos, Francesc Ferrando, Àngels Serra, Josep M. Salla, Xavier Ramis. *Multiarm star with poly(ethylenimine) core and poly(ε-caprolactone) arms as modifiers of diglycidylether of bisphenol A thermosets cured by 1-methylimidazole*. Premio al mejor Póster procedente de un país no Báltico. Baltic Symposium 2013, Trakai (Lituania)

Cristina Acebo, Xavier Fernández-Francos, Francesc Ferrando, Àngels Serra, Josep M. Salla, Xavier Ramis. *Modification of diglycidylether of bisphenol A thermosets with multiarm star polymers with poly(ethylenimine) core and polyester arms cured by 1-methylimidazole*. Presentación oral en el VII Congreso de Jóvenes Investigadors en Polímeros (JIP), Cala Galdana (Menorca, 2013).

Cristina Acebo, Annamaria Picardi, Àngels Serra, Xavier Ramis, Xavier Fernández-Francos, Silvia De la Flor. *Modification of epoxy resins with star-like polymers with poly(ethylenimine) core and polyester arms, cured by anhydride*. Presentació oral en el VIII Congrés de Joves Investigadors dels Països Catalans (Andorra, 2013).

Cristina Acebo, Àngels Serra, Xavier Ramis, Xavier Fernández-Francos, Francesc Ferrando. *Multiarm star with poly(ethylenimine) core and poly(lactide) arms as modifiers of diglycidylether of bisphenol A thermosets cured by 1-methylimidazole*. Póster en el III Simposio Internacional: Frontiers in Polymer Science, Sitges (Barcelona, 2013)

Cristina Acebo, X. Fernández-Francos, Silvia De la Flor, Xavier Ramis, Àngels Serra. *New epoxy thermosets modified with 10-undecenoyl modified polyethyleneimine*. Póster en el XIII Meeting del Grupo Especialzado en Polímeros (GEP) (Girona, 2014).

Cristina Acebo, Xavier Fernández-Francos, Massimo Messori, Xavier Ramis, Àngels Serra. *Novel epoxy-silica hybrid coatings by using ethoxysilyl-modified hyperbranched poly(ethyleneimine) with improved scratch resistance*. Poster on the 8th ECNP International Conference on Nanostructured Polymers and Nanocomposites (Dresden 2014)

Cristina Acebo, Xavier Ramis, Xavier Fernández-Francos, Àngels Serra. *Novel thiol-ene/thiol-epoxy thermosets based on allyl modified hyperbranched poly(ethyleneimine) and DGEBA.* Poster on the European Polymer Congress (EPF) (Dresden, 2015).

Vicente Lorenzo, **Cristina Acebo**, Àngels Serra. *Instrumented indentation characterization of sol-gel coatings based on silylated hyperbranched poly(ethyleneimine) and DGEBA*. Poster on the European Polymer Congress (EPF) (Dresden, 2015).

José María Morancho, Xavier Fernández-Francos, **Cristina Acebo**, Xavier Ramis, Josep María Salla, Àngels Serra. *Thermal curing of an epoxy-anhydride system modified with hyperbranched poly(ethyleneimne)s with different terminal groups.* Poster on the 3rd Central and Eastern European Conference on Thermal Analysis and Calorimetry (CEEC-TAC3) (Ljubljana, 2015).

Stay Abroad

Organization: Leibniz-Insitute für Polymerforschung

Department: Institute of Macromolecular Chemistry

City: Dresden **Country:** Germany

Lenght: 6 months **Year:** 2015